NASA Contractor Report 182075

LABORATORY TEST AND ACOUSTIC ANALYSIS OF CABIN TREATMENT FOR PROPFAN TEST ASSESSMENT AIRCRAFT

H.L. Kuntz and R.J. Gatineau

LOCKHEED AERONAUTICAL SYSTEMS COMPANY
Burbank, California

Contract NAS1-18036
May 1991

NASA
National Aeronautics and Space Administration
Langley Research Center
Hampton, Virginia 23665-5225

FOREWORD

The tests described herein were made possible through the efforts of many people. Messrs. D. L. Morrow, J. L. Hayward, and C. J. Looper organized and performed the acoustical tests. Mr. J. R. Trott and Dr. A. Abtahi improved the Masscomp data acquisition capabilities. Messrs. R. A. Prydz and F. J. Balena supplied administrative help and supplied technical suggestions. A number of people from the Kelly Johnson Research and Development Center shops worked on construction, instrumentation, and changing room and fuselage configurations for the various laboratory tests. Dr. L.D. Pope (L.D. Pope Associates) modified the Propeller Aircraft Interior Noise (PAIN) computer program to model the inclusion of resonators within the cabin sidewall and made cabin noise prediction computations with this program. Dr. Kevin Shepherd of NASA-Langley Research Center was the Technical Contract Monitor during this period.

The original version of this document was a Lockheed Aeronautical Systems Company - Burbank Report **LR**31879, May 1990.

SUMMARY

In the Spring of 1988 seven flight tests were conducted at LASC-Georgia with a cabin acoustic enclosure, which was installed in the Propfan Test Assessment (PTA) Gulfstream II aircraft. These tests were performed to evaluate the effectiveness of using sidewall-mounted Helmholtz resonators to increase the spatially averaged cabin noise reduction <NR> of an aircraft with a near-constant rotational speed propfan. With the resonators active during the flight tests, cabin <NR> improvements were observed, but additional information was required to clarify our understanding of the test results. In order to obtain this information, a series of laboratory tests were performed during 1989. This report describes the laboratory tests in detail and compares the laboratory test results with flight test results.

The results of the laboratory tests show that the resonators operate as predicted. During the flight tests the resonator and ambient sidewall temperatures were higher than anticipated. These elevated temperatures caused the resonator resonance frequency to be higher than the design frequency. For the laboratory tests the resonator resonance frequency (236 Hz @ 27° C) was centered in the simulated propfan tonal excitation frequency range of 225 through 245 Hz. In addition, <NR> tests were performed with a broadband noise source between 150 and 800 Hz. During the flight tests it was determined that cabin noise flanking around the enclosure ends was a serious problem. Although barrier materials were added to the enclosure ends and the gap between the enclosure and the fuselage sidewall, the barriers were not complete, since some airflow had to be maintained between the fore and aft cabins. During the laboratory tests, measurements were made without and then with complete double wall vinyl barriers over the enclosure and fuselage section ends.

Because flight test resonator effects were observed over a much broader frequency range than anticipated, it was postulated that this broad tuning effect was due, in part, to the presence of sidewall insulation near the resonator nozzles. Other causes of this tuning spread were thought to be temperature variations within the sidewall and tuning scatter caused by resonator dimensional variations. However, statistical testing of a sampling of resonators showed the dimensional variation effects to be small.

As a result of the laboratory tests, it was determined that without sidewall insulation, the additional <NR> from the resonator operation was 11 dB at the resonance frequency. With sidewall insulation present, the <NR> was 9 dB. The sidewall insulation increased the <NR> at all frequencies greater than 200 Hz.

TABLE OF CONTENTS

LIST OF FIGURES

LIST OF TABLES

NOTATION

BPF Blade Passage Frequency
Hz Frequency in hertz (cycles/second)
IL Insertion Loss - Difference between the SPLs before and after and acoustical element has been introduced, dB.
NR Noise Reduction - Difference between the incident and the transmitted SPLs across an acoustical element, dB.
PTA Propfan Test Assessment
rpm Revolutions per Minute
SPL Sound Pressure Level - dB re 20 uPa
TL Transmission Loss - Difference between the incident and the transmitted sound power levels across an acoustical element, dB.
<.> Brackets to indicate spatial averaging of transducer data.

Normalization SPLs (Fuselage <SPL>):

Blade Passage Frequency:	142 dB
Second Harmonic Tone:	136 dB
Third Harmonic Tone:	128 dB
Broadband Random Noise:	120 dB

NAS### The ### denotes the laboratory test number. These numbers may be used to compare data between plots (see Table II).

1.0 Introduction

The objective of the NASA Acoustic Treatment Technology Program contract with the Lockheed Aeronautical Systems Company (LASC) was to evaluate the acoustic performance of an advanced cabin wall treatment equipped with acoustic resonators* in the Propfan Test Assessment (PTA) Gulfstream II aircraft. Except for flight testing, this program was performed in the Acoustics Laboratory at the Kelly Johnson Research and Development Center at Rye Canyon, Saugus, CA and was funded by the NASA-Langley Research Center. This program was in support of the overall PTA program awarded to LASC-Georgia, funded by NASA-Lewis Research Center, and completed in 1989[1,2].

Initial acoustic resonator testing and development for use within double walls was accomplished utilizing flat panels in a 1.08 by 1.08 m transmission loss facility in Lockheed's Rye Canyon Acoustics Laboratory[3,4]. These tests were aimed at improving the transmission loss (TL) of various double-wall assemblies at and near specified tonal frequencies. The test results indicated that a large increase in TL and noise reduction (NR) could be achieved for a specified frequency band.

The flat panel assembly tests led to a design validation program that tested the effectiveness of resonators attached to aircraft cabin trim panels. These trim panels and the fuselage skin form a curved double-wall assembly similar to the flat double-wall assemblies tested in the laboratory. The results from the design validation program guided the construction and test of an acoustic cabin enclosure, described below.

As part of the associated PTA program, a tractor propfan powerplant was mounted on the left wing of a modified Gulfstream II test bed aircraft. In the Spring of 1988 the enclosure was flown in the aircraft to determine the effectiveness of acoustic resonators in reducing the propfan fundamental blade passage frequency (BPF) sound pressure levels (SPL) within the aircraft cabin. Since this aircraft had a bare fuselage interior, the acoustic test enclosure installed in the cabin consisted of a metal framework, plywood ends, and a plywood floor. The enclosure was constructed as a trim panel support frame and was centered near the propfan rotational plane. Figure 1 is a photograph showing this trim panel support framework attached to its shipping base. Most of the framework fasteners are bolts. The bolts permit the framework to be dismantled for installation and re-assembly within the aircraft cabin. The enclosure is designed to accommodate high-level crash loads. The test aircraft, with its propfan powerplant, is shown behind the enclosure framework.

Twenty-eight aluminum trim panels, each supporting sixteen acoustic resonators, are supported by this rigid framework. Installation of the two end access doors, the floor, and the 28 trim panels form the acoustic enclosure, which was placed within the aircraft cabin. This cabin-within-a-cabin was used to evaluate the performance of resonators as noise

*A resonator is a device in which it is very easy to excite oscillations at one or more discrete frequencies. The resonators used during the laboratory and flight tests are described in Appendices A and B.

attenuating devices during cruise flight. The enclosure was attached to the cabin floor seat tracks with twenty-one vibration isolators. The isolators were to prevent most of the vibration-borne noise from being admitted into the enclosure.

As part of the PTA acoustic test program, and in support of the enclosure test program, an analysis of acoustic data obtained inside and outside the cabin of the untreated PTA aircraft was performed[1,2,5]. The spatially averaged noise reduction (<NR>) of the untreated fuselage was determined to be dominated by the airborne acoustic input. Structure-borne noise originating from the propfan became important only at low altitude (1520 m) and at higher frequencies (i.e., 675 Hz, 3rd harmonic). The untreated fuselage <NR> averaged 25 dB for each of the first three harmonics when the fundamental frequency was varied from 172 through 237 Hz.

Interior noise predictions were made with the Propeller Aircraft Interior Noise (PAIN) computer model[3,6,7] for comparison with the flight test data. The predictions indicated that the resonators should have been more effective than measured. At an altitude of 10,700 m and flight speed of 0.8 M, the predicted increase in <NR> from the resonator operation was 15 dB and the measured increase was 6 dB. The laboratory investigations described in this report were undertaken to further understand resonator performance, and to identify the reason(s) for the differences between predicted and the flight test results.

1.1 Flight Tests

The flight test evaluations of the acoustic enclosure were performed at LASC-Georgia. Some results are summarized in Ref. 8. In summary, the flight test analysis revealed three complications:

(1) The external and internal sidewall temperatures were higher than those assumed for the resonator design, thus, the resonator tuning frequency was higher than the design target frequency.
(2) Noise flanking of the enclosure treatment at the enclosure ends reduced the measured <NR> values.
(3) The measured <NR> with resonators active was lower than predicted at the tuning frequency and exhibited a broader than anticipated attenuation bandwidth.

1.2 Laboratory Tests

The flight tests with the acoustic enclosure installed in the aircraft were performed before there was an opportunity to evaluate the resonator-equipped enclosure in the laboratory. The laboratory tests described in the present document were performed to help clarify the understanding of resonator operation in the flight test configuration, and to answer questions raised concerning the flight test results.

The laboratory tests were performed in the Acoustics Laboratory of the Kelly Johnson Research and Development Center, Saugus, CA. The tests were performed in a nearly anechoic room using a Gulfstream II fuselage test section (similar to the PTA fuselage). Figure 2 is a photograph of the test section positioned within the semi-anechoic room.

The test room volume (781 m^3) was much larger than test section volume (16 m^3). The acoustic enclosure was installed within this fuselage section in a way similar to the flight test installation. The same thermal insulation was installed for both the flight and laboratory tests.

The acoustic excitation fields used in the laboratory were generated by an electro-pneumatic driver attached to an exponential horn. The tonal SPLs exciting the fuselage shell were adjusted to be similar to the flight test tonal SPLs in both distribution and level.

In this report, the results of a variety of laboratory tests are compared directly to the flight test results. Comparisons of data trends and magnitudes between flight and ground tests are good, especially when considering the large differences between the two environments. Some of the differences between the flight and laboratory tests were: cabin pressurization, partial fuselage section, different fuselage support, different acoustic source size, different source phasing on fuselage, different end conditions, and forward velocity effects on the sound field during flight. These effects were not treated in a quantitative manner in the analyses of the test results.

The remainder of this report is divided into the following sections:

SECTION 2 contains descriptions of the test methods, including: the acoustic source, the measurement equipment, the test chamber, and the acoustic signals.
SECTION 3 presents the results of the laboratory tests, including: the source signal, comparisons to flight data, and the effects of configuration modifications.
SECTION 4 summarizes the laboratory study.
APPENDIX A describes individual resonator tests.
APPENDIX B describes the peripheral vibration testing of resonators and panels, and tap testing of the enclosure frame, without and with the resonator-loaded trim panels.
APPENDIX C summarizes the laboratory thermal environment.

2.0 Test Methods

Acoustic and vibration tests were performed on the Gulfstream II fuselage test section. The test section contained the acoustic enclosure previously flight tested in the NASA Gulfstream II aircraft. Enclosure configurations identical to flight test configurations were re-tested in the Acoustics Laboratory under conditions closely duplicating those of the acoustic flight test program. Numerous tests were performed in order to identify and eliminate detrimental effects on resonator performance.

Figure 2 shows the fuselage test section which simulates the Gulfstream cabin just ahead of the wing leading edge. This is the cabin area where the enclosure was located during the flight tests. The enclosure was centered at fuselage station FS307 in the aircraft, close to the propeller plane at FS301. Aircraft windows were not provided with the fuselage test section. Windows were simulated with an aluminum skin and limp vinyl septa. Four simulated windows were constructed. Each window consisted of two weighted-vinyl septa, a 1 mm-thick aluminum plate, and an airspace. The measured TL of this treatment equalled or exceeded the measured TL of the metallic portion of the fuselage shell. Limp, weighted vinyl outer barriers were installed over the ends of the fuselage section. In this figure, the fuselage exterior microphones and cables can be seen on the left side of the fuselage. The large rolls of glass fiber insulation shown on the room surfaces are very effective sound absorbers. The room surface treatment was added to permit testing in a near-anechoic environment.

Acoustic excitation of the fuselage was provided by an air-driven acoustic driver and horn, which can be seen in Fig. 2. The acoustic driver was adjusted to simulate the propfan tonal noise radiated to the fuselage. This source was located in a plane such that the sound pressure distribution patterns exciting the fuselage shell closely duplicated the tone input patterns measured during cruise flight. Acoustic and vibration data were recorded with a digital computer. Thermal data were recorded with a strip chart recorder.

2.1 Acoustic Source

The laboratory acoustic fields used to excite the fuselage shell were generated by an electro-pneumatic driver (Ling EPT-94A) attached to an exponential horn (Emilar EH-330). The drive and monitoring systems for generating the acoustic signals are shown schematically in Fig. 3. The electrical signal was generated with either the Allison white noise generator or with the HP waveform synthesizer. The signal was then shaped with the GR filter/equalizer and was band-limited by the Ithaco filter before being fed into the amplification system. Power, voltage, and current inputs to the driver were monitored in the control room. In order to generate the desired acoustic pressures, the Ling EPT-94A modulated the 30 psi compressed air supply according to the electrical signal input. The acoustic loading was monitored at a fuselage reference microphone (M323) location, which was located 1.6 m from the bottom of the fuselage and 0.69 m behind the simulated propeller plane. A typical acoustic spectrum measured by this fuselage reference microphone is shown in Fig. 4. This spectrum was generated by a sawtooth electrical input signal from the HP3325A synthesizer.

A broadband acoustic source was used during portions of the testing. The source signal was obtained from the white noise signal generator. As indicated in Fig. 5, most of the energy of the broadband signal was between 180 and 850 Hz and the overall level was 138 dB.

Figure 6 shows the excitation spectrum variation envelope of the spatially averaged sound pressure level (<SPL>) data measured on the fuselage for all laboratory testing with broadband noise. When normalized values were calculated, a fuselage <SPL> of 120 dB was utilized at each frequency, since this level was similar to the input <SPL> near the resonator tuning frequency. Normalized levels were calculated with the following equation:

$$\text{Normalized Level} = \text{Measured Level} - \text{Fuselage <SPL>} + 120 \text{ dB}.$$

For example, if the measured cabin <SPL> was 90 dB and the measured fuselage <SPL> was 118 dB, then the normalized cabin <SPL> would be 90 - 118 + 120 = 92 dB. This normalization must be calculated at each frequency in the spectrum.

The broadband signal was limited at low frequencies by the characteristics of the horn and driver combination. At frequencies above 800 Hz the 1/3 octave band filter outputs of the noise generating system were turned off, thus reducing the energy input at the higher frequencies.

2.2 Acoustic Measurement

Twenty-nine channels of data were digitized in a Masscomp computer. The Masscomp computer was used to simultaneously capture and average 16 channels of data at a time. A block diagram of the complete measurement and monitoring system is shown in Fig. 7. Two fuselage microphones and one cabin microphone were used as reference channels for each bank of 16 channels recorded. The incoming data were monitored with the SD 375 analyzer, B&K 2032 analyzer, Scanscope 1810, HP 1205B oscilloscope, and the Masscomp computer. Two 16 channel banks were switched via a patch panel and the changeover was rapid. The digitization rate of the Masscomp was 5 Khz for each channel. The 1024 point FFT data were recorded from 0 through 2000 Hz (frequency spacing 1.953 Hz). The data were backed up on magnetic tape and sent to a MicroVAX II for analysis and plotting.

SPL measurements were made near (12 mm) the fuselage exterior surface, between the fuselage and enclosure walls, under the enclosure floor, inside selected Helmholtz resonators, and in the enclosure cabin. The tonal SPLs measured on the fuselage shell were similar to the flight test SPLs. The external sound field was initially measured at 16 positions to define the sound field on the fuselage. The mounting of a typical 1/2 inch microphone (B&K 4134) on the fuselage is shown in Fig. 8. The positions of the 16 microphones are indicated in Fig. 9, as viewed from the source side of the fuselage. These positions correspond to the external microphone locations used during the flight tests, except that four more locations were used in flight (shown by the "**X**" symbols in Fig. 9). After the sound field was adjusted to approximate the flight acoustic environment, four microphone locations (M303, M304, M323, and M324) were used to characterize the

field. After the initial sound field was set-up, it remained constant and these four microphones were sufficient to monitor the input sound field throughout the tests. The SPL difference between the average of the 16 and the 4 microphones was 4.2 dB in the frequency region near the fundamental propfan tone. Figure 10 shows the SPL differences from 150 through 500 Hz. This 4.2 dB correction was applied to all the data which used the spatially averaged SPL of the four fuselage microphones. During the flight tests there were 20 microphones on the outside of the fuselage, used for input level characterization and averaging.

Four microphones (B&K 4165) were placed between the fuselage shell and the enclosure. Three of these microphones were located between the walls on the loudspeaker side and one microphone was centered under the floor of the enclosure. The microphone positions are shown in Fig. 11. Microphones WA01 and WA03 differ in position relative to the flight tests, where these two microphones were in the prop plane above and below WA02. In order to detect noise flanking effects around the ends of the enclosure, these microphones were repositioned for the laboratory tests.

Fourteen microphones (B&K 4165) were placed inside the cabin. Their locations are shown in Fig. 12, as viewed from the source side. The laboratory microphones were in the same positions as for the flight test, but there were fewer microphones (14 versus 24). For specific resonator tests, two of these microphones were replaced with probe microphones.

2.3 Test Room Description and Absorption Characteristics

The room in which the fuselage was tested is shown in Fig. 2 and has inner dimensions of 16.2 x 7.9 x 6.1 m (53 x 26 x 20 ft). Acoustical decay characteristics of the room were measured in 1/3 octave bands from 100 through 1000 Hz. Decay times were measured at two positions. One position was at fuselage microphone M323 and the other position was 2.4 m above the floor and 2 m from the aft end of the fuselage. Five measurements were taken at each position and in each 1/3 octave band. Measured decay times, standard deviations of decay times, and calculated average statistical absorption coefficients for all the room and fuselage surfaces are listed in Table I. Each average statistical absorption coefficient (α_{St}) was calculated by using the Norris-Eyring equation[9]

$$\alpha_{St} = 1 - e^{\left(0.161 \frac{V_a}{S_a T_{60}}\right)}$$

where V_a is the room volume minus the fuselage volume in m^3, S_a is the room surface area plus the fuselage exterior surface area in m^2, and T_{60} is the reverberation time in seconds. The reverberation time is the time required for a sound field to decay 60 dB after the sound source is abruptly terminated. The added absorption consisted of large rolls of glass fiber material and some large blocks of an acoustic reticulated foam (see

Fig. 2). The volumes and surface areas of these rolls were not included in the calculations.

2.4 Broadband & Tonal Tests

Tests were performed in the laboratory to simulate acoustic conditions experienced during the flight tests. The test numbers, test conditions, and the related flight numbers are listed in Table II. This table lists the laboratory test variables such as resonator operation, end treatment, cabin absorption, acoustic source, sidewall glass treatment, etc.

Typical tonal (235 Hz) and broadband laboratory signals measured on the laboratory fuselage section at M323 are shown in Figs. 4 and 5. Flight test spectra measured at location M323 (10,700 m MSL, 0.8 M, 225 Hz BPF) are shown in Fig. 13. Except for the third harmonic, which varied with flight conditions, the relative levels of the other harmonics at this microphone location were similar between the flight and laboratory tests. The dashed curve in Fig. 13 shows the acoustic environment at this location when the propfan was removed. At the BPF, the tone is 37 dB higher than without the propfan. This large difference shows the necessity for a high TL cabin structure.

2.5 Fuselage Vibration Test Methods

Vibration levels were measured at seven locations on the fuselage and enclosure during the laboratory tests. The accelerometer locations are listed in Table III. Their locations relative to the microphone locations may be seen by comparing these coordinates to the microphone location plots of Figs. 9, 11, and 12. Accelerometers AG02 and AG01 were used to measure the vibrations of a typical trim panel and of a resonator mounted on the panel, respectively. This resonator was located in the area of the highest exterior sound pressure level. The difference between the measured levels indicated some isolation of the resonator from the panel by its "Velcro"* mounting tabs. Accelerometers AG03 and AG04 were used to measure the vertical responses of the fuselage floor and the enclosure floor, respectively. These accelerometers were placed on each side of an aft end floor vibration mount. The vibration level difference between these accelerometers indicates the isolation properties of the mount. Accelerometers AG05 through AG07 were used to measure the response of the fuselage skin at three locations. AG06 was located in the area of highest sound pressure level, near microphone M323.

Additional vibration testing was performed in the laboratory. These tests, which included enclosure tap testing and steady state panel vibration testing, are described in Appendix B.

*Velcro is a registered trademark of Velcro USA Inc., Manchester, NH. Velcro and similar materials, manufactured by several companies, were used in this project.

3.0 Laboratory Test Results and Comparisons to Flight Test Results

Laboratory tests were performed in order to repeat flight test conditions, improve resonator operation, and define resonator limitations.

The main differences between the laboratory and flight test configurations were the lack of fuselage pressurization, a truncated fuselage test section, and superior annular sealing between the acoustic enclosure and the fuselage test section of the laboratory test configuration. Other differences between the ground and flight test configurations are the fuselage shell end conditions which result in differences in the longitudinal modal response of the fuselage shell for the two test cases. Since the sound transmission frequencies investigated were well below any coincidence effects that might have occurred during flight because of airflow on the fuselage, the forward flight effects were not considered a factor in comparing the ground and flight test results. As noted in Section 2.0, the laboratory fuselage contained four simulated windows.

SPL data were obtained in the cavities between the enclosure and fuselage section ends while flight-typical tones excited the fuselage at the simulated propfan plane. The cavity SPLs were quite similar to the SPLs measured at the ends of the acoustic enclosure during cruise flight.

In order to reduce the SPLs at the ends of the enclosure, and to reduce acoustic flanking through the annular space between the fuselage and the enclosure wall, an acoustic treatment was added at each end of the fuselage section. The acoustic treatment consisted primarily of a heavy, limp vinyl septum bolted to a heavy, rolled aluminum frame which terminated the shell at each end. A second layer was attached directly to the end walls of the enclosure. In addition, limp septa covered the annular airspace between the enclosure and the fuselage skin and floor. This latter treatment was the so-called end barrier treatment which acoustically isolated the sidewall and under-floor resonator spaces from the fuselage section end cavities. The overall length of the fuselage section was 3.49 m, and the overall length of the enclosure centered within the fuselage section was 3.05 m. This provides a cavity 0.22 m long at each end between the enclosure end wall surface and the end septum surface attached to the fuselage. Fifty resonators were placed in the cavity at each end of the enclosure to absorb the fundamental excitation tone within each end cavity.

After the end barriers and resonators were added and the flanking effects determined, the effectiveness of the sidewall resonators was determined. Three tests were performed: one with the sidewall resonators active, one with the sidewall resonators inactive (tape was placed over the nozzle openings), and one with the sidewall resonators removed. For all tests, the resonators under the enclosure floor were active, as they were during the flight tests.

After the above tests had been performed, the bagged insulation batts were removed from the sidewalls and resonators were re-installed on the sidewall trim panels. These materials were removed in order to test the hypothesis that the proximity of the insulation

to the nozzles could be affecting resonator performance. Tests were performed with the sidewall resonators active and then inactive.

In addition to the basic tests listed above, some peripheral tests were performed. These peripheral tests consisted of measuring the effects of cabin absorption, the influence of ambient SPL on the cabin <NR>, the performance characteristics of individual resonators (Appendix A), the vibration characteristics of the enclosure structures (Appendix B), and the effects of relocating the resonators to the cabin side of the trim panel rather than on the outer trim panel surface facing the fuselage sidewall.

3.1 Exterior Sound Field

The sound field on the fuselage skin during flight was measured at 20 positions. For the laboratory tests the sound field on the fuselage skin was measured at 16 microphone positions. Once the sound field had been established, four selected microphones were used to monitor the exterior sound field. The fuselage external sound field was adjusted for spectrum shape, amplitude, and spatial distribution to simulate the sound field detected during cruise flight. The laboratory sound fields for the fundamental (235 Hz) and second harmonic are shown in Fig. 14. Figure 15 shows the corresponding harmonic sound fields measured on the aircraft fuselage during a high altitude cruise flight. The sound field utilized in the laboratory had similar fundamental levels in the area of the highest SPL (147 dB at FS301 and FS328), but the laboratory sound field gradient was steeper away from this area than it was during the flight tests. For example, at FS354 and WL119, aft of the propeller plane, the flight test SPL, was 143.6 dB and the laboratory SPL was 139.9 dB.

The fuselage surface <SPL> values for the first three harmonics are shown in Fig. 16 for various simulated propfan rpm settings. Figure 17 compares <SPL> values for the fundamental measured at three different flight altitudes and also in the laboratory. Figures 18 and 19 show the frequency distributions at the second and third harmonics, respectively. Each figure shows that the laboratory fuselage <SPL>s closely represent the flight test fuselage <SPL>s. Figure 4 shows a spectrum of the input tones on the fuselage at position M323 for one of the laboratory tests and Fig. 13 shows a flight test spectrum measurement at the same position.

In addition to utilizing simulated propfan tones, a shaped broadband spectrum was used for exciting the fuselage shell. Figure 5 shows a typical broadband input spectrum measured at microphone position M323. The levels are much lower than for the tone tests. The overall level was about 10 dB lower. Because of the sound field distribution, the levels between the 16 and 4 microphone averages differed. Figure 20 shows the spectra of the 16 and 4 microphone broadband <SPL>s. In the frequency range spanning the propfan BPF fundamental tone there is a 4.2 dB difference (Fig. 10). As noted in Section 2.1, this value is utilized in the data normalizing process whenever a 4 microphone broadband <SPL> was used during the test analysis.

3.2 Flanking Effects

During the course of PTA flight testing with the acoustic enclosure installed in the cabin, it was determined that the <NR> of the enclosure could be improved by sealing the end annular gaps between the enclosure and the fuselage. This <NR> increase was most noticeable at the propfan fundamental tone frequency. Limp vinyl and tape were utilized to effect this annular gap sealing. During flight, the gap between the fuselage and enclosure floors was not sealed because of safety considerations in the event of cabin depressurization. High SPLs were measured in the cabin during flight forward and aft of the enclosure. SPLs in the 250 Hz octave band were read during cruise flight with an octave band analyzer in the main cabin regions just forward and aft of the enclosure, because high SPL values within the untreated cabin were thought to interfere with resonator effectiveness by admitting noise into the annular gap. The octave band SPLs ranged from 100 through 124 dB. The level in the 250 Hz octave band is controlled by the SPL of the propfan fundamental BPF within the cabin at the point of measurement. Figure 21 shows the 250 Hz octave band levels measured at the annular gaps and end surfaces of the enclosure during cruise flight.

Figure 22 shows the effect of installing the annular gap seals on the fundamental tone <NR> during the flight tests. A significant increase in <NR> was obtained at all fundamental BPFs with the barriers installed. This noise entered the fuselage sidewall regions of the enclosure through the peripheral annular gaps at each end of the enclosure. When partial limp vinyl barriers were installed, a 4 to 5 dB BPF <NR> increase was achieved over the frequency range of 200 to 235 Hz. The effect of resonators and the barrier seals will be discussed later.

Figures 23 and 24 show the effect of the end barriers on the second and third harmonic tone <NR> during flight. At these higher frequencies, the <NR> improvements with the annular seals (acoustic barriers) are less pronounced. Therefore, it may be concluded that the <NR> improvement with barriers becomes less important as the frequency increases.

Because of the pronounced barrier effect on the fundamental tone <NR> of the enclosure noted during the flight test program, the laboratory test program was directed at studying this effect under more controlled test conditions.

An objective of the laboratory testing was to ensure that all significant noise entering the fuselage section and the test enclosure was admitted via the sidewalls only. Prior to adding the end treatments to the fuselage test section and to the acoustic enclosure, the tone SPLs were measured at four locations near the annular gaps between the fuselage and enclosure ends. Figure 25 is a sketch showing the measurement locations and the tone SPLs obtained at the enclosure end annular gaps. Also shown are the tone SPLs of reference microphone M323 located on the fuselage near the noise source. Note that these tone SPLs are very similar to those obtained during cruise flight (Fig. 21). However, the SPLs at the enclosure ends were much lower during much of the laboratory testing because of the presence of the fuselage section end barriers.
In order to ensure that most of the generated noise entered the acoustic enclosure directly through the fuselage sidewall, annular vinyl seals and other acoustic treatments

were installed. These treatments are described in Section 3.0. Fifty resonators were attached to each end wall of the enclosure. Figure 26 is a photograph which shows vinyl and resonator installations on one end wall of the enclosure. Also, shown is the heavy 9.8 kg/m^2 (2.0 psf) weighted vinyl curtain which is bolted to each end of the fuselage test section.

Figure 27 compares the acoustic enclosure fundamental tone <NR> obtained without the various acoustic barriers (flanked) and end cavity resonators described above, to the <NR> with barriers and end cavity resonators installed. Note that as in flight (Fig. 22), the <NR> for the fundamental tone is generally greater with the end barriers installed. In comparisons with the flight data, however, the <NR> level differences during the laboratory tests were not as constant. In addition, the resonator peak response at 234 Hz is somewhat more obvious in Fig. 27 than it is in Fig. 22, both with barriers installed. The reasons for these differences are not known, but may arise out of the differences in the configurations between the flight and laboratory tests. The resonators were active in all cases described above. Note that for the flanked (no barrier) case in Fig. 27, that the <NR> average peak is at approximately 236 Hz. This slight upward shift in <NR> without barriers is difficult to explain. Also note, the double peaks occurring at about 235 and 243 Hz, for the case with barriers installed.

Figures 28 and 29 compare the <NR>s of the second and third harmonic simulated propfan tones with and without barriers installed. The <NR> variations are unrelated to resonator operation since the resonators were tuned only to the fundamental tone frequency. Figure 28 shows a localized <NR> difference of about 5 dB centered near 470 Hz between the flanked and unflanked (barriers installed) cases. The highest <NR> was obtained for the flanked condition. This could be attributed to a standing wave condition set up in the sidewall and floor resonator cavities by the barriers. Figure 29 shows another <NR> difference occurring at the third harmonic tone frequencies from about 675 to 735 Hz. Note the seven dB higher <NR> near 675 Hz with barriers installed. In this case, the barriers generally improved the average <NR> of the third harmonic tone at the lower frequency range of the <NR> curve.

In addition to tonal excitation, broadband noise excitation of the fuselage shell was used to investigate the effect of flanking noise. The broadband excitation yields a better picture of how the enclosure functions over the complete frequency range. Typical broadband SPL spectra measured on the fuselage are shown in Figs. 5 and 6. Figure 30 shows a broadband noise excitation <NR> comparison from 150 to 500 Hz for cases with and without end sealing. The resonators were active and full cabin absorption was installed for these comparison tests. Note the higher <NR> (4 dB) at the resonator tuning frequency with the end sealing treatment in place. The <NR> improvement is less above the resonator tuning frequency than it is at or below the tuning frequency.

For the case with end barriers, a comparison of Figs. 27 and 30 near the resonator tuning frequency shows general agreement in the <NR> levels. For the case without barriers, the dual peaks observed between 225 and 240 Hz in Fig. 30 are not present in Fig. 27.

3.3 Sidewall Thermal Blanket Effects

Thermal insulation blankets contained in Kapton bags are used on the inside walls of the fuselage shell to assist in controlling the thermal environment within the passenger cabin. In addition, these glass fiber blankets act as high frequency sound absorptive barriers in the sidewall. Bagged glass fiber blankets, approximately two inches thick, were attached to the inner sidewalls and ceiling of the fuselage test section to duplicate the thermal insulation present within the sidewalls and ceiling of the PTA aircraft when the resonators and enclosure were evaluated during flight. The laboratory insulation blankets were the same ones used during flight testing.

The thermal blankets filled a large portion of the ceiling and sidewall annular cavity containing the Helmholtz resonators. The proximity of the blankets to the resonator nozzles can affect resonator performance. This proximity tends to broaden and lower the resonator response and to lower the resonance frequency (see Appendix A). For this reason, the hemispherical resonators utilized during the testing were designed and built with side nozzles slanted 45 degrees (see Appendix B), so as to position the nozzle entrances as far as possible from the thermal blankets.

Tests were run with the enclosure to determine the effect of this insulation on resonator performance. During these tests the vinyl end barriers remained in place. Tests were conducted with and without sidewall and ceiling insulation and with sidewall resonators active and inactive.

Figure 31 shows the effect of the presence of thermal insulation on the fundamental tone <NR> for the input frequency range from 225 through 245 Hz. Upon removal of the thermal insulation, the enclosure <NR> increased about 3 dB @ 235 Hz, the average resonator tuning frequency. A crossover occurs in the <NR> curves at 241 Hz. At 245 Hz the presence of insulation gives an <NR> improvement. The gap between the fuselage skin and the trim panel skin is 15.7 cm (6.2 inches). The resonator and the thermal blanket, theoretically, utilize 11.7 cm (4.6 inches) of volume depth within the sidewalls. This leaves a theoretical clearance of 4.0 cm (1.6 inches) between the resonator surfaces and the blanket surfaces. The 45° nozzle inclination increased the nozzle clearance to almost 5 cm. Blanket sag can eliminate most of this clearance. It was found that some Kapton bags sagged enough to touch the top of the resonators, thus reducing the actual nozzle clearance to less than 1.5 cm. The fuselage frames were also covered with 1.3 to 1.9 cm (1/2 to 3/4 inch) deep bagged insulation to duplicate the flight test installation. Some of this thin blanket material was positioned very close to some resonator nozzles.

Figures 32 and 33 show the effects of the presence of thermal blankets on enclosure <NR> at the second and third harmonics of simulated propfan tones. Figure 32 shows the effects of the thermal blanket removal on the second harmonic tone from 450 to 490 Hz. Two decibels of <NR> are lost at the lower end of the band; the loss is as much as 6 dB at frequencies above 470 Hz. Note that the best <NR> with thermal blankets is about 43 dB @ 490 Hz. In addition, note that this second harmonic maximum <NR> is less than the fundamental tone <NR>s shown in Fig. 31. With the thermal blankets, the maximum fundamental tone <NR> is about 47 dB, compared to 43 dB for the second harmonic,

even though the excitation tone is an octave higher in frequency. This is primarily due to resonator activity in the fundamental tone range of excitation frequencies.

Figure 33 shows the effects of the thermal blankets on the third harmonic tone from 675 to 735 Hz. With the thermal blankets, the <NR>s are now as high or higher (53 dB) than the <NR>s for the fundamental tone (47 dB). Note the large change in <NR> at the lower end of the tone excitation band when the thermal blankets are removed. A mid-band peak in <NR> occurs at about 700 Hz after the sidewall insulation is removed. The reason for this peak is not clear.

Again, broadband noise was used to investigate the effects of thermal blankets near resonator nozzles on resonator performance. Figure 34 shows an <NR> comparison from 150 to 500 Hz with and without thermal blankets on the sidewalls and ceiling of the fuselage shell. There is little <NR> difference at the resonator tuning peak near 235 Hz. The -3 dB bandwidth was reduced from 27 Hz to 22 Hz, both of which are larger than the tonal excitation frequency range. The difference seen with tone excitation is not exactly duplicated with the broadband excitation. At other frequencies, the <NR> is significantly reduced with thermal blanket removal.

In Fig. 34 the effect of the thermal insulation is more noticeable in the frequency ranges above and below the resonance frequency. This difference indicates that the resonator effect at resonance prevails over the absorption effect. In order to depict the effect of the sidewall insulation on the resonator function, the spatially averaged resonator insertion loss (<IL>) was calculated for each case. In Fig. 35 the <IL>s are plotted for the two cases. The values for each curve are calculated from $\langle IL \rangle = \langle NR \rangle_{active} - \langle NR \rangle_{inactive}$, where the subscripts denote the resonator operation. Note that the differences above and below the resonance frequency tend to average 0 dB. Essentially, the effects of the insulating materials are removed from the comparison; the inactive resonator <NR>s become the baseline comparisons. In Fig. 35 the effects of the resonators under the two conditions become obvious. With the insulation removal, the peak frequency was shifted from 225 to 236 Hz and the -3 dB bandwidth of the main peak was reduced from 34 to 20 Hz. At 236 Hz the <NR> difference increased from 7.5 to 11 dB. The minimum at 275 Hz appears to be a result of an interaction between the resonators and sidewall acoustical properties[3]. In the case where the insulation was installed, this minimum was attenuated by the absorptive properties of the sidewall insulation.

3.4 Enclosure Absorption Effects

The data shown in Figs. 31 through 35 were obtained with six 0.3x0.3x1.2 m (1x1x4 ft) Scott reticulated foam blocks distributed within the acoustic enclosure to simulate cabin absorption and to minimize internal reverberation effects. In addition, the two enclosure end walls were each covered with a 0.1 m thick glass fiber blanket in Kapton bags.

Figures 36 through 38 show the effects of the foam block absorption on enclosure <NR> for the first three simulated propfan tones. Note that the effect of the absorption is most noticeable at the fundamental frequency (Fig. 36), where the average difference is approximately 2 dB. The flight test data showed a difference of about 1.5 dB in this

frequency region (Ref. 8, Fig. 5). The average differences at the second (Fig. 37) and third (Fig. 38) harmonics in the laboratory were negligible, whereas in the flight tests the average differences were approximately 2 dB at the second harmonic and 3 dB at the third harmonic. The reason for these flight and laboratory test differences is not obvious, as the external configuration differences should not affect the sound field inside the enclosure.

3.5 Resonator Effects

The effectiveness of resonators attached to cabin trim panels in reducing cabin enclosure tone levels was demonstrated in the laboratory in a way similar to the flight test demonstrations.

Figure 39 shows typical first harmonic (fundamental) tone <NR>s for the fuselage/enclosure laboratory combination for three test configurations: 1) trim-panel resonators active; 2) trim-panel resonators inactive (nozzles taped); and 3) trim-panel resonators removed. With the trim panel resonators inactive (nozzles taped) the <NR> dropped significantly (7 dB). The highest fundamental tone <NR> of 47 dB was obtained with active trim panel resonators. With the resonators inactive the <NR> was 40 dB. Removing the resonators from the trim panels reduced the highest fundamental tone <NR> to 32 dB. This drop is attributed to trim panel weight reduction, panel stiffness reduction, and panel damping reduction - all being the result of resonator removal (see Appendix B). These tests were similar to the flight tests conducted in 1988 and reported in Ref. 8. Figure 40 contains the data from Fig. 1 of Ref. 8 and shows flight data similar to the laboratory data shown in Fig. 39.

The main differences between these two sets of data, other than ground-to-flight test variables, are:

1) for the laboratory ground tests the barriers or annular gap seals were in place,
2) due to the presence of the fuselage section end barriers, the noise fields on the ends of the acoustic enclosure were of lower levels than they were during cruise flight, and
3) during flight test the annular gaps were unsealed for the data curves shown in Fig. 40.

Partial annular gap seals were installed during the flight testing. Figure 22 shows the effects on <NR> of this sealing made during cruise flight. The Flight 71 data curve of Fig. 22 with barriers or annular seals is comparable to the top curve of Fig. 39 with barriers. Both show data with active trim panel resonators. Note that somewhat higher <NR>s were obtained during flight with the barrier configuration. Without barriers installed during flight, the <NR> was very close to that obtained in the laboratory with barriers installed. Cabin pressurization effects on the fuselage sidewall could account for somewhat higher <NR>s for similar barrier or annular seal configurations during the two test series. The soft, vinyl annular barriers were attached between the fuselage and enclosure frames. There is a small, but unlikely, possibility of a small mechanical vibration flanking effect, which may have affected the high TL case. The absorption within the enclosure and

sidewalls was identical for both the ground and flight test series.

All of the laboratory and flight <NR> data shown in Figs. 22 and 39 through 42 were obtained with thermal blankets in the proximity of the trim panel resonators. The damping effects of these thermal blankets on the resonator tuning response can account for reductions in resonator peak response and broadening of the resonator response curves, as seen in Fig. 35. Even with the thermal blanket removal, the 3 dB down bandwidth is still 20 Hz and, since the tone tests were made within this 20 Hz range, significant <NR> peaks or valleys were not observed. An advantage of a 20 Hz bandwidth is that moderate changes in the thermal environment or in the prop rotation speed will not significantly affect the <NR> of the treatment.

Note that in Fig. 22 the peak <NR> of the Flight 71 data is at 228 Hz and the -3 dB frequency is at 205 Hz. The calculated resonance frequency is 232 Hz @ 18° C. In the analogous laboratory situation, Fig. 34 shows the peak <NR> at 240 Hz (calculated resonance frequency 235 Hz @ 25°C) and the bandwidth is 29 Hz (lower limit 218 Hz). In considering the physical differences between the flight and laboratory tests, we conclude that the results of these tests are generally similar.

Figures 41 and 42 show the effects of deactivating and then removing the resonators from the trim panels on the <NR> at the second and third harmonics of simulated propfan blade passage frequencies. It is interesting to note that when the resonators were removed from the trim panels, the <NR> for both the second and third harmonic excitation tones increased significantly. In other words, the average levels within the enclosure dropped when the panels were lightened by removal of the resonators from the panels. This is opposite to the effect observed with the fundamental tone, where the <NR> dropped significantly with the removal of the resonators from the trim panels. Possibly, these reverse effects on <NR> for the second and third harmonic tones could be caused by enclosure or trim panel structural modal activity being affected by the resonator masses on the enclosure panels, or by the change of sidewall volume resulting from removing the resonators from this volume. (See Appendix B for a discussion of additional vibration measurements.)

Deactivating the resonators by taping over the nozzles did not significantly affect the <NR>s at the second and third harmonics, but there were some small level changes that might be accounted for by volume changes within the sidewall brought about by isolating the sidewall volume from the resonator volumes. Another explanation is that these data changes are within the range of the experimental error of the measurement systems. More testing would be needed to define the variations seen between the two lower curves of Fig. 41, which compare the <NR>s with resonators active and inactive, and to determine how the resonator volumes relate to the sidewall volumes between the trim panels and the fuselage skin.

A single test for resonator nonlinear behavior was performed at the resonator tuning frequency with active resonators in the fuselage. Nonlinear behavior of resonator operation is caused by the change in the nozzle flow resistance as a function of SPL at high SPLs. At low SPLs the nozzle flow resistance is independent of SPL, and this is

called the linear region.[3,10] Figure 43 shows that as the SPL on the fuselage increased the <NR> of the wall was slightly reduced. Because the measured effect is small, it may be caused by resonator nonlinear behavior, or by experimental error. This result needs to be explored in future resonator tests, which are more easily performed on a bench or in the flat panel TL facility. The nonlinearity effect may be reduced through a redesign of the nozzle (change diameter and length, or modify shape).

3.6 Fuselage/Enclosure Measurements with Random Noise Input

This section describes additional <NR> data obtained with random noise input. Noise reduction data were obtained with this random noise input spectra shown in Figs. 5 and 6. In each figure the test number (e.g. NAS117) is given for each condition. Test numbers are listed in Table II and may be used to compare data between figures.

Figure 44 shows the <NR>s of the fuselage and enclosure combination when the assembly was excited with random noise. The three curves represent the <NR>s of three configurations: active resonators, taped resonators, and sidewall resonators removed. For these configurations the end barriers, or annular seals, and other end seals were installed. The thermal blankets were also installed on the inside surfaces of the fuselage test section. This figure can be compared to similar laboratory data obtained with discrete tone excitation (Figs. 39, 41, and 42) and to the flight data with propfan tone excitation (Fig. 40). The resonators are effective in the frequency range from 200 through 250 Hz. The maximum difference between the active and inactive resonators is 9.5 dB @ 225 Hz. The average difference in <NR> levels between the tests of inactive and removed resonators shows the effect of the resonator mass and damping (see Appendix B) on the <NR> of the panel and, to a minor degree, the effect of the volume displacement on the <NR> of the airspace/panel combination.

The difference in <NR> levels between the active and the removed resonators tests show the total effect of the resonators installed on the trim panels. In this case, the positive effect occurs over the 150 Hz to 380 Hz frequency range. The maximum increase is 18 dB @ 243 Hz. The <NR> has been reduced by 8 dB @ 424 Hz. This reduction is below the frequency of the second harmonic and, for the present application, would not be significant.

Figure 45 shows a comparison of broadband <SPL>s measured on the fuselage exterior, within the wall cavity where the sidewall resonators are located, and within the enclosure. All end barriers were installed and the resonators were active. Figure 46 shows similar data obtained with taped (inactive) sidewall resonators. Figure 47 shows similar data with the panel resonators removed from the sidewall cavity between fuselage and the enclosure. In this last figure only 10 spectrum averages of the data were obtained, instead of the usual 100 averages. The <NR>s shown in Fig. 44 were obtained from the differences of the fuselage and cabin <SPL>s shown in Figs. 45 through 47. The fuselage input spectrum is essentially constant in the above three figures. The sidewall cavity and cabin spectra are affected substantially by resonator activity. When the resonators were removed there was minimal change in the sidewall cavity spectrum, but a large change in the cabin spectrum between 150 and 400 Hz. The conclusions are that the resonator

mass, volume, and damping have a marginal effect on the SPL between the walls, but have a large effect on the trim panel properties and the transmitted sound. The acoustical action of the resonator affects both sidewall cavity and cabin SPLs near the resonance frequency.

3.7 Sidewall Cavity Noise Measurements

The middle curves of Figs. 45 through 47 show the average sidewall cavity levels of three microphones located within the cabin sidewall nearest to the excitation noise source at water line (WL) 113 (Fig. 11). A central microphone (WA02) was located close to the vertical plane (simulated prop plane) of the noise source at FS301. In addition, microphones WA01 and WA03 were located at each end of the cavity near the enclosure end walls and at WL113. During the flight test program, sidewall cavity noise data were obtained with three microphones located in the prop plane but at three different water lines. The central microphone utilized during the laboratory testing was located at the same location as the central prop plane sidewall microphone used during the flight test program[8].

Figure 48 compares the normalized sidewall tonal SPLs measured with the central sidewall cavity microphone during the flight tests (MD3C, at three altitudes) and during the laboratory tests (WA02). The normalized sidewall cavity SPLs for the fundamental blade passage tone are similar. These data were obtained without annular seals or end barriers. Note the obvious cavity SPL minima near the resonator tuning frequency of 233 Hz. The minimum obtained at the 4600 meter cruise condition is particularly pronounced. At the two other cruise conditions the minima are not well defined. The resonator tuning had shifted upward because of the higher-than-predicted resonator ambient temperatures for these conditions.

Figure 49 shows the fundamental tone NR comparison for the same flight and laboratory test conditions. The central sidewall cavity microphone levels are similar for the high altitude cruise flight and laboratory test conditions. The fuselage <SPL> and central sidewall microphone SPL and NR values for the test points described in Figs. 48 and 49 are listed in the following table.

Altitude, m	370 (Lab)	4600	7600	10700
Frequency, Hz	233	234	233	234
Fuselage <SPL>, dB	141	138	144	139
Sidewall SPL, dB	104 (WA02)	93 (MD3C)	108 (MD3C)	104(MD3C)
Sidewall NR, dB	37	45	36	35

The fuselage sidewall BPF NR values obtained in the laboratory and during high altitude cruise flight are similar. The reason for the greater NR value obtained during low altitude cruise flight cannot be explained at this time.

3.8 Comparison of Under-Floor Sound Pressure Level Versus Sidewall Cavity Spatially Averaged Sound Pressure Level

A single microphone was located between the fuselage section floor and the enclosure floor at the center of the enclosure (FS300, WL71, BL0). The location is depicted in Fig. 11. The microphone was centered among the resonators located between floors. These resonators were active during all laboratory and flight test configurations.

Within the sidewall cavity three microphones were located at the noise source height (see Section 3.7 and Fig. 11). The SPLs of these three microphones were averaged, and are compared to the SPL of the central microphone located below the enclosure floor.

Figure 50 compares the normalized average sidewall and the under-floor SPL spectra with the sidewall resonators active. (The normalized SPL spectra of individual sidewall cavity microphones are discussed in Sections 3.7 and 3.10). Note the sharp minimum in the under-floor SPL at 238 Hz, near the resonator tuning frequency. The minimum is less-pronounced for the sidewall microphone averages, which indicates that the sidewall resonators did not respond as well as did the under-floor resonators. At other frequencies the sidewall <SPL> is similar to the average under-floor SPL.

A similar test was performed with inactive sidewall cavity resonators. The average sidewall to under-floor SPL comparison is shown in Fig. 51. The under-floor microphone normalized SPL is still about 72 dB at the resonator tuning frequency, but the sidewall cavity <SPL> increased from about 90 dB with active resonators to 97 dB with inactive resonators at the resonator tuning frequency. This is similar to the change in the cabin <SPL> for the same conditions (see Section 3.6).

Removing the resonators from the trim panels causes another <SPL> increase at the resonator tuning frequency. The sidewall normalized SPL increased 3 dB to about 100 dB by resonator removal. Figure 52 shows this 100 dB sidewall cavity <SPL> as well as the under-floor SPL. Note that the curves of Fig. 52 show more oscillations than the curves of the two previous figures. The latter curve represents averages of ten spectra whereas the curves of Figs. 50 and 51 represent averages of 100 spectra.

3.9 Comparison of Under-Floor Sound Pressure Level versus Enclosure Spatially Averaged Sound Pressure Level

Figure 53 compares the normalized under-floor SPL obtained with the single central under-floor microphone to the normalized <SPL> of 11 enclosure microphones when the fuselage section was excited with broadband noise. The sidewall cavity resonators were active for this test. The under-floor microphone SPL is typically about 25 dB higher than the enclosure <SPL>, except at the resonator tuning frequency where the levels are similar. A typical 25 dB <NR> (inactive resonators) is estimated for the enclosure alone since the under-floor microphone SPLs and the three sidewall microphone average SPLs are similar (ref. Fig. 50), except at the resonator tuning frequency where the SPL minimum is less apparent in the sidewall cavity, as explained above.

Figure 54 compares the normalized <SPL> within the enclosure with the under-floor normalized SPL measured with the single central microphone with sidewall resonators inactive. Note that at resonator tuning, the enclosure <SPL> has increased from 69 dB (Fig. 53) to 76 dB (Fig. 54) with sidewall cavity resonators inactive (taped).

Removing the resonators from the sidewall trim panels produces an even greater effect. At the under-floor resonator tuning frequency (238 Hz approx.), the enclosure normalized <SPL> increased from 76 dB (Fig. 54) to 87 dB (Fig. 55).

Although the under-floor resonators were active during each test, there appears to be little effect on the <SPL> in the enclosure from these resonators. The under-floor resonators were effective in reducing the under-floor SPL and essentially eliminated the flanking path of sound through the floor.

3.10 Effects of End Barriers and Sidewall Insulation on the Sidewall and Under-Floor Sound Pressure Levels

The flanking path between the fuselage skin and the enclosure trim panels at each end of the enclosure degraded the effectiveness of the enclosure treatments. The resonator effectiveness depends on its local environment and the elimination of flanking paths. Figures 56 through 58 show normalized SPLs at each of the 3 sidewall microphones for three cases:

1) with the barriers in place and without sidewall insulation,
2) with end barriers and sidewall insulation, and
3) without the end barriers but with sidewall insulation.

In all three cases the resonators were active. Figure 59 shows normalized SPLs at the below floor microphone for the same three cases.

Figures 56 through 58 show that the resonators tend to be more effective in the middle of the fuselage than in proximity to the ends of the fuselage. At the forward microphone (WA01, Fig. 56) the response spectra are affected significantly by the sidewall configuration variables. Note the SPL minima near the resonance frequency of 235 Hz. These SPL minima are centered at different frequencies depending on the presence of thermal blankets near the resonators, and on the presence of barriers at the enclosure ends. For example, with blankets removed, the SPL is 81 dB at the nominal resonator tuning frequency of 234 Hz. For the other two configurations (barriers and no barriers) with thermal blankets installed, the SPL minima at 83 and 85 dB are shifted to frequencies less than 234 Hz. For the case without end barriers, a second more pronounced dip to 80 dB occurs at 251 Hz, possibly caused by a change of end conditions of the sidewall cavity as a result of the absence of the barrier near the end microphone.

At the central microphone (WA02, Fig. 57) the SPL minima are lower and closer to the resonance frequency for all three configurations. The SPL minima of 80, 78, and 76 dB can be seen near 234 Hz, the nominal resonator tuning frequency. On the average, these

minima are lower than those seen at the end microphones WA01 and WA03 even though sidewall microphone WA02 is nearest to the noise source. Other sidewall cavity noise minima occur above and below 235 Hz, but these appear to be unrelated to resonator activity.

At the aft position (WA03, Fig. 58) the flanking effects are the most obvious. Without the barriers the minimum near the resonance frequency is 99 dB @ 231 Hz After the barriers are added the minimum drops to 94 dB @ 234 Hz. With the removal of the sidewall insulation the minimum becomes well defined and the SPL drops to 74 dB @ 236 Hz. At this microphone location, the presence of thermal insulation near the resonators appears to seriously degrade resonator effectiveness.

The data in the above figures indicate that the under-floor microphone response is only slightly affected by sidewall cavity changes. As noted in Sections 3.8 and 3.9, the SPL minima at resonator tuning are very pronounced under the floor. It should be pointed out that no thermal blankets were installed in the under-floor cavity, and that the sidewall cavities extend into the under-floor cavity. No barriers were installed between the floor cavity and the sidewall cavity to minimize sound transmission from cavity to cavity.

Because of its central location, the below-floor microphone is not greatly affected by the flanking sound around the ends of the fuselage. The data in Fig. 59 are for the same conditions as that in Figs. 56 through 58, and show some changes in the spectrum away from the resonance frequency. Near the resonance frequency there was a shift (from 236 to 240 Hz and from 66 to 73 dB) of the minimum SPL when the barriers were added. After the sidewall insulation removal, the minimum became 70 dB @ 238 Hz. The shift may result from the somewhat higher sidewall environmental temperature, which raises the tuning frequency.

3.11 Effects of Resonators Mounted Inside the Enclosure Cabin

For a number of tests the resonator trim panels were reversed and the sidewall resonators faced the cabin interior, instead of between the walls. Only broadband excitation was used for these tests. The end barriers were in place, the resonators under the floor were active, and the sidewall thermal insulation was in place. The <NR> was measured with and without absorptive foam blocks in the cabin. Figure 60 compares the <NR>s obtained across the fuselage and cabin wall with the inside-mounted resonators active and inactive. The absorptive foam blocks had been removed from the enclosure during these two tests. The fundamental tone <NR> increase with the active resonators is much higher (57 dB @ 236 Hz) and sharper than in the case where the resonators were placed between the walls (see Fig. 62).

In order to determine if the proximity of the microphones to the resonators was affecting the results, four microphones were placed on a horizontal line across the cabin and their signals were compared to the microphone signals at standard cabin locations. The four microphones were placed at mid-cabin, at 1 m above the floor, and at 0.41, 0.74, 1.22, and 1.63 m from the propfan side resonators. At the resonance frequency the range of NRs, between the fuselage external <SPL> and each individual standardly positioned

microphone, was from 47 through 65 dB. The NR range for the four mid-cabin microphones was from 54 through 58 dB. This latter range is similar to the overall <NR> shown in Figs. 60 and 61.

Figure 61 compares the <NR> with the resonators operating, with and without absorption in the cabin. Note that the <NR> at the resonance frequency remains constant for these two cases. Away from the resonance frequency the <NR> changes, much in the same manner as when the sidewall absorptive blankets were removed while the resonators were located between the walls. The large <NR> (57 dB) at resonance achieved with the resonators inside the enclosure is comparable to some of the large noise reductions achieved with double-wall panels in the 1.08 x 1.08 m panel test facility at Rye Canyon when resonators were mounted inside the panel assemblies.

Figure 62 compares the <NR> of the fuselage/enclosure combination with active resonators inside the sidewall to active resonators inside the enclosure. For each case, the absorptive foam blocks were installed within the enclosure and the sidewall thermal insulation was present.

The effect of resonator operation is more obvious for the case with the resonators inside the cabin enclosure. The <NR> peak at the resonator tuning frequency is 4 to 5 dB greater for the case with the resonators inside the enclosure. In addition, the response peak is much sharper than it is for the case with the resonators within the sidewall and close to the absorptive thermal blankets. Test results (see Appendix A) showed degradation of test panel <NR> when the in-wall resonator nozzles were within one to two nozzle diameters from the insulation blanket. When the resonators were tested inside the enclosure, the resonator nozzles were located six inches or more from the nearest absorptive foam blocks. Only a small percentage of the nozzles were close to the blocks, which displaced but a small amount of the free air volume within the enclosure.

The off-peak <NR> levels of Fig. 62 show moderate <NR> variations between the two test configurations. The <NR> levels for the higher propeller harmonics are expected to be similar for these two configurations.

When comparing the resonator operation inside the sidewall cavity versus inside the cabin, it is not obvious which is the preferred design approach. Some investigators have theorized that resonators positioned within the sidewalls with nozzles facing the fuselage skin act as "anti-noise" or passive phase canceling devices which cancel the plane radiated waves radiated by the fuselage skin. Others theorize that the sidewall cavity contains a diffuse sound field consisting of plane radial waves mixed with a multitude of cross modes, and the "anti-noise" function is merely an absorption function much like that which occurs when the resonators are installed within the cabin.

There are pros and cons for both resonator configurations and the choice of which to use in attenuating high-level propeller tones within cabins would depend, in part, on the aircraft cabin configuration and which resonator installation would be most acceptable.

Resonators mounted inside the cabin could create problems with near-field sidewall noise.

Free-field scattering experiments with spherical Helmholtz resonators[11] show strong local sound pressure amplifications near the nozzles within one resonator diameter from the nozzle. Since the ears of cabin occupants sitting near the sidewalls could be close to sidewall-mounted resonators, local tone amplifications could occur that would make this configuration unacceptable, unless the proximity of the passenger's ear to resonator nozzle is avoided. Since sidewall resonators are not in a free-field, the sound pressure contours around such resonators would have to be determined in a laboratory environment before such a resonator installation concept is utilized.

3.12 Fuselage Sidewall and Trim Panel Vibrations and Sidewall Cavity <SPL>

The incident sound induces vibrations in the fuselage skin and stiffeners. Velocity levels were measured at three locations (AG05, AG06, and AG07) on the fuselage during the test program. Accelerometer locations are listed in Table III. Measurements made with and without the internal sidewall resonators operating showed minor changes in the fuselage vibrations. Figure 63 shows the three normalized accelerometer spectra with the resonators active. Figure 64 shows the three normalized accelerometer spectra with inactive resonators. The velocity levels shown in Figs. 63 and 64 are similar for this small data sampling. The minima at 227 Hz, well below the 235 Hz resonance frequency, is likely a result of fuselage shell modal activity unrelated to resonator operation.

Figures 65 through 67 compare sidewall cavity <SPL>s (3 microphones) to spatially averaged fuselage sidewall vibrations (3 vibration transducers) when the fuselage shell was excited with broadband noise. Figure 65 shows data obtained with active resonators, Fig. 66 with resonators inactive, and Fig. 67 with resonators removed. From this small data sampling, there is no obvious interaction between sidewall cavity noise levels and fuselage sidewall vibration levels.

A single accelerometer was mounted on a trim panel in the area of the highest fuselage SPL. The difference in the velocity levels of the fuselage and the trim panel is an indication of the NR provided by the wall. Figure 68 is a plot of the fuselage and trim panel velocity levels with the resonators active and without the end barriers present. There is a large difference between the levels near the resonance frequency (37 dB @ 233 Hz). Figure 69 is a plot of the same test after the end barriers had been added and the resonators inactivated. The trim panel vibration levels at the resonance frequency were reduced by 20 dB by resonators activity. The accelerometer data from the tests with the resonators removed was faulty and no results were obtained.

The difference between fuselage and trim panel velocity levels (velocity reduction) for the two cases (Figs. 68 and 69) are plotted in Fig. 70. The velocity reductions are modified by resonator activity over a much larger frequency range than just around the resonance frequency. Similar broadband effects (both advantageous and detrimental) were measured during the acoustic tests.

3.13 Vibration Isolation of the Enclosure

In order to structurally isolate the enclosure from the aircraft cabin floor, 21 vibration isolators were used. This isolation was used in an attempt to reduce the structure-borne vibration flanking path through the enclosure attachment points. In order to test the effectiveness of a vibration isolator, an accelerometer was placed on each side of a single aft isolator. The velocity level spectra plotted in Fig. 71 show, for the greater part of the spectrum, that there is a moderate isolation of the cabin. The primary exception is between 226 Hz and 260 Hz where the isolators amplify (up to 6 dB) the input signal to the enclosure floor. It is not known whether the other isolators operate in this fashion, but in the flight tests without the enclosure in the aircraft cabin, it was determined that the structure-borne vibrations were not major contributors to the cabin SPLs[5]. Laboratory tests were not performed with the vibration isolators inactivated.

4.0 Summary and Conclusions

The use of Helmholtz resonators integrated with the cabin trim of an aircraft cabin was demonstrated to be effective in reducing high SPL propeller blade passage tones within an aircraft cabin. Only the reduction of the propeller fundamental BPF tone was considered in the laboratory and flight tests. This tone dominates and controls cabin sound levels. Generally, low frequency tones are more readily admitted through the fuselage shell than the high frequency tones. However, fuselage shell panel resonances can significantly affect fuselage shell noise transmission.

Questions as to resonator operation, acoustic flanking paths, temperature effects, and sidewall insulation effects, which were raised in the flight test data analysis, were answered as a result of the laboratory tests. In addition, acoustic testing was performed with resonators inside the cabin and vibration testing was performed on the enclosure structure and on the frame/panel/resonator structure.

4.1 Resonators Mounted Inside the Cabin Trim

The use of Helmholtz resonators within the cabin sidewalls and under the floor appear to be a cost-effective approach to cabin quieting. Other methods of quieting, utilizing stiffness, mass, and damping, likely involve more treatment weight and construction costs. Other methods were not considered in this investigation. However, the test results lead to the conclusion that a resonator-equipped trim panel system design could be significantly lighter than some current trim designs for reducing propeller noise within a cabin. Laboratory tests show that new resonator shapes are feasible for significantly reducing the sidewall volume needed to contain such resonators. Resonator designs are also on hand that have the potential to attenuate two or more tones within a cabin.

4.2 Resonators Mounted Inside the Cabin

Laboratory tests were performed to show the effectiveness of resonators coupled to the cabin volume in attenuating simulated propeller propfan tones within a fuselage cabin. The <NR> obtained with this installation was more pronounced at the resonator tuning frequency, compared to the <NR>s obtained with the resonators coupled to the sidewall and ceiling cavities. The cabin <NR> at the resonator tuning frequency is 4 to 5 dB higher for the cabin-coupled resonators. In addition, the bandwidth at tuning is much narrower and better-defined.

From an acoustic point of view, locating the resonators inside the cabin seems preferable to installing them out of sight within the cabin sidewall. However, internal installation presents problems from a practical point of view. Protrusions from the sidewalls and ceiling might not be tolerated from a safety or aesthetic viewpoint. Exposed nozzles would be an invitation for storing debris or trash thereby rendering the resonators only partially effective. Protective screens over the nozzles could reduce resonator effectiveness by introducing damping within the resonators, but this may have an advantageous effect of increasing acoustic dissipation. The resonator nearfield noise could exceed the sidewall noise without resonators installed, thus increasing tone levels at the sidewall passenger

ear height. The nearfield sound pressure surrounding an active resonator was investigated by Ingard in the early 1950's[11]. The nearfield sound pressure surrounding an active resonator mounted on a wall should be investigated before such a resonator configuration is considered seriously. (It may be a more acceptable design for a ceiling treatment where nearfield considerations are not as important).

4.3 Isolated Enclosure Noise Attenuation

The acoustic enclosure utilized for this investigation consisted of a lightweight skeletal framework covered with aluminum "trim" panels, a heavy plywood floor, and two, heavy plywood double-wall end barriers to prevent noise from entering the enclosure through the end walls. This enclosure was attached to the fuselage floor and acoustically isolated through the use of vibration isolators attached to the cabin seat tracks. There were no other structural connections between the acoustic enclosure and the fuselage.

In the frequency range of interest, near the resonator tuning frequency, the total <NR> of the fuselage/enclosure combination was about 50 dB with active sidewall cavity resonators.

4.4 End Flanking Effects

The end flanking effects on enclosure <NR> were significant during a portion of the laboratory program and during all of the flight test program. These effects tended to obscure the resonator effectiveness in suppressing the propeller fundamental tone. End barriers installed to eliminate these effects tended to degrade resonator operation in the vicinity of the barriers. This was likely caused by longitudinal acoustic modes within the sidewall cavities bounded by the end barriers. These longitudinal modes seemed to interact with the resonator operation. The understanding of these effects could be the subject for further study and laboratory investigation.

4.5 Effect of Sidewall Thermal Insulation on Resonator Operation

The effect of placing sidewall thermal insulation blankets in the vicinity of resonator nozzles had been determined during tests conducted in the 1.08x1.08 m (4x4 ft) noise reduction test facility with flat square test panel assemblies. Test data (Appendix A) show that the presence of thermal blankets within 5 cm (2 inches) of the nozzle had negligible effect on resonator operation. The theoretical design clearance for the enclosure investigations was 4 cm (1.6 inches), as discussed in Section 3.3. Because of blanket sag, the resonators were close enough to some of the thermal blankets to cause a degradation in <NR>. Although the resonators utilized for the enclosure tests had 45° inclined nozzles, this inclination still did not always provide optimum nozzle clearance. Theoretically, the 45° nozzle inclination gave about a 5 cm (2 inch) nozzle to blanket separation gap for the enclosure tests, for the cases where the bag and insulation did not sag. In many cases, the clearance was less than 1.5 cm because the bags in which the blankets were wrapped tended to contact some of the resonator bodies.

Increased resonator-to-blanket gap, reduced profile (thickness) resonators, and thinner thermal blankets are all means of improving sidewall cavity resonator operation while maintaining sidewall trim thickness. These topics should be investigated to determine their effects on different resonator shapes and types.

4.6 Effect of Enclosure Absorption

The effect of enclosure absorption was determined to be minor, possibly because the enclosure microphones were all placed near to the radiating sidewall surfaces. Had the microphones been distributed across the cabin, the effect may have been more obvious. An <NR> improvement on the fundamental tone with the presence of absorptive foam within the cabin was obtained. For the second and third harmonic tones, the presence of foam blocks had negligible effect.

REFERENCES

1. B.H. Little, H.W. Bartel, N.N. Reddy, G. Swift, C.C. Withers, and P.C. Brown, "Propfan Test Assessment (PTA) Flight Test Report", NASA **CR**-182278 (April 1989).

2. B.H. Little, D.T. Poland, H.W. Bartel, C.C. Withers, and P.C. Brown, "Propfan Test Assessment (PTA) Final Project Report", NASA **CR**-185138 (July 1989).

3. R.A. Prydz, L.S. Wirt, H.L. Kuntz, and L.D. Pope, "Transmission Loss of a Multilayer Panel with Internal Tuned Helmholtz Resonators", **J. Acoust. Soc. Am. 87**:1597-1606 (1990).

4. R.A. Prydz, H.L. Kuntz, D.L. Morrow, and L.S. Wirt, Transmission Loss of Double Wall Panels Containing Helmholtz Resonators", **Proceedings of NOISE-CON 88**, 243-248, Purdue University, West Lafayette, IN (20-22 June 1988).

5. H.L. Kuntz and R.A. Prydz, "Interior Noise in the Untreated Gulfstream II Propfan Test Assessment Aircraft", **J. Aircraft 27**:647-652 (1990).

6. L.D. Pope, E.G. Wilby, and J.F. Wilby, "Propeller Aircraft Interior Noise, Part I: Analytical Model", **J. Sound Vibration 118**:449-467 (1987).

7. L.D. Pope, E.G. Wilby, and J.F. Wilby, "Propeller Aircraft Interior Noise, Part II: Scale-Model and Flight-Test Comparisons", **J. Sound Vibration 118**:469-493 (1987).

8. H.L. Kuntz, R.J. Gatineau, and R.A. Prydz, "Acoustic Transmission Loss Flight Test Results for an Aircraft Cabin Enclosure", **Proceedings of INTER-NOISE 89,** 211-216, Newport Beach, CA (4-6 December 1989).

9. T.F.W. Embleton, "Sound in Large Rooms", in Noise and Vibration Control, L.L Beranek, Ed., (McGraw-Hill, Inc., New York, 1971).

10. J. Wu and I. Rudnick, "Measurements of the Nonlinear Tuning Curves of Helmholtz Resonators", **J. Acoust. Soc. Am. 80**:1419-1422 (1986).

11. Uno Ingard, "The Near Field of a Helmholtz Resonator Exposed to a Plane Wave", **J. Acoust. Soc. Am. 25**:1062-1067 (1953).

APPENDIX A - Resonator Tests

A.1 Resonator Test Method

The method of testing individual resonator response is relatively simple and rapid. A photograph of the test setup with a single resonator is shown in Fig. A-1. A block diagram of the test system is shown in Fig. A-2. The measurements do not have to be made in a free field environment, although the further the reflecting surfaces are from the system, the better the accuracy. The requirement for a free field is avoided by performing the test with two fixed microphone probes. One probe is positioned about 7 cm from the broadband noise source and the second about 15 cm farther from the source than the first probe.

Two transfer functions are measured between the probe signals - the first measurement is without the resonator in position and the second is with the resonator in position, as shown in Fig. A-1. The transfer function without a resonator in place is saved and used as a system normalization transfer function. This normalization transfer function is used to eliminate the effects of the test bench and the room surface reflections on the test results. The introduction of the resonator volume into the noise field is not a significant factor on the test results, because the resonator dimensions are small compared to the wavelength at the frequency of interest.

A 1 mm hole is drilled in the resonator body opposite the resonator nozzle and, without moving either probe microphone, the #2 probe is inserted into the resonator volume. The resonator nozzle is pointed at the loudspeaker and duct seal is packed around the probe where it enters the resonator. The second transfer function is measured and the previously saved transfer function is used to normalize the second transfer function. The resonance frequency is determined by reading the frequency at which the transfer function magnitude has its main peak, or, in the case of a low amplification factor, when the phase equals 90 degrees. The amplification factor is the maximum value of the normalized transfer function amplitude near or at the resonance frequency.

A.2 Statistical Testing of Resonators

Thirty resonators were randomly selected from the 600 fuselage resonators and the resonance frequencies and amplification factors were measured. The temperature range during the test was from 21 through 24.5° C. Temperature corrections were made such that the normalized temperature was 23° C (the maximum frequency shift was 0.7 Hz). The frequency variation was from 232.4 through 235.5 Hz, the average 233.8 Hz, and the standard deviation was 0.767 Hz. Because of environmental factors, the temperature during a test on any realistic fuselage will have a variation of at least $\pm 5°$ C, which will lead to a resonance frequency variation of at least ± 2 Hz. This frequency broadening of the tuning range will have the effect of lowering the peak <NR>, but it will also lead to a broader frequency range for achieving a consistently high <NR>.

The amplification factor is almost unaffected by temperature. The average amplification factor was 36.2 dB and the standard deviation was 0.57 dB.

A.3 Environmental Interference of Resonators

In addition to temperature, the proximity of other resonators and sidewall insulation may affect the resonance frequency and amplification factor of the resonators. Two tests were made to determine these effects. The first test used two resonators attached next to each other on a panel and the resonance frequency of one resonator was tested relative to the proximity of the two resonator nozzles. The second test was to explore the effect of materials in the proximity of the nozzle. In this test a single resonator was used and boards with and without absorptive surfaces were brought into the region of the nozzle as the frequency and amplification factor were monitored.

The resonator proximity test results indicated that the nozzles of resonators should not face each other. As a baseline, a single resonator was measured to have a resonance frequency of 234 Hz. A second resonator was added such that the nozzles both faced in the same direction and were co-linear. The resonance frequency was re-measured to be at 234 Hz. The nozzle of the second resonator was rotated 90 degrees toward the reference resonator and the measured resonance shifted to 233.5 Hz. Next, the second resonator was rotated such that the nozzles faced each other (center-to-center nozzle separation was 4 cm) and the measured resonance shifted to 231 Hz. Three additional resonators were attached to the panel (none of the nozzles directly faced the reference nozzle) and the measured resonance frequency was 237 Hz. Finally, the panel was filled with an additional 11 resonators (16 total) and the measured resonance frequency was 235.5 Hz. The above test was performed in an open space and the scattering and diffraction are different than when the resonators are placed in an enclosure, such as the sidewall of an aircraft. The measurements that were performed in the fuselage sidewall and with 64 resonators in the 1.08 by 1.08 m TL facility did not show large shifts in the aggregate resonance frequency.

In order to determine the effect of surrounding materials on the resonance frequency and amplification factors, some resonators tuned to 170 Hz were tested during a separate resonator study. The basic results of these tests indicate that there is minimal interference from a surface (whether solid or porous) when the material is two times the nozzle diameter from the throat opening.

The proximity of materials to the nozzles, closer than two nozzle diameters, was determined to have an effect on the resonance frequency and the amplification factor of the resonators. When a surface approaches the nozzle from the side (parallel to the nozzle axis) the effects are noticeable at about one nozzle diameter from the nozzle edge. At this distance, the effect is negligible on the amplification factor and the frequency shift is less than -1 Hz. When the surface is perpendicular to the nozzle axis the effect is detrimental to the resonator function at a distance of about 1.5 times the nozzle diameter.

APPENDIX B - Vibration Tests

B.1 Steady State Resonator/Panel/Frame Assembly Vibration Response

In order to test the vibration response of a sample panel, resonator, and frame structure, a curved frame assembly segment was constructed. A single panel was attached to the assembly and the system was mounted on a vibration shaker table. The single panel held 16 resonators, each mounted on three Velcro-like tabs. The panel itself was attached to the frame assembly with Velcro-like strips around its perimeter. Swept sine vibration tests were run between 100 and 1000 Hz at several vibration levels of the shaker table. The tests were used to determine the effects of the three Velcro-like mounting tabs on the single panel dynamics. Several resonator configurations were tested. In addition, a single resonator was mounted on the shaker table with three Velcro-like tabs and tests were made to determine the response of a single resonator on its mount. Figure B-1 shows the locations of the accelerometers attached to the panel, resonators, and the shaker head. The shaker was a Ling 300B with a head expander, and the analysis/drive system was a Spectral Dynamics (SD) Model 1500, which consisted of an SD4158 Digital Sine Servo and an SD 400A System Control. In addition, an SD 380 was used for monitoring the four accelerometer outputs. The four accelerometers were Endevco 2226 and their output signals were conditioned with Endevco 2721A Charge Amplifiers.

The vibration response of the single resonator mounted on the shaker indicates that the Velcro-like tab mountings are nonlinear in behavior. The tabs act as nonlinear, softening springs. As the amplitude of the excitation is increased, the resonance frequency of the resonator/mounting system is lowered. This change with level is shown in Fig. B-2 where the excitation levels were varied from 0.75 through 5.0 g. At the lowest drive level (0.75 g) the resonance was near 460 Hz and at the highest drive level (5 g) the resonance was near 170 Hz. An important finding is that the Velcro-like tape mounting characteristics are not repeatable; each time a resonator is removed and replaced, the resonance frequency changes. These changes are illustrated in Fig. B-3 where the frequency responses of the resonator and its mounting are exhibited for two different installations. The measurements were made at the same drive level (1 g), but between tests the resonator was removed and replaced on the mounting tabs. The 225 Hz resonance shift leads to the conclusion that a panel with 16 resonators mounted on its surface will have 16 "tuned" damped vibration absorbers with a very large frequency spread. These absorbers are highly damped with amplification factors between 1.8 and 3. In addition, the direction of frequency sweep affects the shape of the resonance curve. A downward sweeping frequency generates a less defined peak than those shown in Fig. B-3, which contain data for an upward sweep frequency. Although the peak is not as well defined, the amplification factor is approximately the same in each direction. These combined effects tend to make the analysis of the panel dynamics difficult.

As is well known, the Velcro-like material is very tenacious. In order to determine if the resonators would be held onto the panels under a shock load, a single resonator was tested on the shaker. The holding power of the tabs to a half-sine shock (100 Hz) was tested up to 45 g (system limit) without the tabs releasing.

The panel/frame assembly was tested with 0, 1, 2, 4, 8, and 16 resonators installed. The effect of the resonators on the panel vibration is shown in Fig. B-4. The solid curve shows the panel response when 16 resonators are attached to the panel with tabs. The dashed curve shows the panel response with the resonators removed (the panel-side tabs were still in place). There was a large vibration increase at most frequencies when the resonators were removed. The resonator mass and damping effects are not as noticeable on the frame, as shown in Fig. B-5. The frame segment resonance near 250 Hz increased in amplitude and frequency when the resonators were removed, but, for the most part, the two responses are similar. This single panel model cannot be taken as an exact replica of the complex structure of the enclosure, but it is illustrative of the resonator mass and damping effects which may be seen in the enclosure data.

B.2 Vibration Tap Tests

Tap tests were performed at various locations on the enclosure panel supports and panels. Table IV contains a list of the test positions for the tests with and without the panels in place. Figure B-6 is a photograph of the cabin enclosure structure on its plywood shipping base. Only two resonator-equipped panels are installed on the frame. Figure B-7 is a photograph of the cabin interior with all the panels installed. These tests were used to determine the enclosure sidewall structural resonances in the region of the propfan tones. Before the enclosure was flown in the PTA Gulfstream II, tap tests were run on the structure without any resonators or panels. After the enclosure was installed in the laboratory fuselage section, tap tests were run with the panels and resonators in place. Tap test data were obtained through the use of a single channel spectrum analyzer (HP 3561A) and a moveable accelerometer (Endevco 2251). The panel (or framework) was lightly tapped with a plastic-tipped hammer which included a force transducer. The signal from the force transducer triggered the spectrum analyzer data capture. Changes in the input force were not taken into account. The relative spectrum shapes and frequency shifts were used to analyze the vibration response differences between the two test conditions.

Vibration tap tests were performed on the various structural components of the acoustic enclosure. The circular frames, longerons, floor beams, floor panels, end panels, and trim panels were tapped with the instrumented hammer to determine the frequencies at which these components responded to these transient excitations. A knowledge of the resonance frequencies existing in the structural components of the acoustic enclosure should be used in the design of enclosures or cabin trim configurations for the attenuation of propfan tonal harmonics.

The tight construction schedule for the enclosure did not allow time to optimize the tuning of the enclosure structural components for achieving maximum enclosure noise reduction at the propfan generated tone frequencies. However, prior to flight testing, tap testing was performed on the enclosure frame without the trim panels attached. Resonance activity was observed close to fundamental propfan blade passage frequency (190 to 240 Hz) on the circular frames. This activity was located at mid-span between the frame-to-longeron junction points. Figure B-8 shows typical responses at these mid-span locations to a single radial tap at mid-span. The spectral plots are linear acceleration responses to tap

excitation over the frequency band of zero to 500 Hz. Note the resonance activity in the propfan fundamental tone frequency band just below 250 Hz.

Sample radial vibration responses at the longeron mid-span locations between circular frames is shown in Fig. B-9. Note the strong resonance response near 285 Hz, well above the propfan fundamental tone band. Vibration responses of the frame-to-longeron junctions to tap excitations was very low near the fundamental tone BPFs as shown in Fig. B-10 for three different junctions. Vibration responses of the plywood double-wall end barriers and plywood floor panels were highly damped and these items were believed to be excellent barriers to noise transmission.

Figure B-6 shows the attachment of the acoustic enclosure to the plywood shipping base with the vibration isolators. The isolators were also used for installing the enclosure within the aircraft cabin. Note the very stiff framework construction which was designed along with its attachment mounts to withstand a forward crash load of nine g's. The frames, longerons, and floor beams are constructed of aluminum alloy 7075 hat sections all heat-treated to a T6 condition. These sections are all 38 mm (1.5 inches) deep, 1.3 mm (0.05 inch) thick, with 1.9 mm (0.75 inch) flanges, and have an overall flange width of 64 mm (2.50 inches). Except for the three trim panels shown attached to the framework with Velcro-like tape, this was the configuration of the enclosure framework during pre-flight tap testing. All trim panels were removed during this initial tap testing.

When the trim panels were attached to the enclosure framework, it became apparent that the panel response to tap excitation was essentially critically damped. The Velcro-like edge attachment plus cloth tape edge sealing contributed to this highly-damped trim panel vibration response. As discussed above, the use of Velcro-like tabs to secure the Helmholtz resonators to the trim panels also contributed to trim panel damping. The tabs can be seen in Fig. B-6 on the single trim panel without resonators attached. The acoustic enclosure was returned to the Kelly Johnson R&D Center in Saugus, California after the conclusion of the 1988 flight testing in Marietta, Georgia. It was then installed in a Gulfstream-II fuselage section for further resonator studies in the Center's Acoustics Laboratory. During the course of such testing, a second tap test investigation was performed inside the enclosure with the trim panels installed. These tests were performed on October 24 and 25, 1989. The same test equipment and procedures were utilized for both vibration tap tests.

Figures B-11 through B-14 are four typical panel vibration response plots to a central radial hammer tap at the center of each respective panel starting from a bottom panel to a top panel near the center of the enclosure. Figure B-11 is the bottom panel response and Fig. B-14 is the top panel response. Again, a linear acceleration response from 0 through 500 Hz is displayed. No attempt was made to normalize the acceleration response to the hammer force input, but the inputs were generally very similar. Note the breadth of the response peaks compared to the very sharp response peaks obtained on the framework without the trim panels attached (Figs. B-8 through B-10). Figures B-11 through B-13 show strong, broad peaks from 230 to 250 Hz corresponding closely to the propfan fundamental tone. This panel peak activity is detrimental to the panel's ability to block sound transmission into the enclosure at the fundamental tone frequency. This

broad peak response might include some frame activity which is masked by panel damping.

Figures B-15 and B-16 are frame mid-span radial vibration response plots to frame mid-span radial tapping. The frames support trim panels and the panel mass and damping effects on the frames affect frame response. These figures should be compared to Fig. B-8 which depicts frame radial mid-span response without panels. The panel effects on the frames effectively cancel frame modal activity near the propfan fundamental frequency input. Note that Figs. B-15 and B-16 show a spectral frequency response from zero to 1000 Hz while Fig. B-8 has a frequency response to 500 Hz.

Figures B-17 and B-18 are longeron mid-span radial vibration response plots to longeron mid-span radial tapping with the trim panels attached. The strong longeron response peak occurring at about 280 Hz is still there (compare to Fig. B-9), even with the trim panels attached to the longerons. The panel damping effect on the longeron vibration response is apparent from the changes in shape and amplitude of the longeron response curves with panels attached.

Tap testing of mockup panels and mockup panel support structure can be a good alternative to panel design calculations for optimizing panel noise reduction in aircraft cabins.

The above figures, which summarize the enclosure vibration responses to transient tap inputs, show that trim panel systems installed in aircraft cabins of propeller-driven aircraft should be designed so as to avoid panel resonances, which could degrade the noise isolation of such panels at the primary tone frequencies of propeller powerplants.

APPENDIX C - Thermal Data

The resonance frequency of a Helmholtz resonator depends on the square root of the absolute temperature. The resonators in this test program had been designed for flight tests in-wall cruise temperatures of 0° C. These low temperatures were never achieved. The flight test and laboratory temperatures were much higher and variable. In order to predict the resonance frequency, twenty-two thermocouples were installed on the fuselage and enclosure surfaces and within the various air spaces. The thermocouple locations are listed in Table V.

During the flight tests the range of sidewall temperatures at a single resonator was from 12° to 22° C. The computed resonance frequency range was from 230 to 234 Hz. Temperatures at other locations were not measured, but it is expected that the temperature variation was much larger than indicated at this single position. Therefore, the resonance frequency variation over a single test, and from test to test, is much larger than indicated.

The laboratory temperatures were quite steady over the duration of a single test. The temperature tended to be most consistent under the floor and between the walls. The cabin temperature and external temperatures tended to be higher and usually rose during a test. The largest and smallest ranges for all the temperatures measured at any one time were 3.1 and 1.4° C (5.5 and 2.5° F, respectively). The largest rise in temperature during a test was 1.1° C (2° F) and the smallest temperature rise during a test was -0.3° C (-0.5° F). The lowest resonator temperature measured was 22.5° C (72.5° F) and the highest was 28.9° C (84° F). For a specific resonator, the computed resonance frequency range was from 234 Hz through 237 Hz.

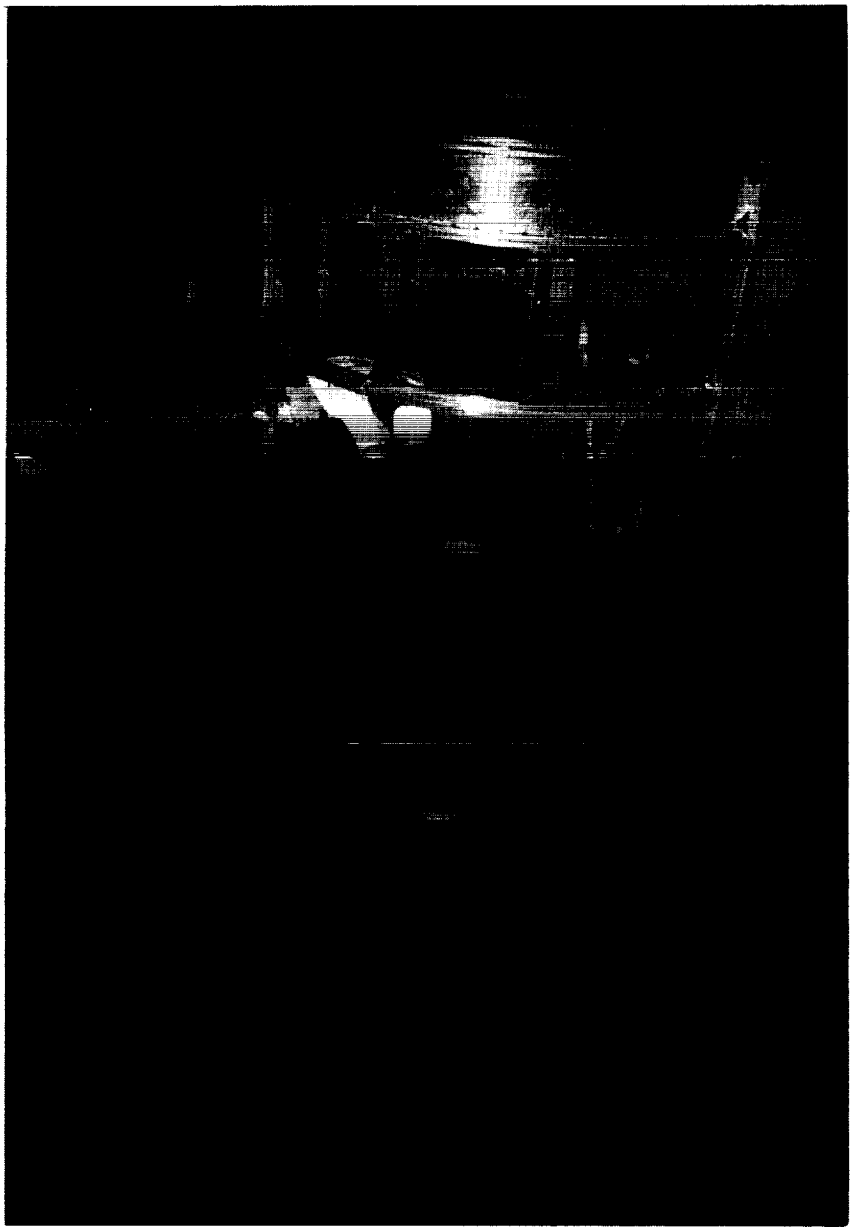

Figure 1: Photograph of the enclosure frame on the shipping platform (PTA aircraft in the background).

ORIGINAL PAGE
BLACK AND WHITE PHOTOGRAPH

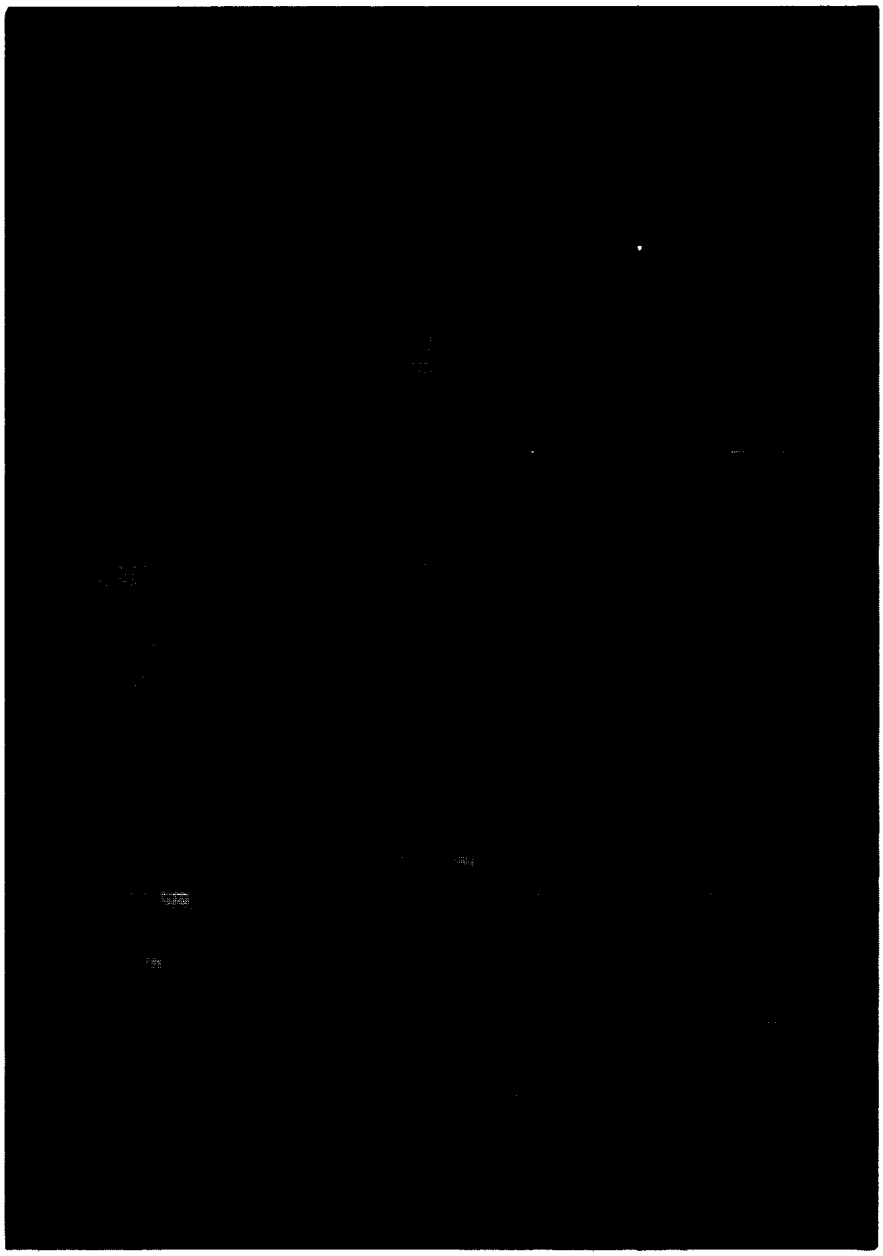

Figure 2: Photograph of the Acoustics Laboratory with the fuselage section and EPT-94 driver with horn.

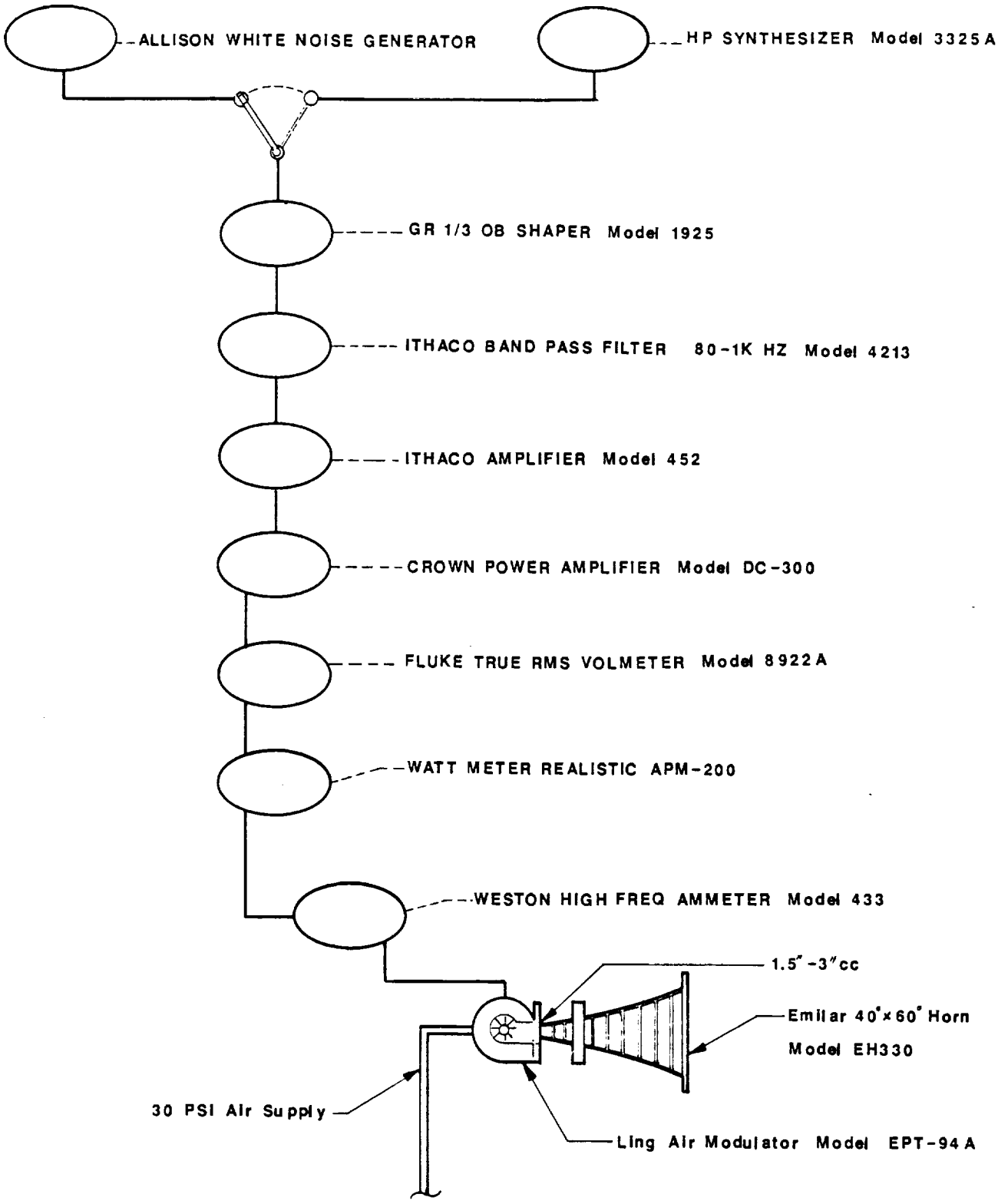

Figure 3: Acoustic source hardware and electronics for the fuselage tests.

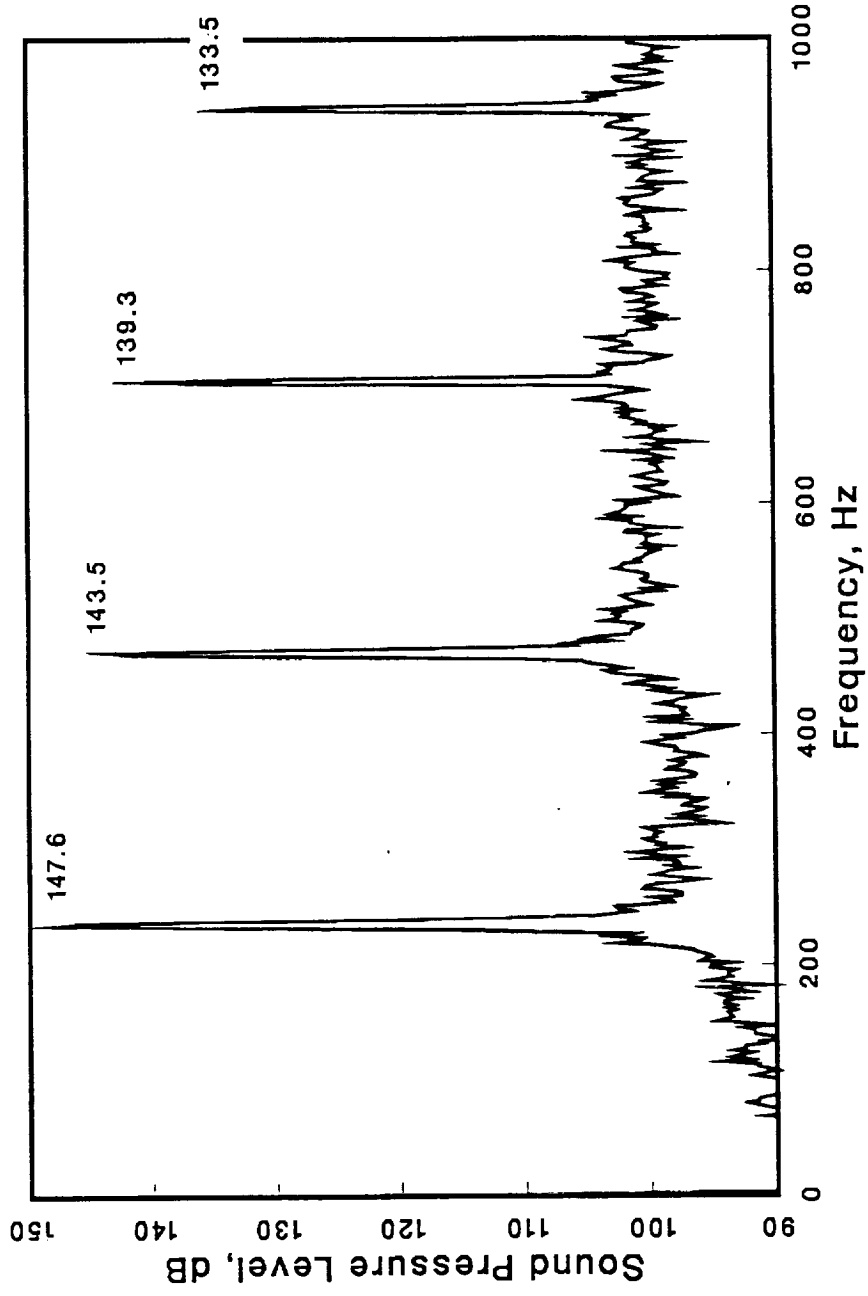

Figure 4: Typical laboratory input tone spectrum at a central, external microphone location.

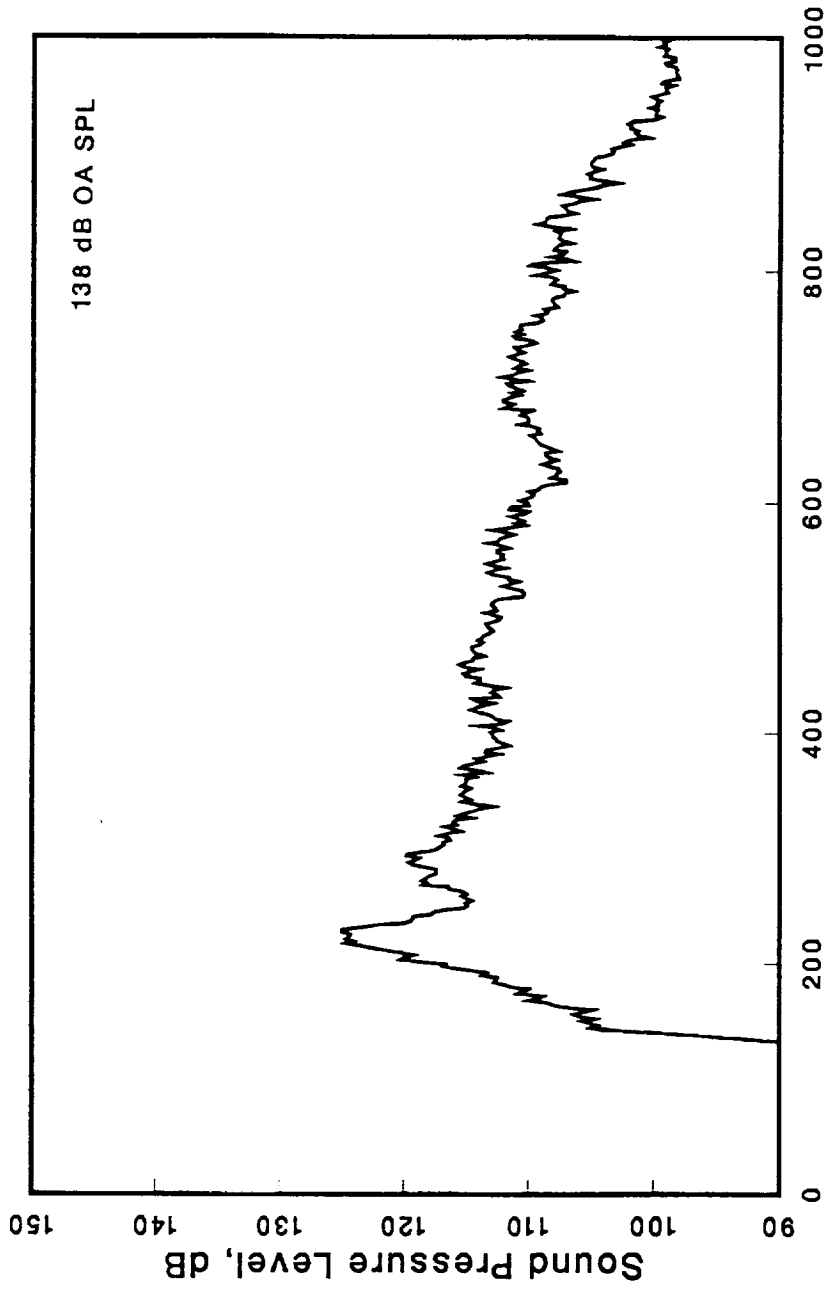

Figure 5: Typical laboratory random noise input spectrum at a central, external microphone location.

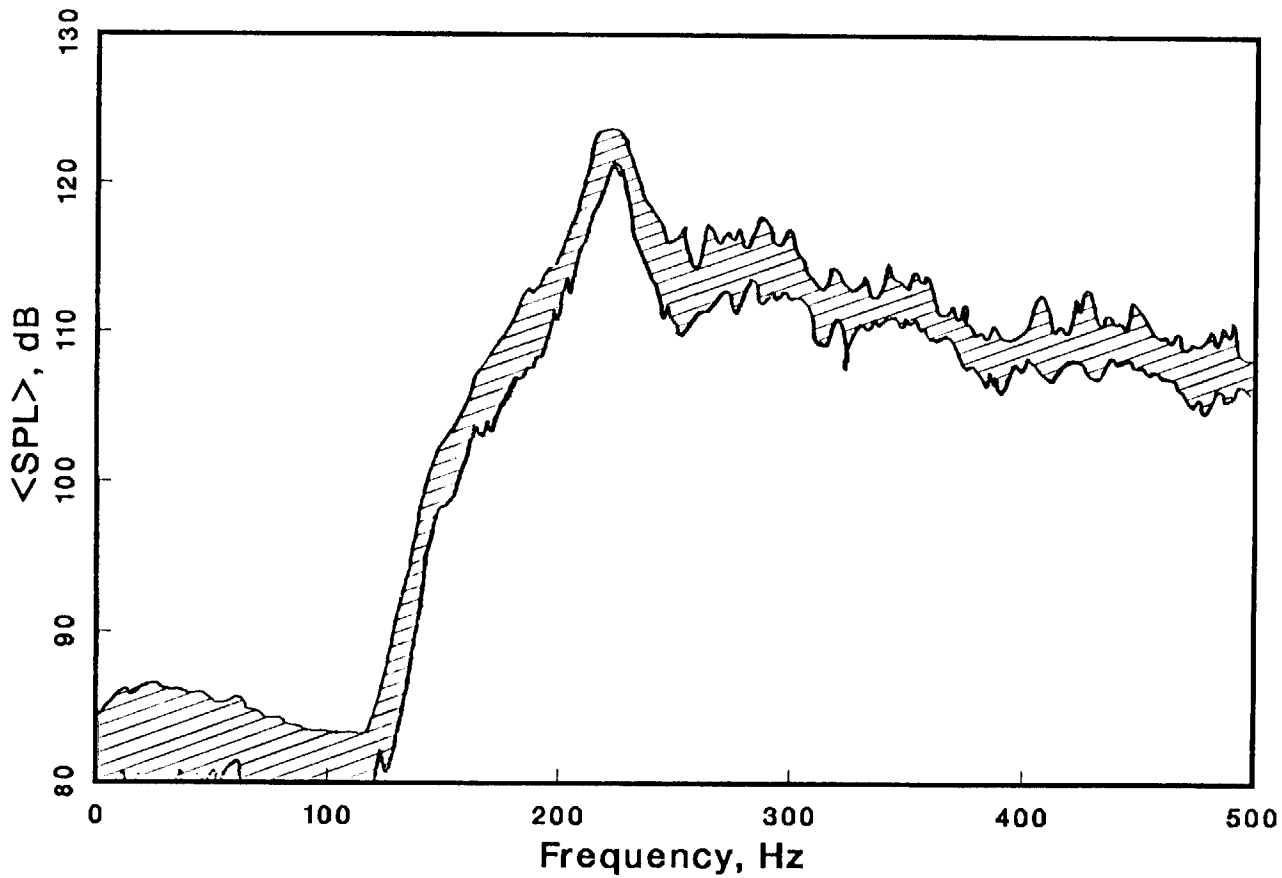

Figure 6: Sound pressure level spectrum variation for all random noise laboratory tests.

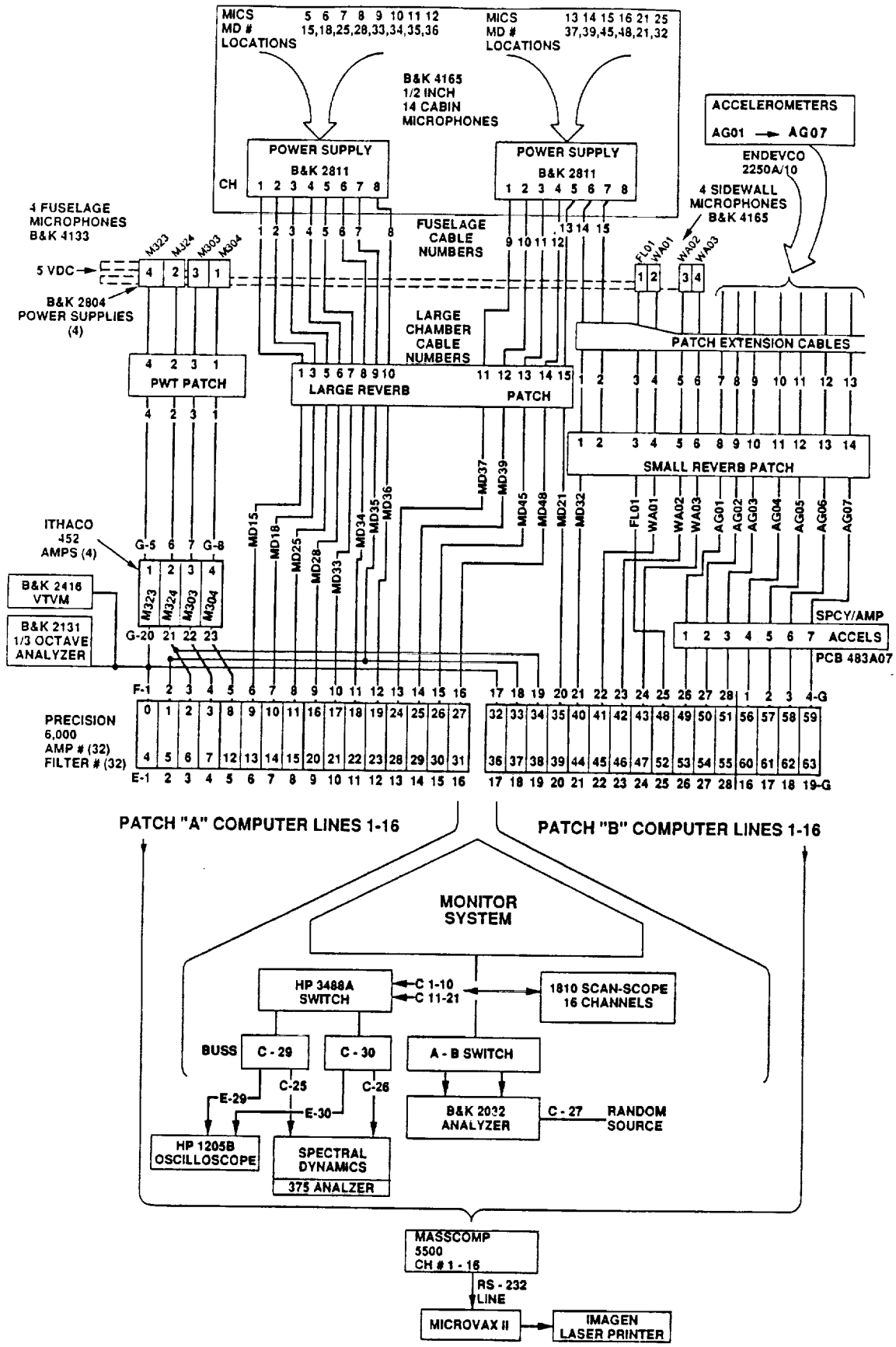

Figure 7: Data measuring and monitoring system block diagram.

RG0052.023
02-12-90

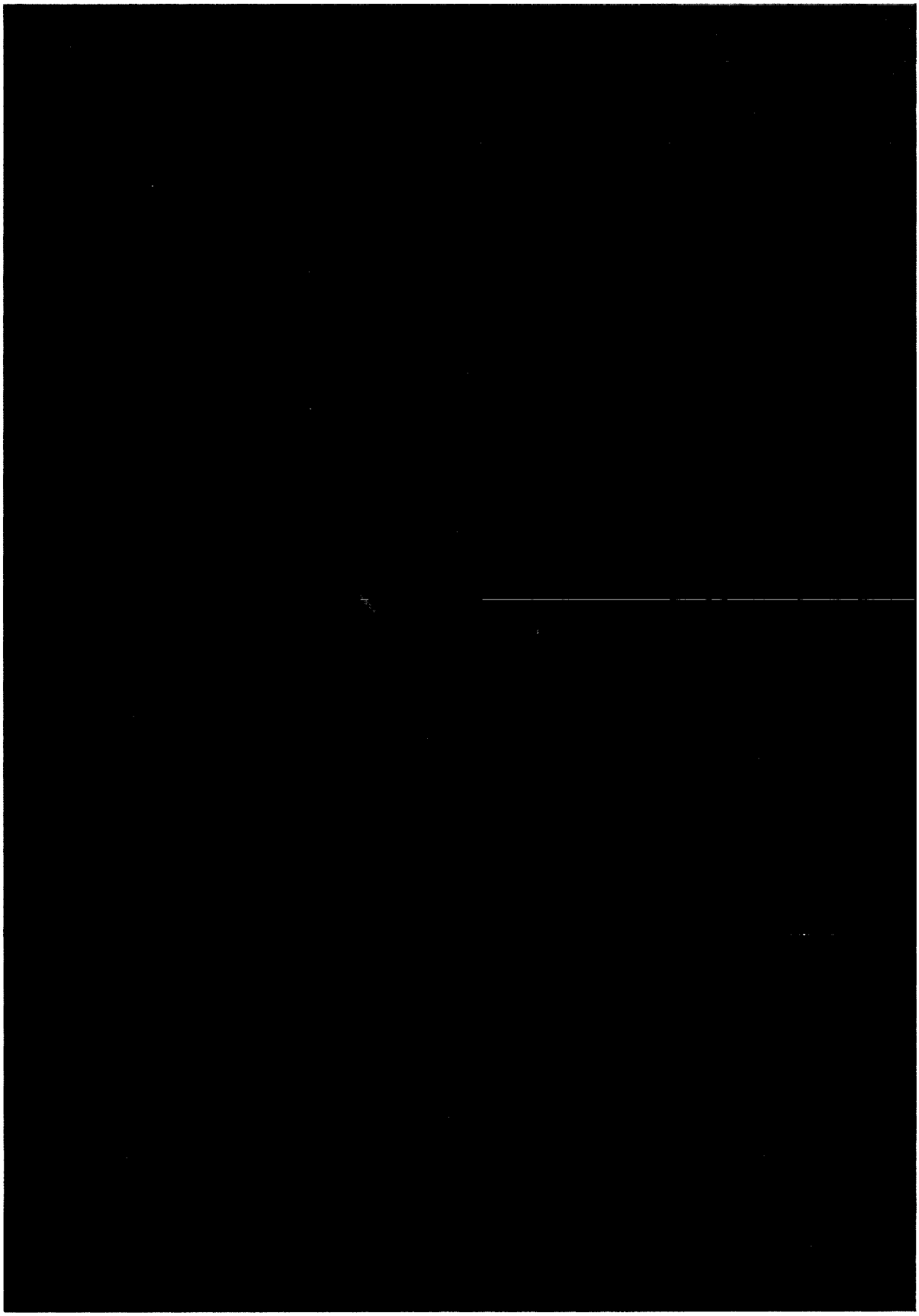

Figure 8: Mounting and placement of a typical external fuselage microphone in the laboratory.

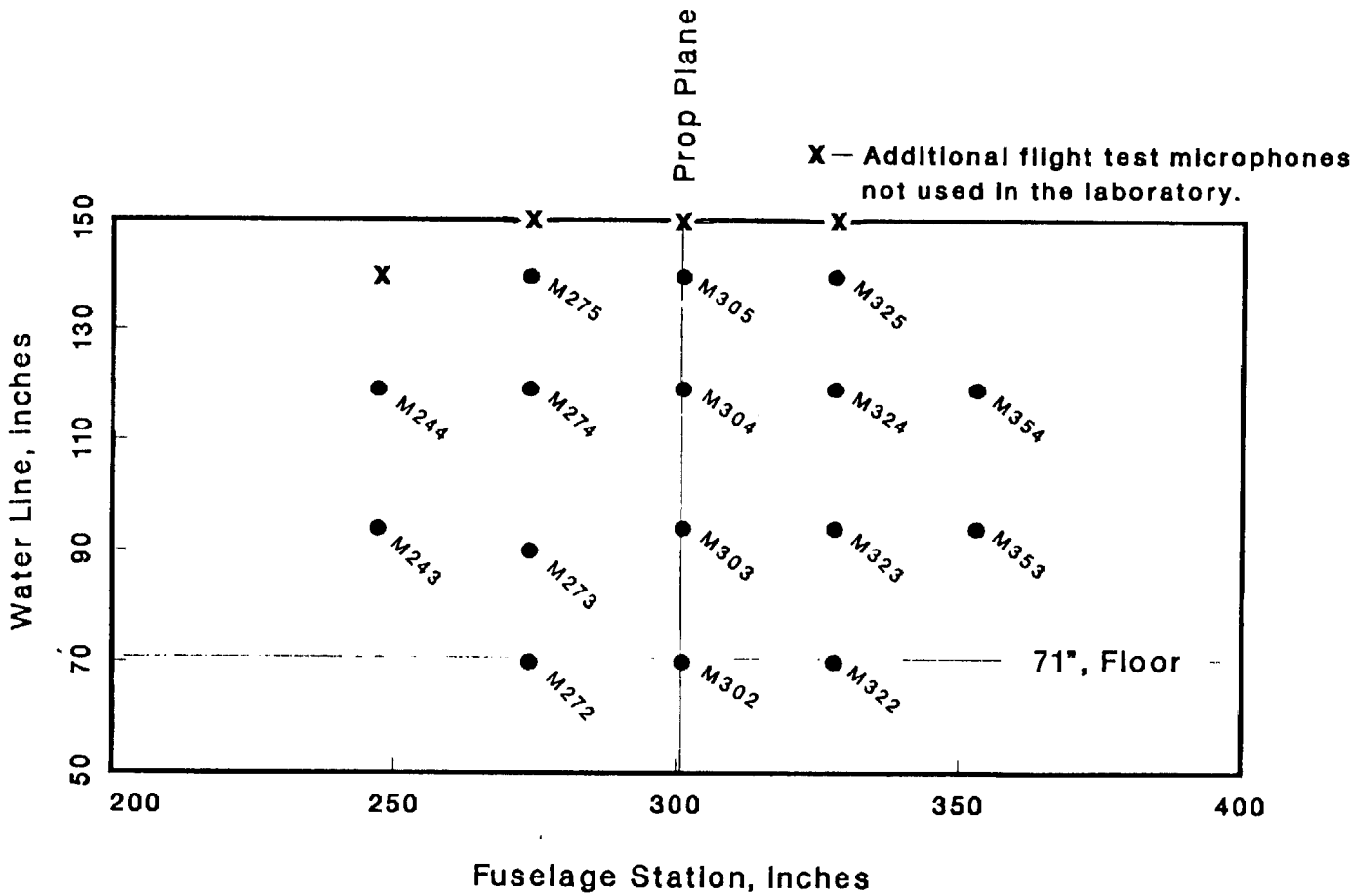

Figure 9: Microphone positions for laboratory measurement of the external sound field. (All microphones positioned 0.03 m from fuselage skin.)

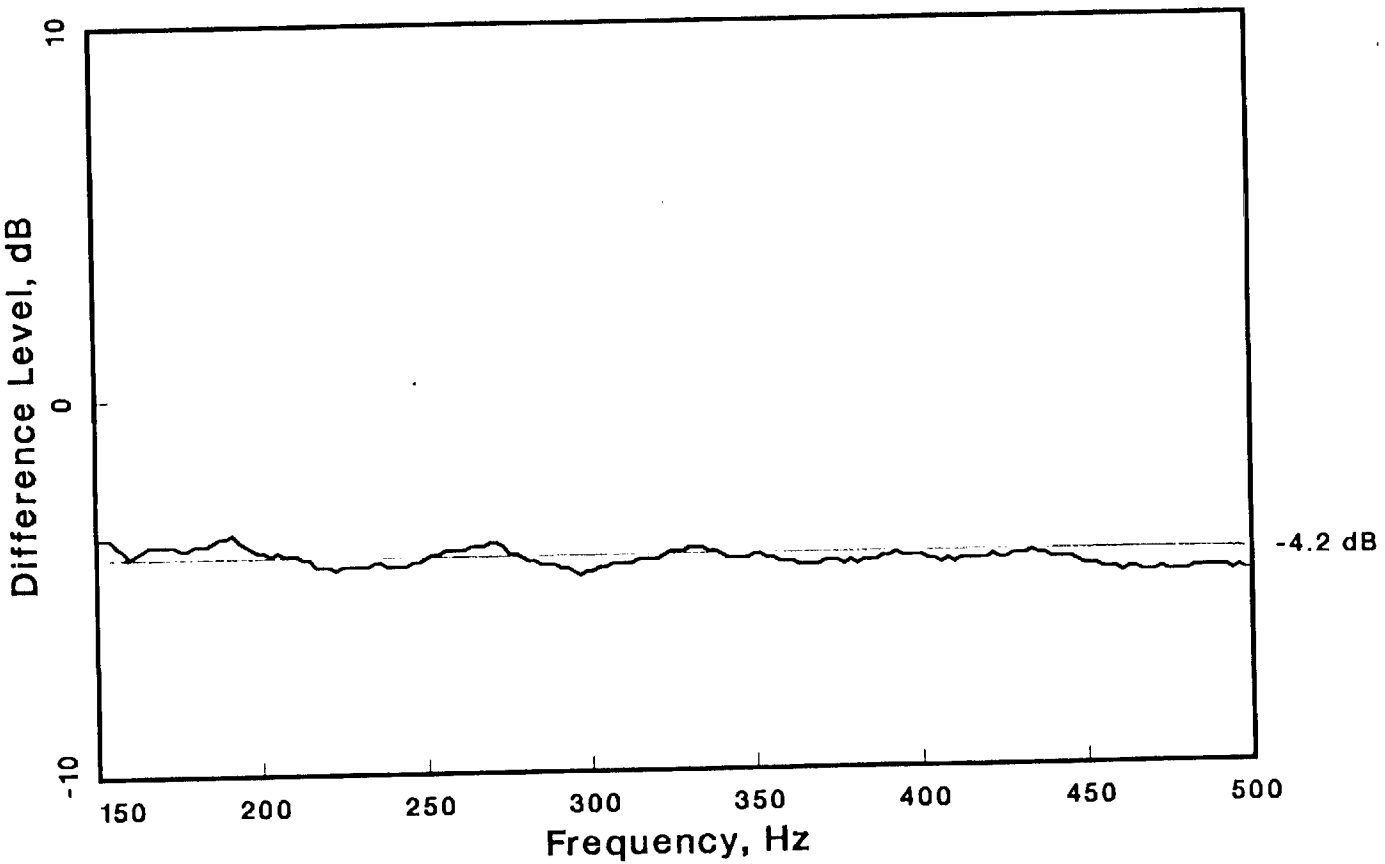

Figure 10: Difference between the average of 16 fuselage surface microphone signals and the average of 4 fuselage microphone (M303, M304, M323, & M324) signals.

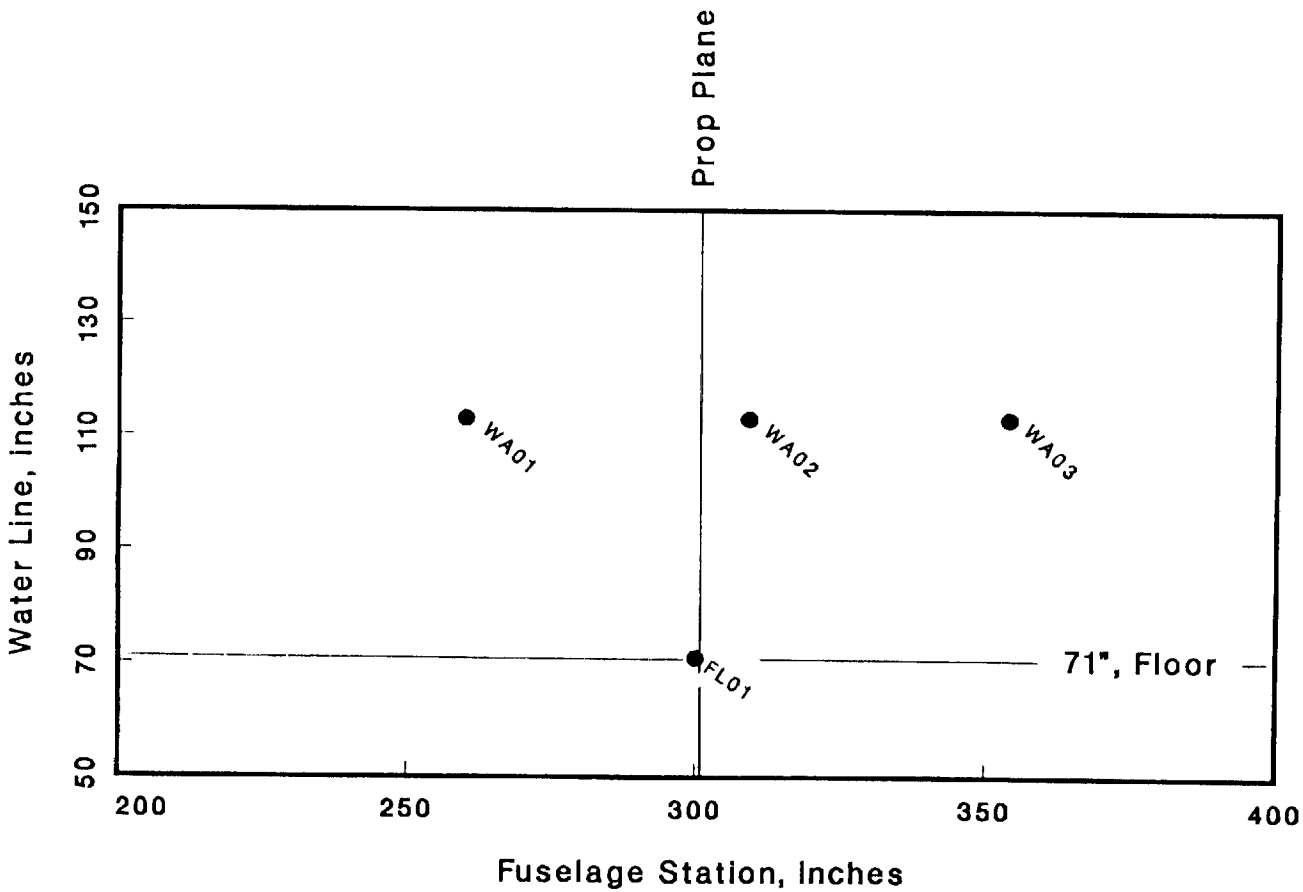

Figure 11: Microphone positions for laboratory measurement of the internal sidewall and underfloor sound fields.

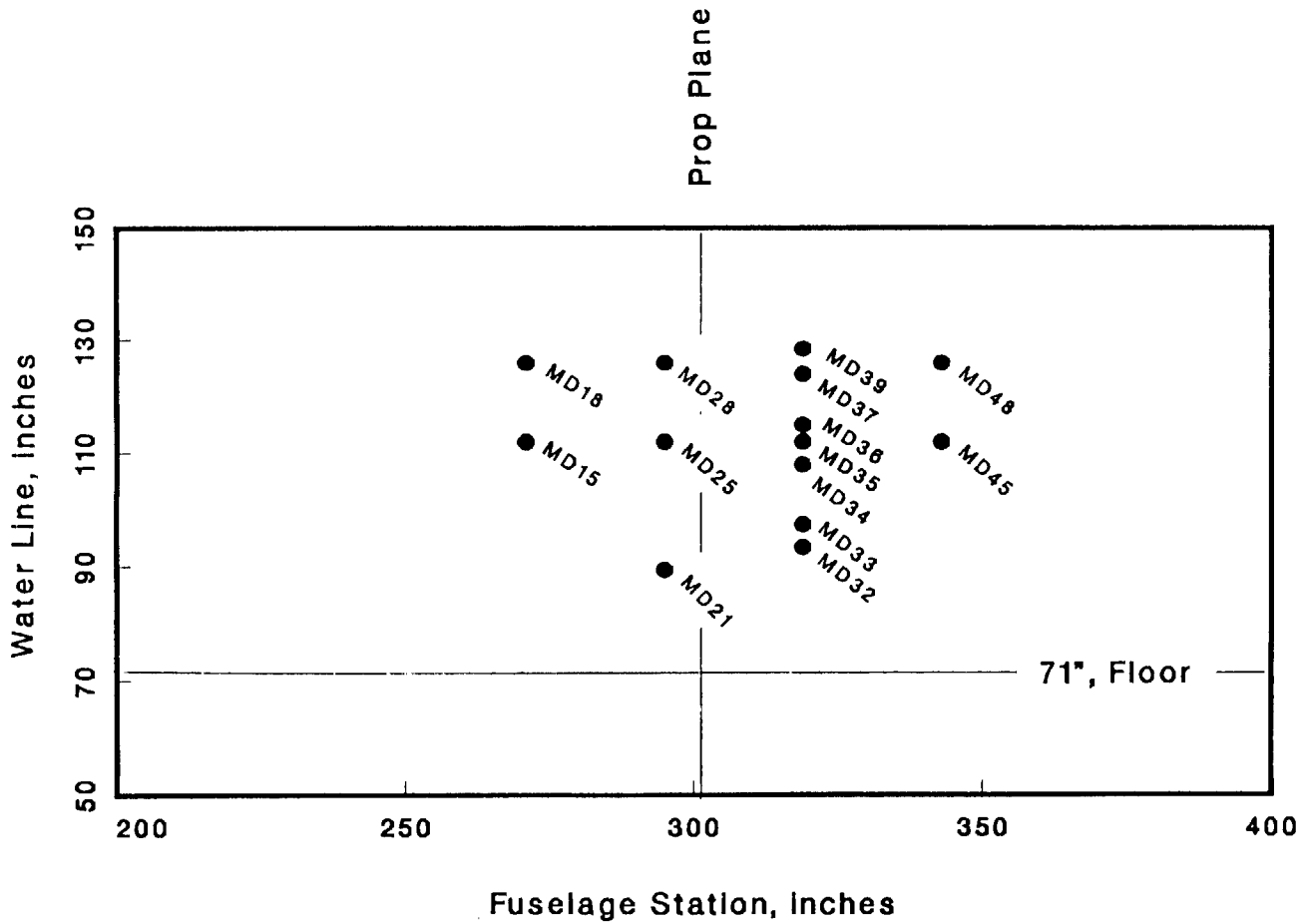

Figure12: Microphone positions for laboratory measurement of the cabin sound field. (All microphones positioned 0.15 m from trim panels.)

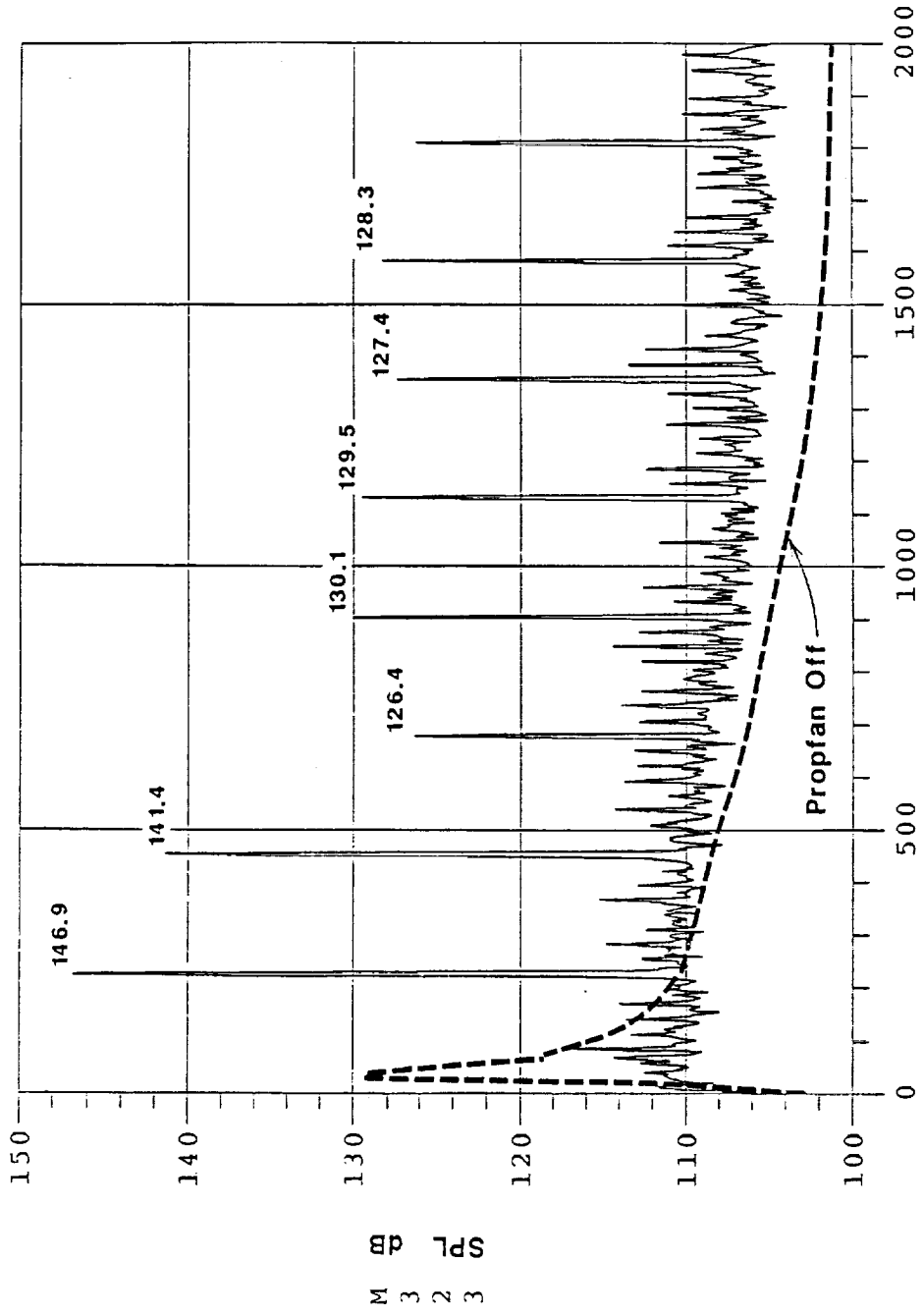

Figure 13: Sound pressure levels measured at fuselage microphone M323 at 10,700 m, 0.8 M, and 225 Hz, with and without propfan in place.

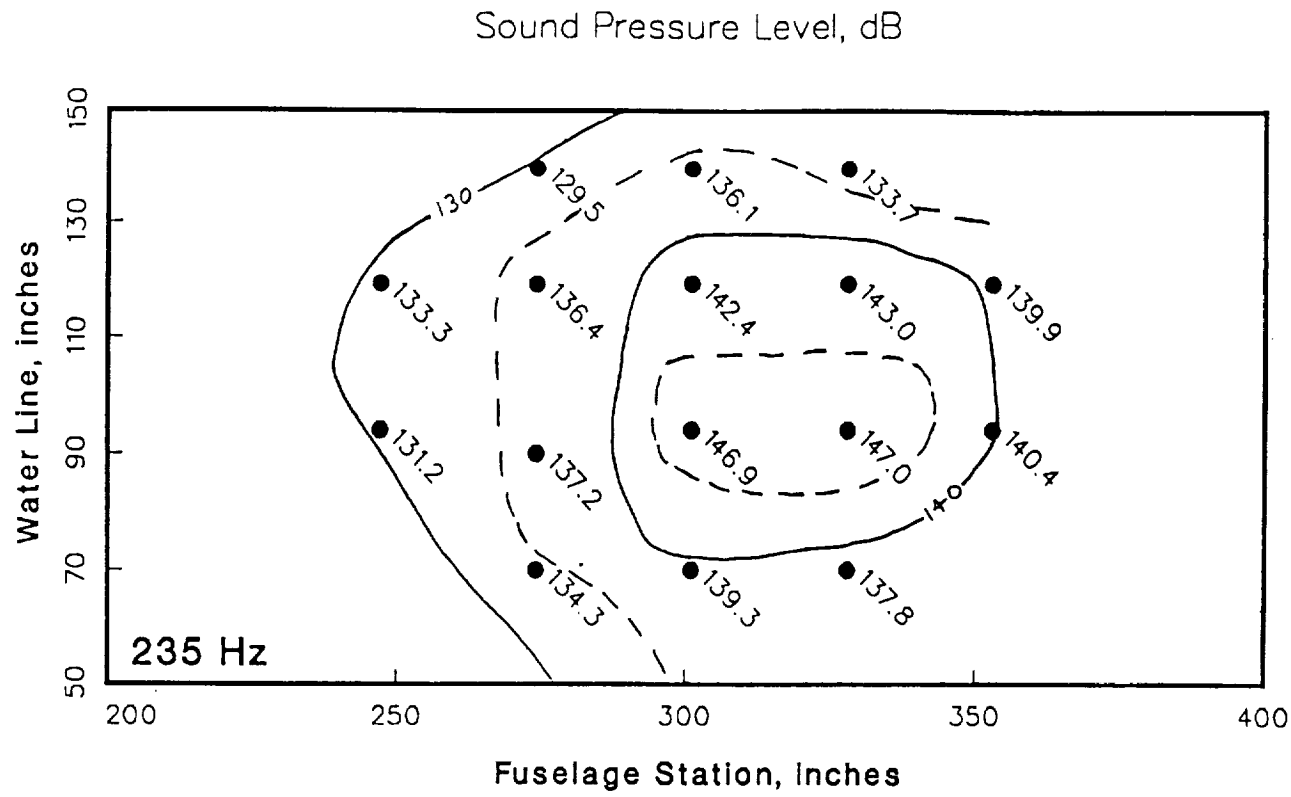

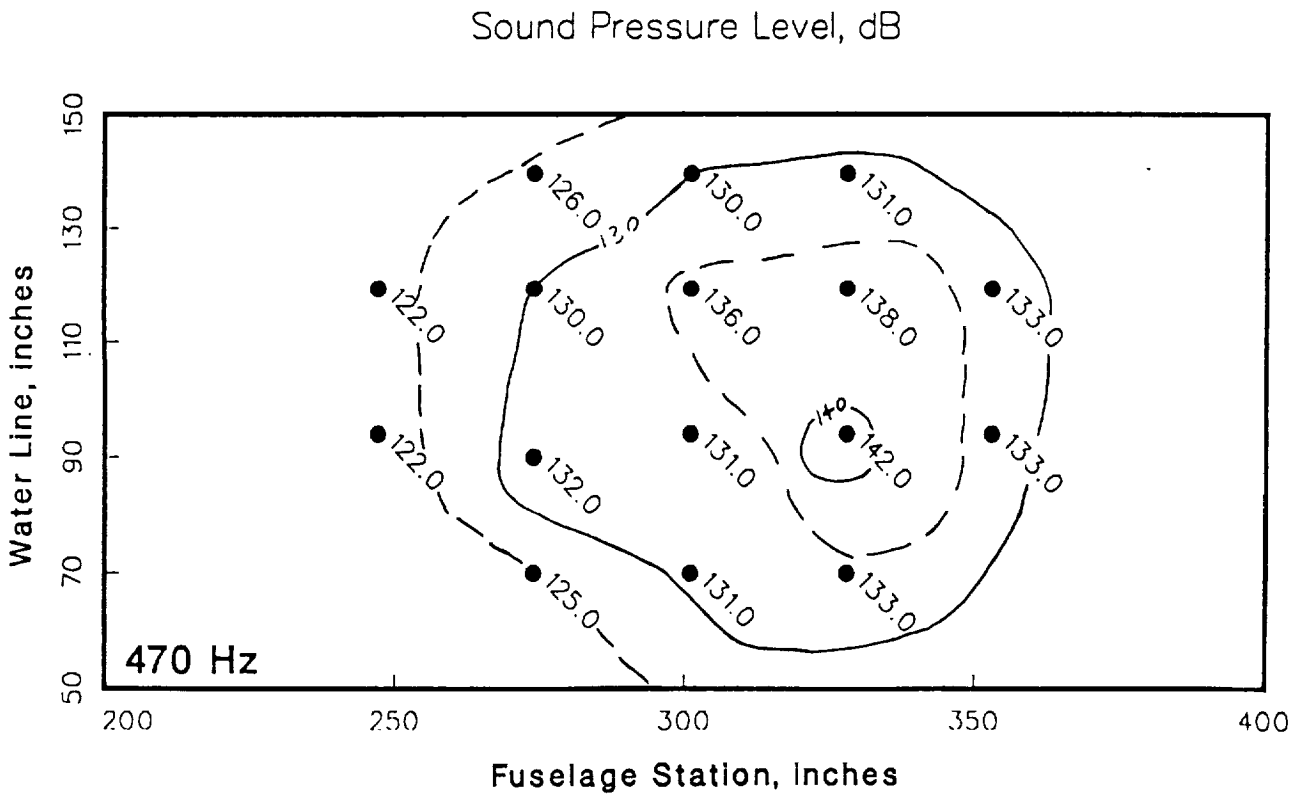

Figure 14: Tonal sound pressure levels measured on the laboratory fuselage.

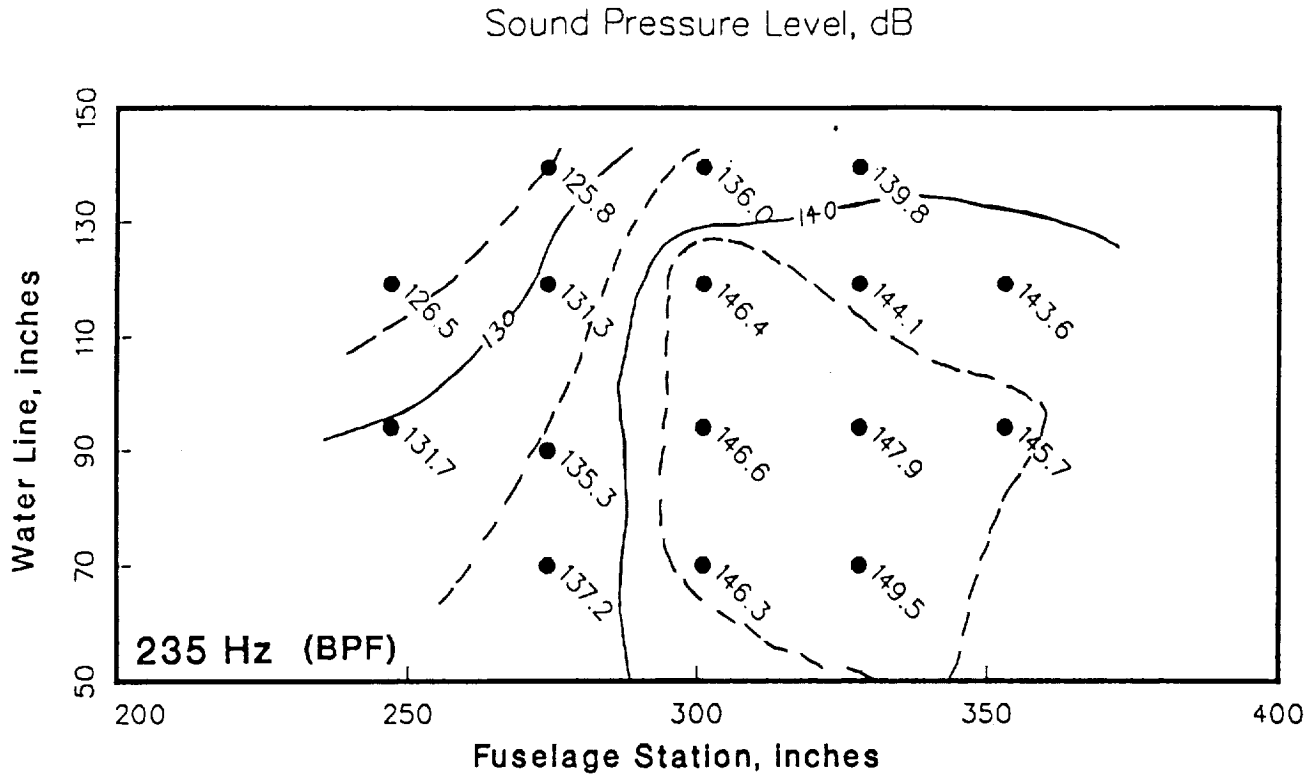

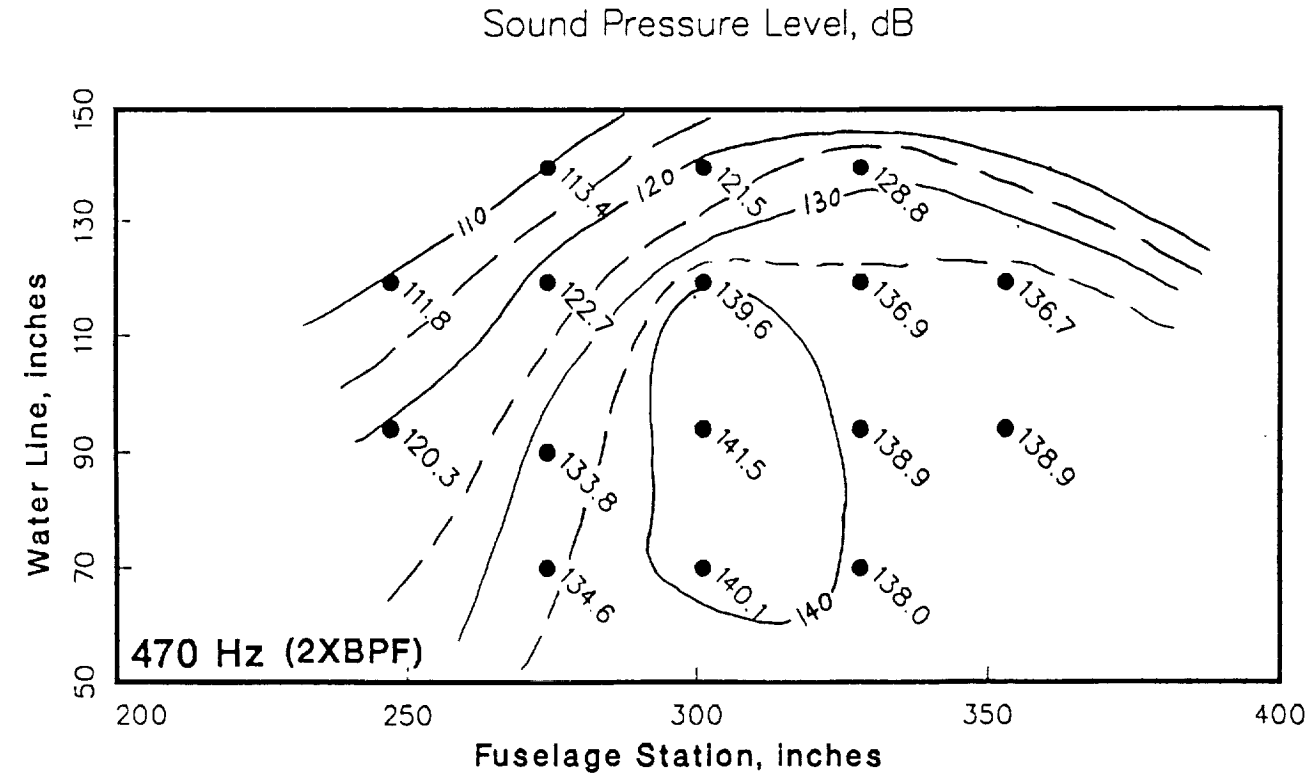

Figure 15: Tonal sound pressure levels measured on the fuselage of the PTA aircraft at 10,700 m and 0.86 M.

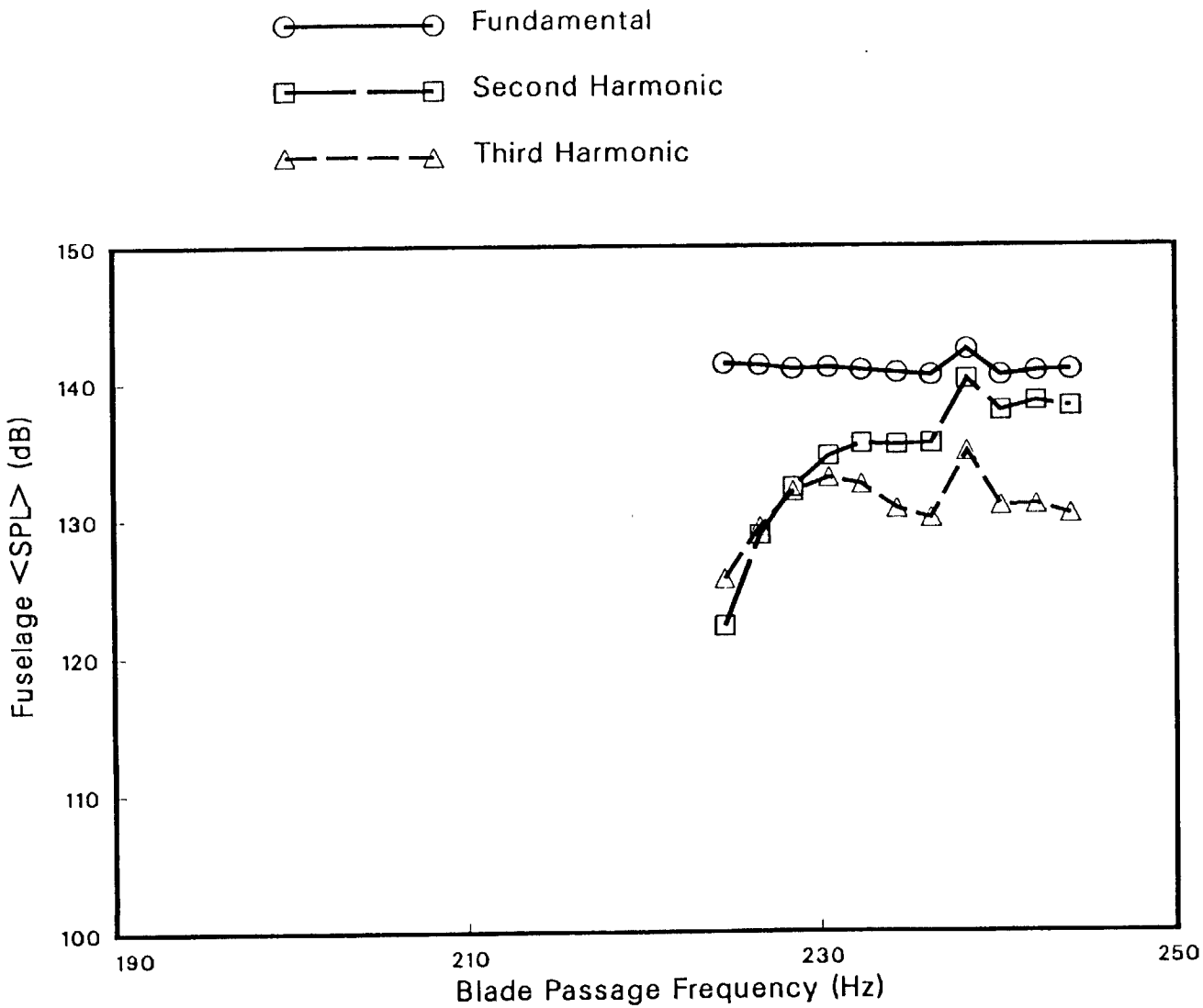

Figure 16 Tonal <SPL>s measured on the laboratory fuselage test section for the first three harmonics of the BPF.

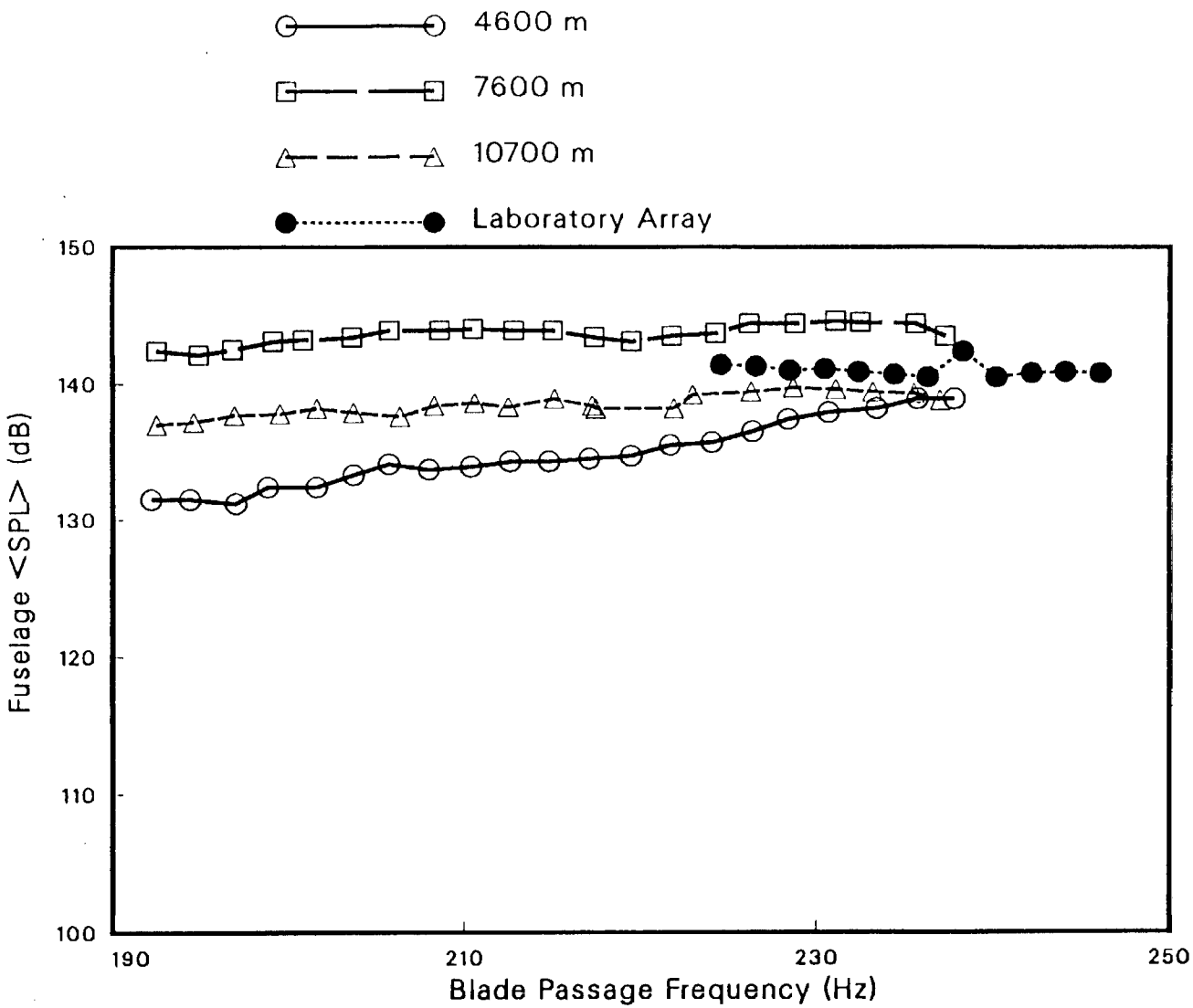

Figure 17: Flight and laboratory fuselage <SPL>s at propeller blade passage frequency.

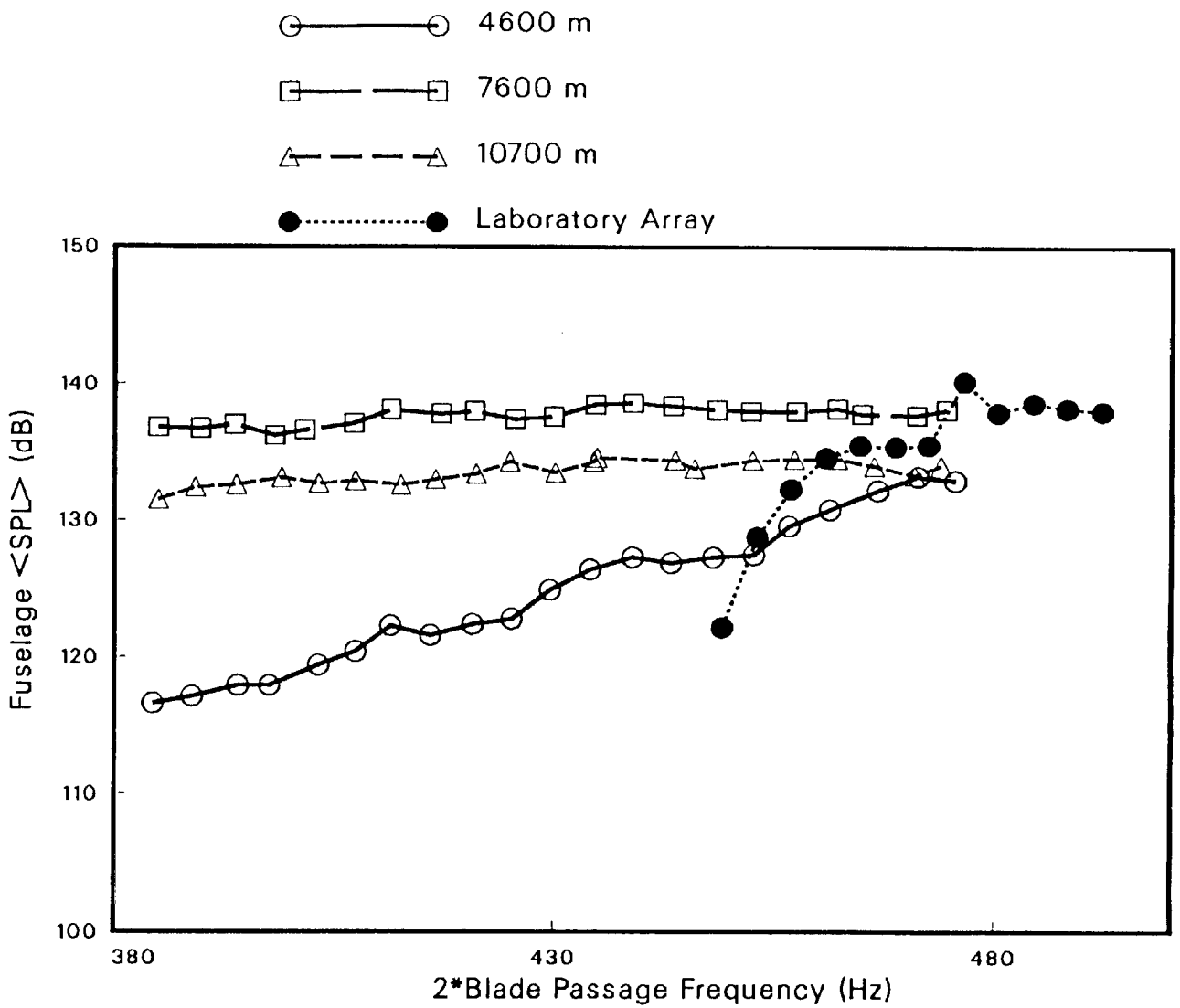

Figure 18: Flight and laboratory fuselage <SPL>s at second harmonic of propeller blade passage frequency.

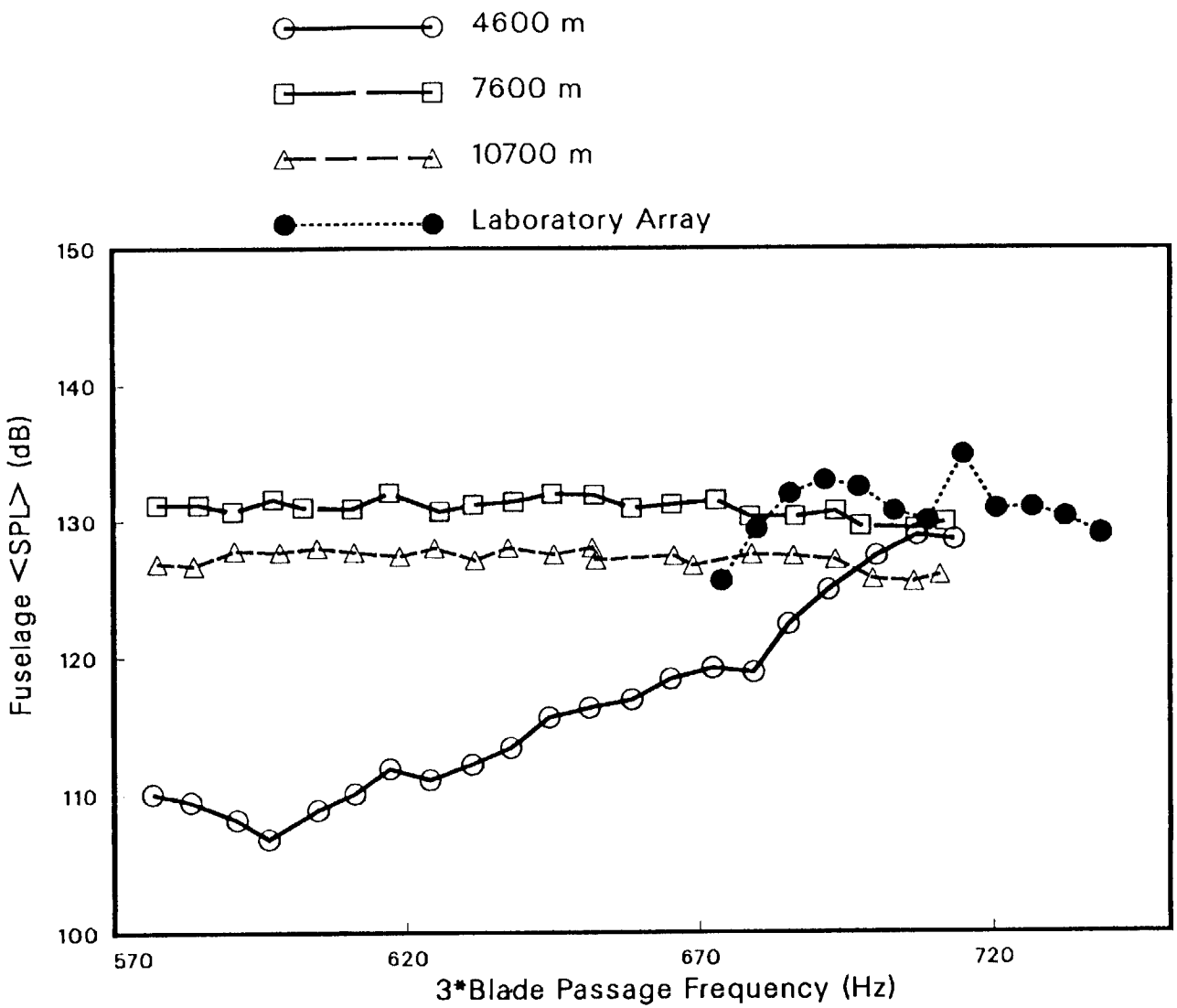

Figure 19: Flight versus laboratory fuselage <SPL>s at third harmonic of propeller blade passage frequency.

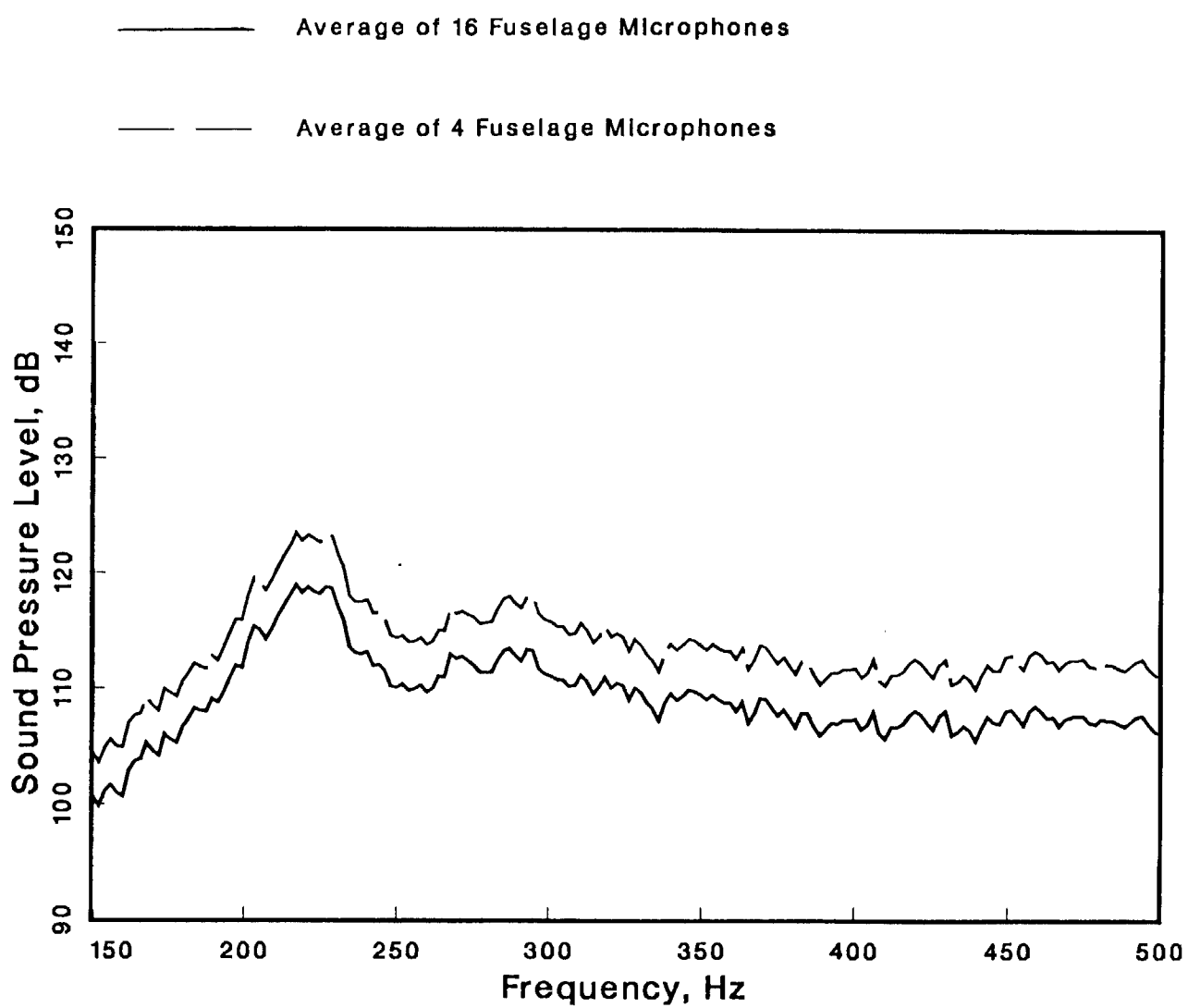

Figure 20: Comparison of <SPL>s by utilizing the four or sixteen microphone average.

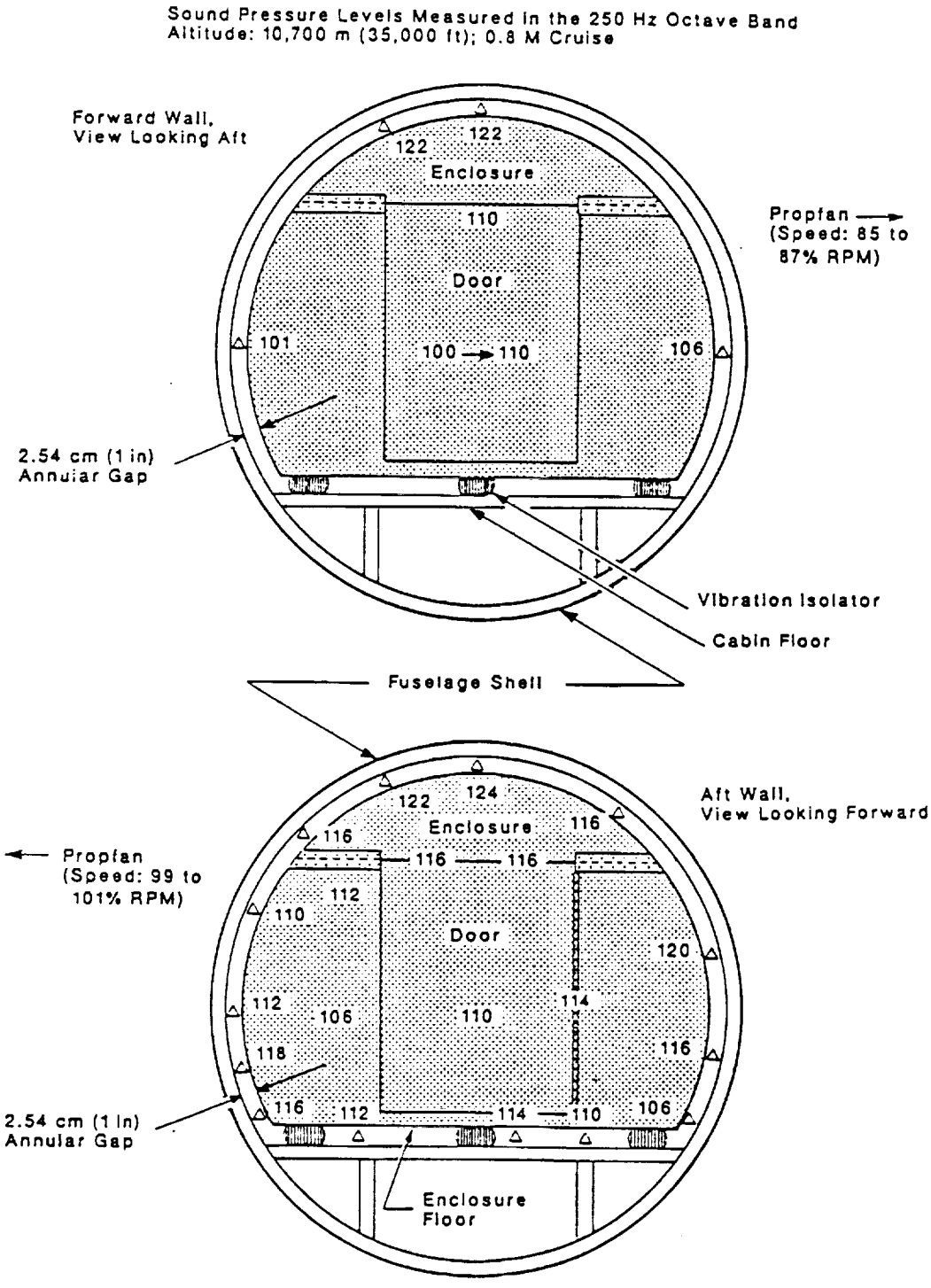

Figure 21: Propfan fundamental tone levels on acoustic enclosure end walls.

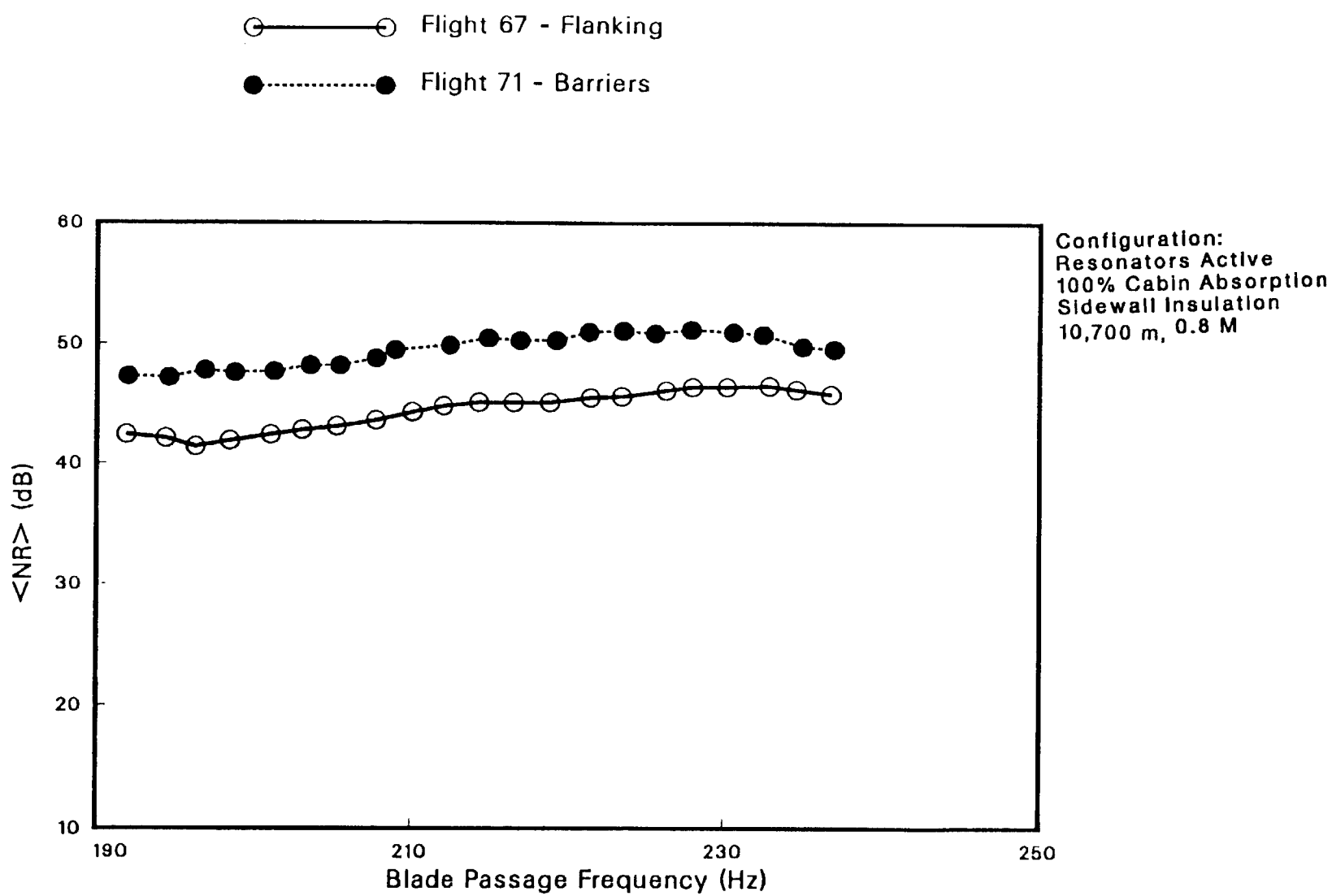

Figure 22: End flanking effect on propfan fundamental tone level reduction.

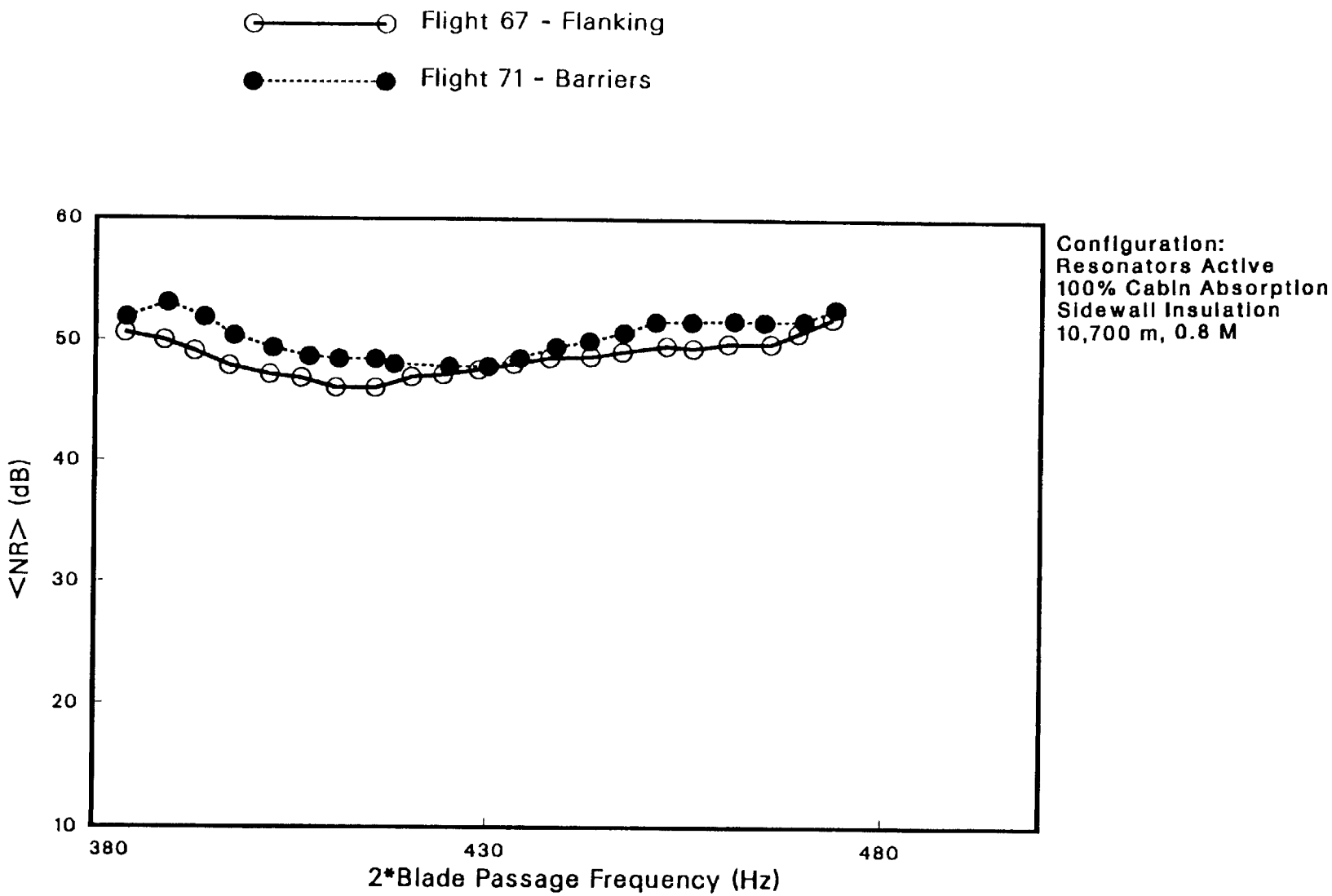

Figure 23: End flanking effect on propfan second harmonic tone level reduction.

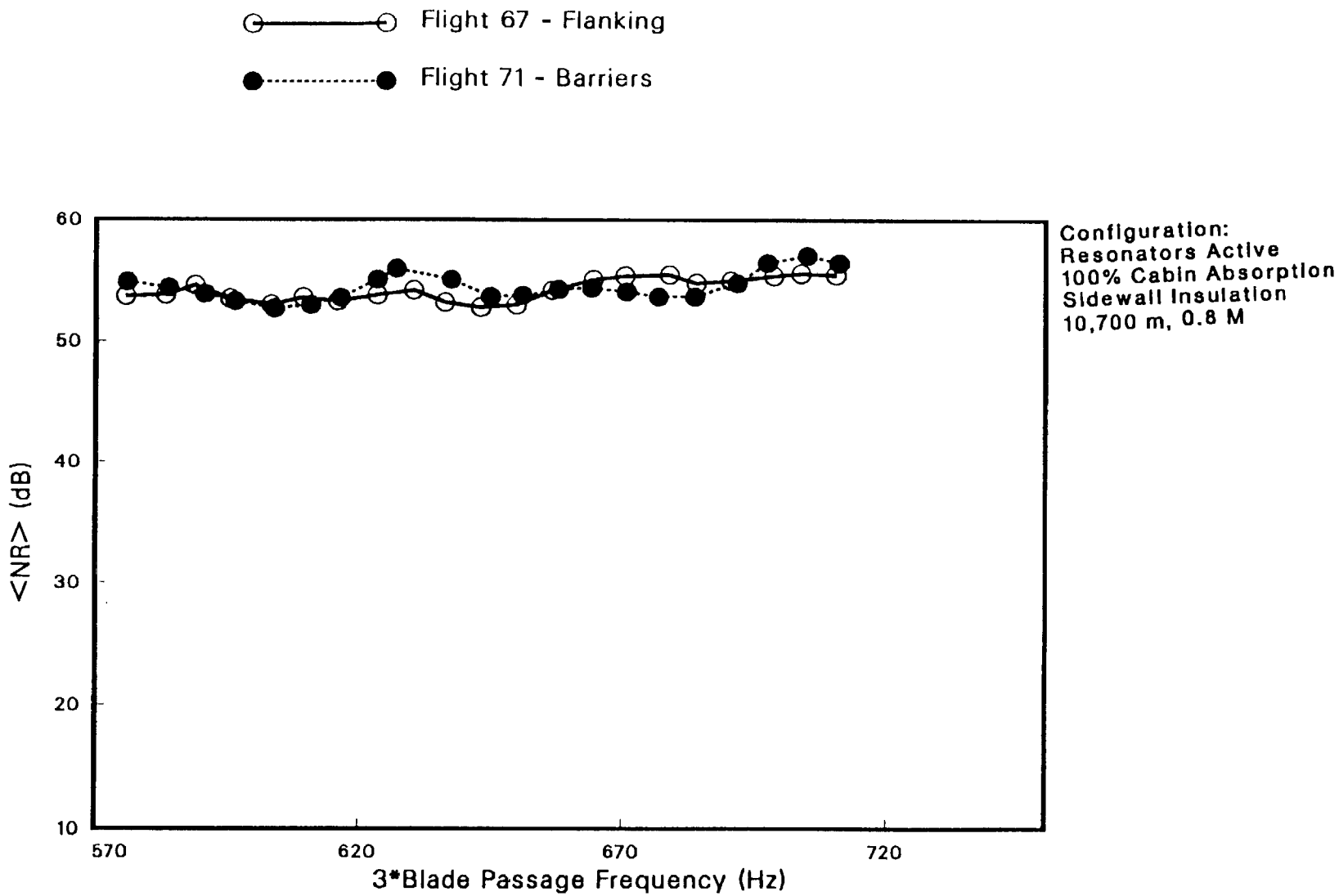

Figure 24: End flanking effect on propfan third harmonic tone level reduction.

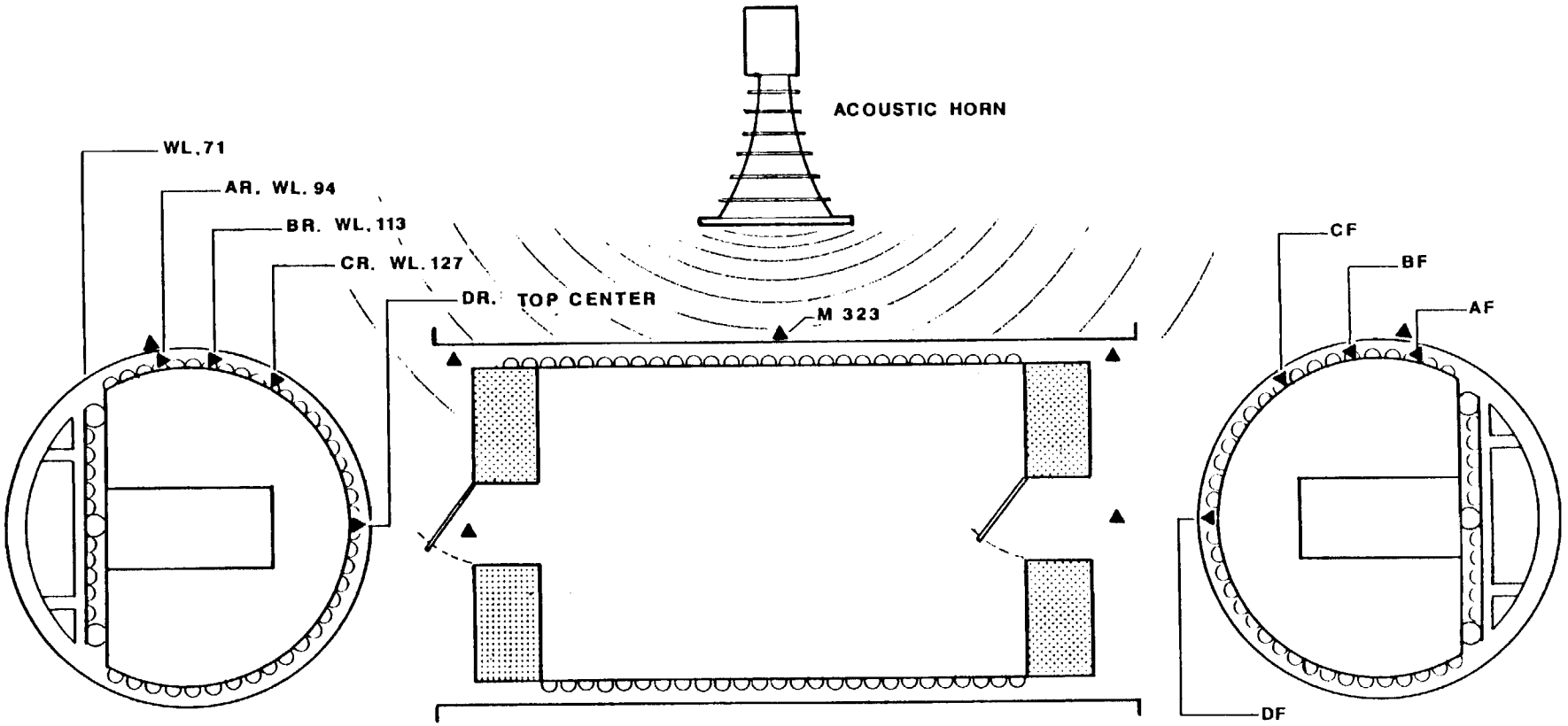

Figure 25: Input tone and annular gap tone levels without end seals and end surface resonators.

Microphone	Fundamental	Second Harmonic	Third Harmonic
M323	148 dB	144 dB	139 dB
AR	120	102	110
BR	121	112	108
CR	126	116	107
DR	123	120	89
AF	117	108	87
BF	113	103	97
CF	117	111	98
DF	113	118	95

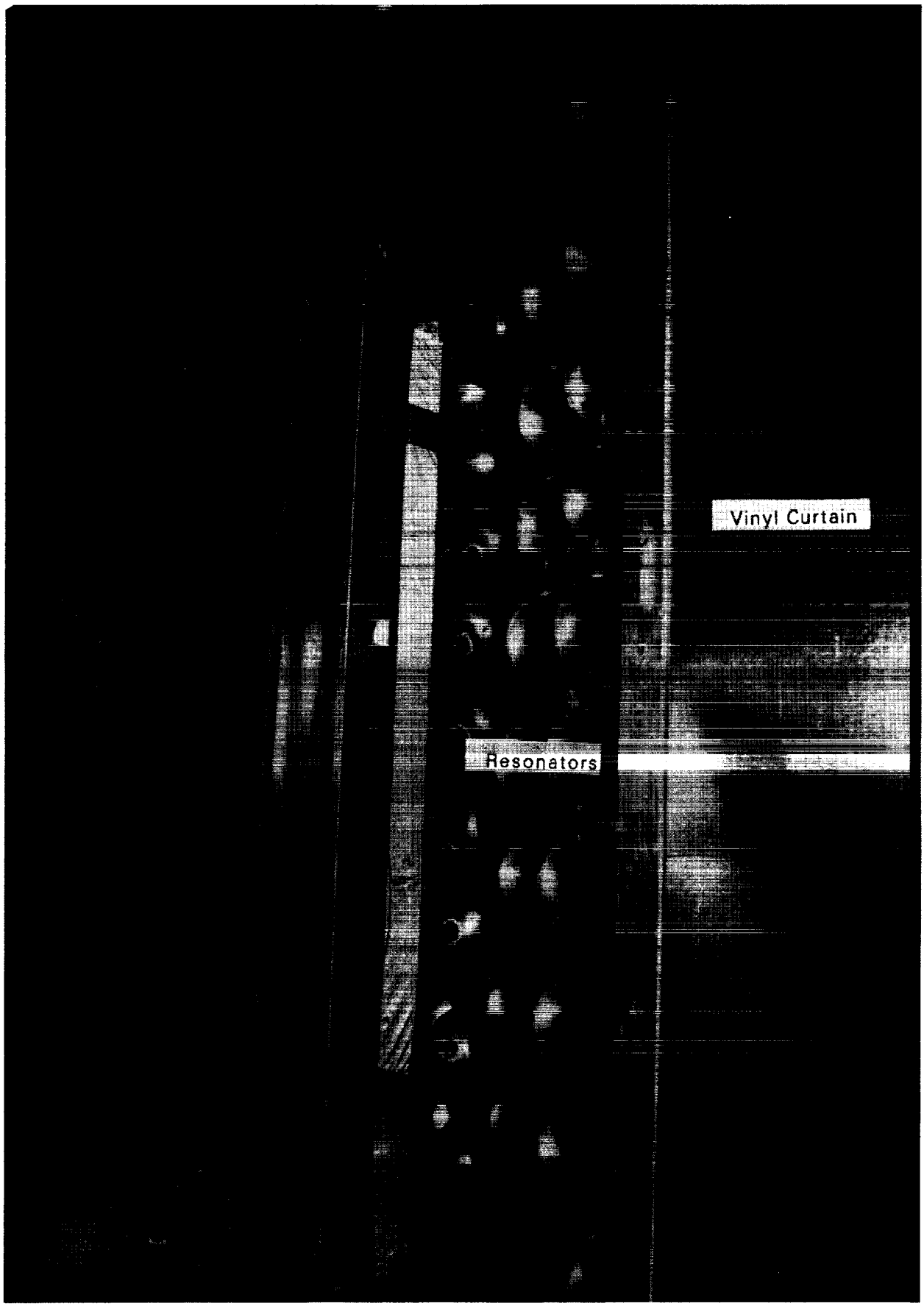

Figure 26: Photograph of vinyl end barriers and resonators.

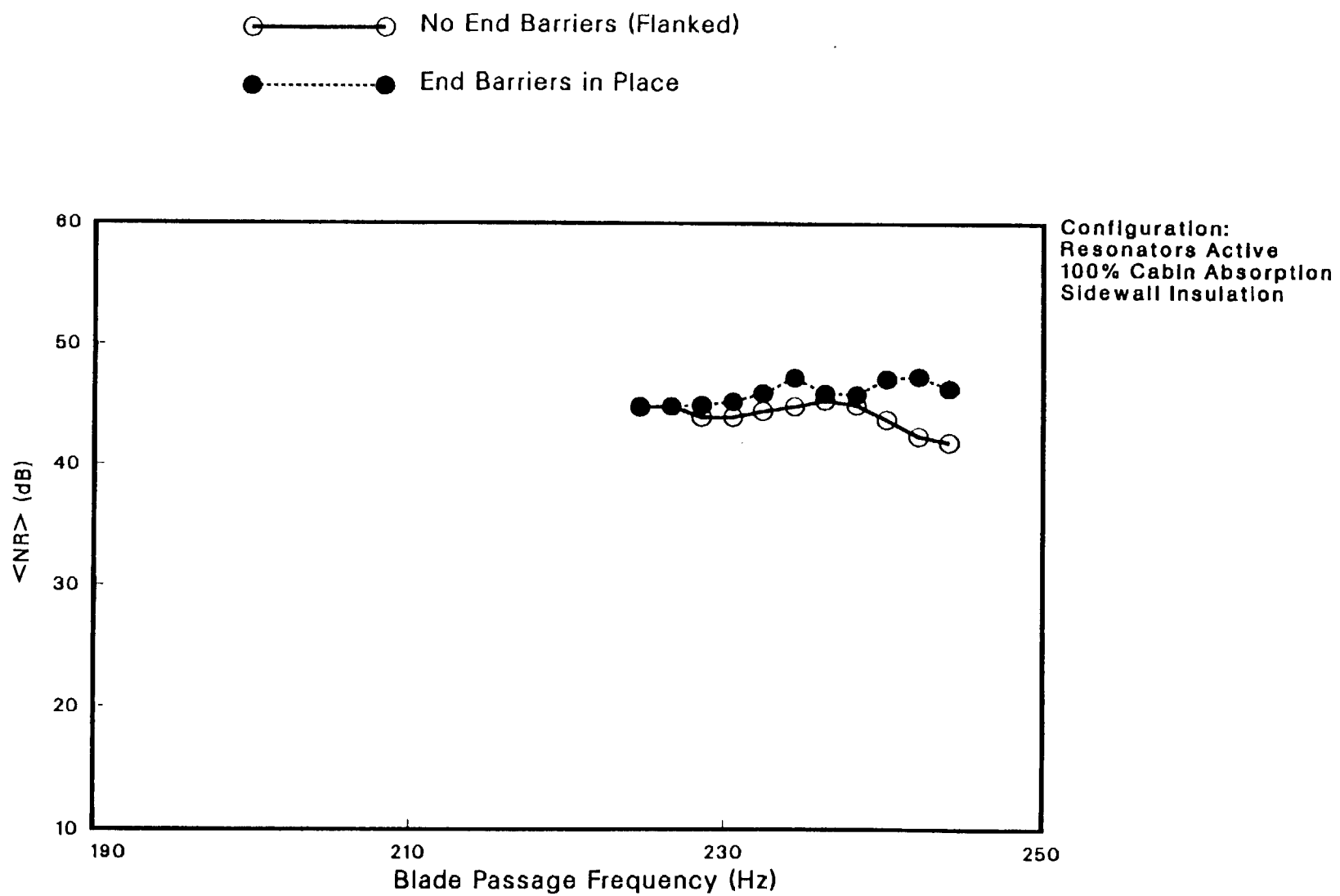

Figure 27: Enclosure <NR>s with and without barrier seals and enclosure external end wall resonators - fundamental tone.

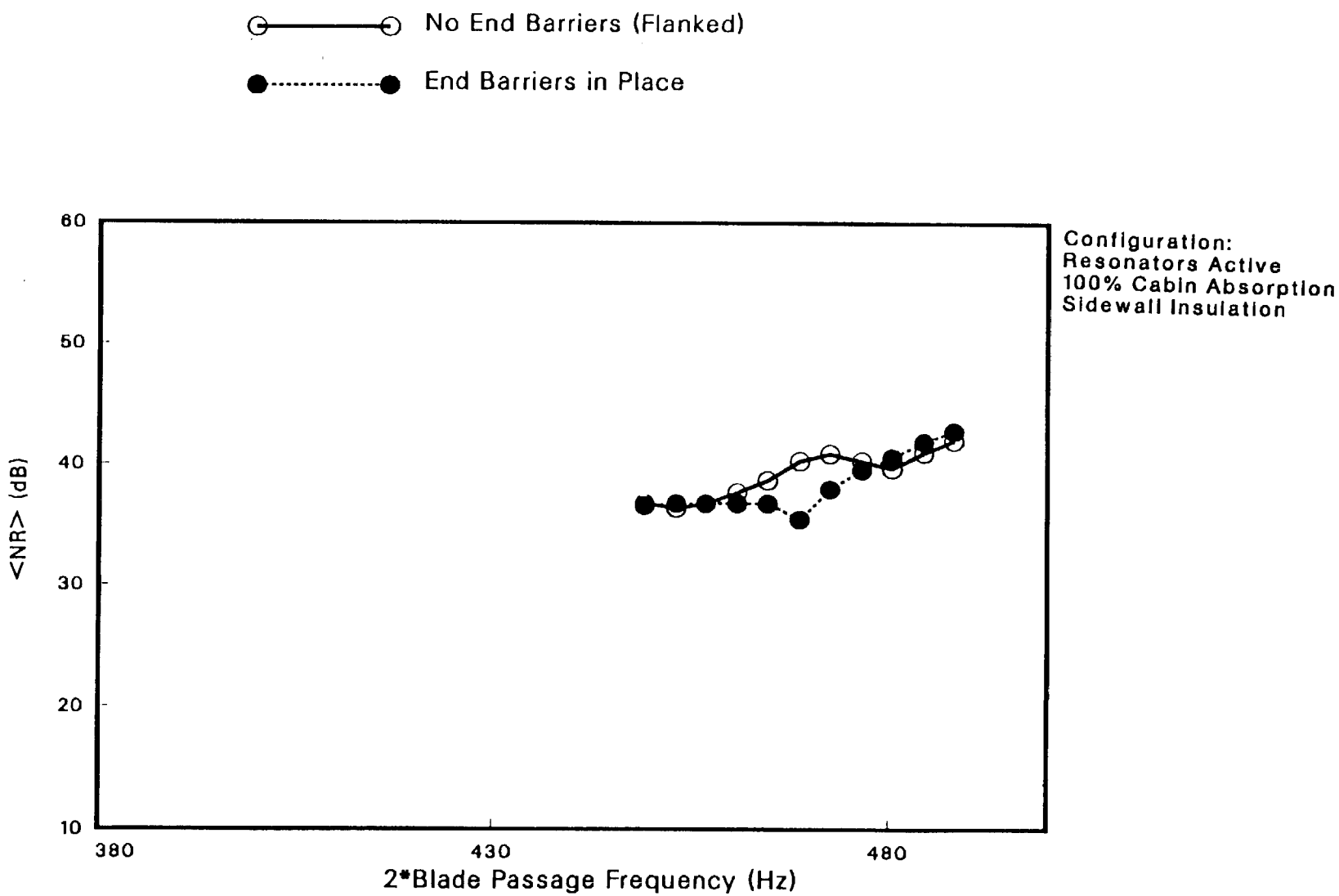

Figure 28: Enclosure <NR>s with and without barrier seals and enclosure external end wall resonators - second harmonic tone.

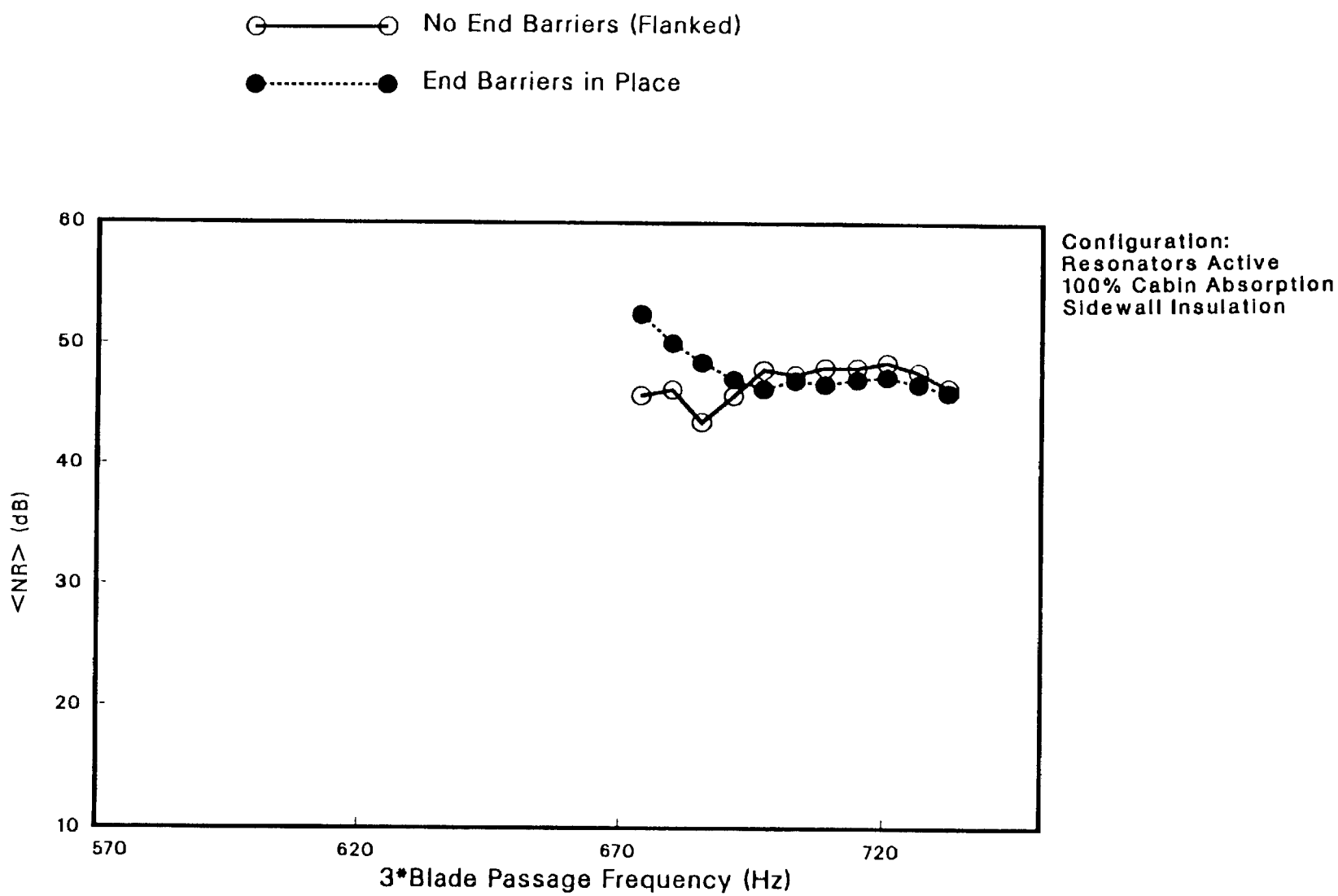

Figure 29: Enclosure <NR>s with and without barrier seals and enclosure external end wall resonators - third harmonic tone.

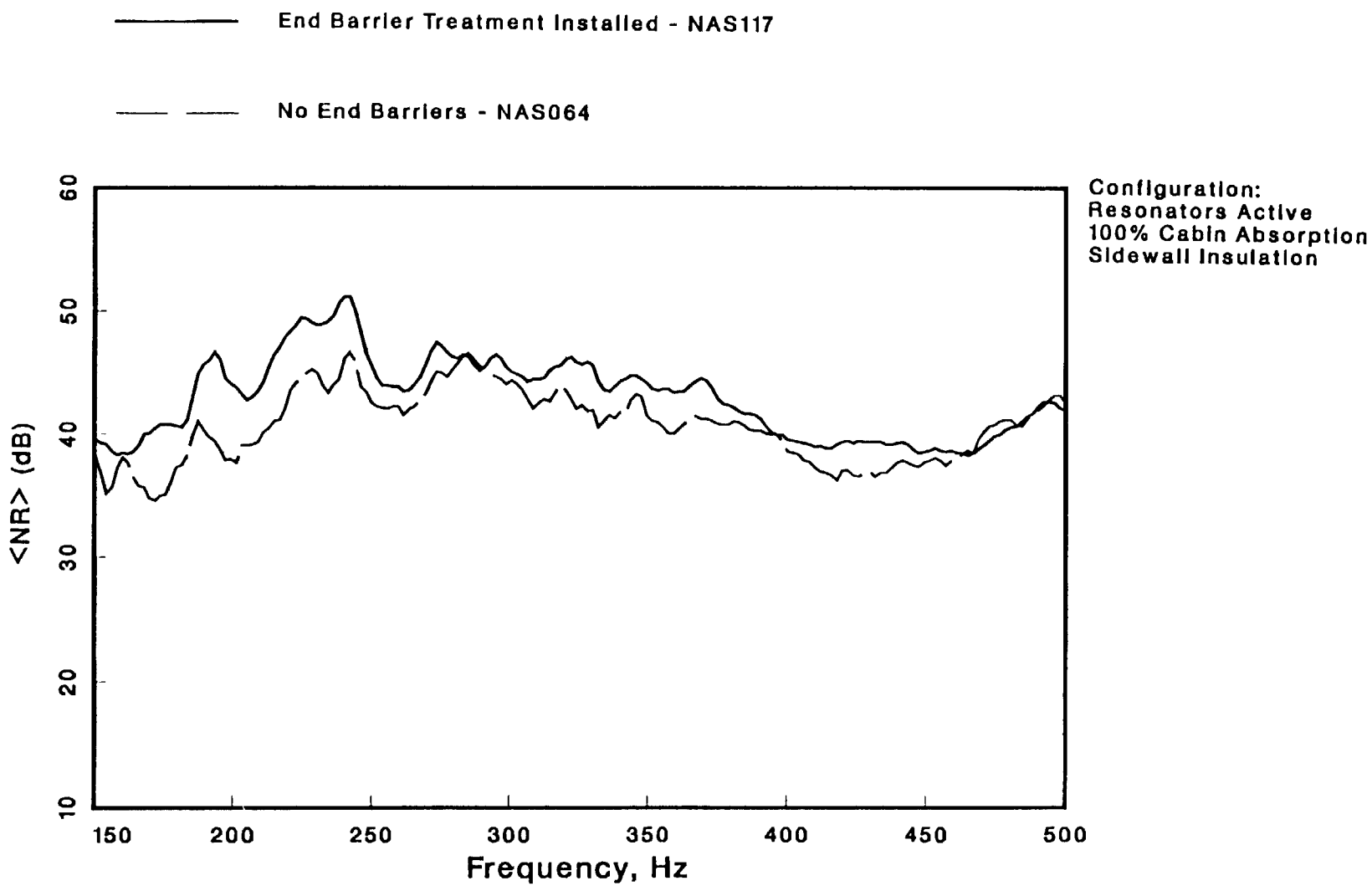

Figure 30: Enclosure <NR>s with and without barrier seals and enclosure external end wall resonators - broadband noise excitation.

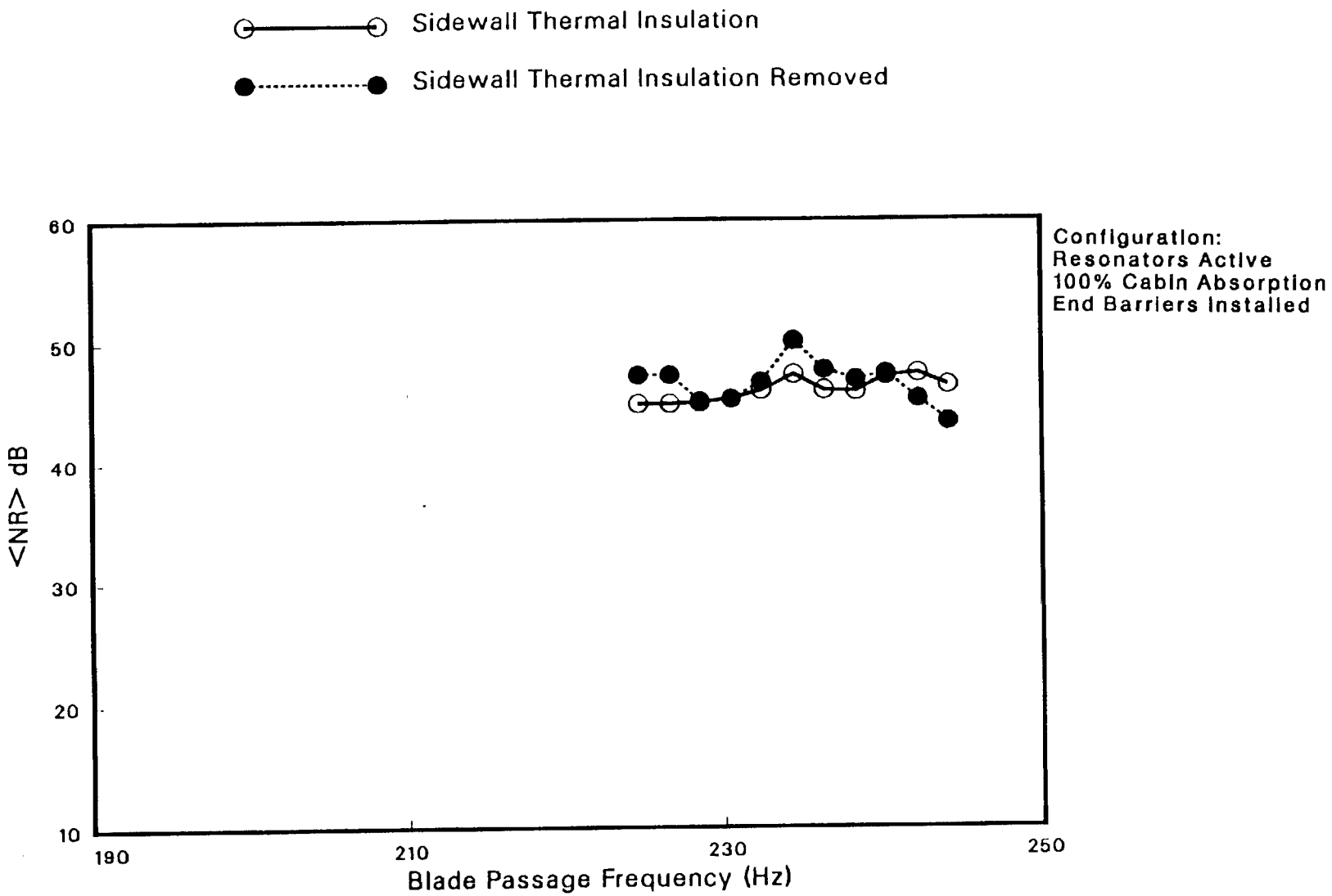

Figure 31: Enclosure <NR>s with and without sidewall thermal insulation in place - fundamental tone.

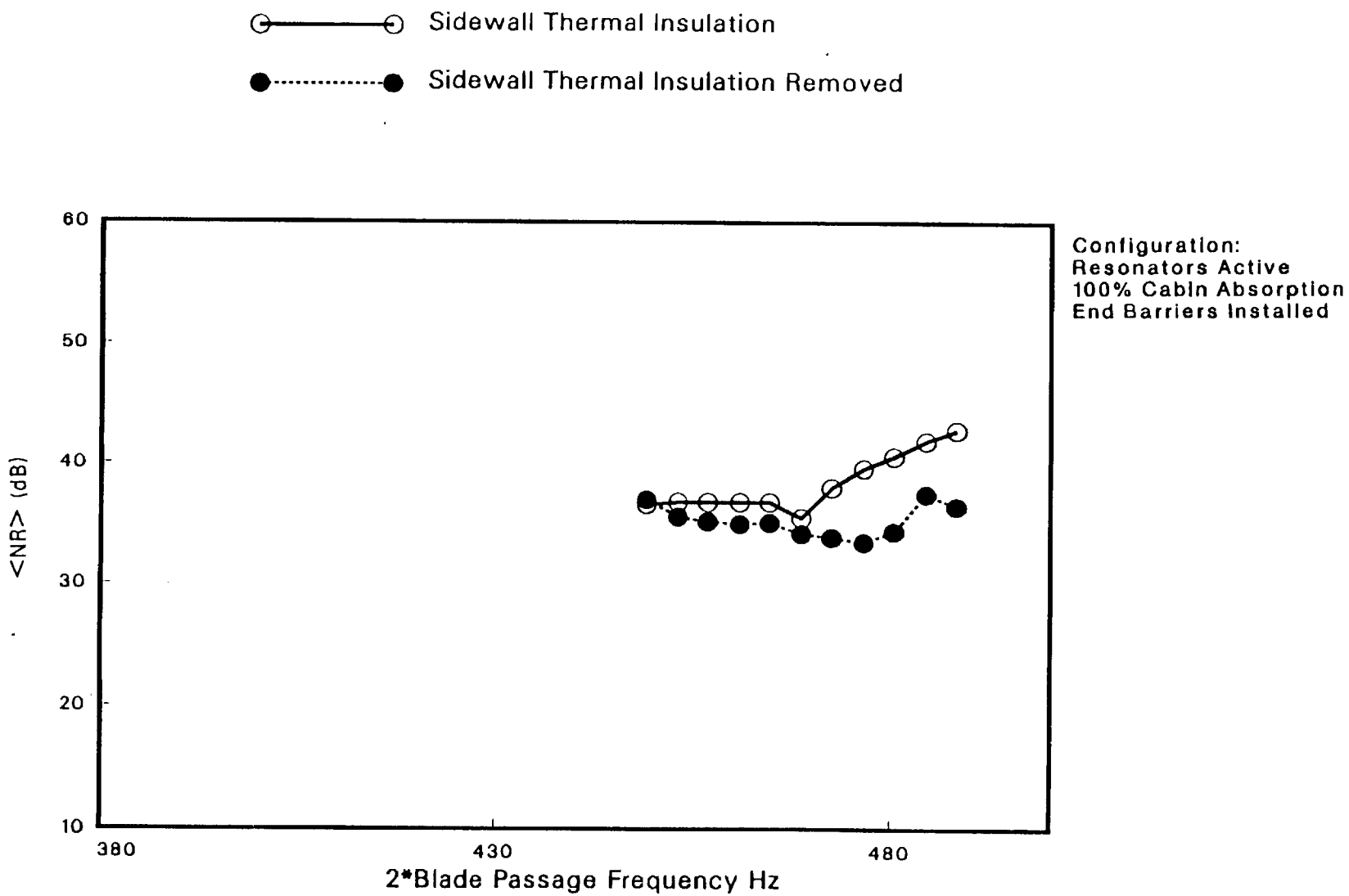

Figure 32: Enclosure <NR>s with and without sidewall thermal insulation in place - second harmonic tone.

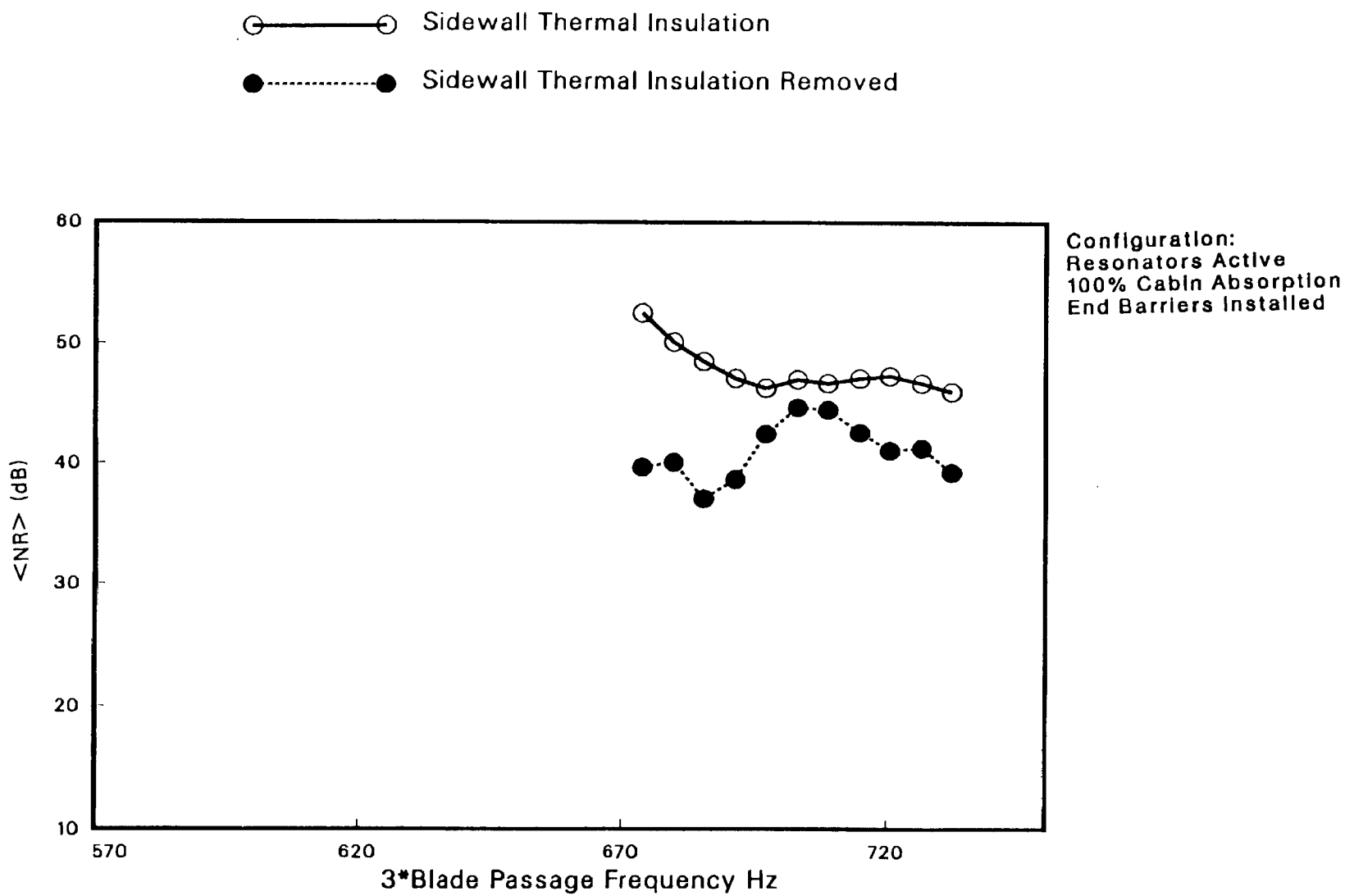

Figure 33: Enclosure <NR>s with and without sidewall thermal insulation in place - third harmonic tone.

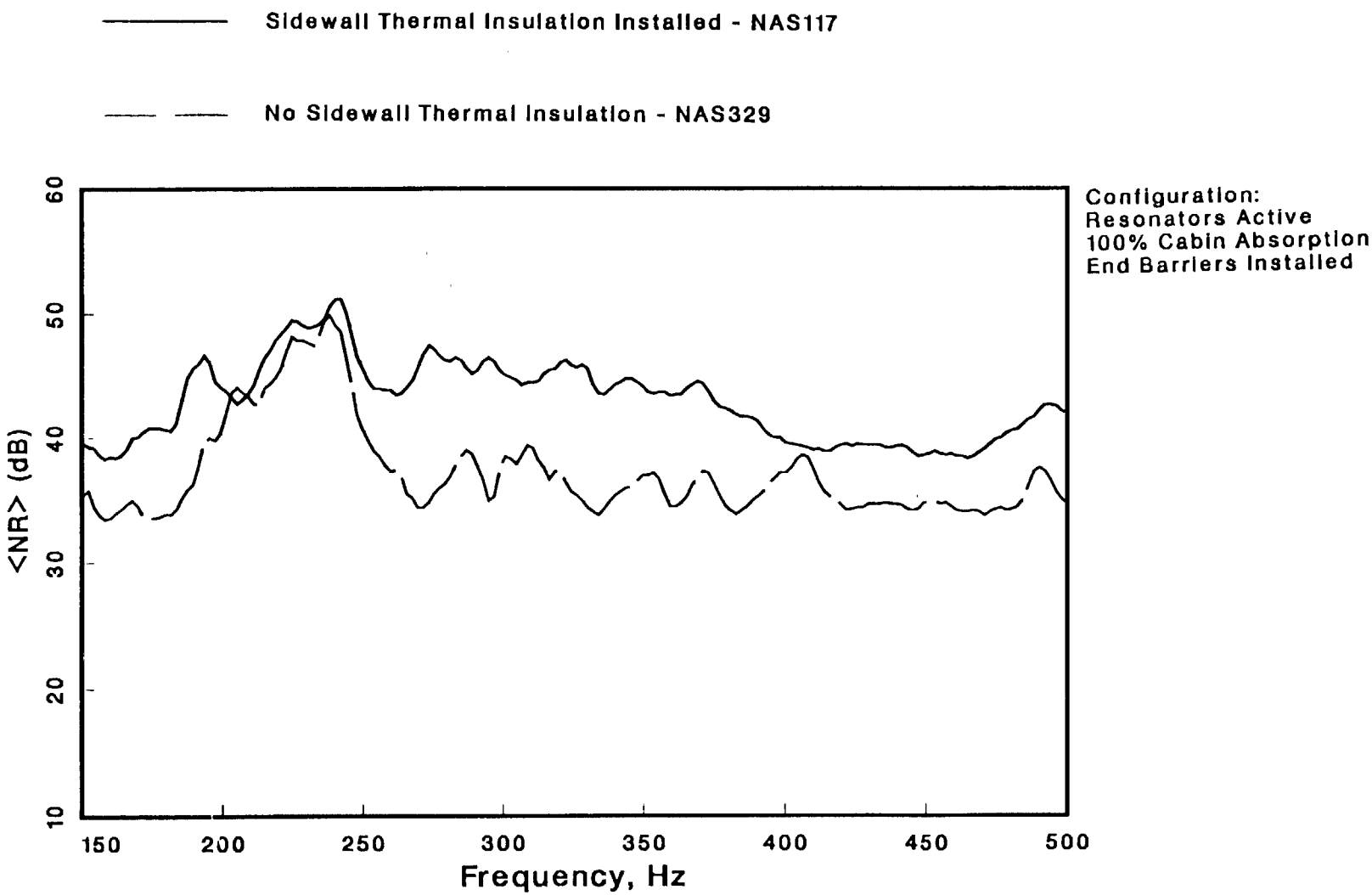

Figure 34: Enclosure <NR>s with and without sidewall thermal insulation in place - broadband noise excitation.

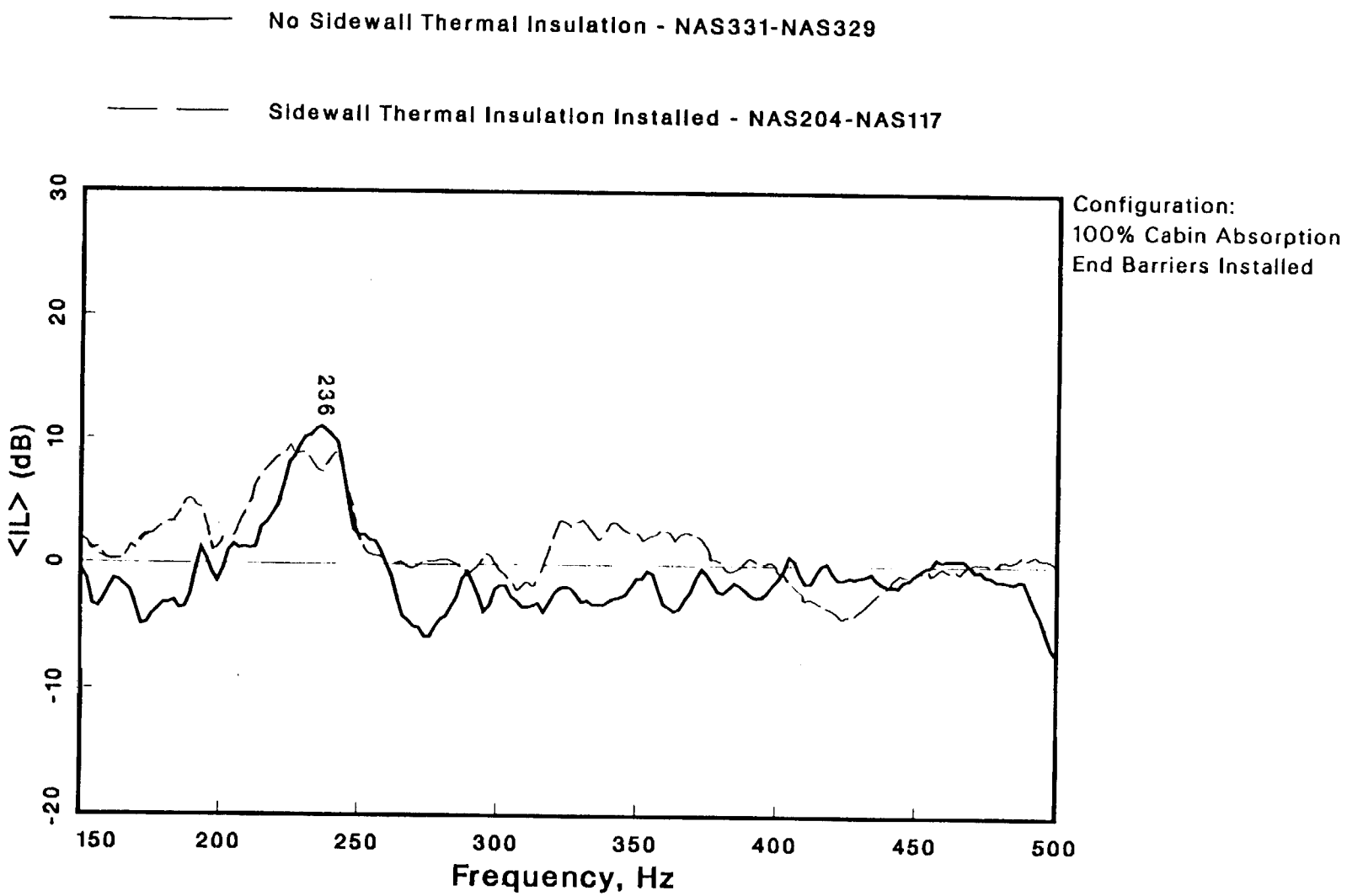

Figure 35: Effect of sidewall thermal blanket installation on resonator <IL> near the resonator tuning frequency.

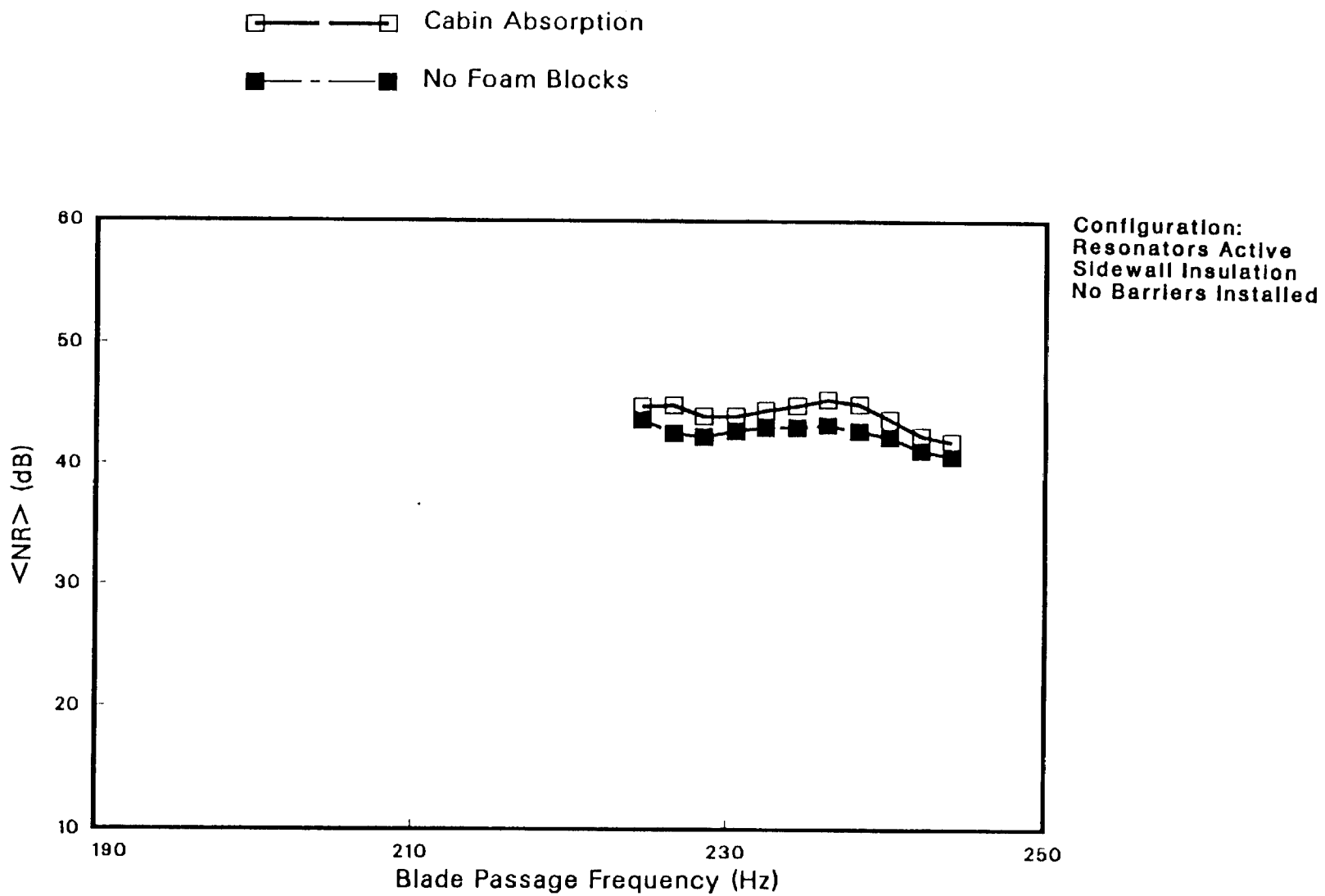

Figure 36: Effect of absorptive materials (six foam blocks) on the <NR> with tonal input - fundamental tone.

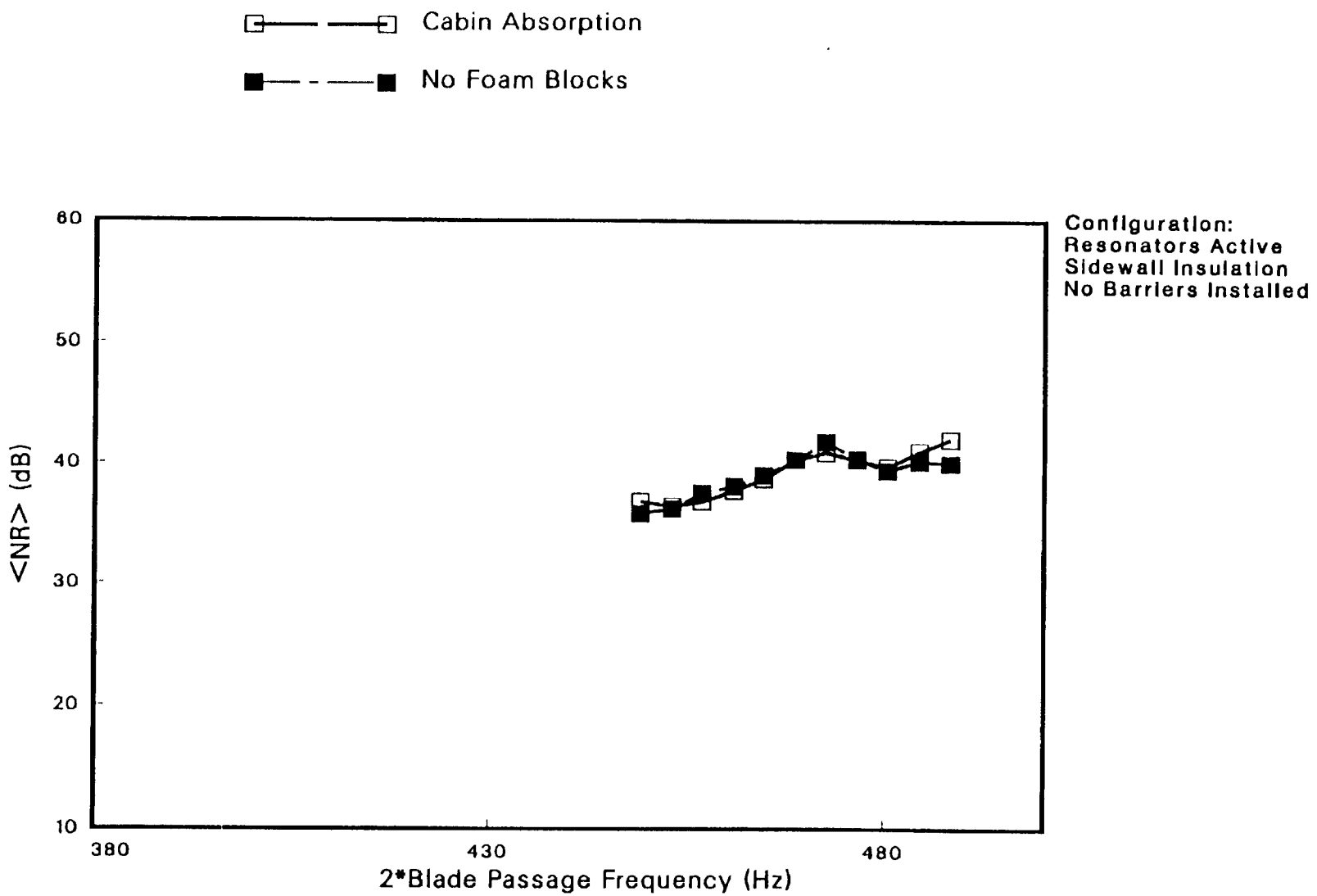

Figure 37: Effect of absorptive materials (six foam blocks) on the <NR> with tone input - second harmonic tone.

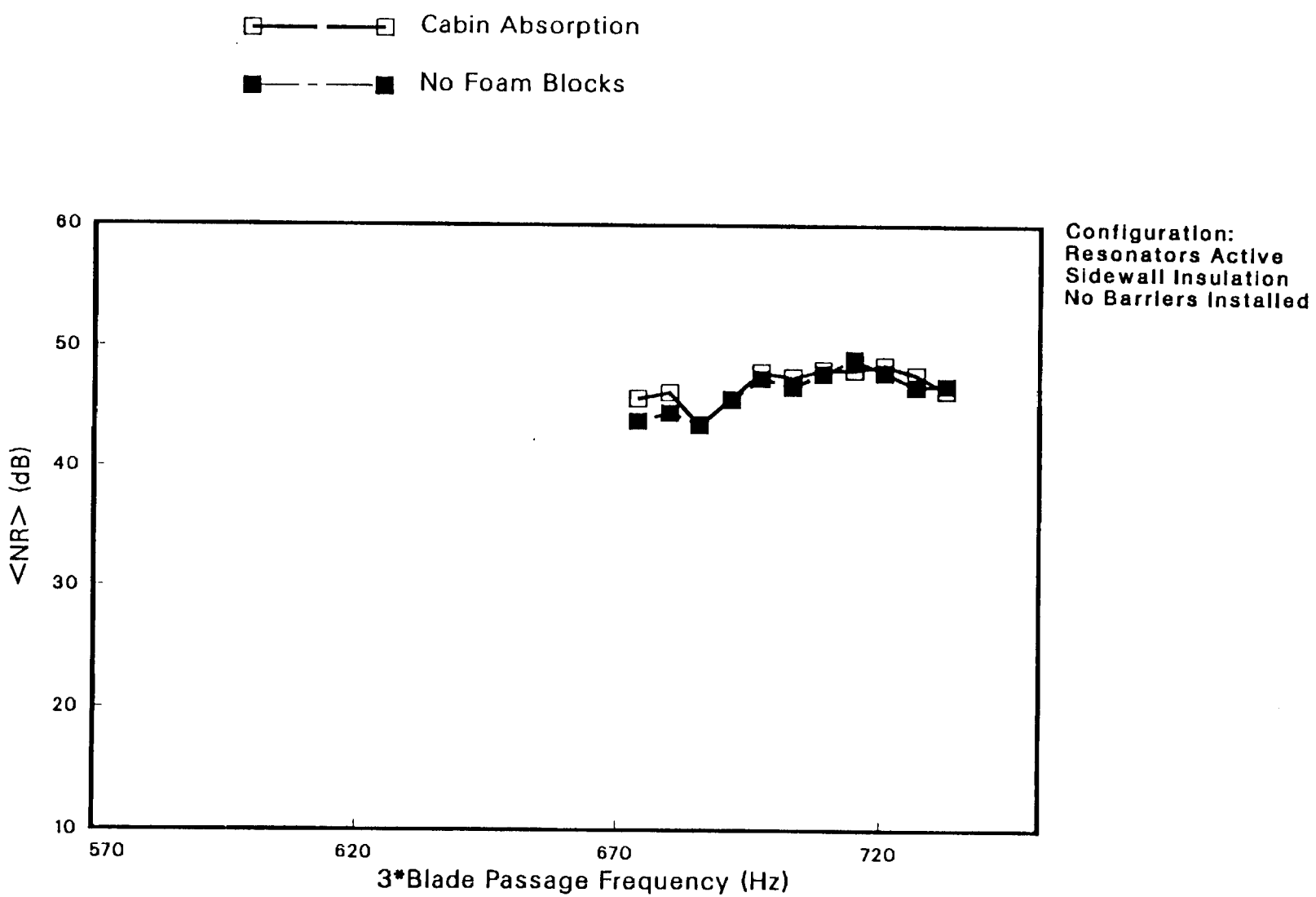

Figure 38: Effect of absorptive materials (six foam blocks) on the <NR> with tonal input - third harmonic tone.

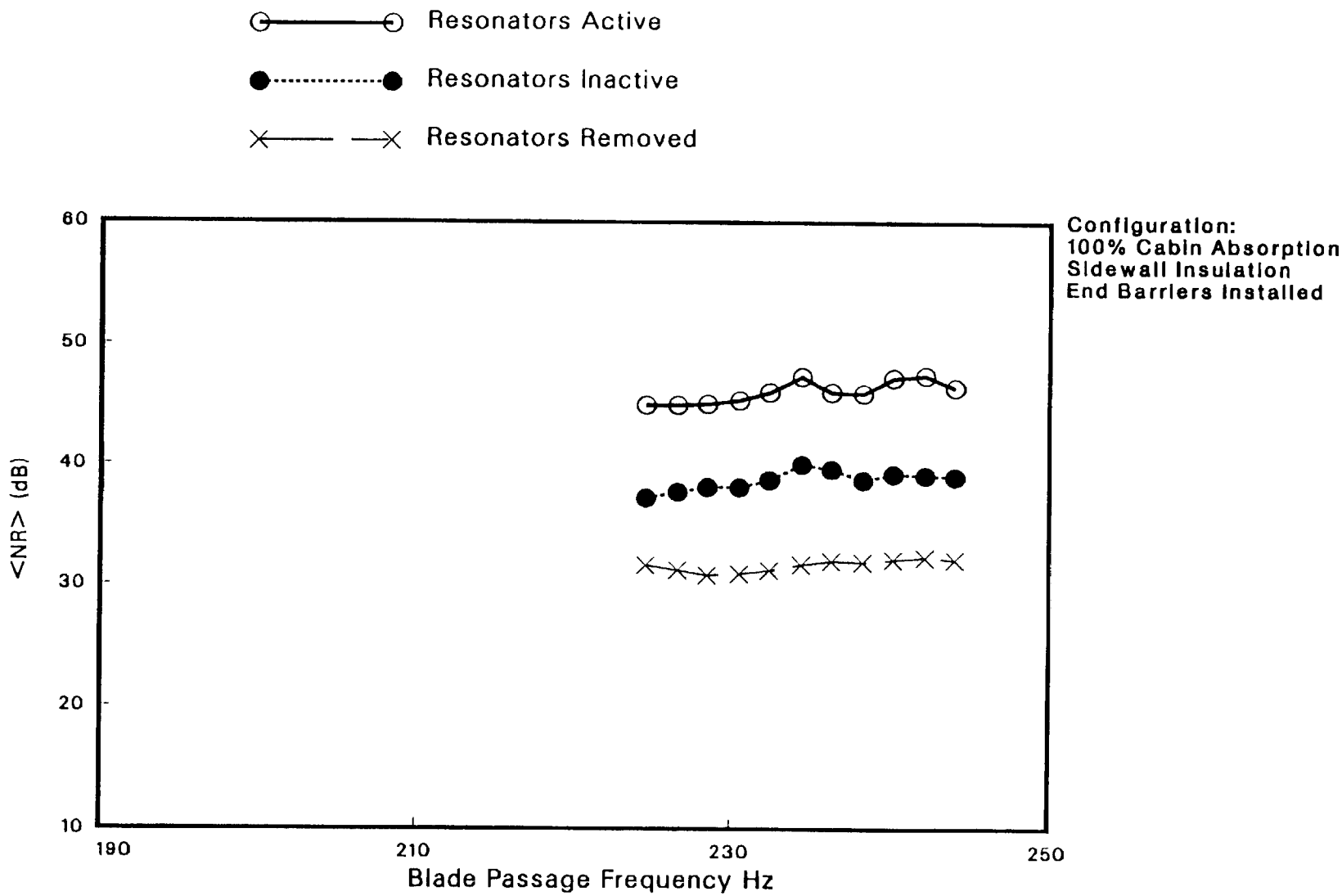

Figure 39: Laboratory test comparison of <NR>s with sidewall resonators active, inactive, and removed - fundamental tone.

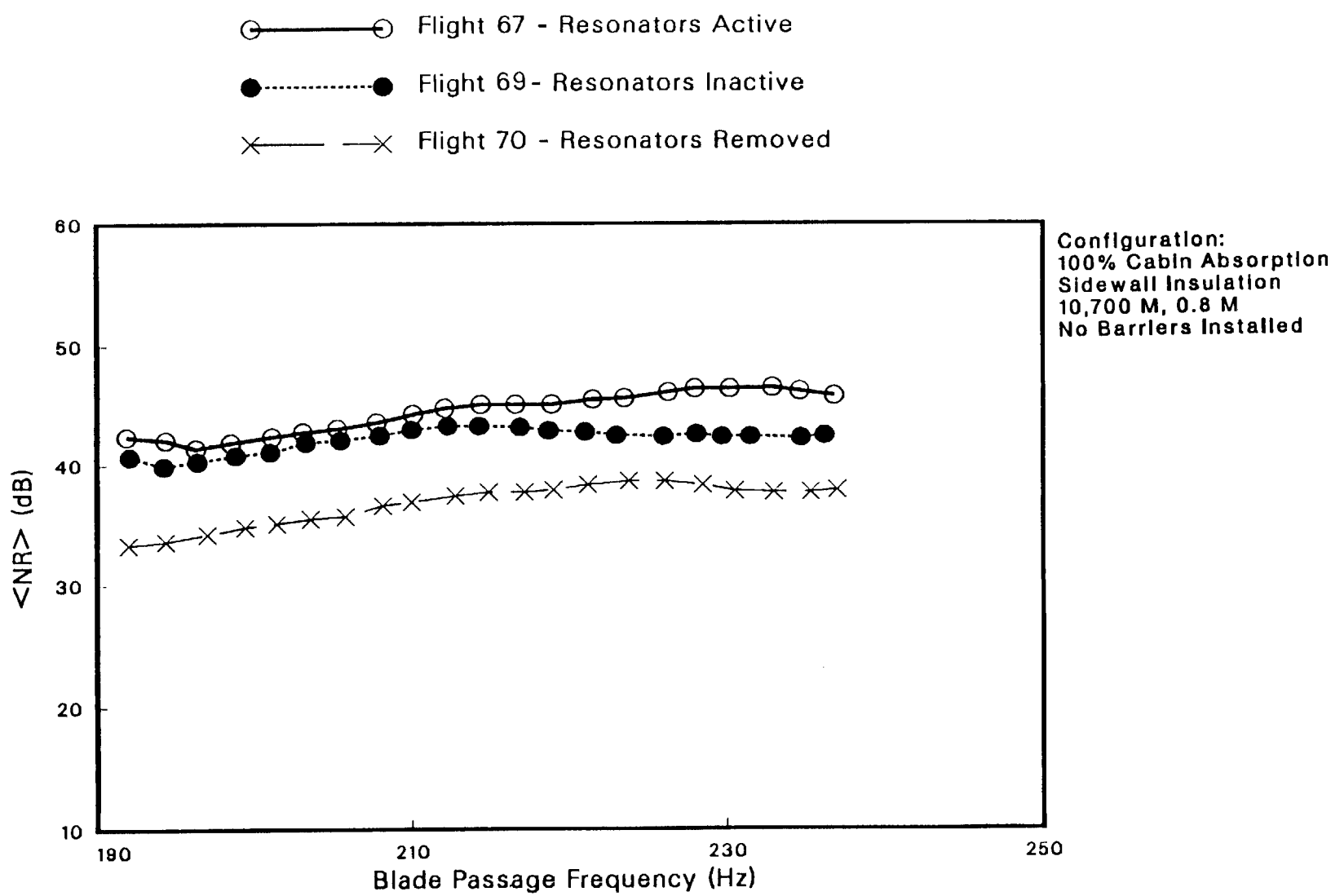

Figure 40: Flight test comparison of <NR>s with sidewall resonators active, inactive, and removed - fundamental tone.

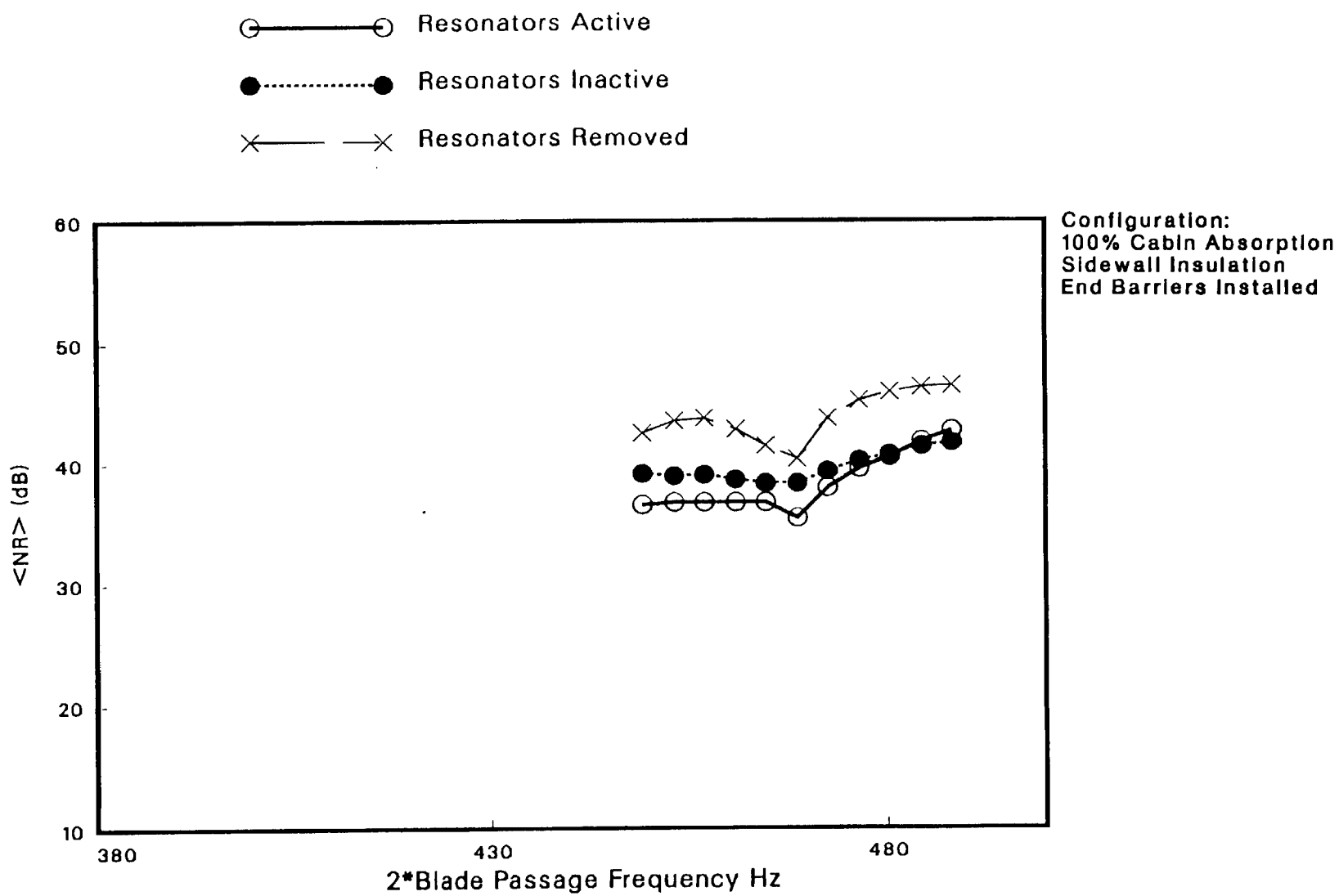

Figure 41: Laboratory test comparison of <NR>s with sidewall resonators active, inactive, and removed - second harmonic tone.

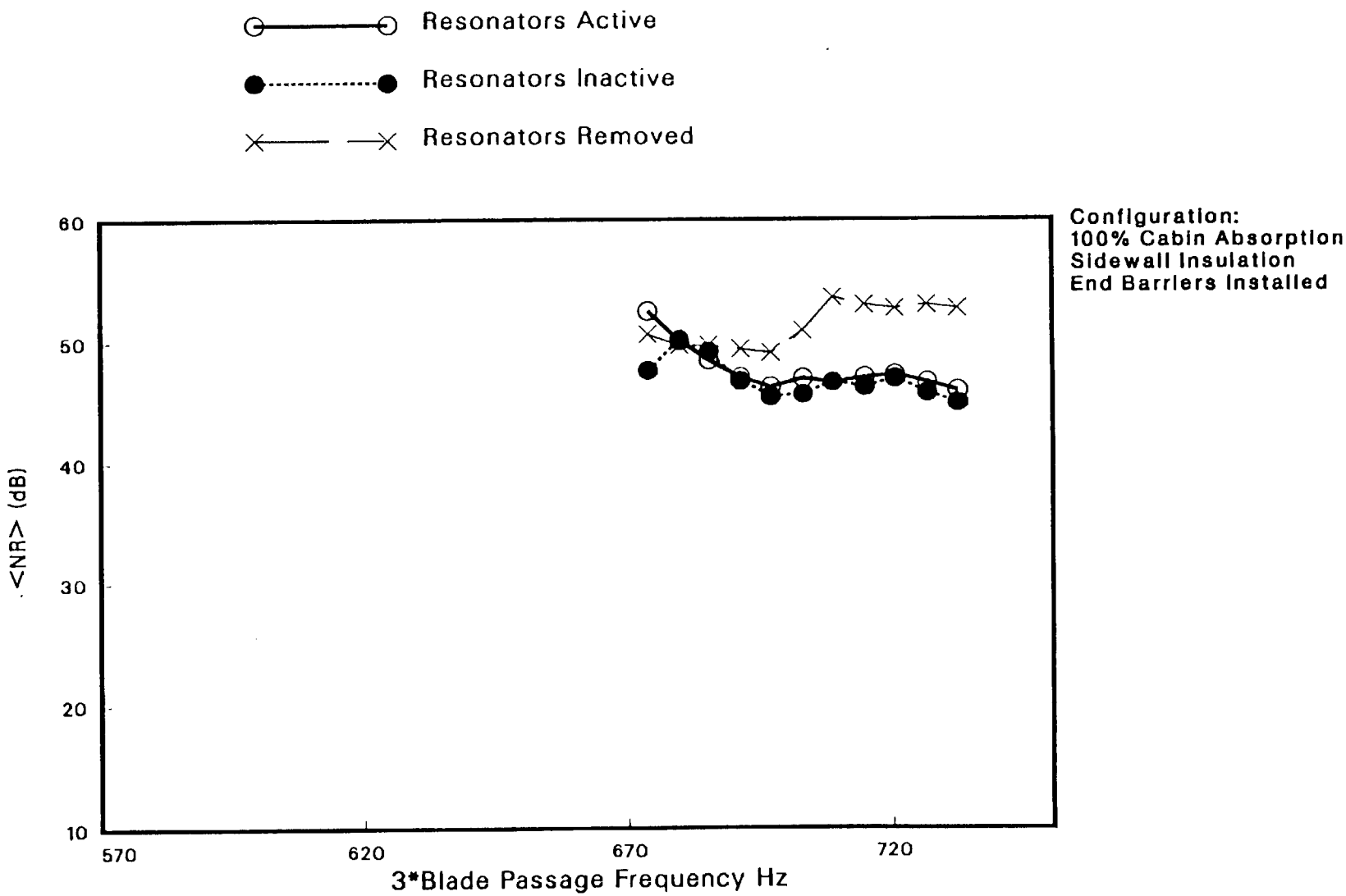

Figure 42: Laboratory test comparison of <NR>s with sidewall resonators active, inactive, and removed - third harmonic tone.

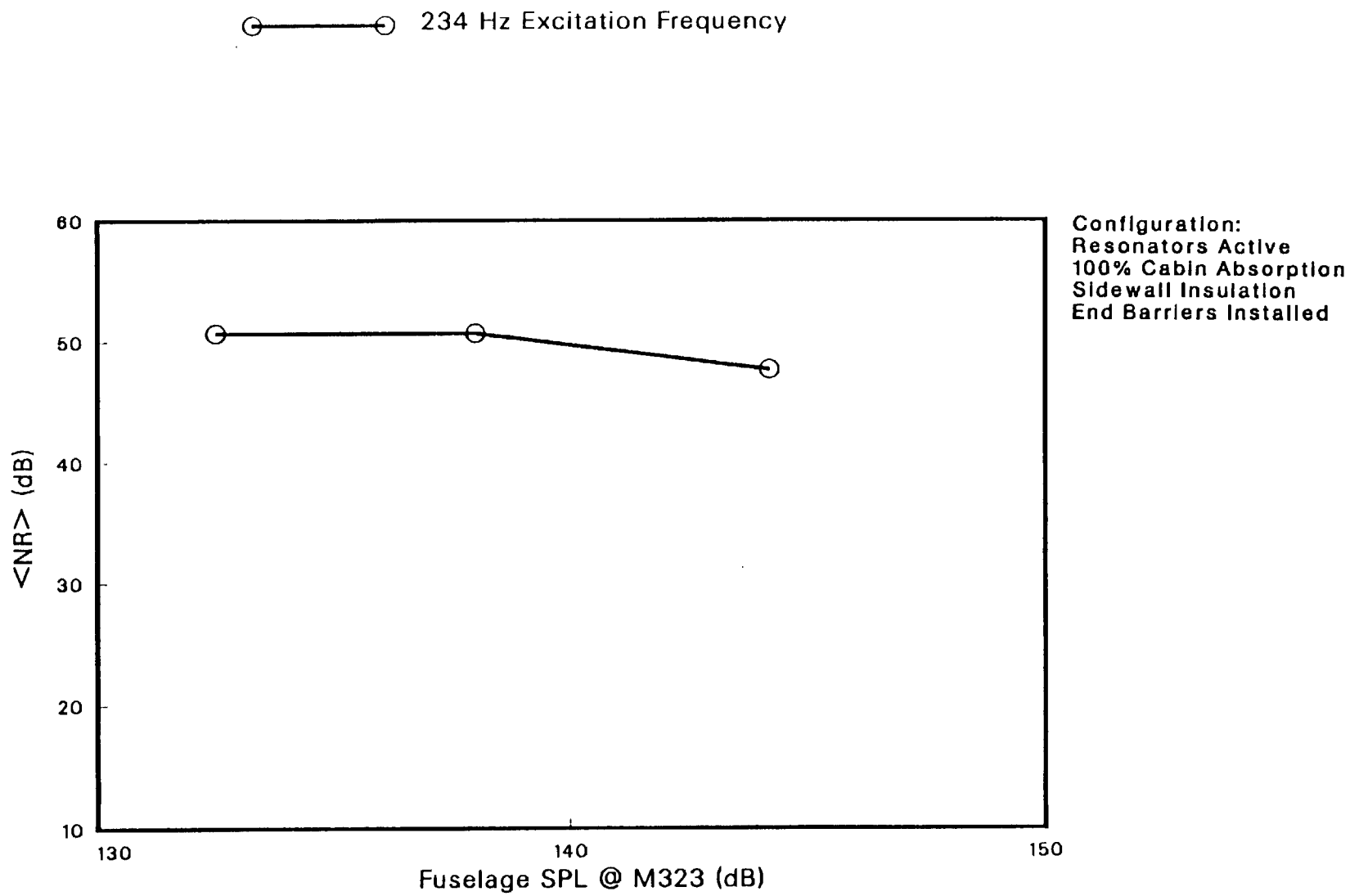

Figure 43: Change in <NR> with input fuselage SPL at M323. Input frequency 234 Hz.

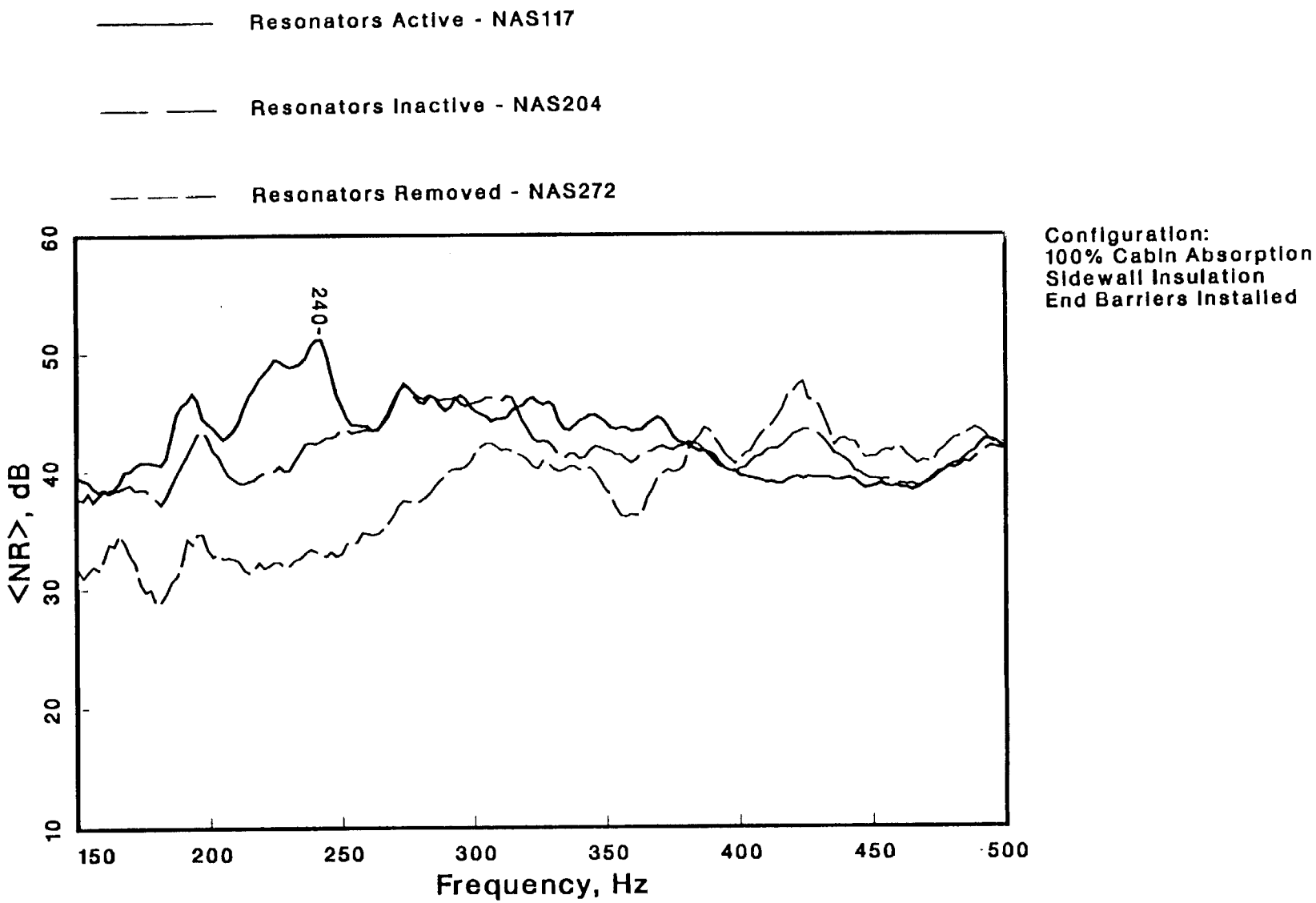

Figure 44: Fuselage/enclosure <NR> obtained in the laboratory with various trim panel configurations - broadband noise excitation.

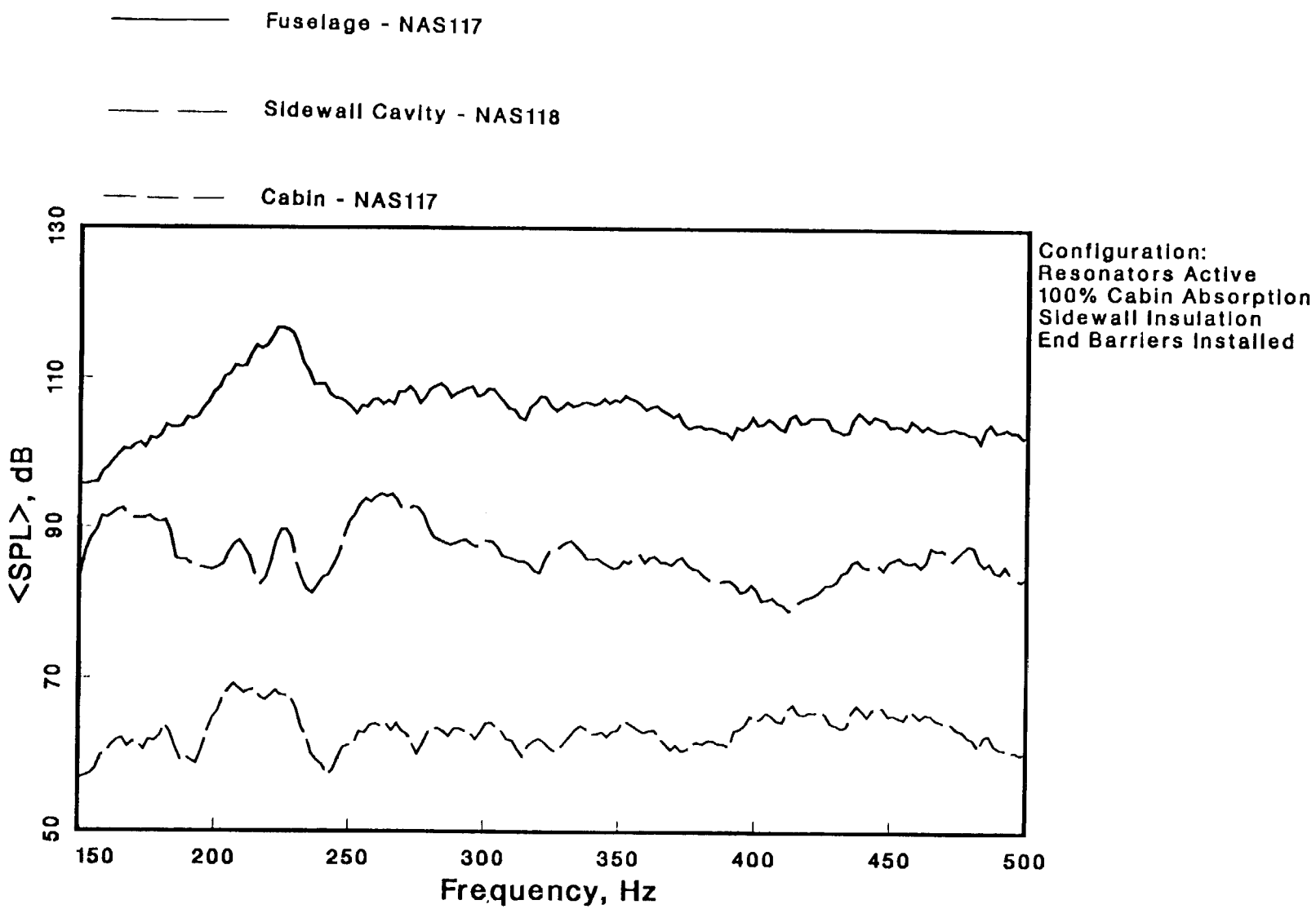

Figure 45: Fuselage, sidewall cavity, and enclosure <SPL> comparisons - resonators active - broadband noise excitation.

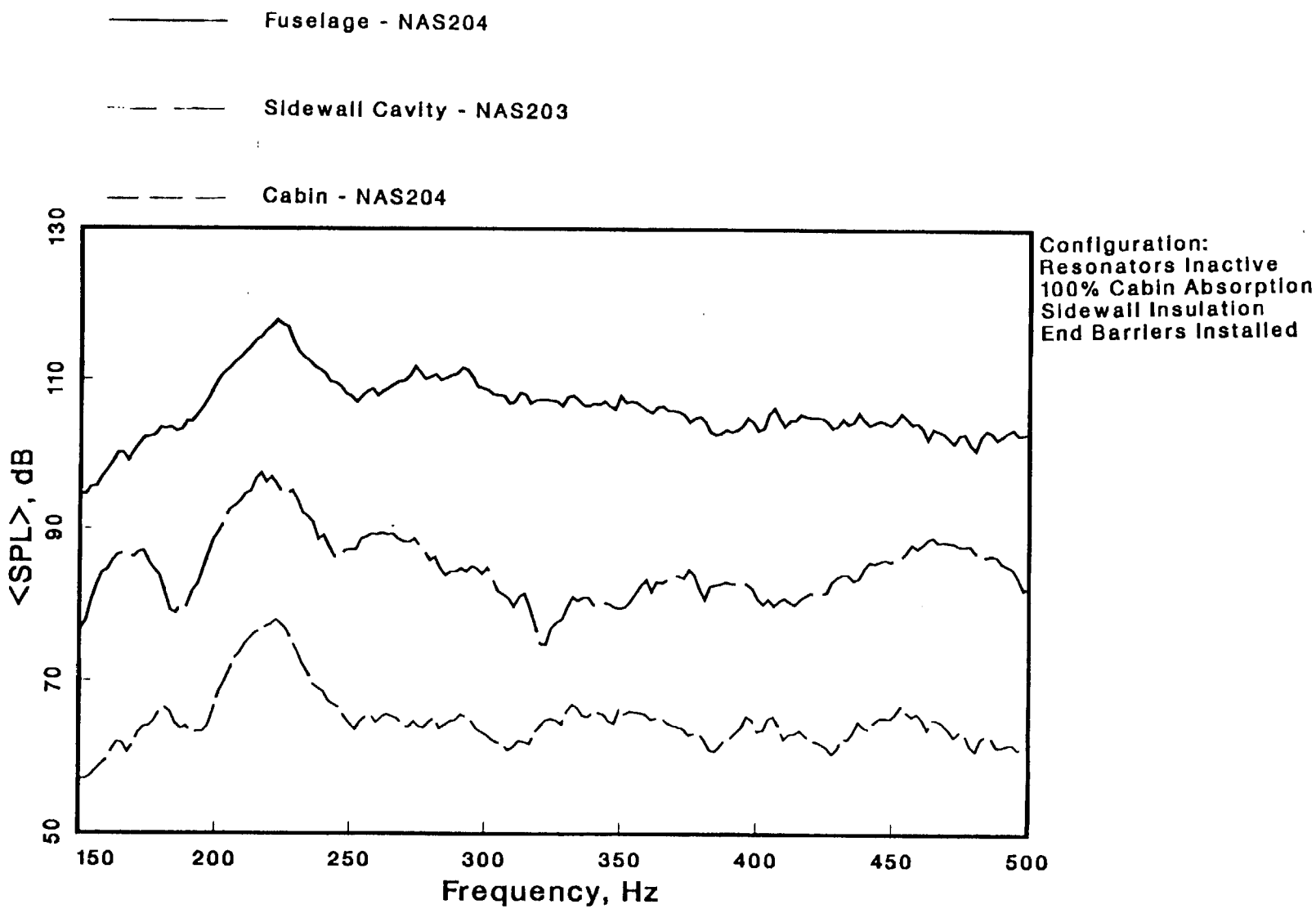

Figure 46: Fuselage, sidewall cavity, and enclosure <SPL> comparisons - resonators inactive.

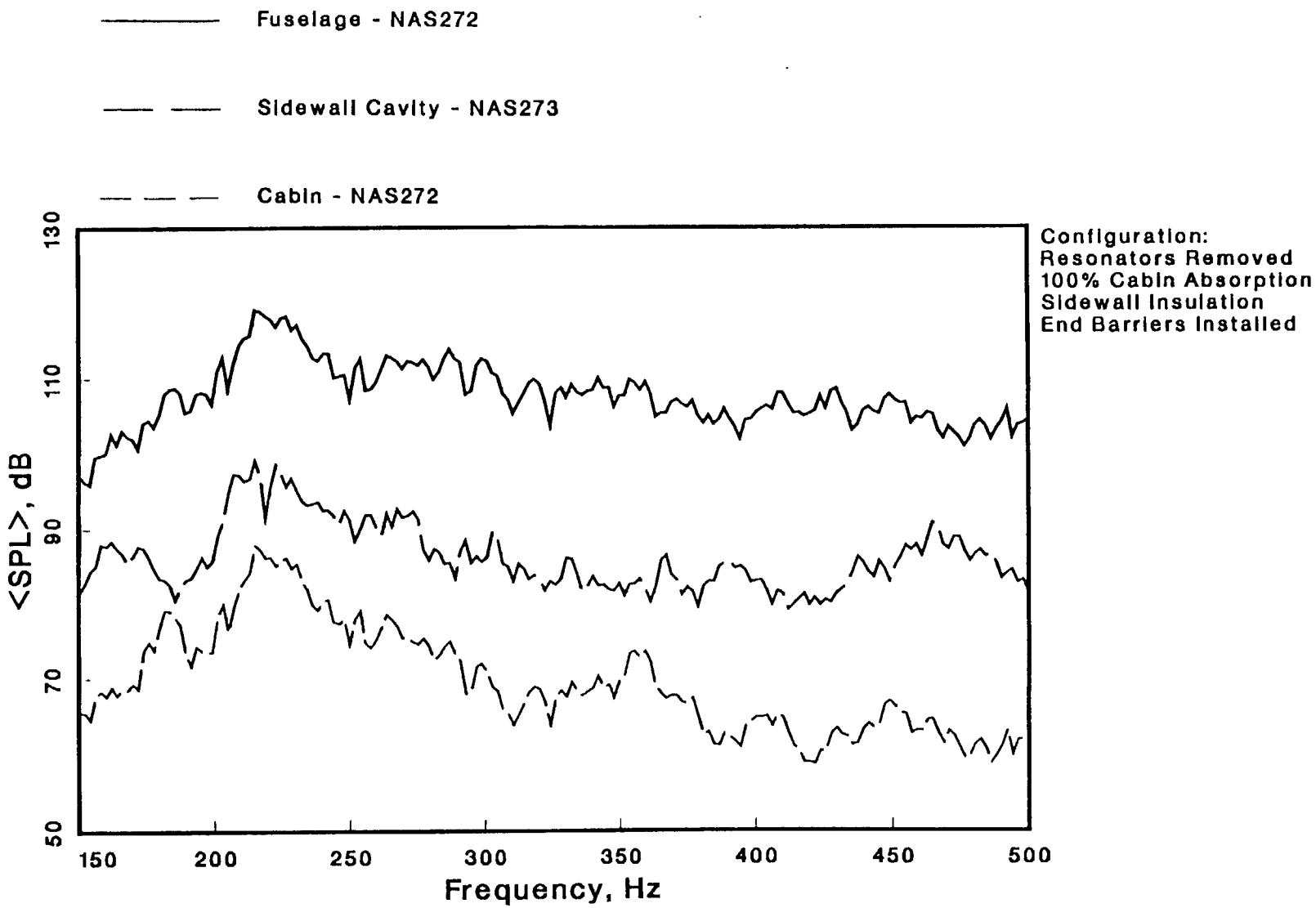

Figure 47: Fuselage, sidewall cavity, and enclosure <SPL> comparisons - resonators removed - broadband noise excitation.

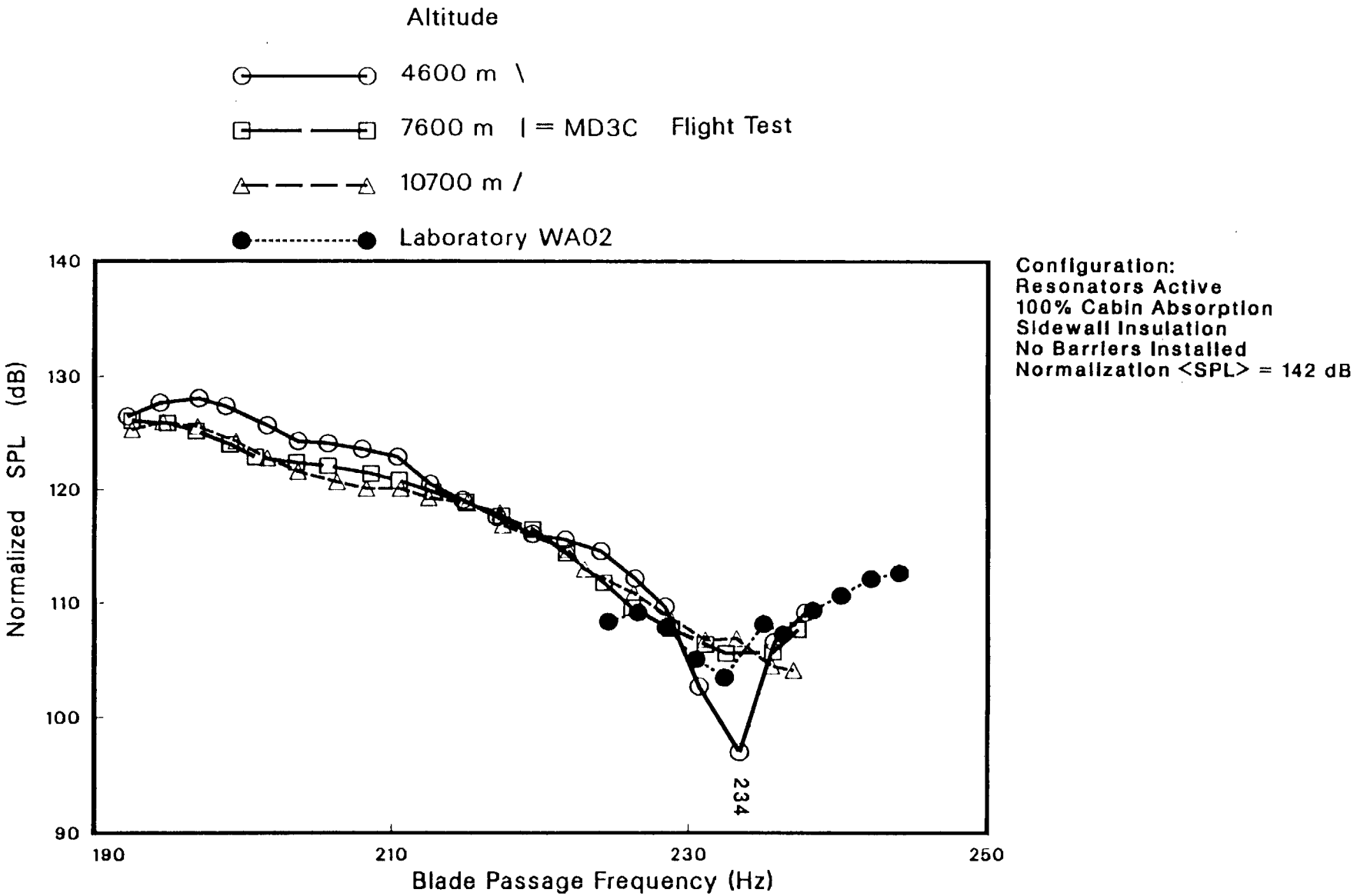

Figure 48: Normalized tonal SPL at sidewall cavity central microphone for flight and laboratory data - fundamental tone.

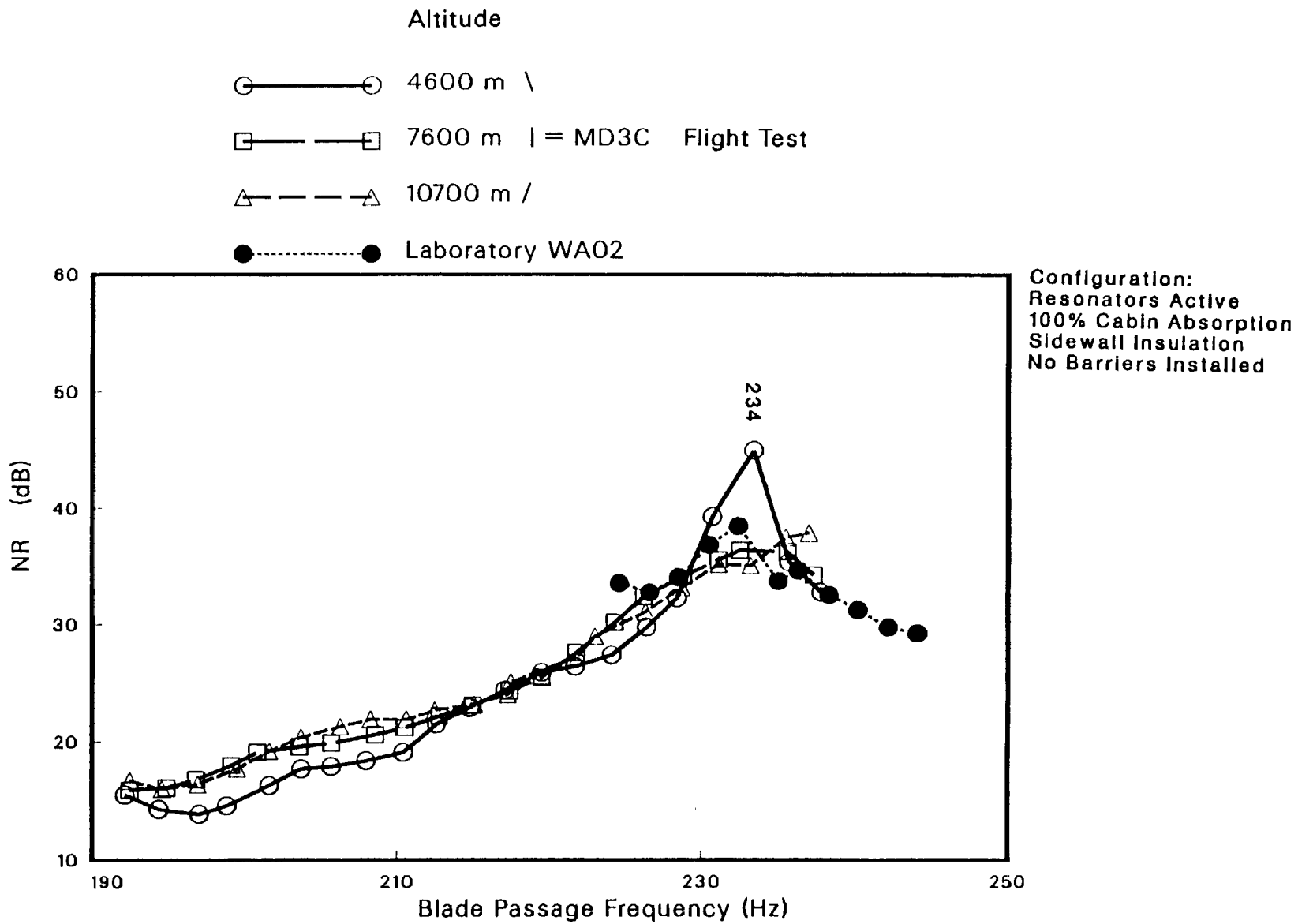

Figure 49: Tonal NR at sidewall cavity central microphone for flight and laboratory data - fundamental tone.

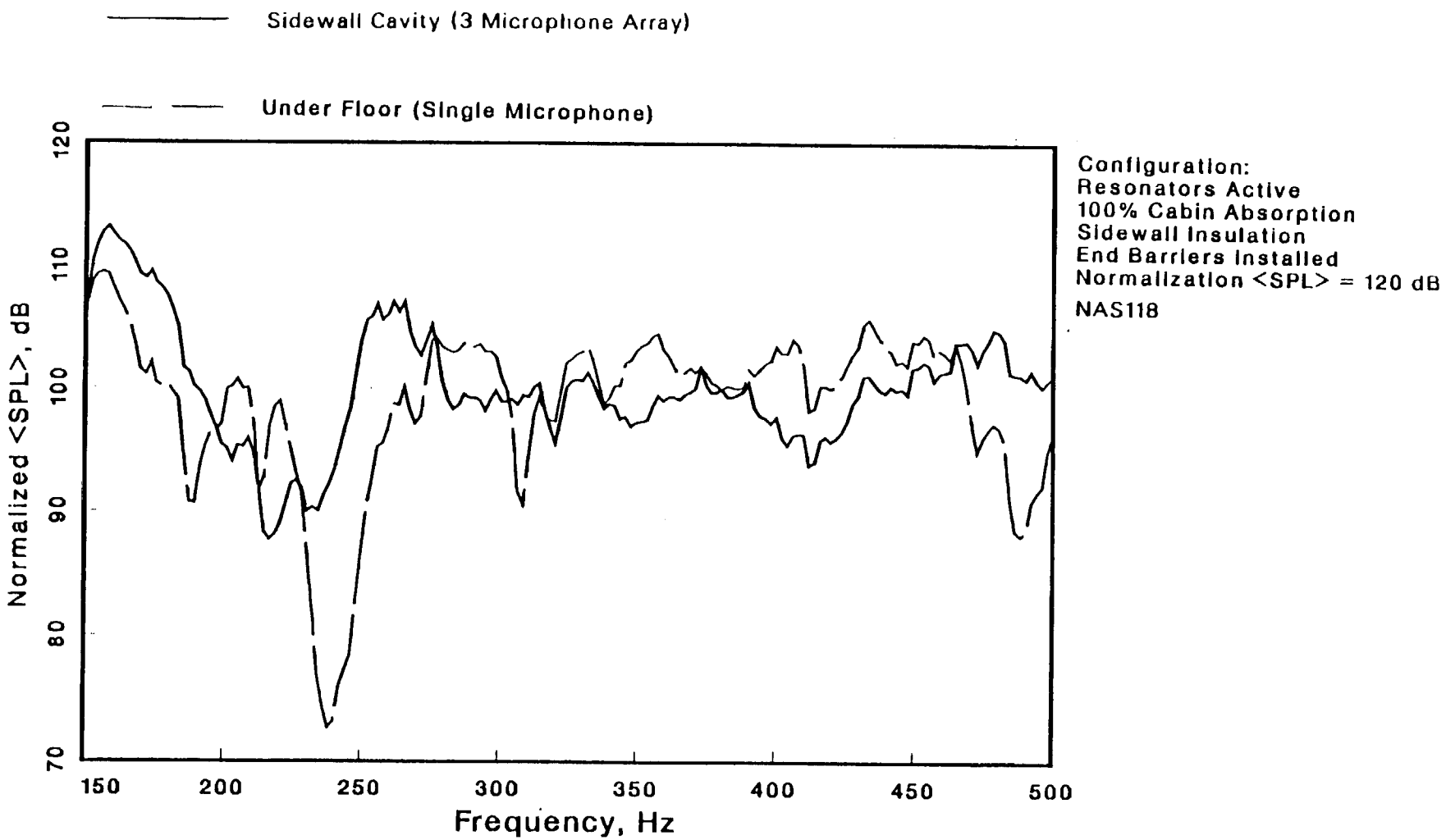

Figure 50: Broadband normalized <SPL> response comparison of sidewall and underfloor spectra - resonators active.

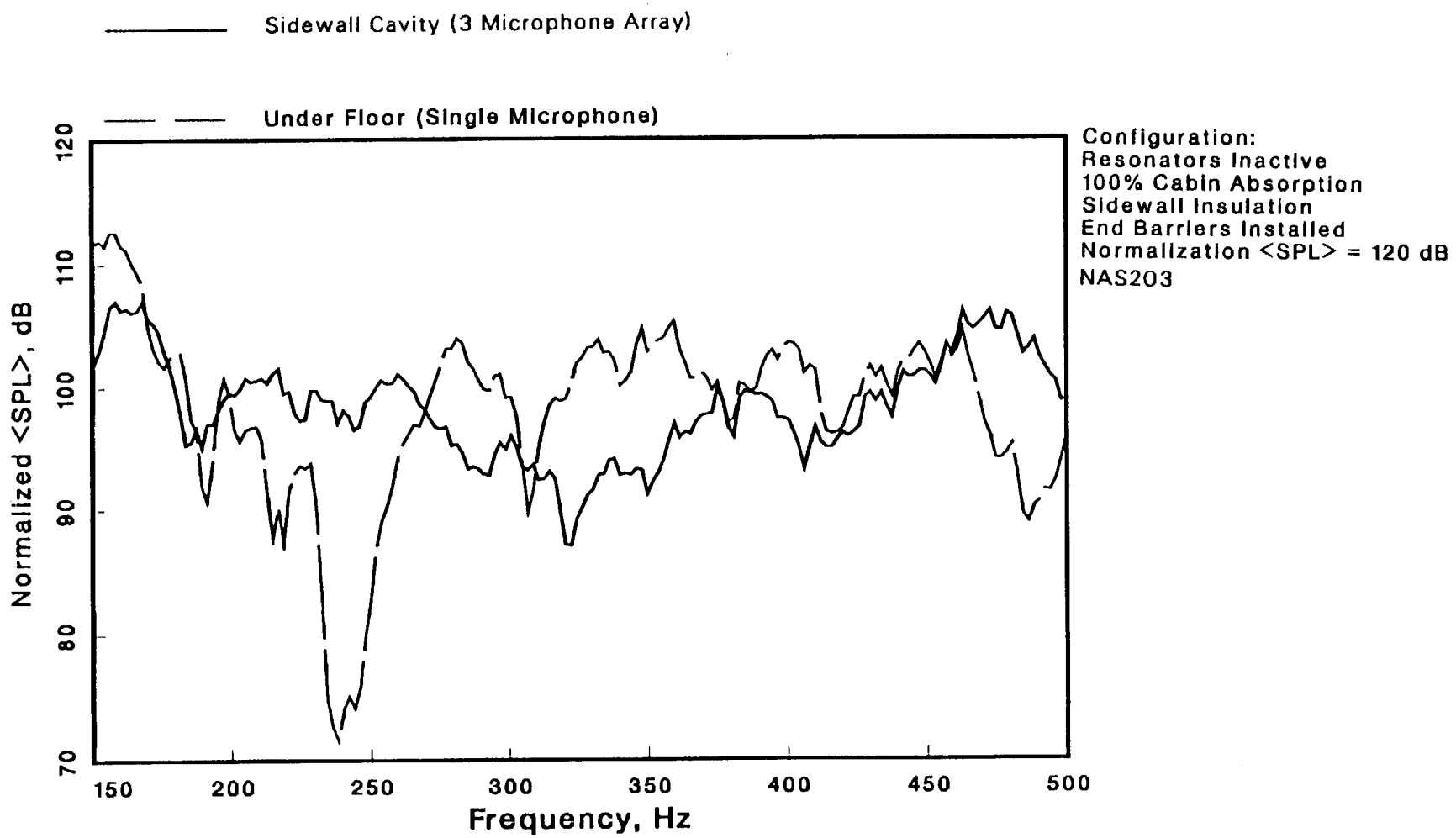

Figure 51: Broadband normalized <SPL> response comparison of sidewall and underfloor spectra - sidewall resonators inactive.

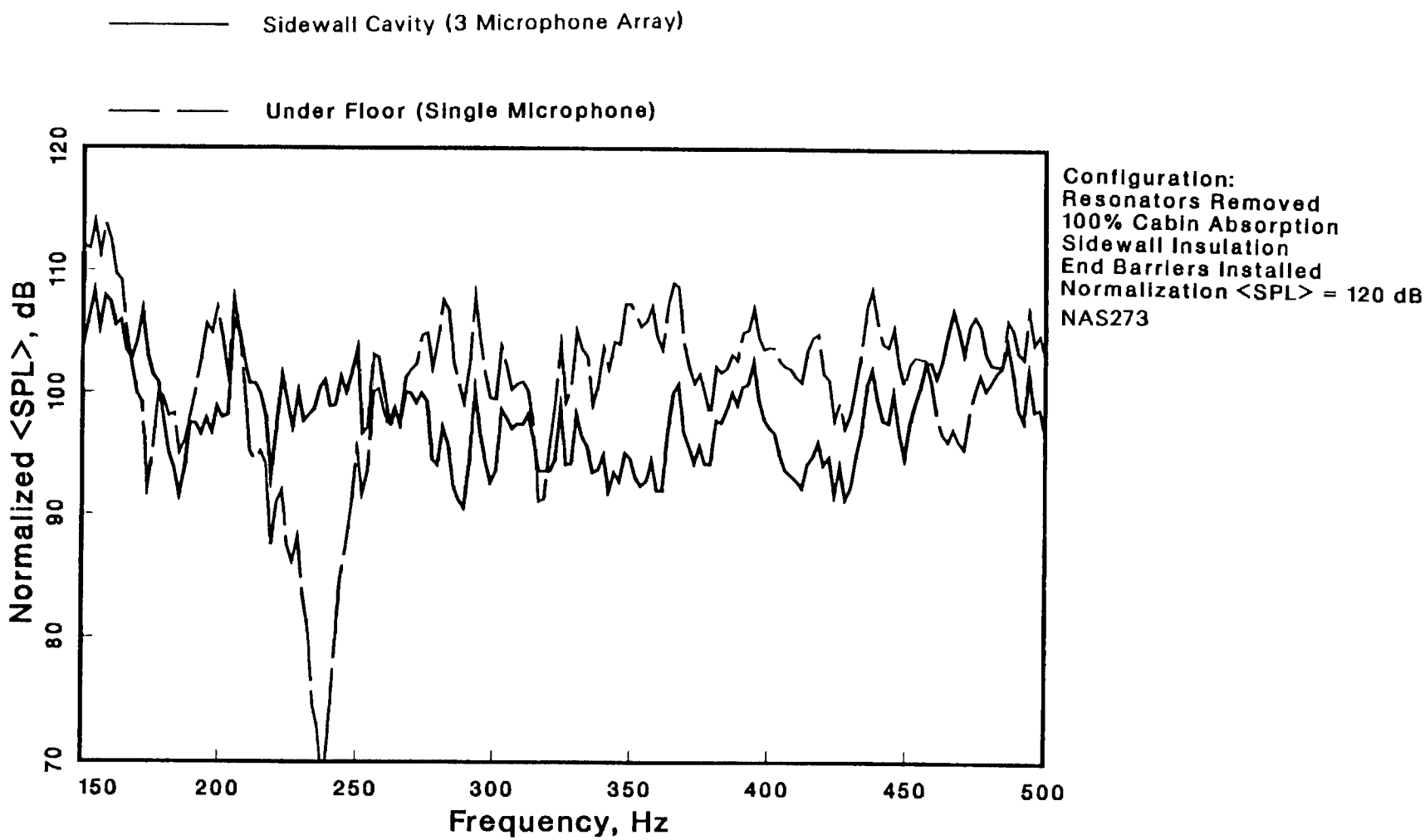

Figure 52: Broadband normalized <SPL> response comparison of sidewall and underfloor spectra - sidewall resonators removed.

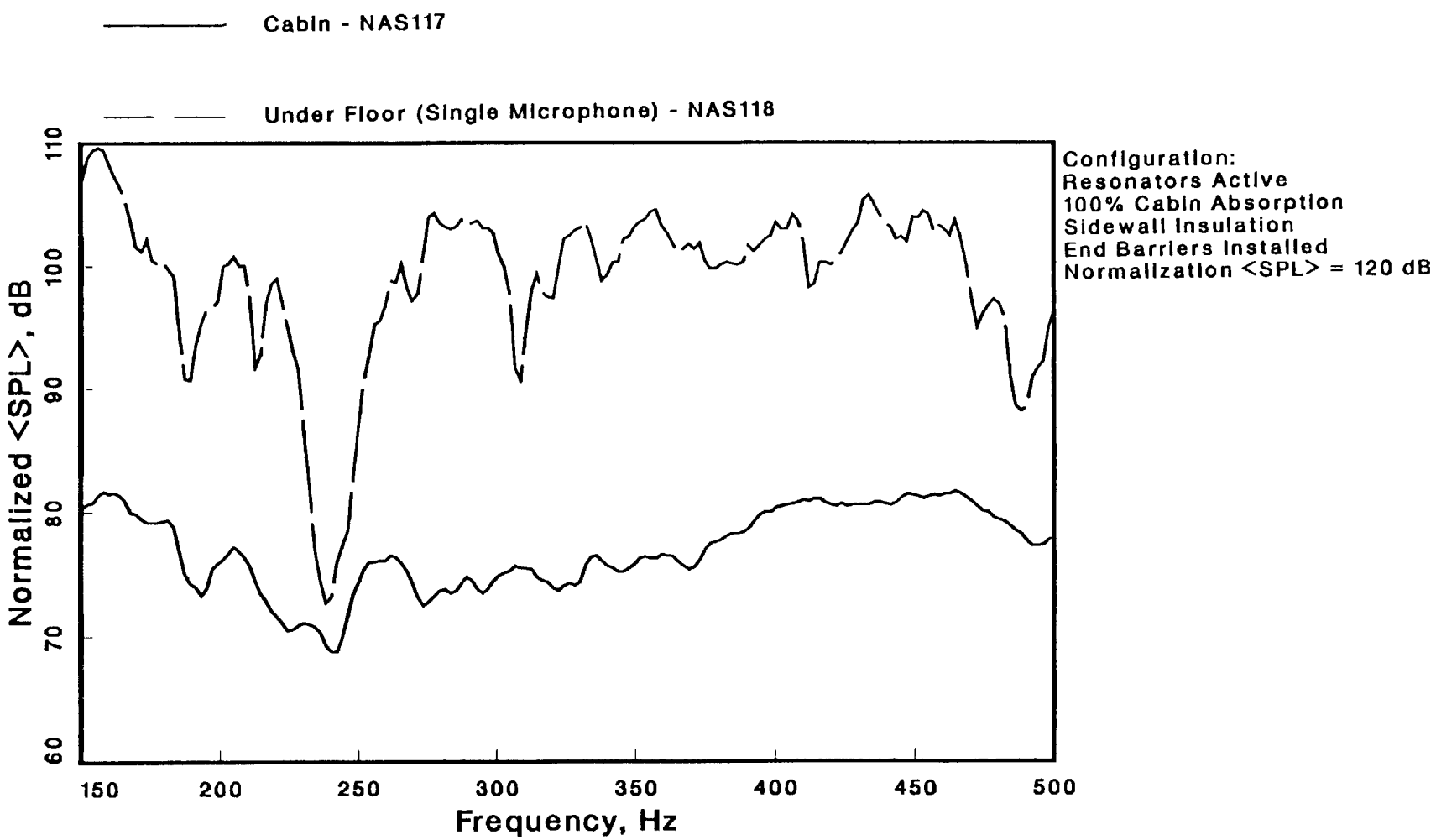

Figure 53: Broadband normalized <SPL> response comparison of enclosure and underfloor spectra - resonators active.

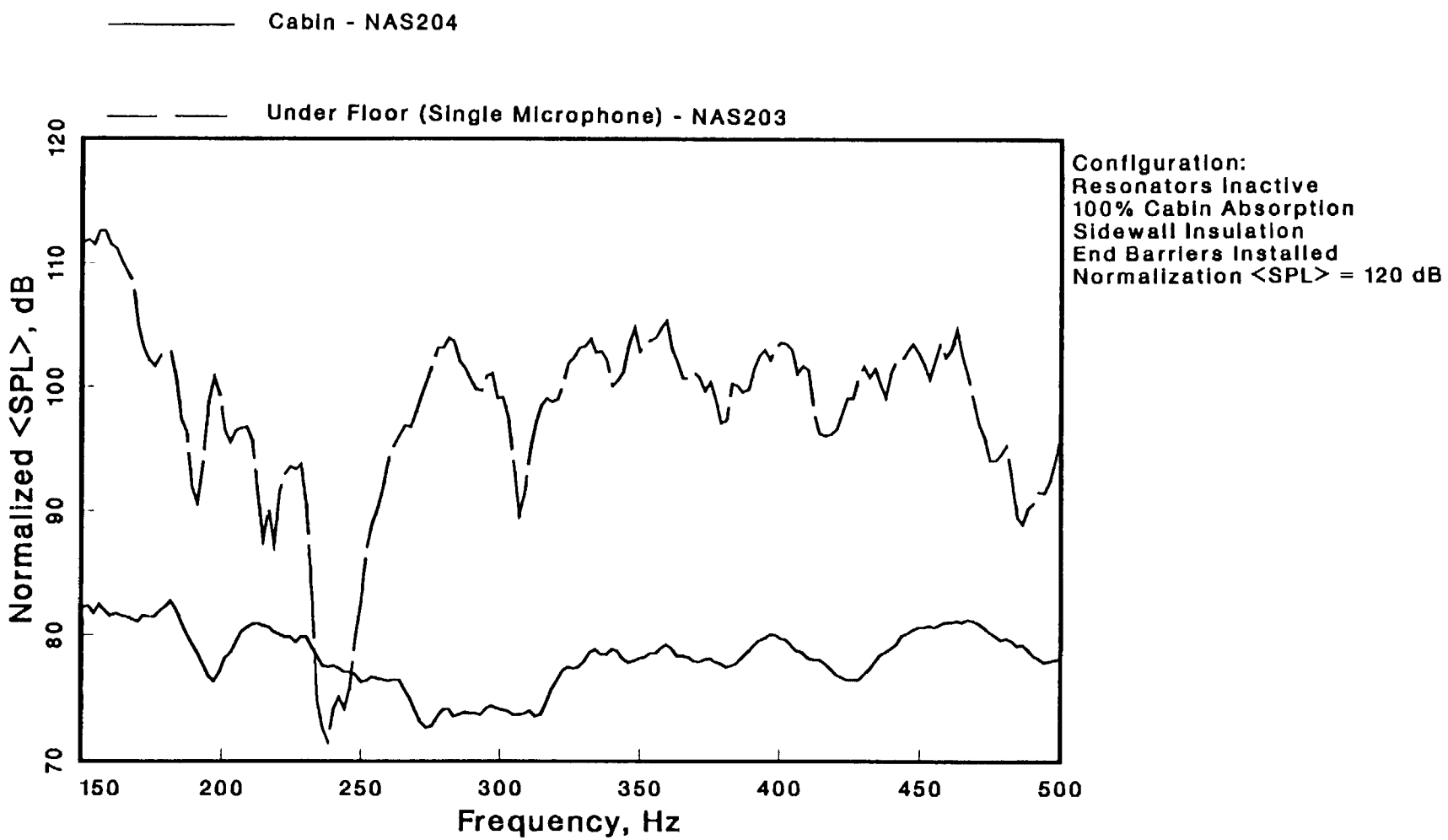

Figure 54: Broadband normalized <SPL> response comparison of enclosure and underfloor spectra - sidewall resonators inactive.

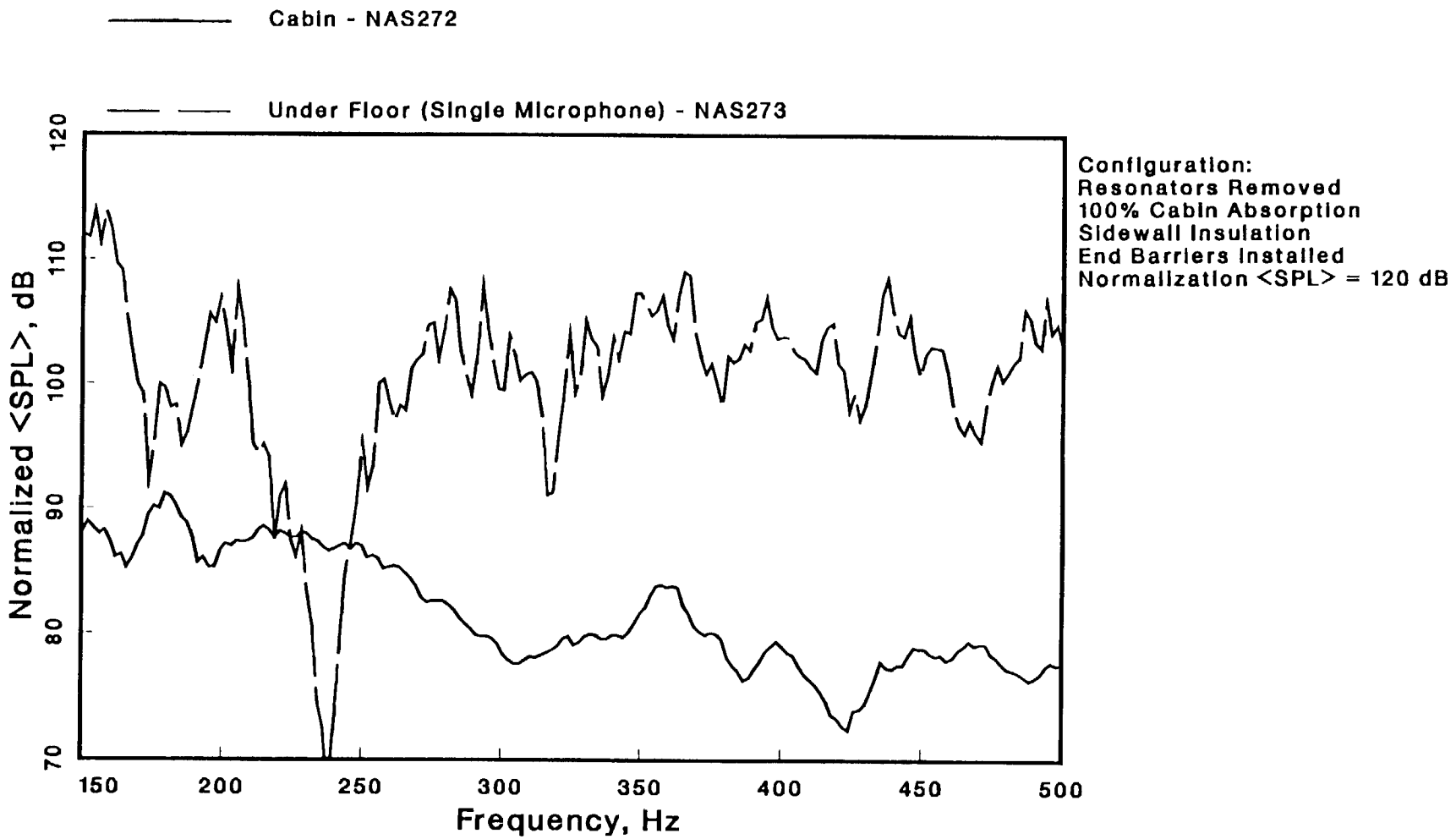

Figure 55: Broadband normalized <SPL> response comparison of enclosure and underfloor spectra - sidewall resonators removed.

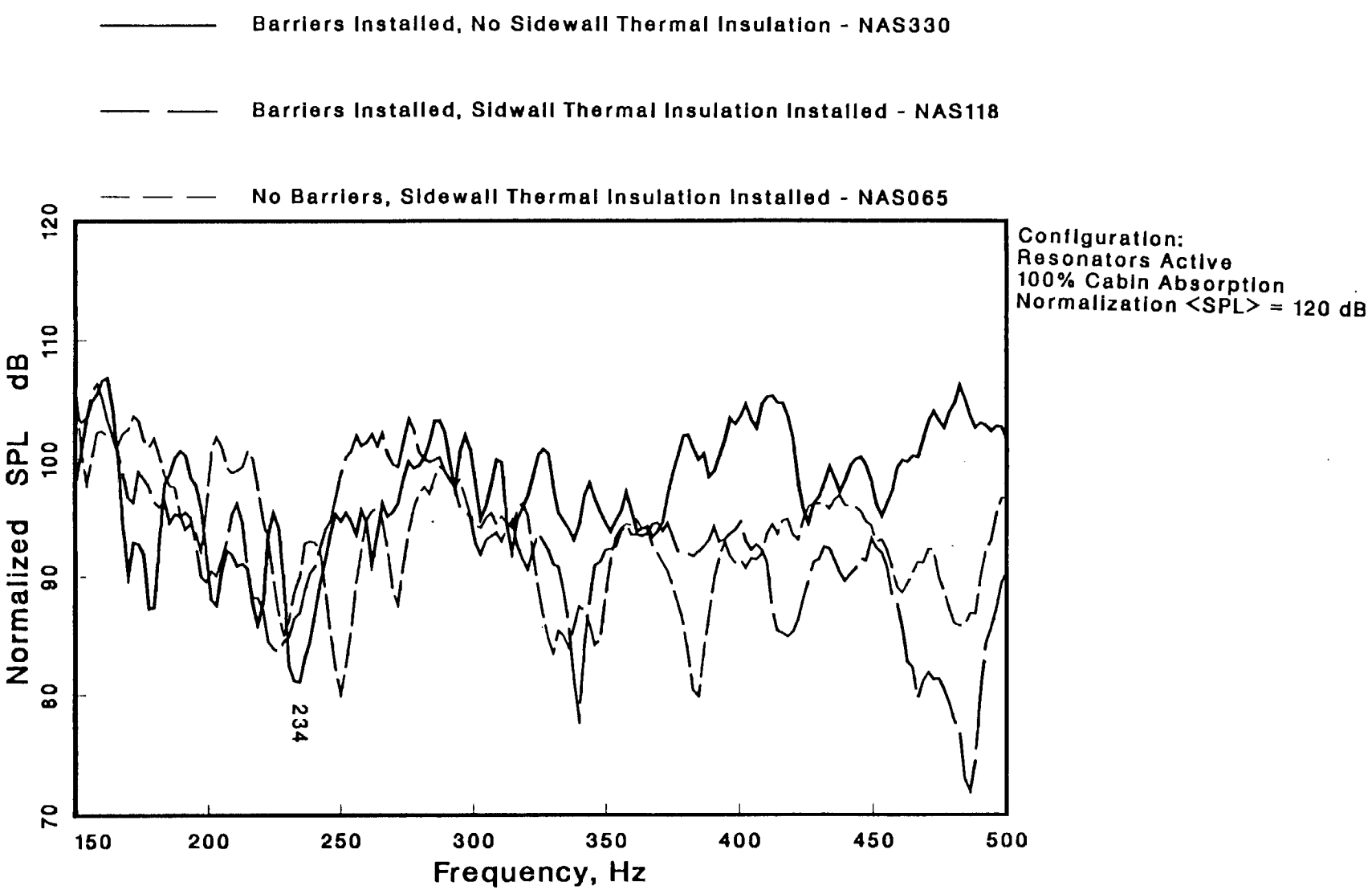

Figure 56: Forward sidewall cavity microphone (WA01) normalized response to sidewall configuration variables - broadband noise excitation.

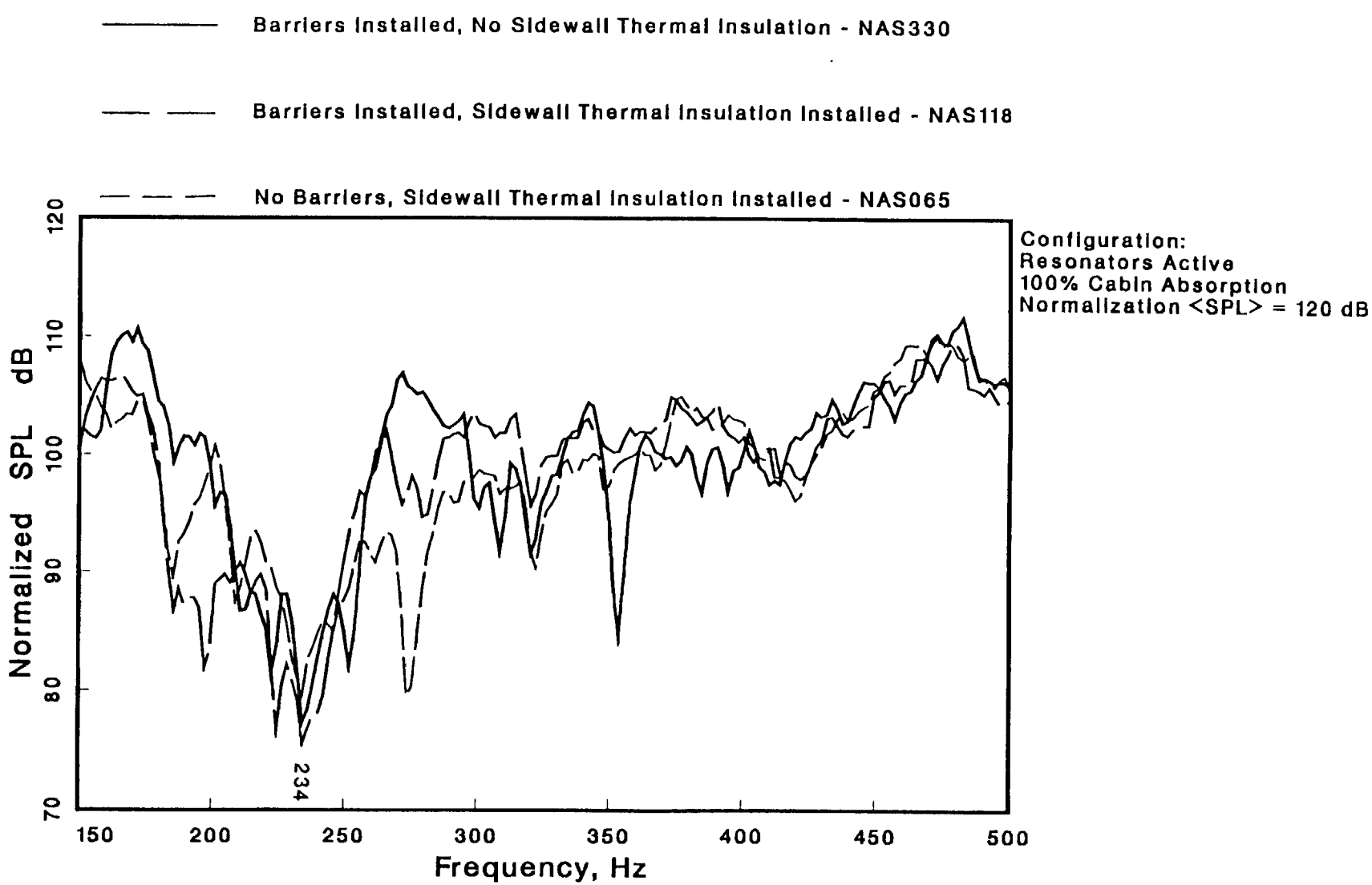

Figure 57: Central sidewall cavity microphone (WA02) normalized response to sidewall configuration variables - broadband noise excitation.

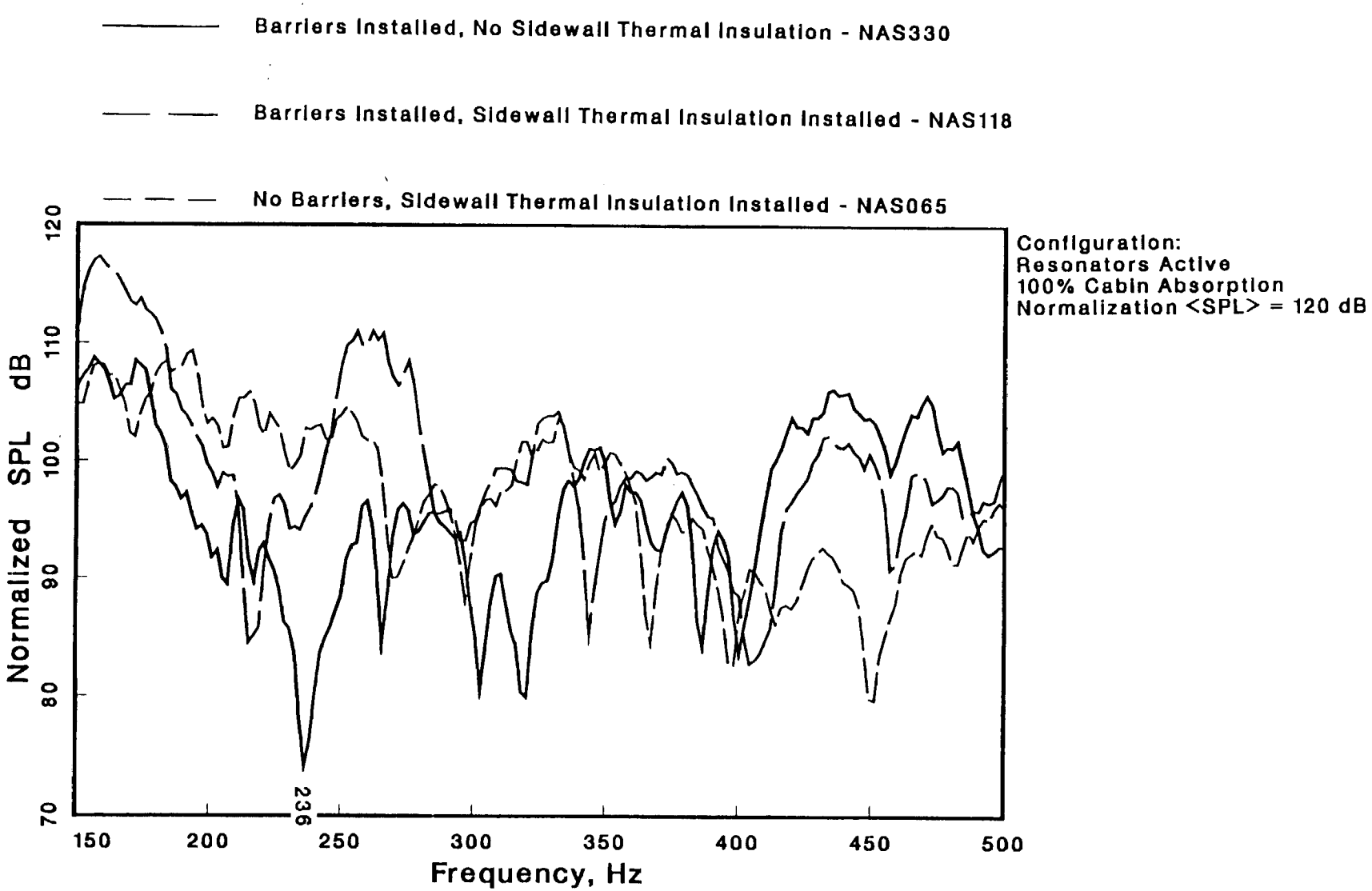

Figure 58: Aft sidewall cavity microphone (WA03) normalized response to sidewall configuration variables - broadband noise excitation.

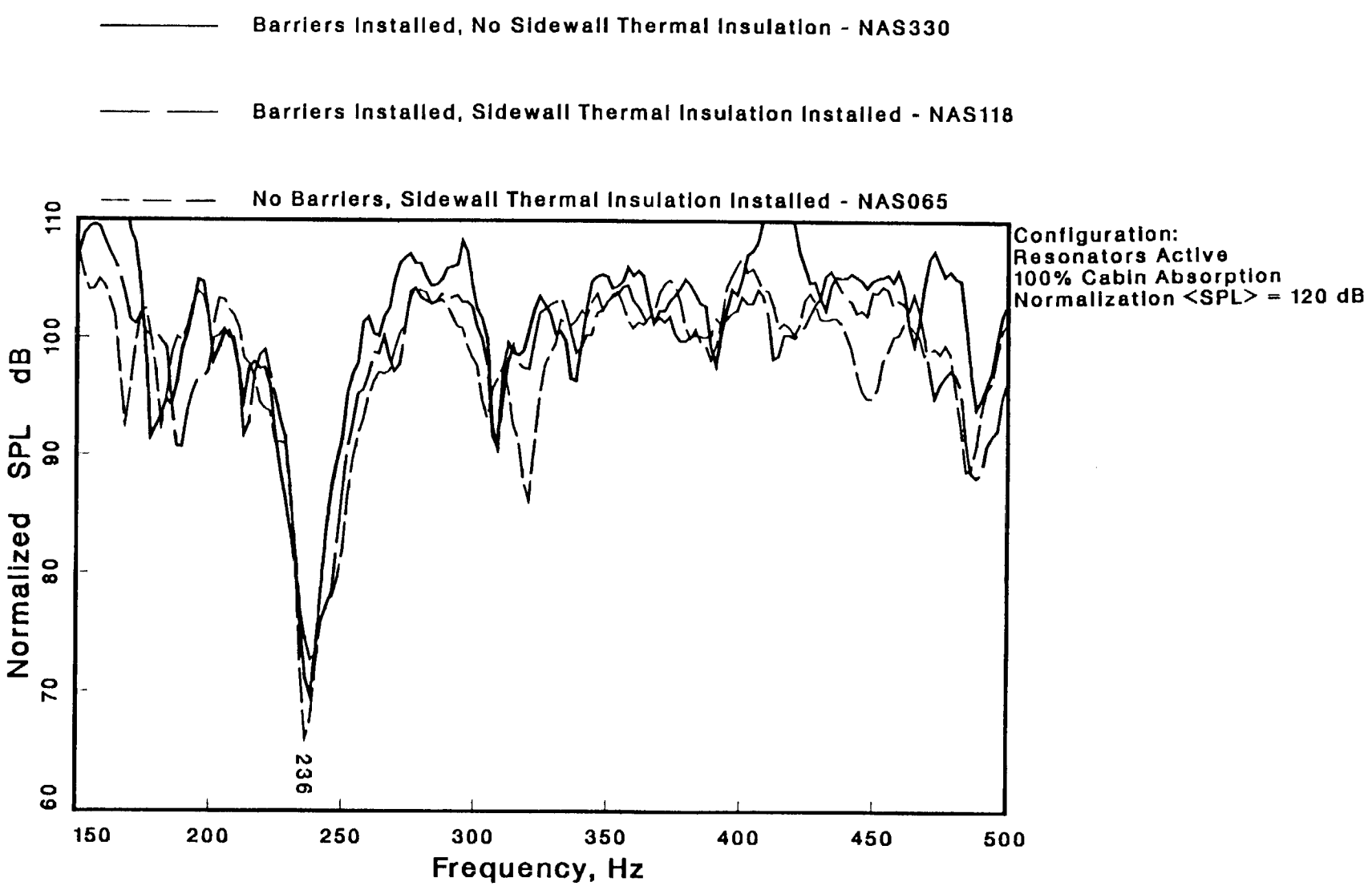

Figure 59: Central under-floor microphone (FL01) normalized response to sidewall configuration variables - broadband noise excitation.

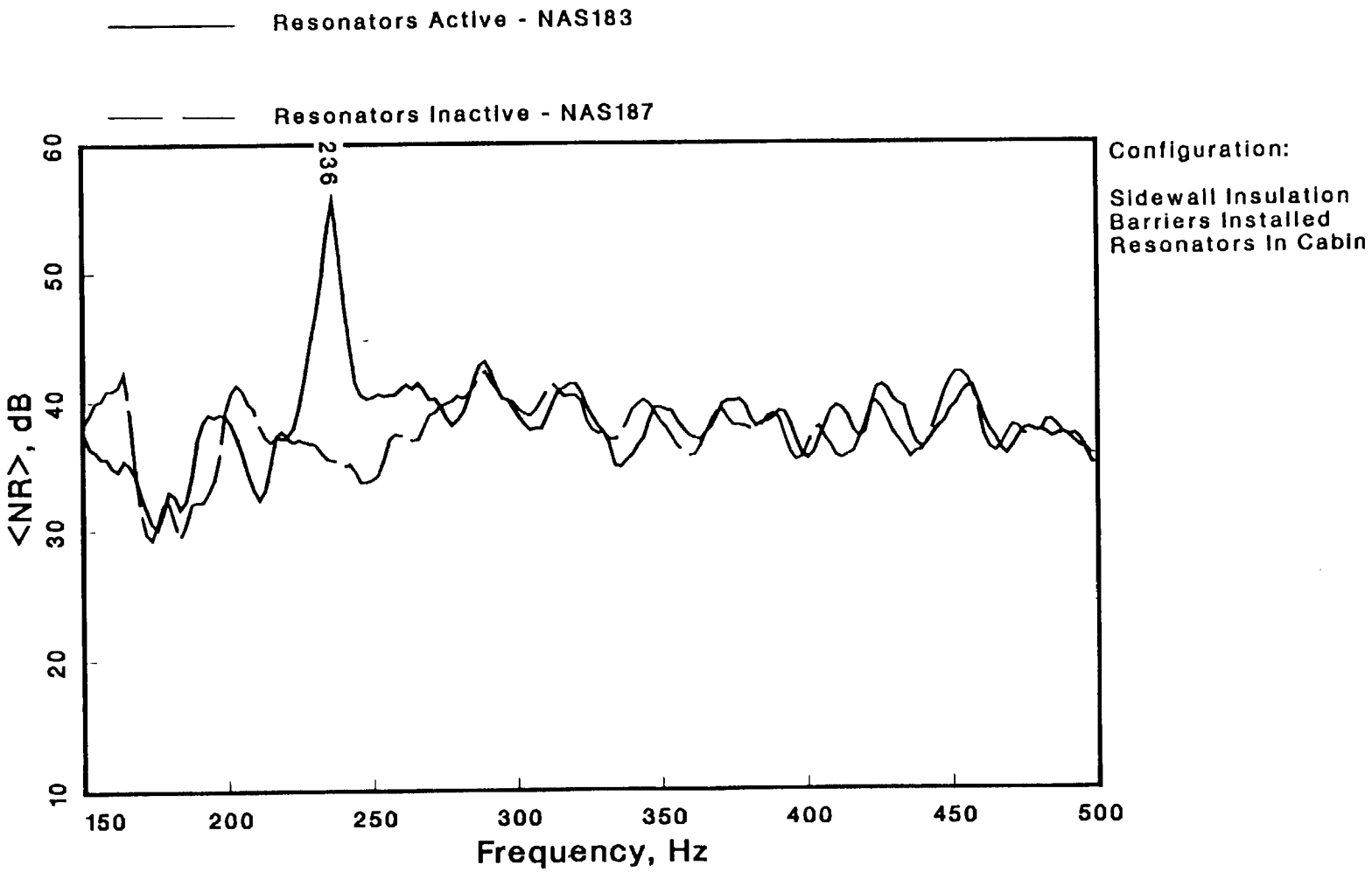

Figure 60: <NR> for the enclosure with resonators, active and inactive, attached to the inner surfaces of the enclosure trim panels - broadband noise excitation.

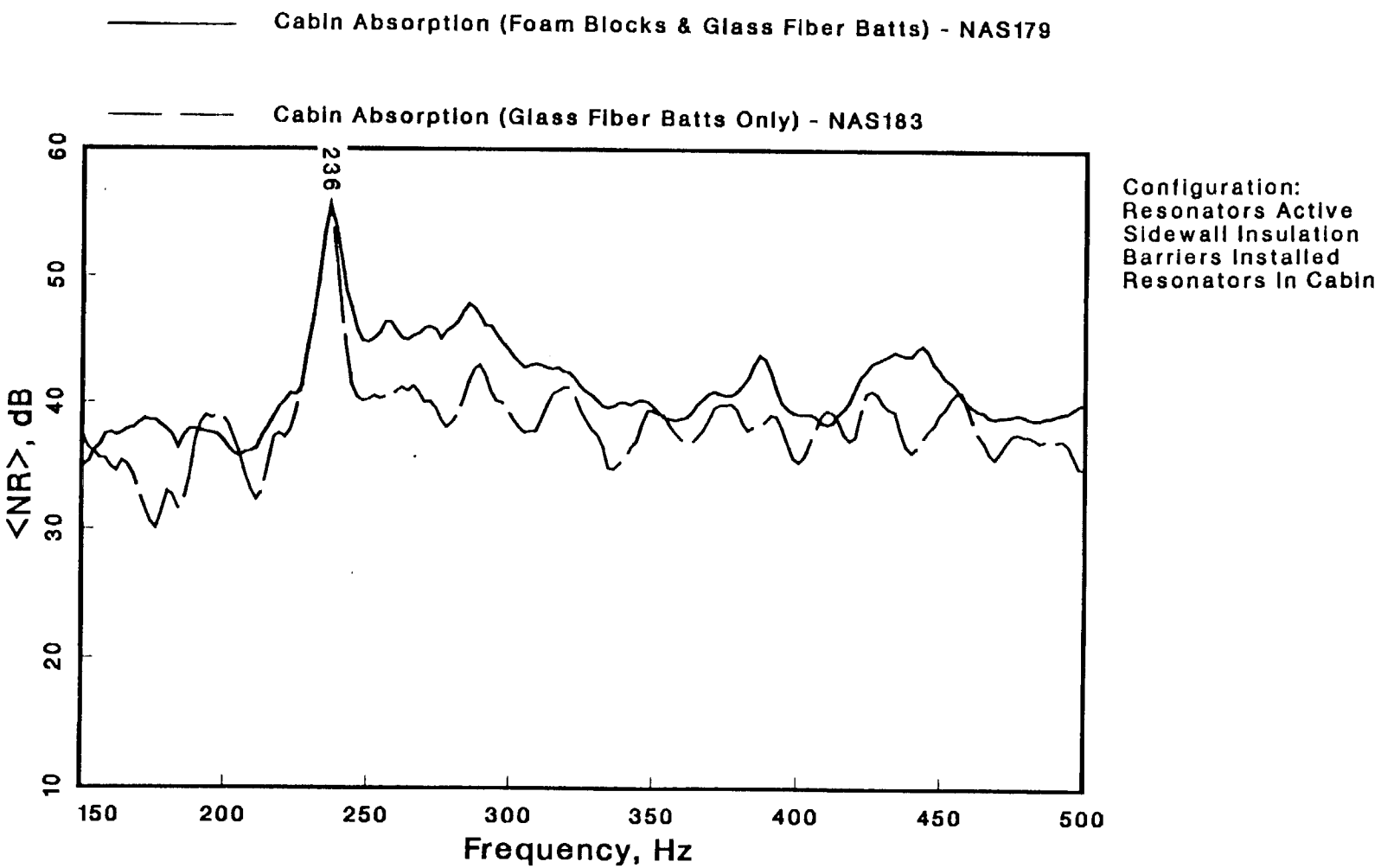

Figure 61: <NR> for the enclosure with active resonators attached to the inner surfaces of the enclosure trim panels, with and without cabin absorption - broadband noise excitation.

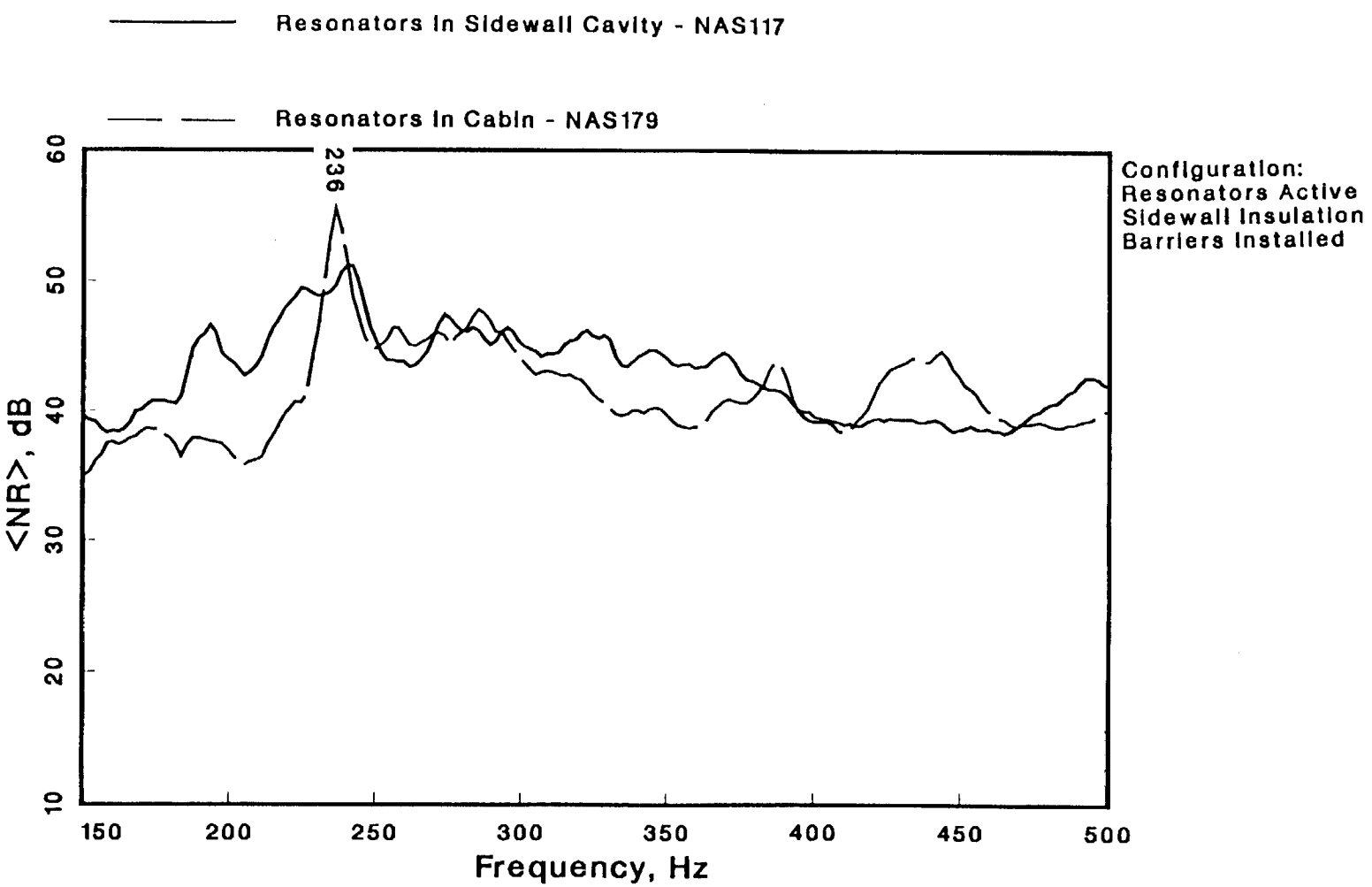

Figure 62: <NR> for the enclosure with active resonators within sidewall versus active resonators within enclosure - broadband noise excitation.

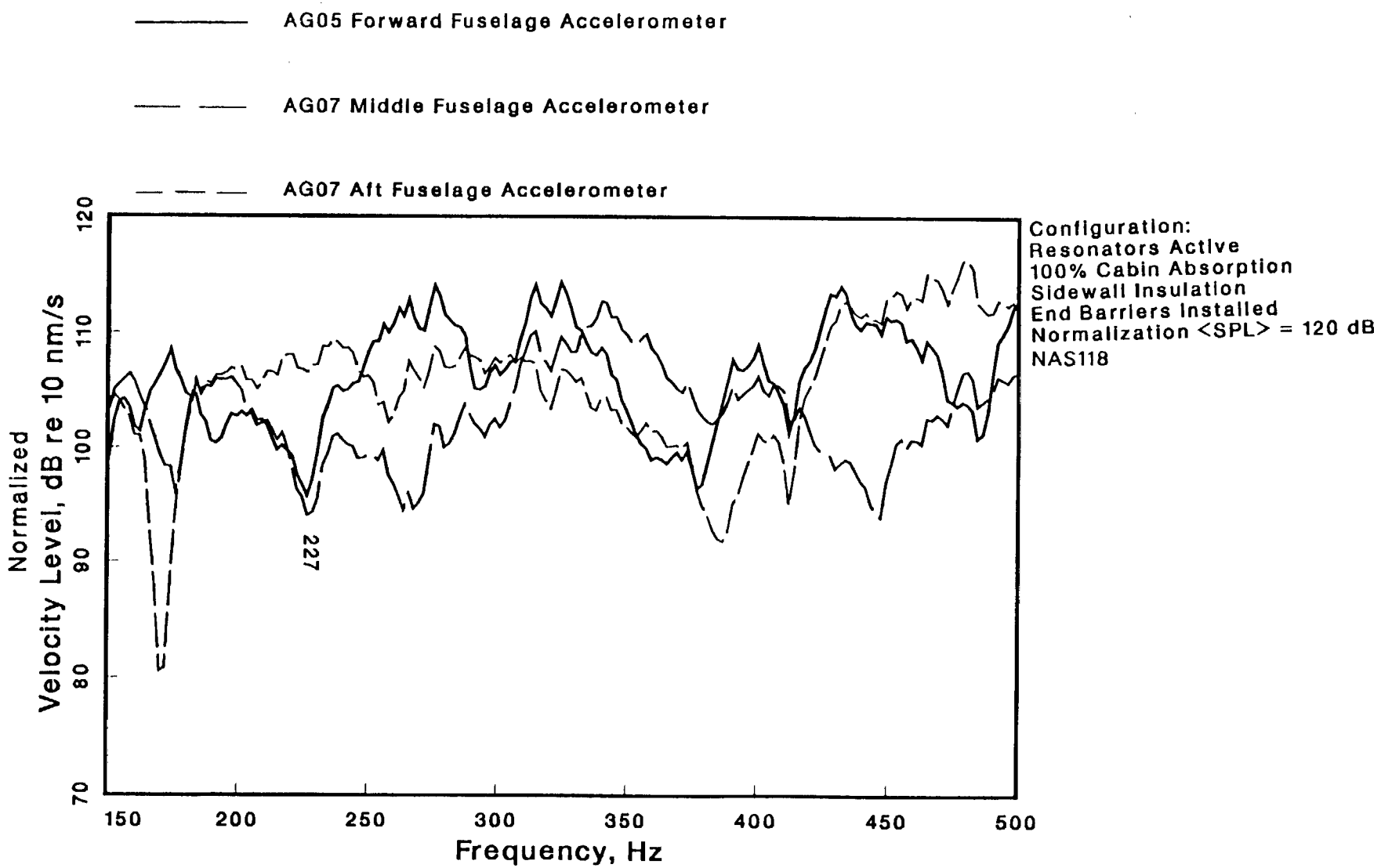

Figure 63: Fuselage shell radial vibration velocity levels at WL113; FS262, FS319, and FS353 - resonators active.

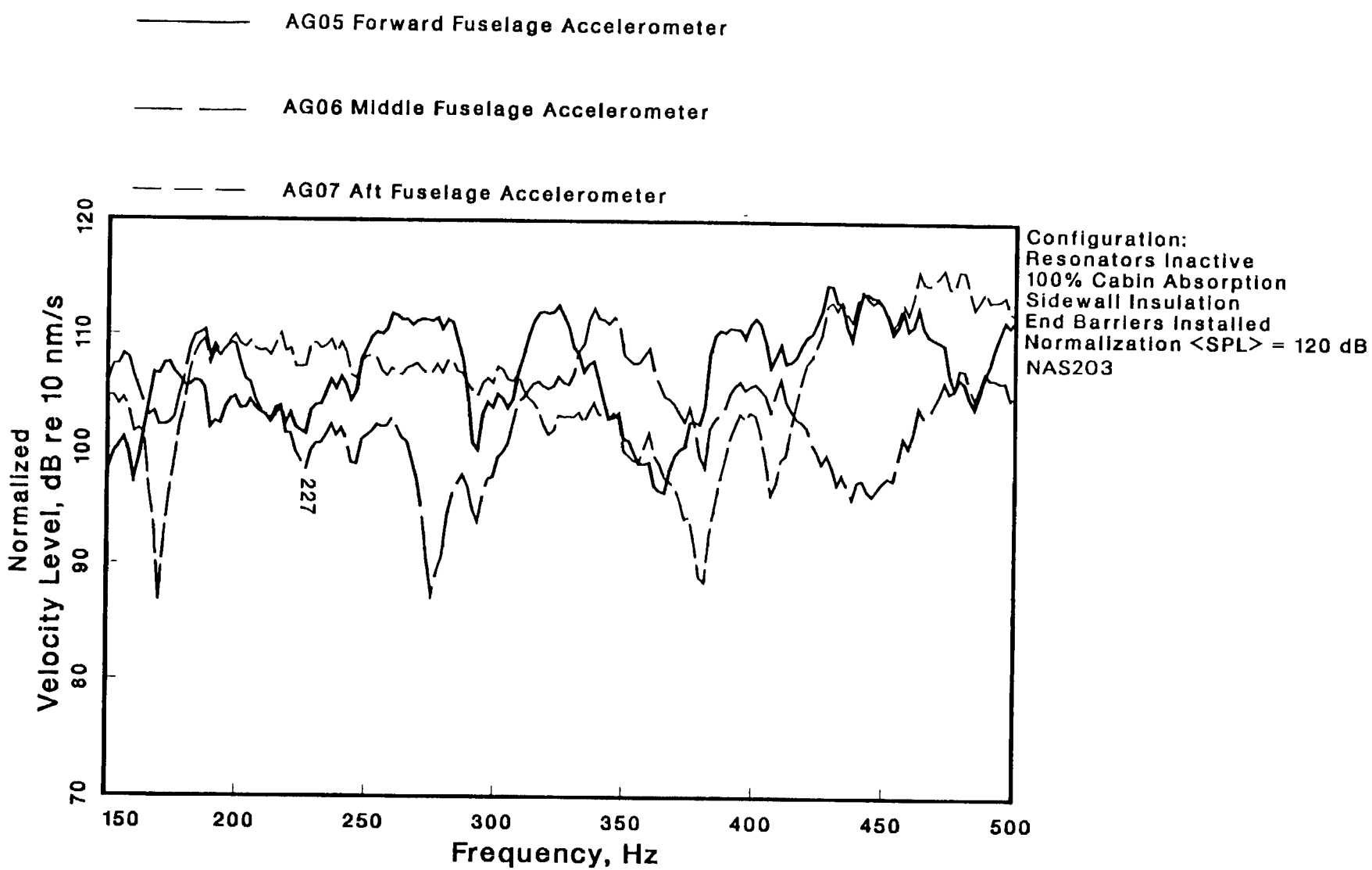

Figure 64: Fuselage shell radial vibration velocity levels at WL113; FS262, FS319, and FS353 - resonators inactive.

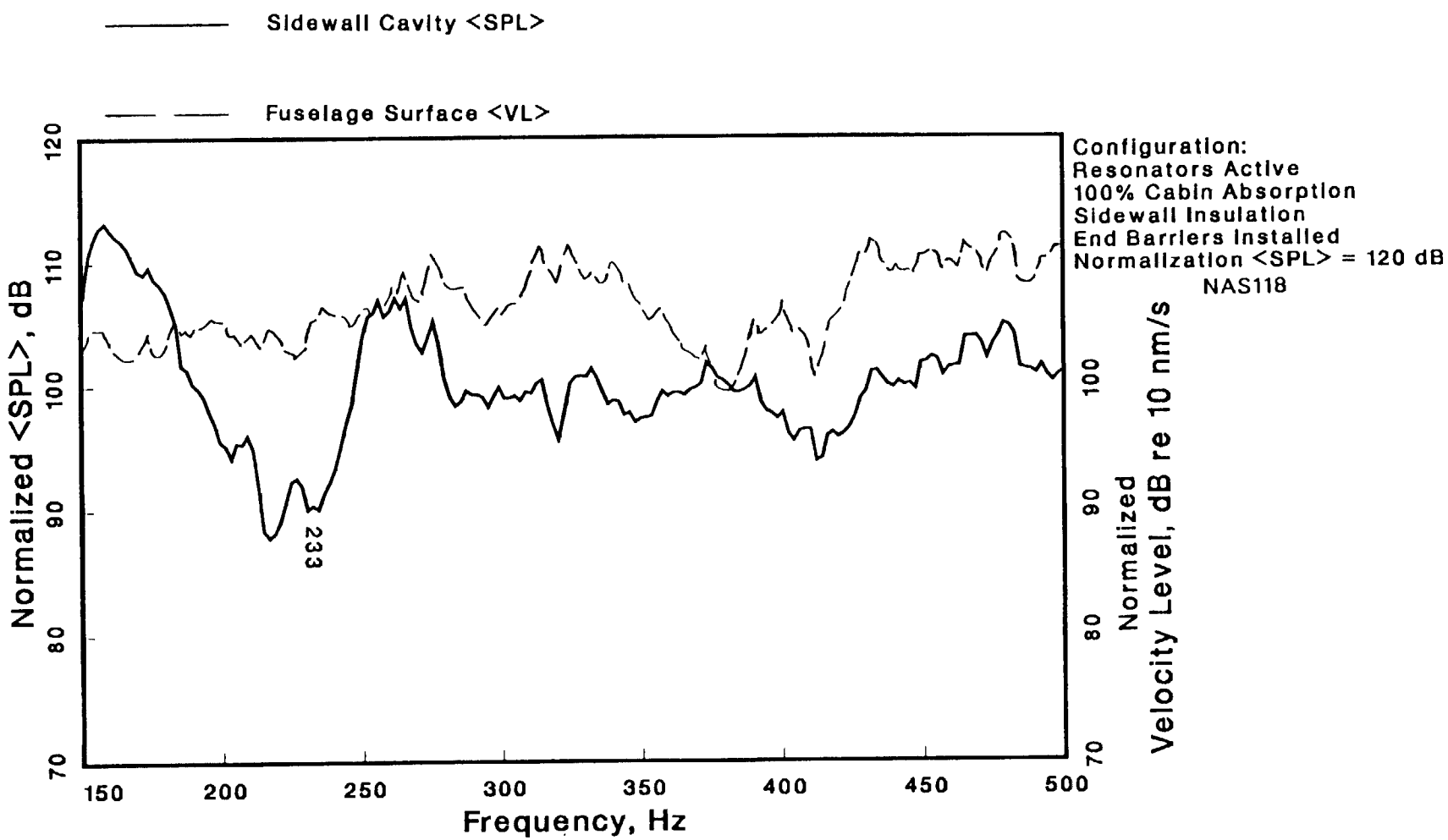

Figure 65: Average fuselage shell sidewall radial vibration velocity level versus sidewall cavity <SPL> - resonators active.

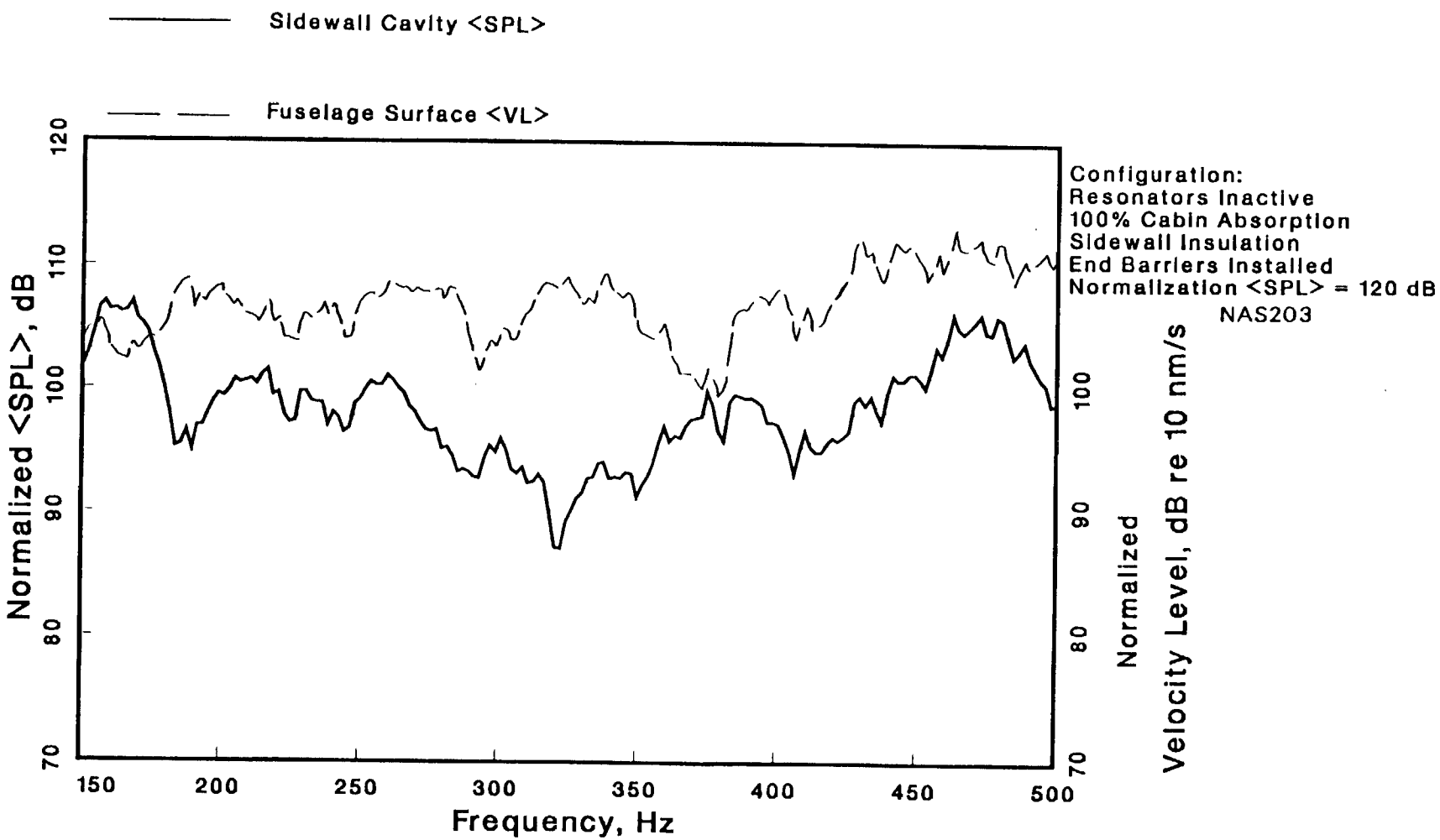

Figure 66: Average fuselage shell sidewall radial vibration velocity level versus sidewall cavity <SPL> - resonators inactive.

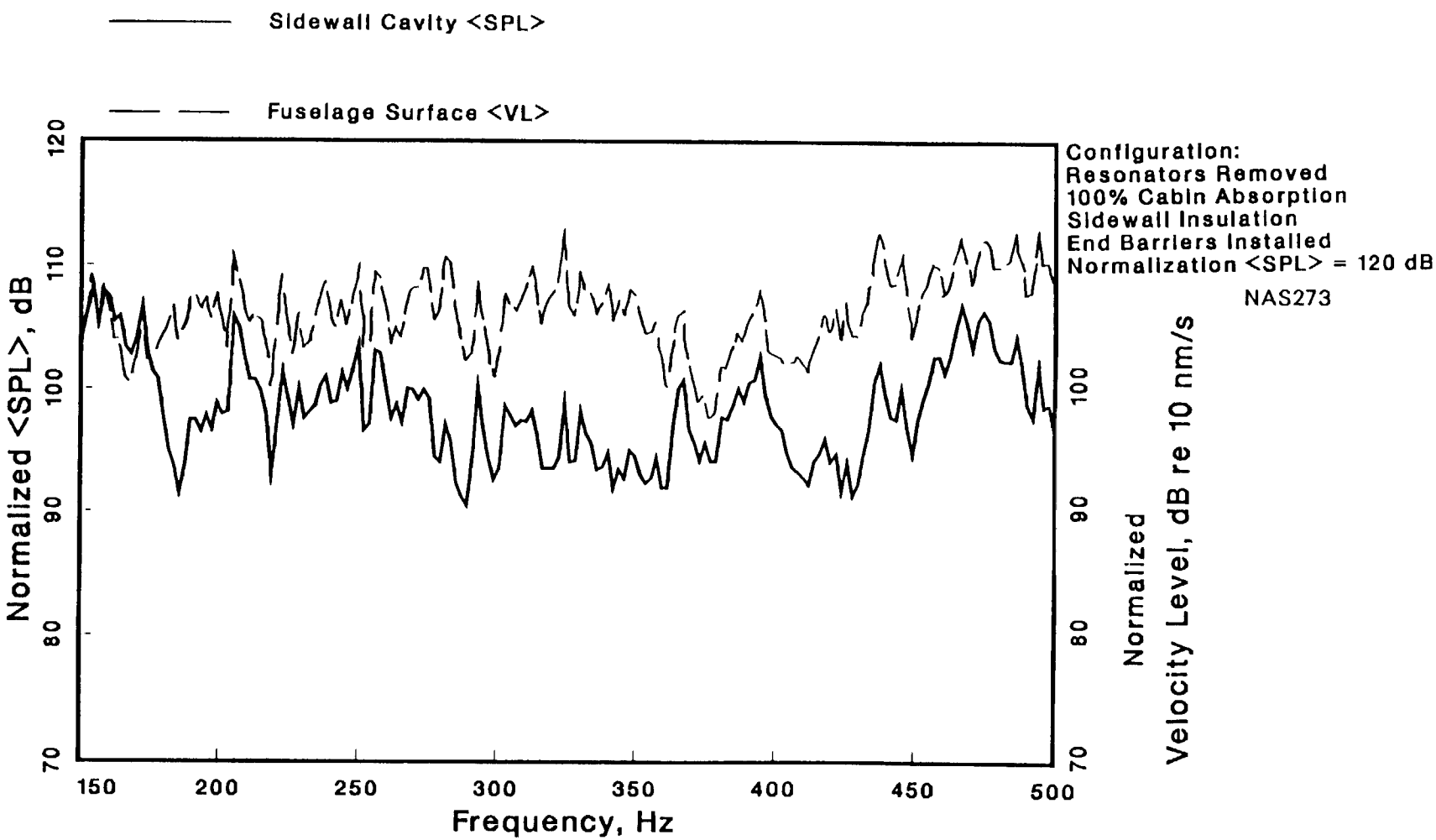

Figure 67: Average fuselage shell sidewall radial vibration velocity level versus sidewall cavity <SPL> - resonators removed.

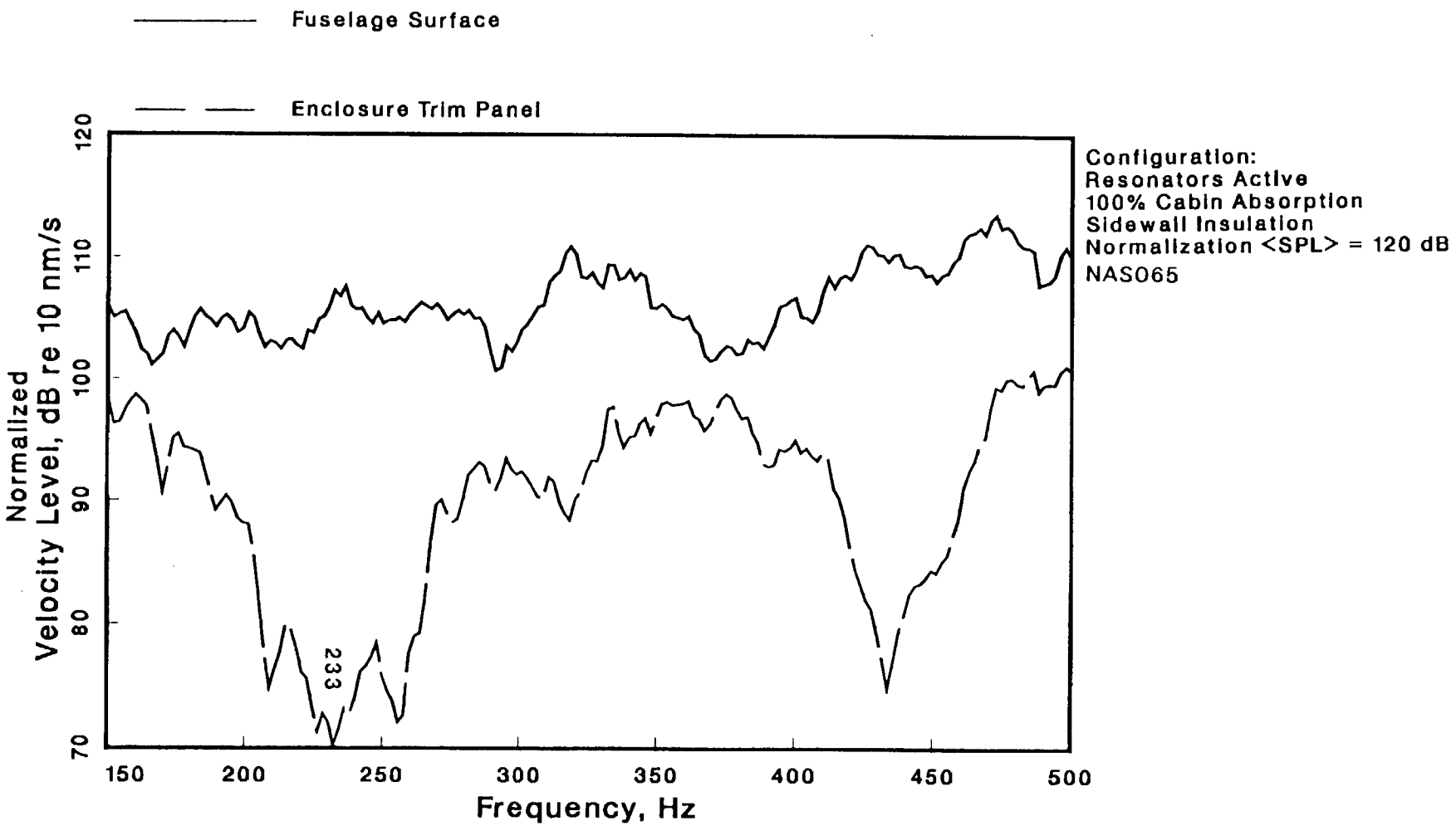

Figure 68: Average fuselage shell sidewall radial vibration velocity level versus enclosure panel radial vibration velocity level - resonators active.

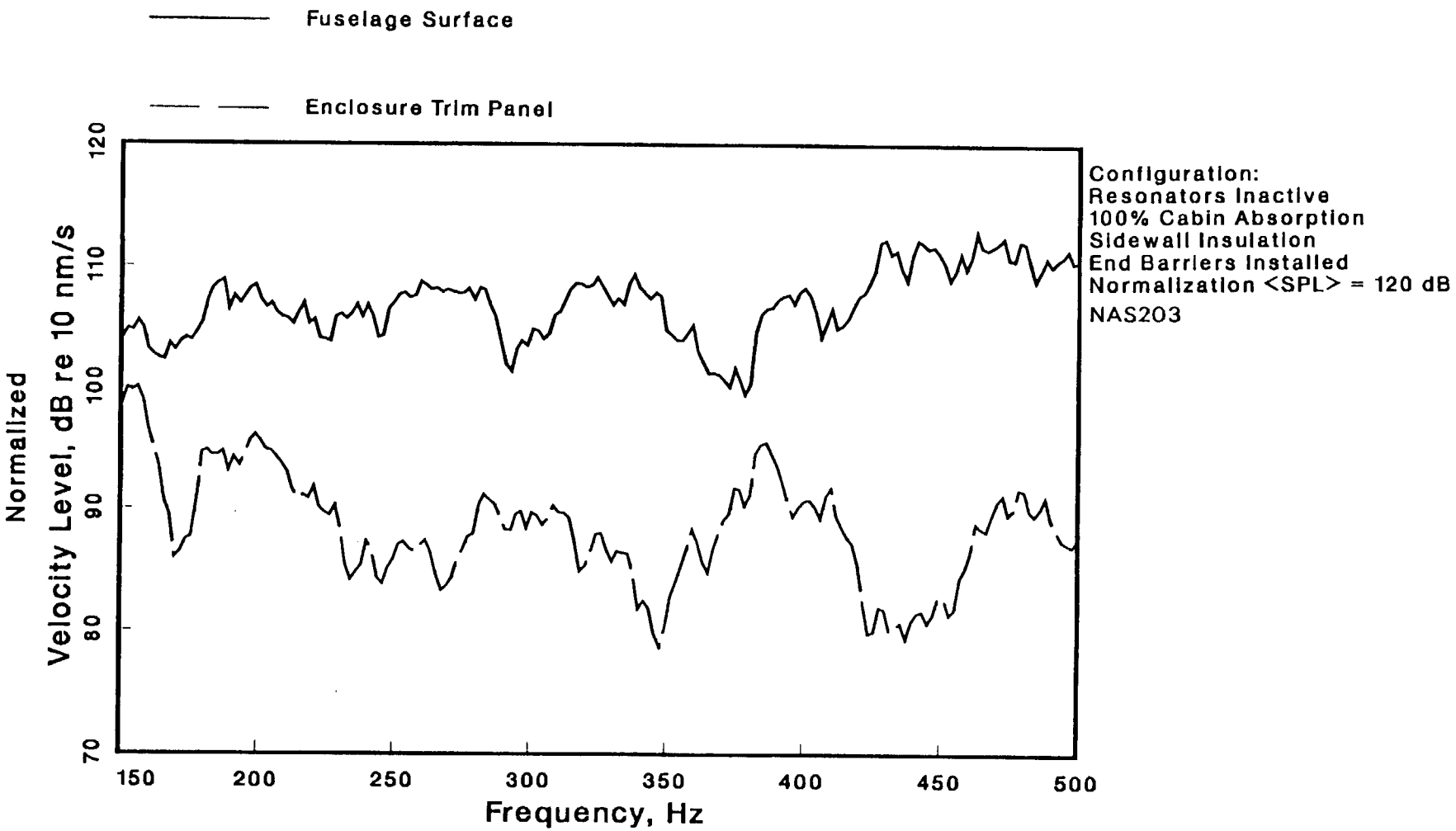

Figure 69: Average fuselage shell sidewall radial vibration velocity level versus enclosure panel radial vibration velocity level - resonators inactive.

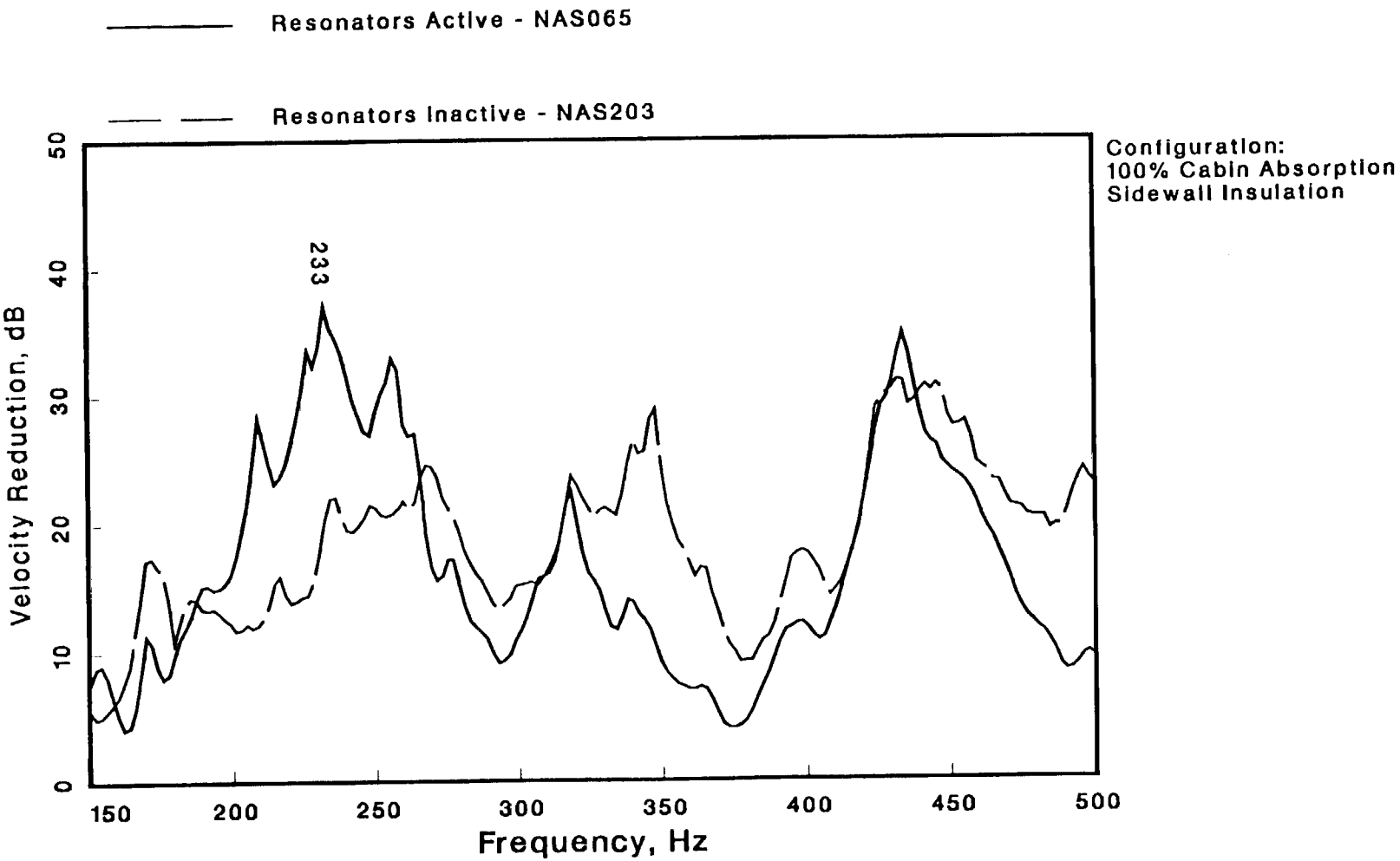

Figure 70: Vibration velocity level reduction between fuselage skin and panel radial velocities - resonators active versus resonators inactive.

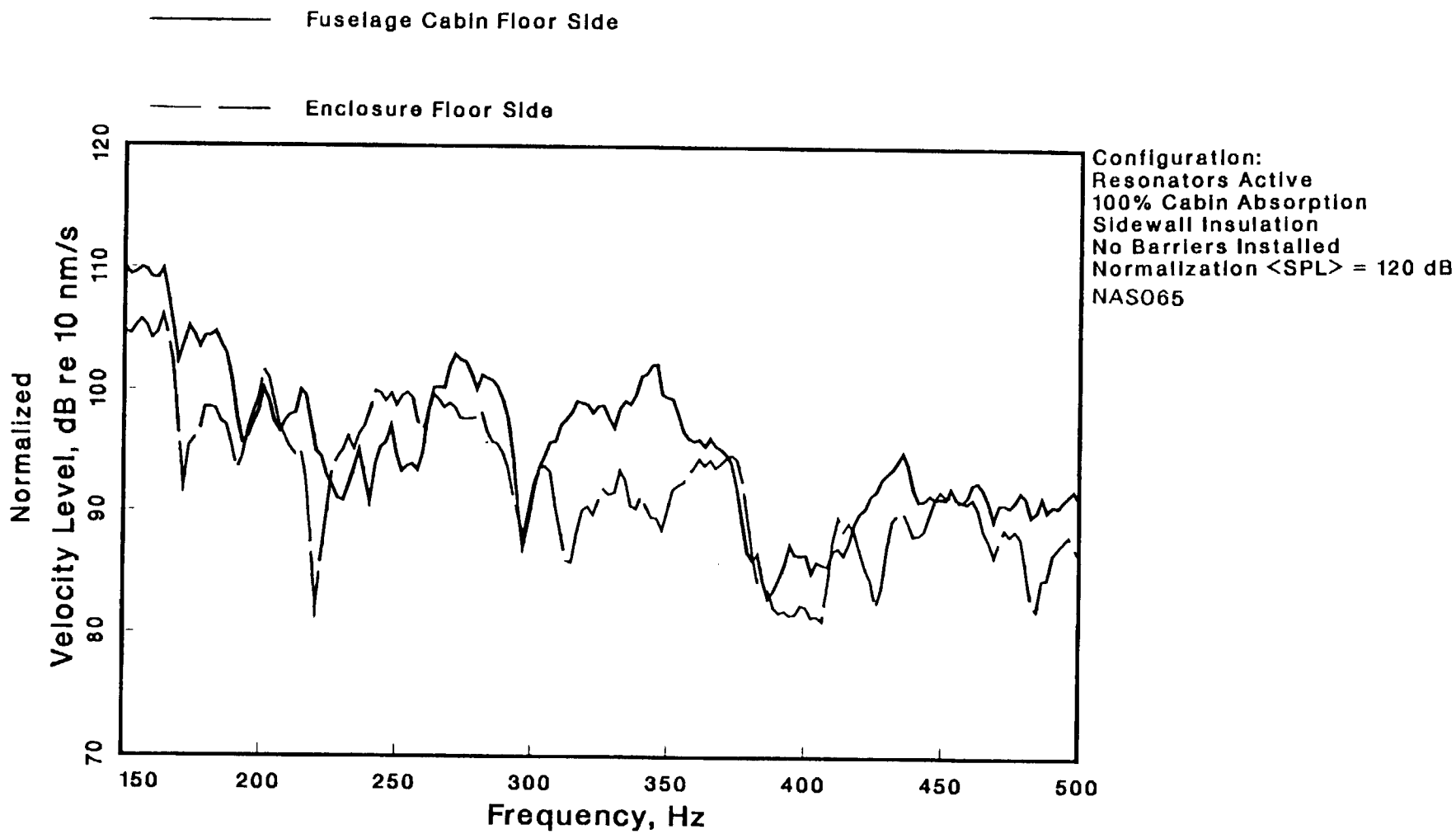

Figure 71: Vertical vibration velocity levels on either side of a single floor vibration isolator.

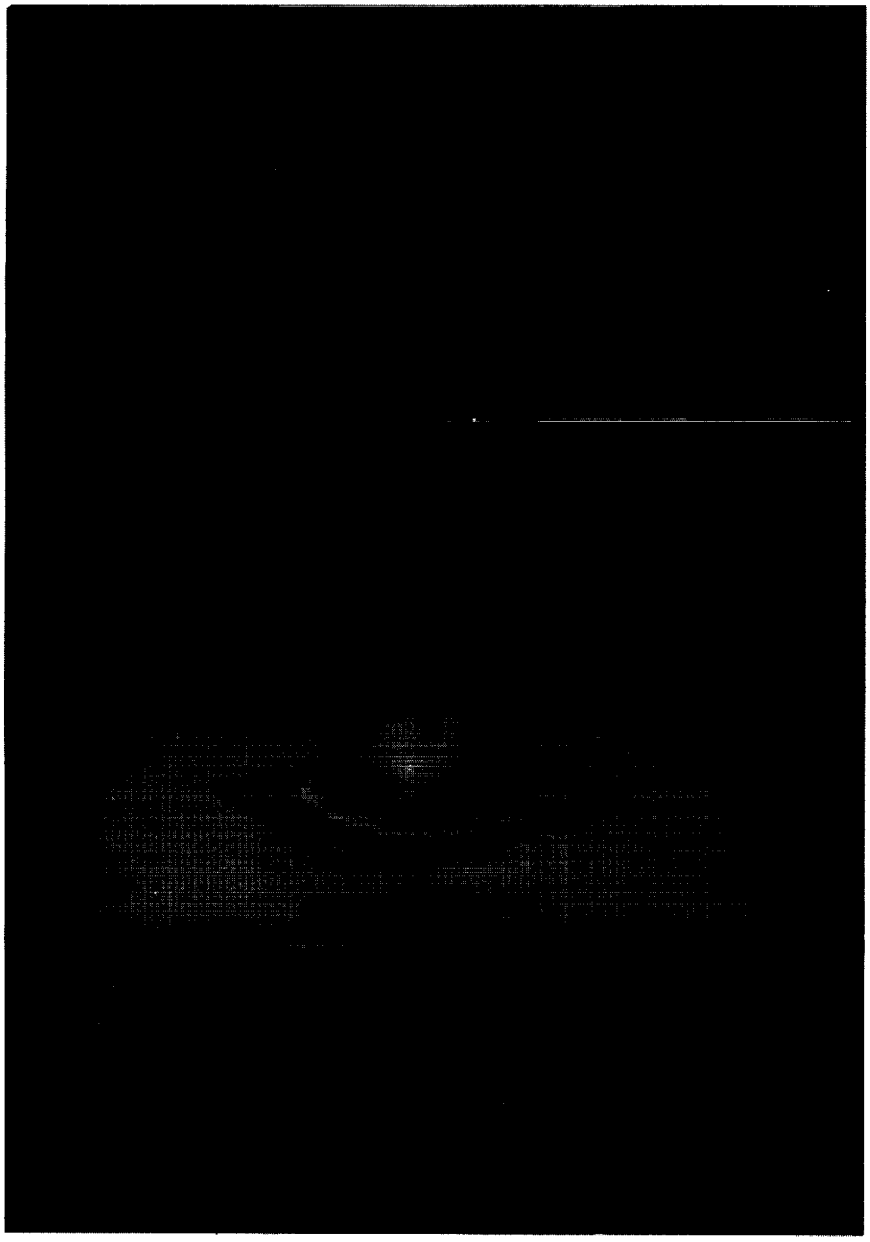

Figure A-1: Photograph of the resonator test setup.

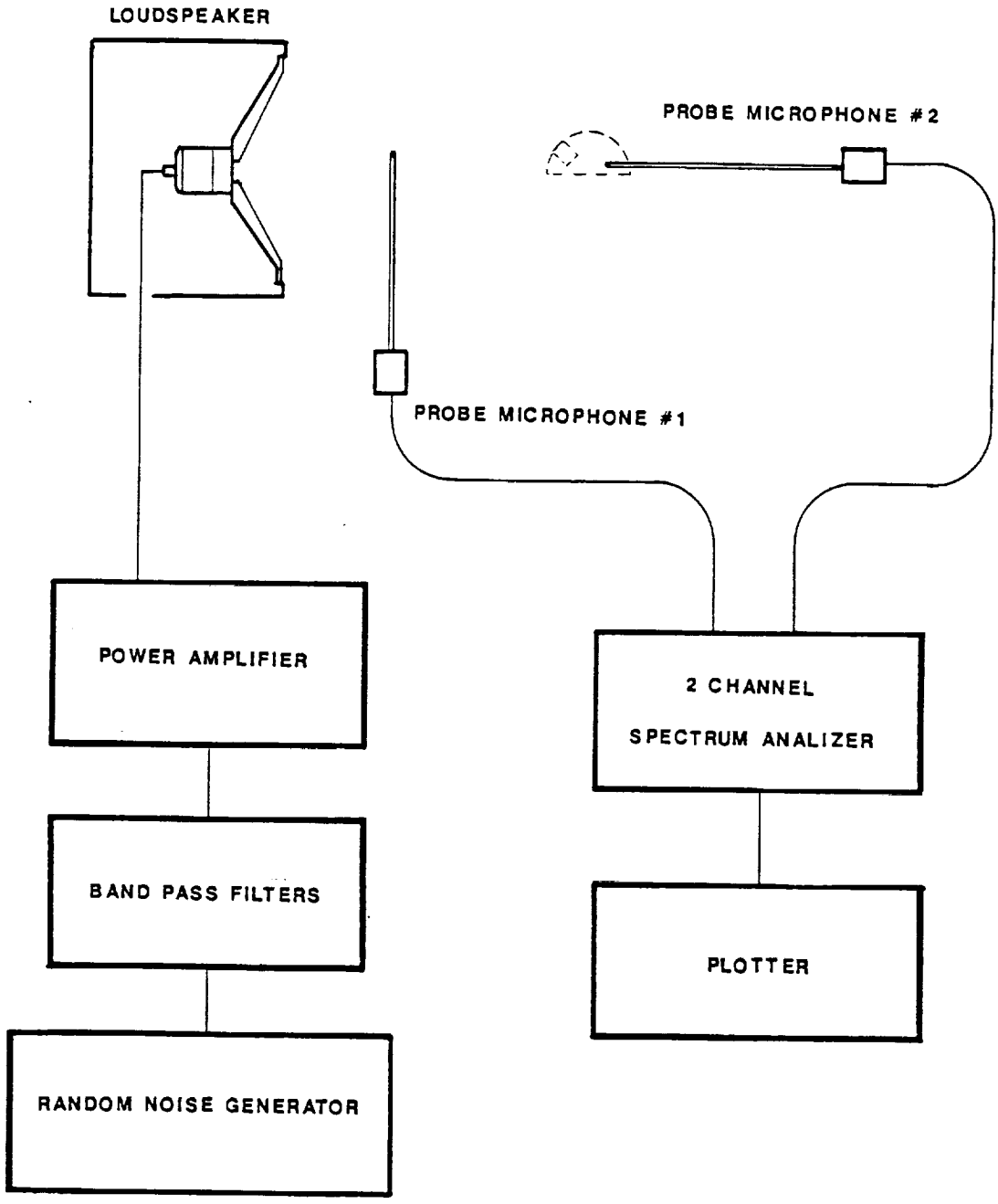

Figure A-2: Block diagram of the resonator test setup.

RESONATOR PANEL VIBRATION TEST

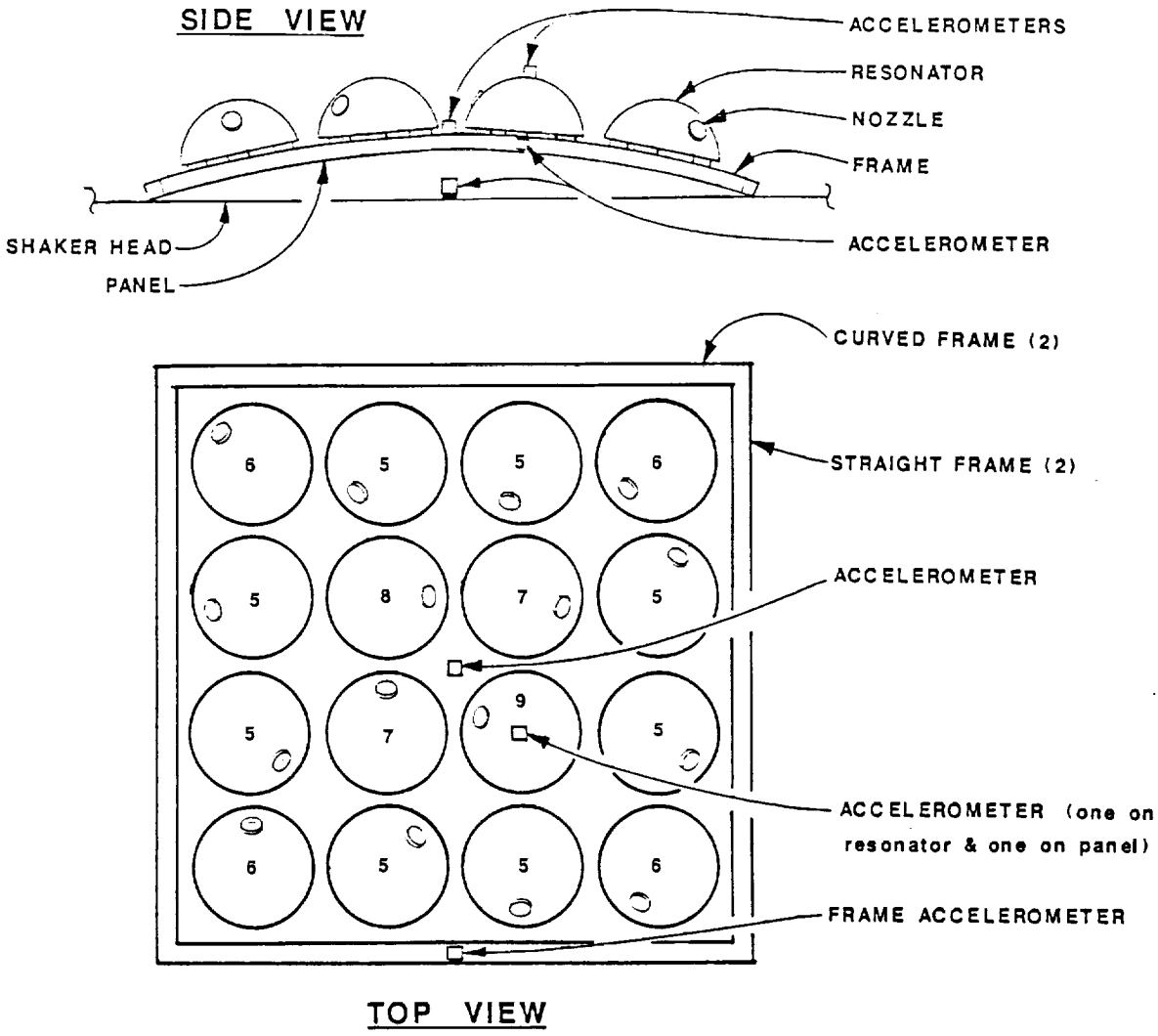

SINGLE RESONATOR VIBRATION TEST

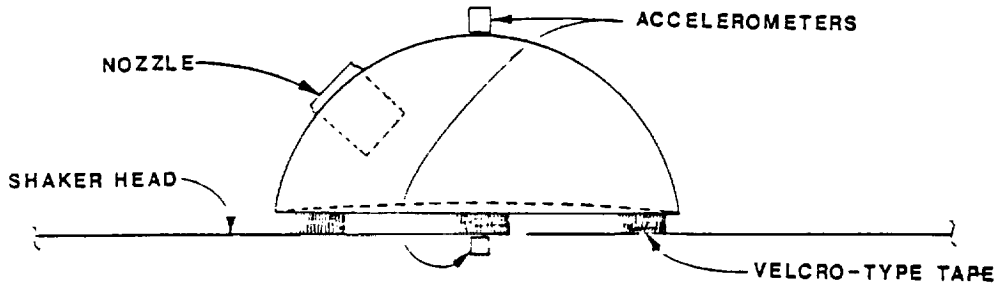

Figure B-1: Accelerometer locations on test panel and single resonator.

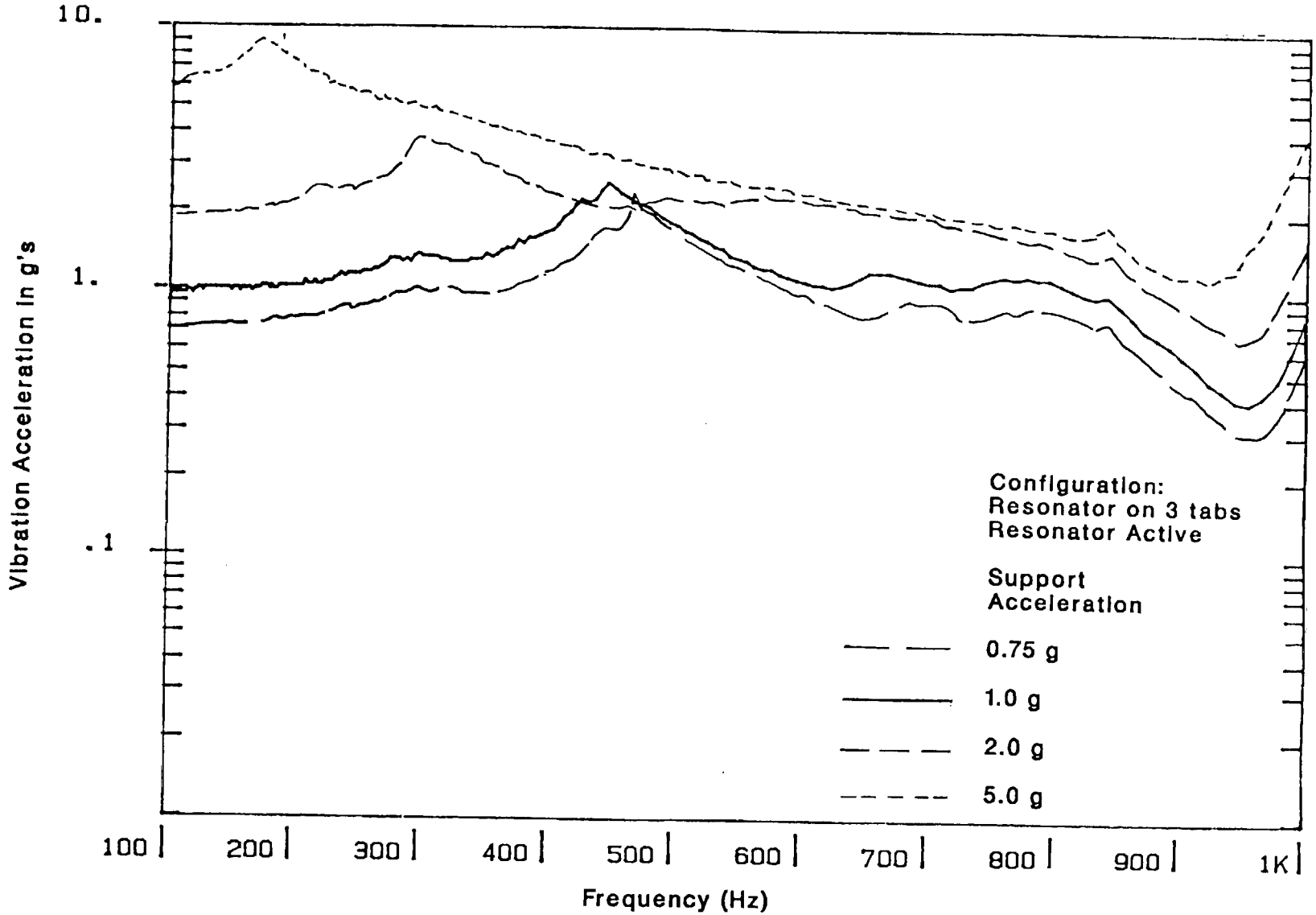

Figure B-2: Effect of vertical vibration excitation on vertical vibration response of resonator on its mounting tabs.

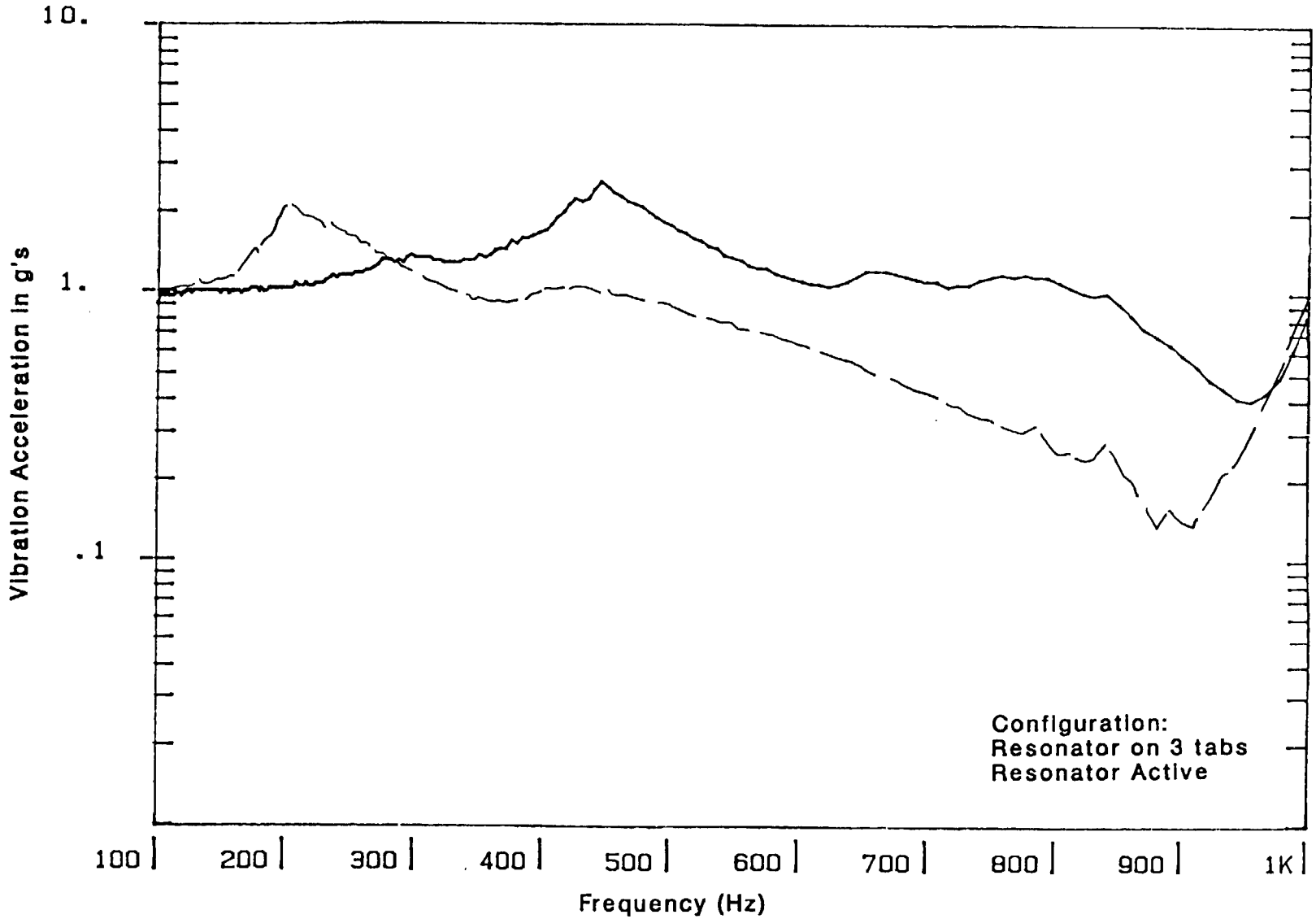

Figure B-3: Effect of resonator removal and reinstallation on vertical vibration response of resonator on its mounting tabs.

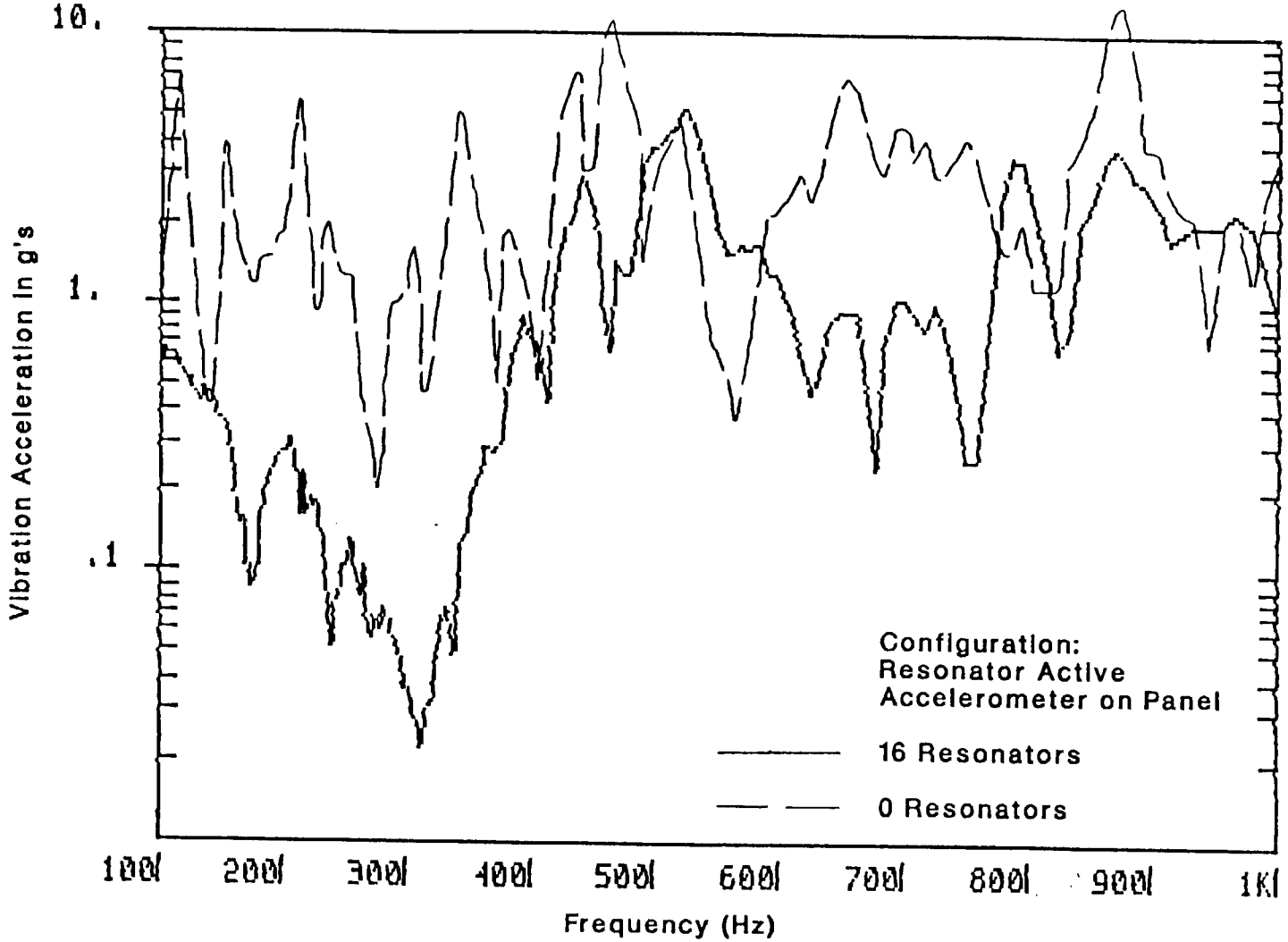

Figure B-4: Panel center vertical vibration response with and without resonators attached to the panel. 0.5 g shaker input level.

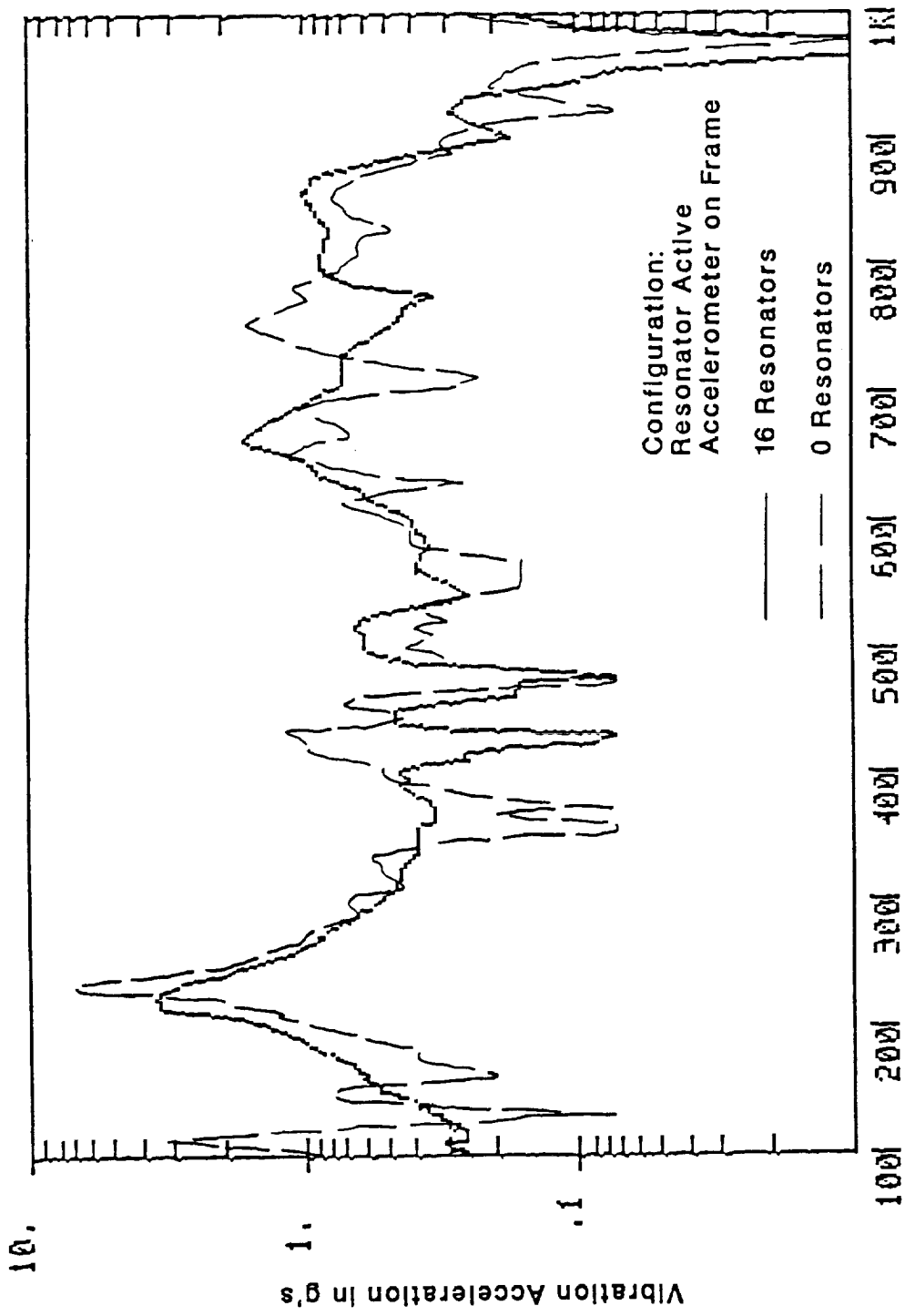

Figure B-5: Frame segment center vertical vibration response with and without resonators attached to the panel. 0.5g shaker input level.

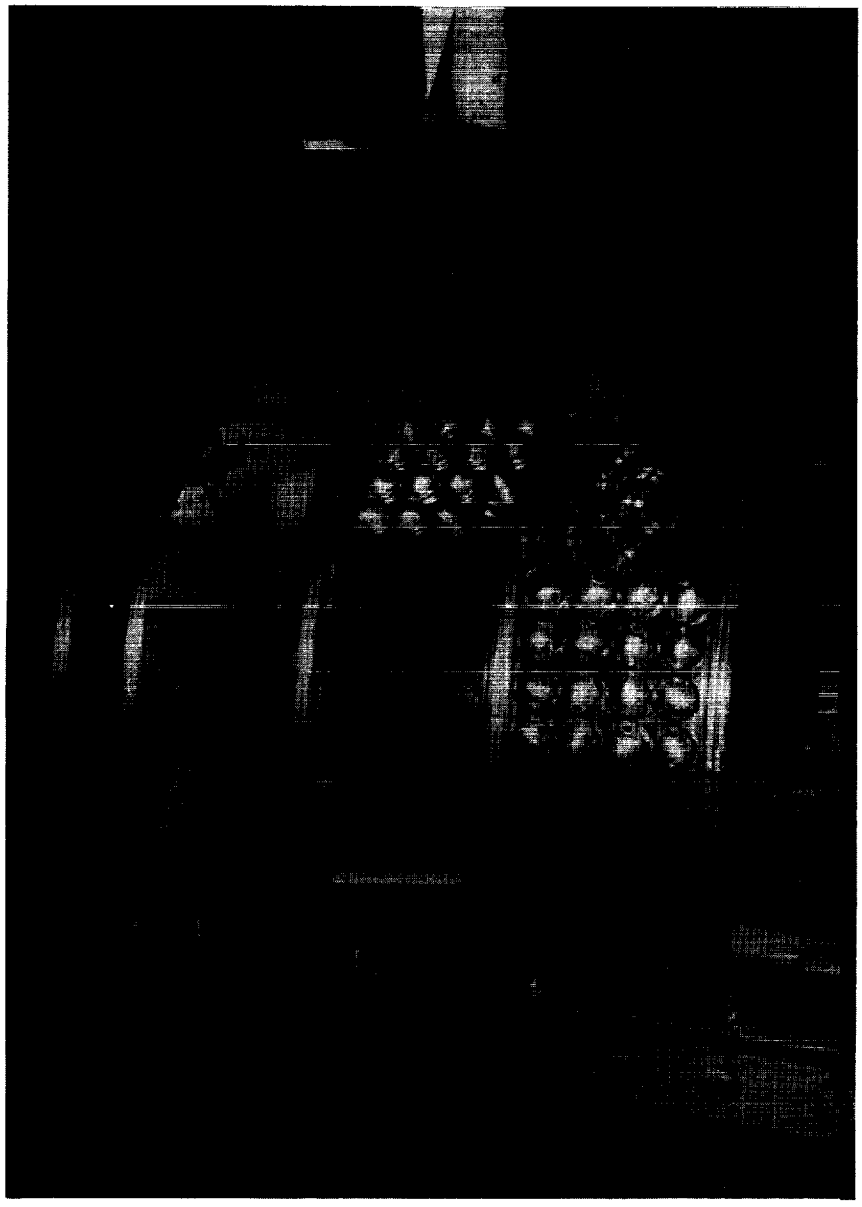

Figure B-6: Acoustic chamber on shipping base with three resonator panel assemblies attached.

Figure B-7: A view of some of the panels tapped (with identification numbers).

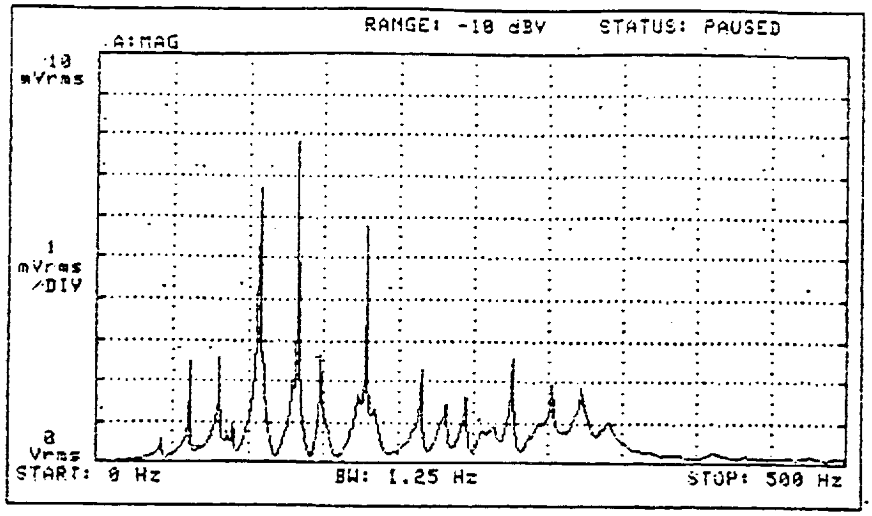

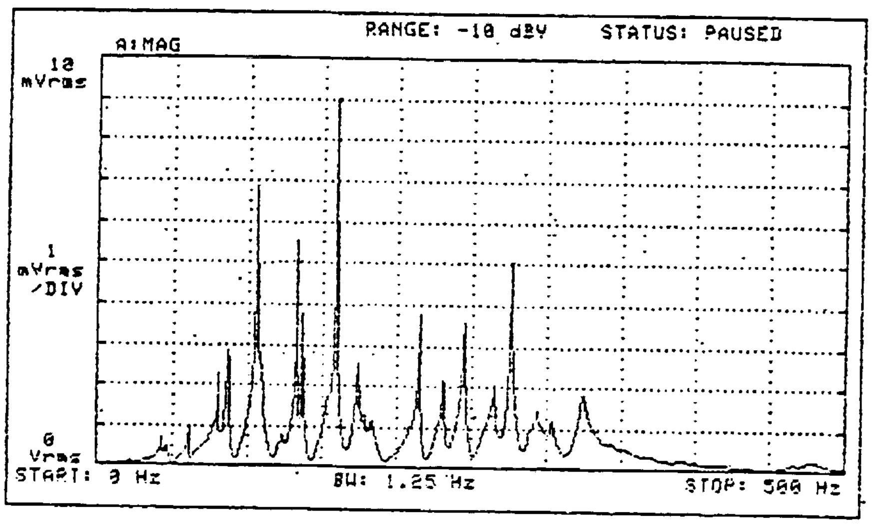

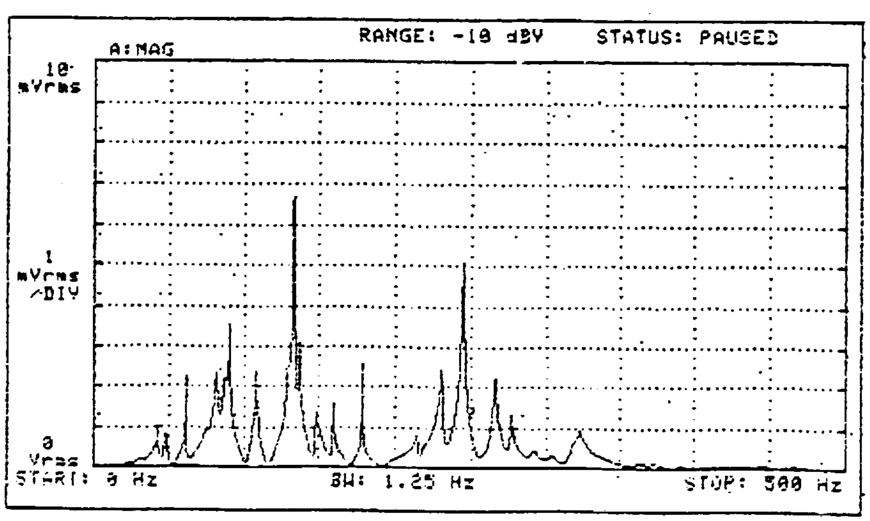

Figure B-8: Circular frame mid-span sample vibration responses.

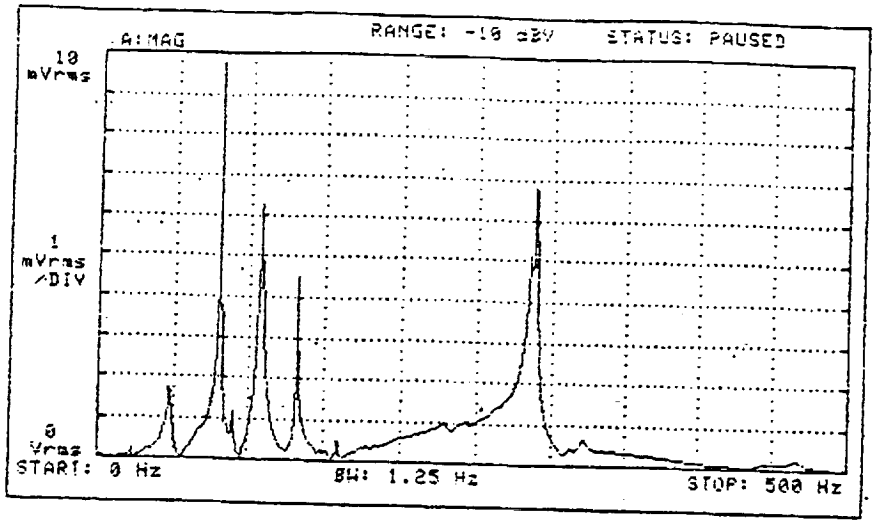

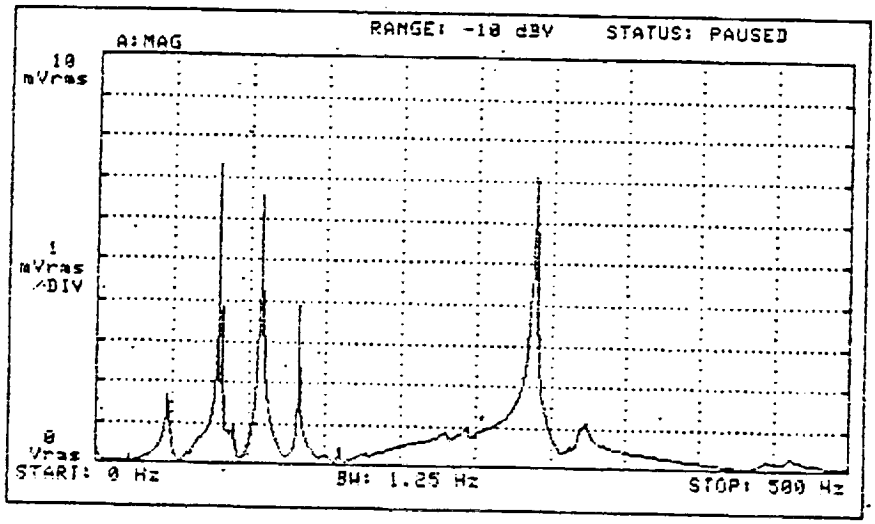

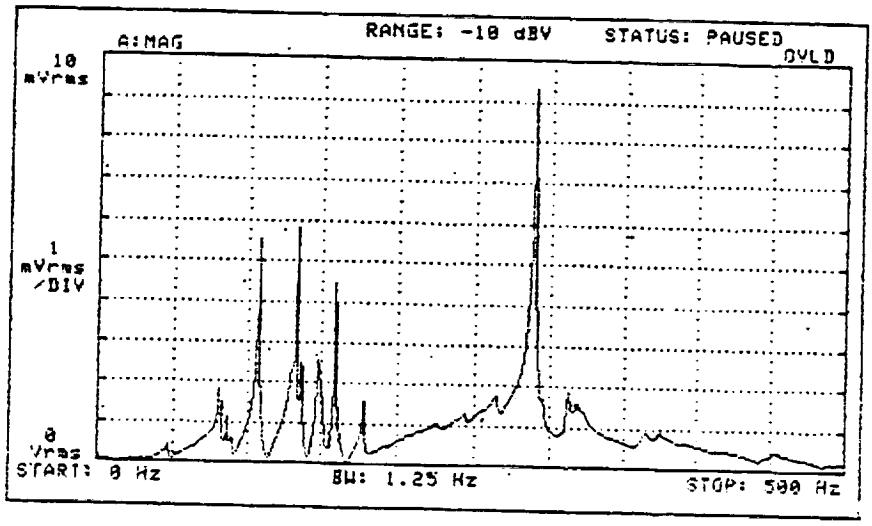

Figure B-9: Longeron mid-span sample vibration responses.

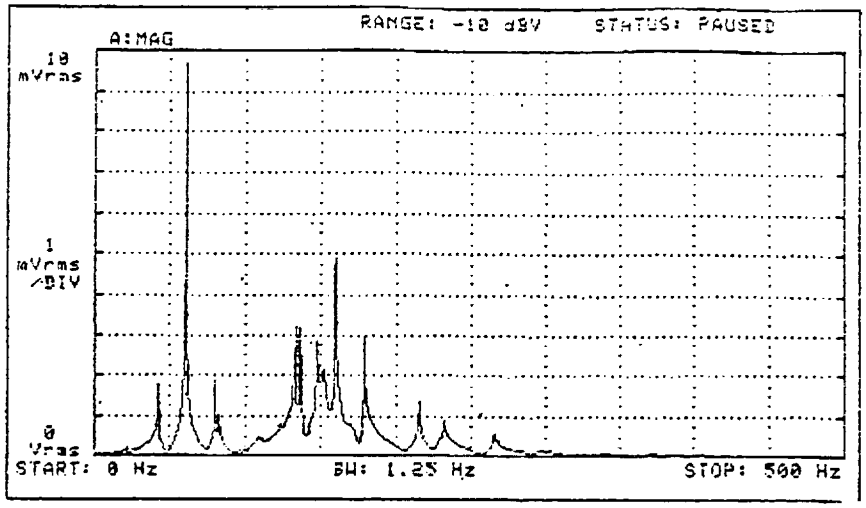

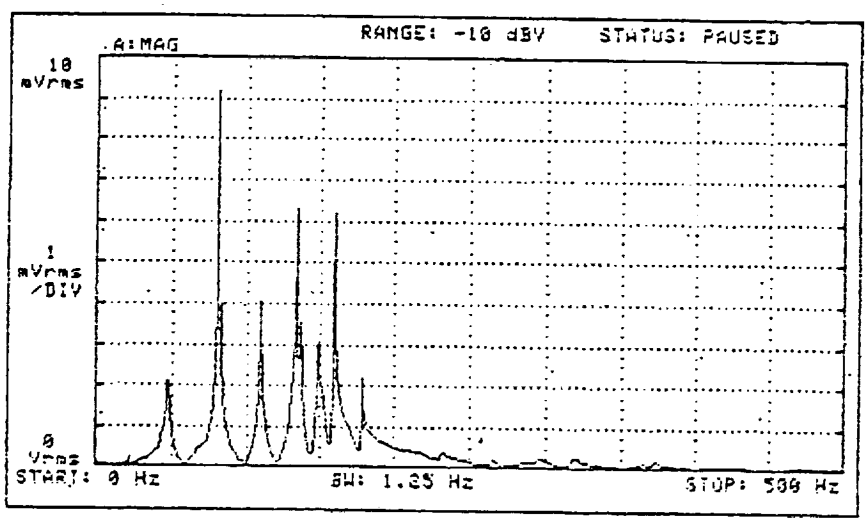

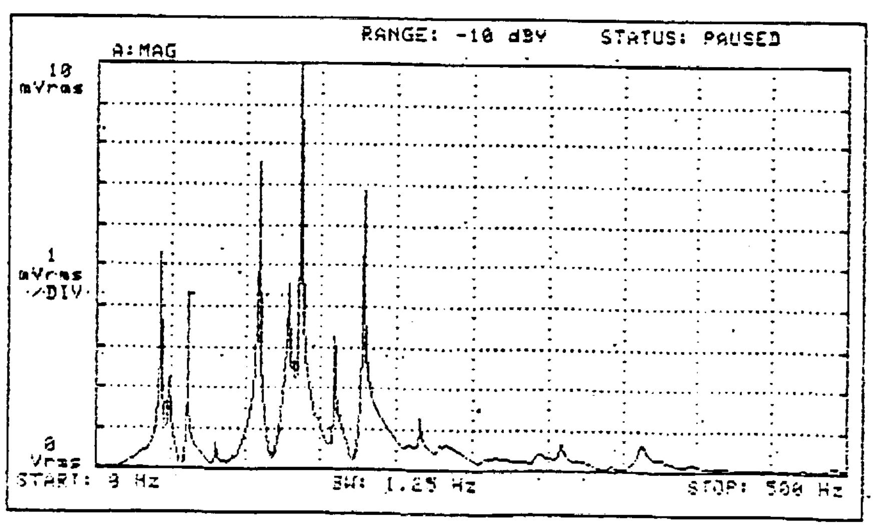

Figure B-10: Frame-to-longeron junction sample vibration responses.

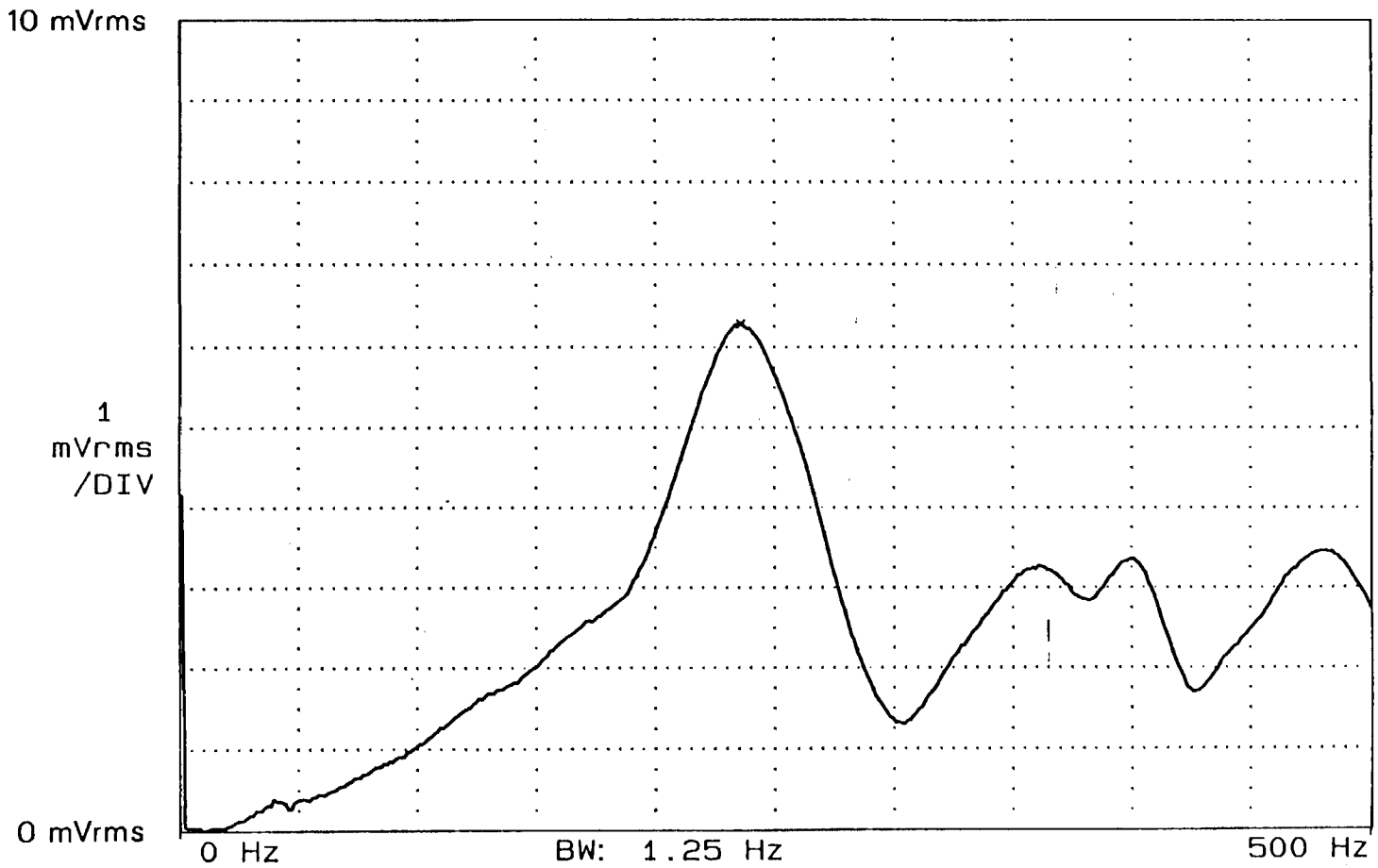

Figure B-11: Top panel 2.4 central vibration response to central radial tap.

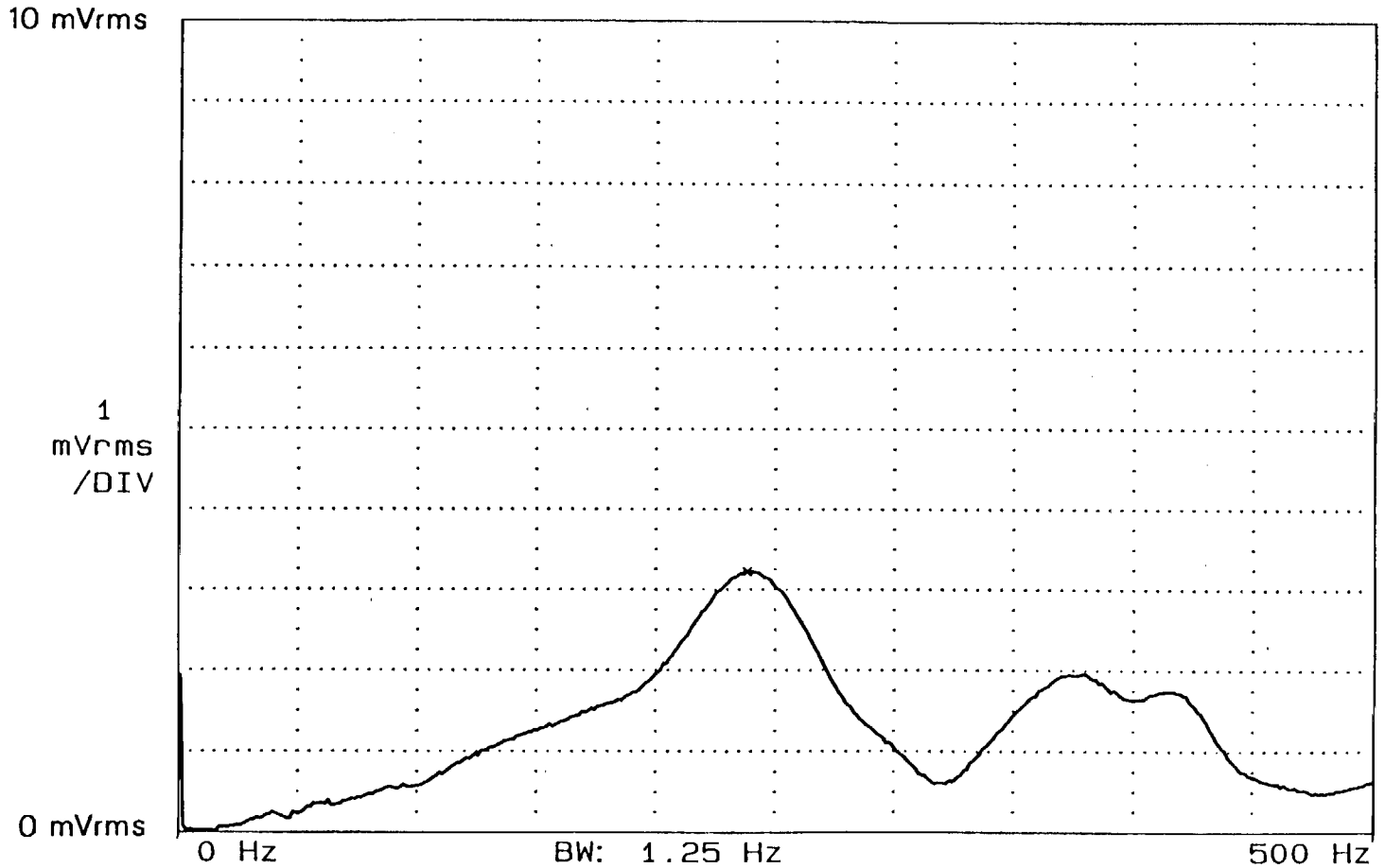

Figure B-12: Side panel 2.3 central radial response to central radial tap.

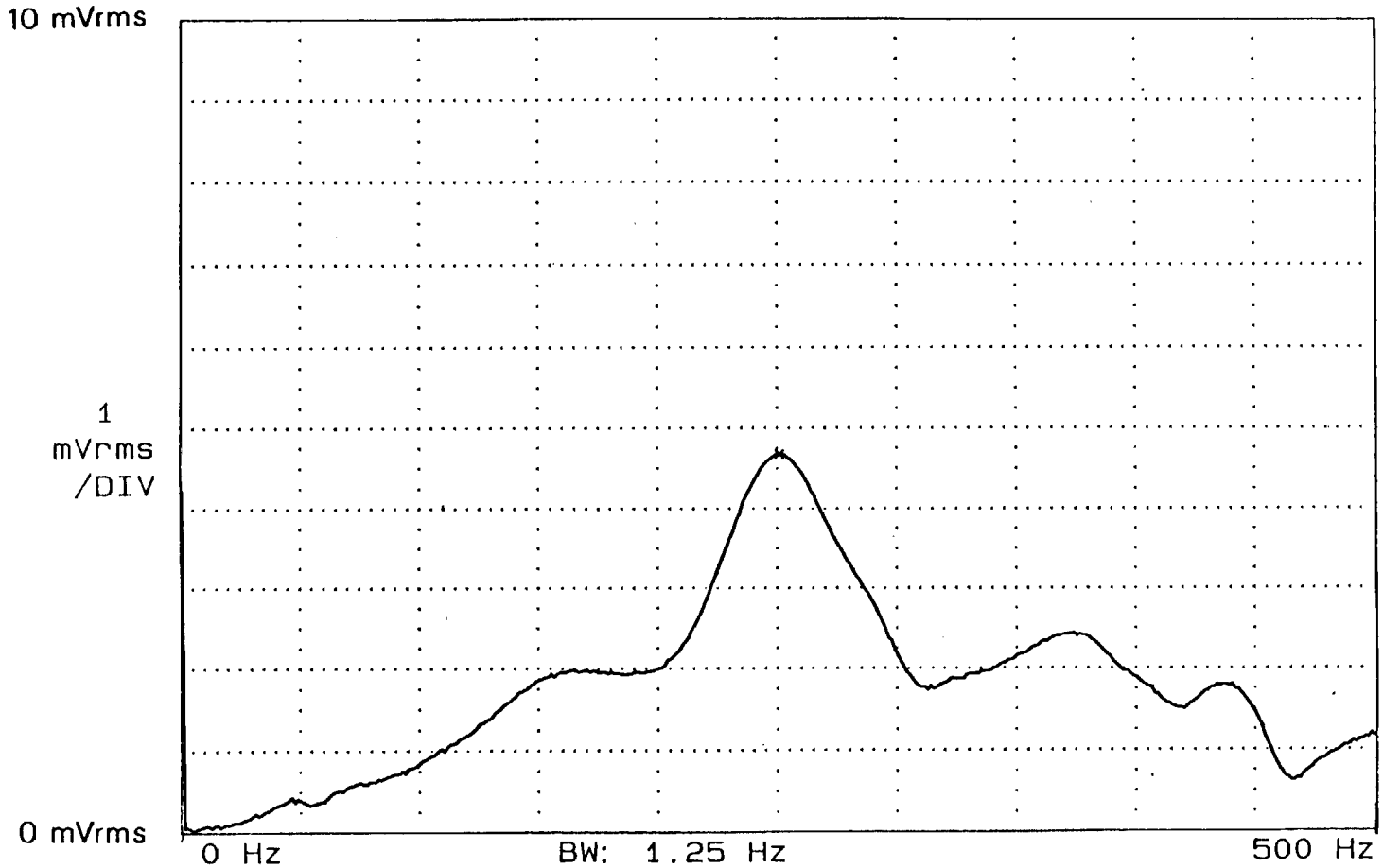

Figure B-13: Side panel 2.2 central radial response to central radial tap.

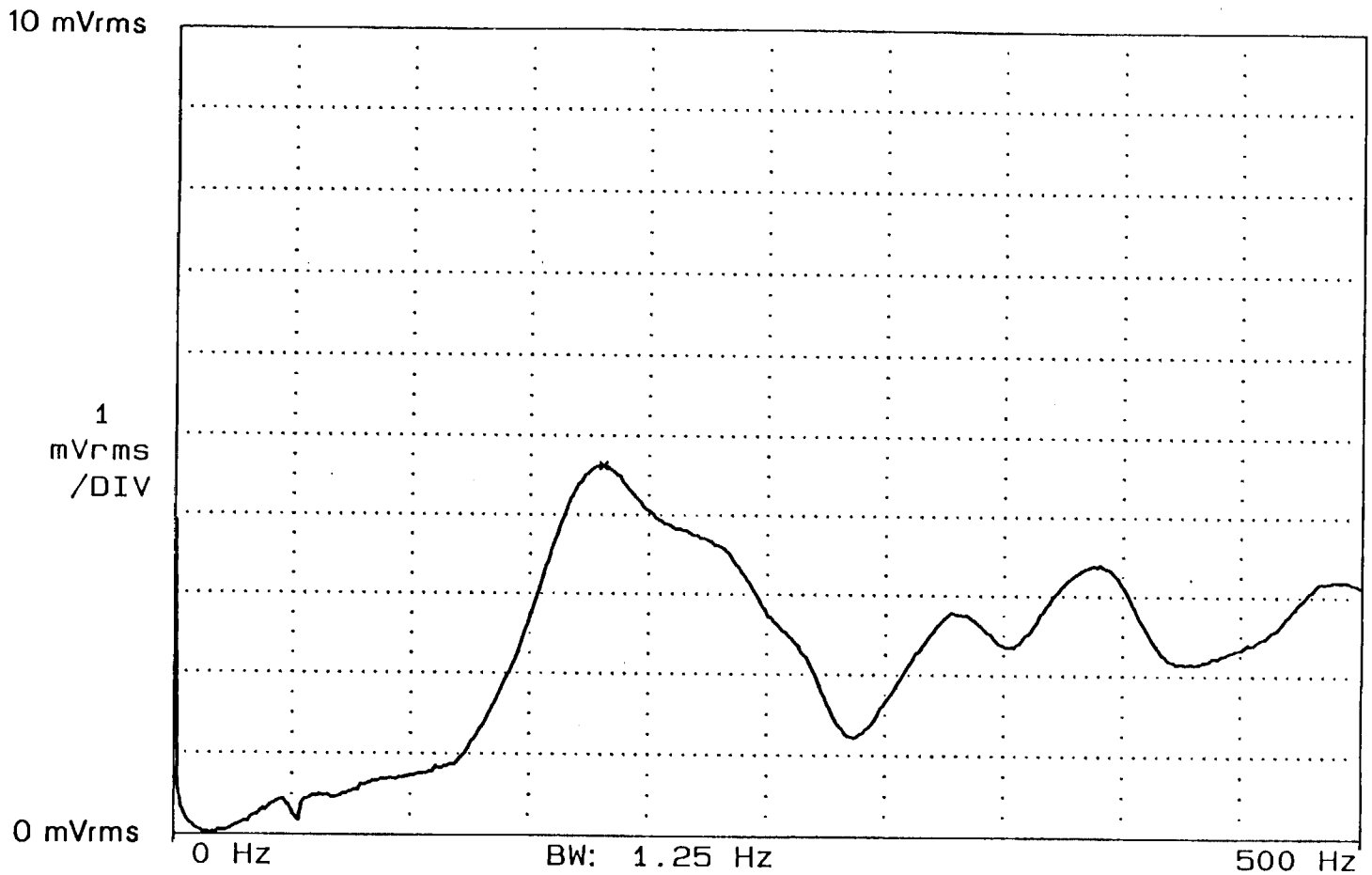

Figure B-14: Side panel 2.1 central radial response to central radial tap.

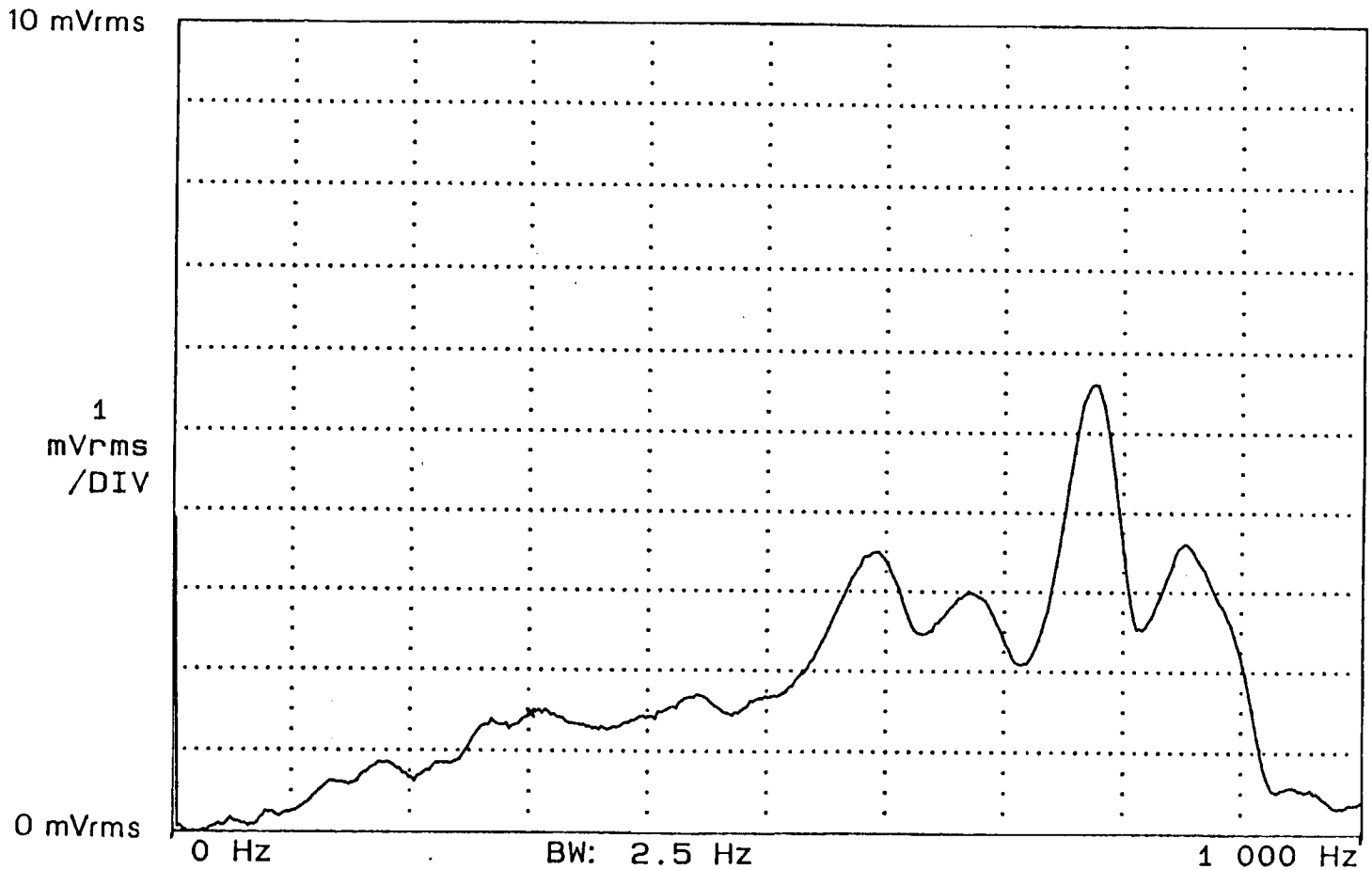

Figure B-15: Frame mid-span radial response to frame radial tap. Frame located just forward of panel 2.2.

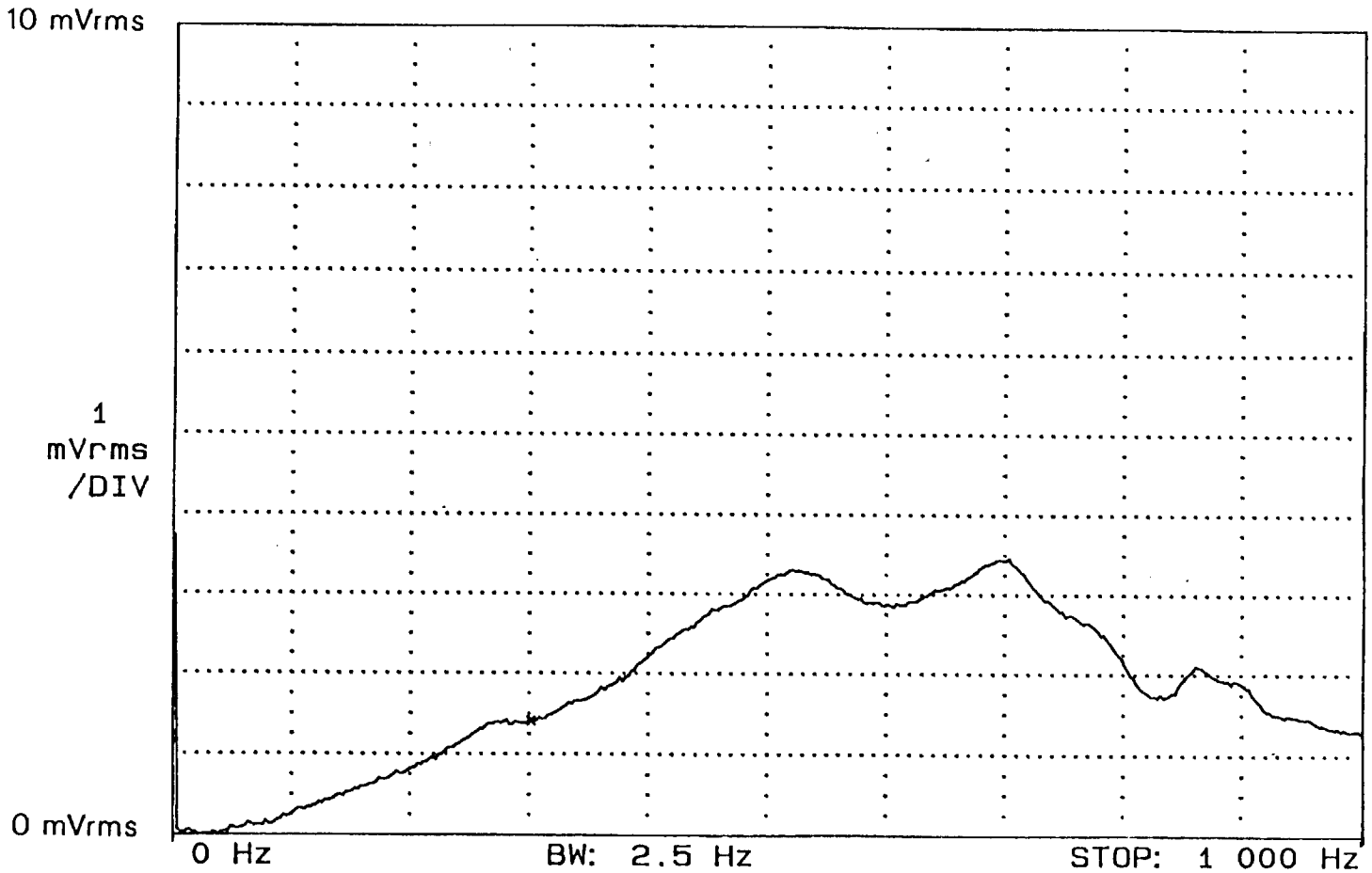

Figure B-16: Frame mid-span radial response to frame radial tap. Frame located just forward of panel 2.3.

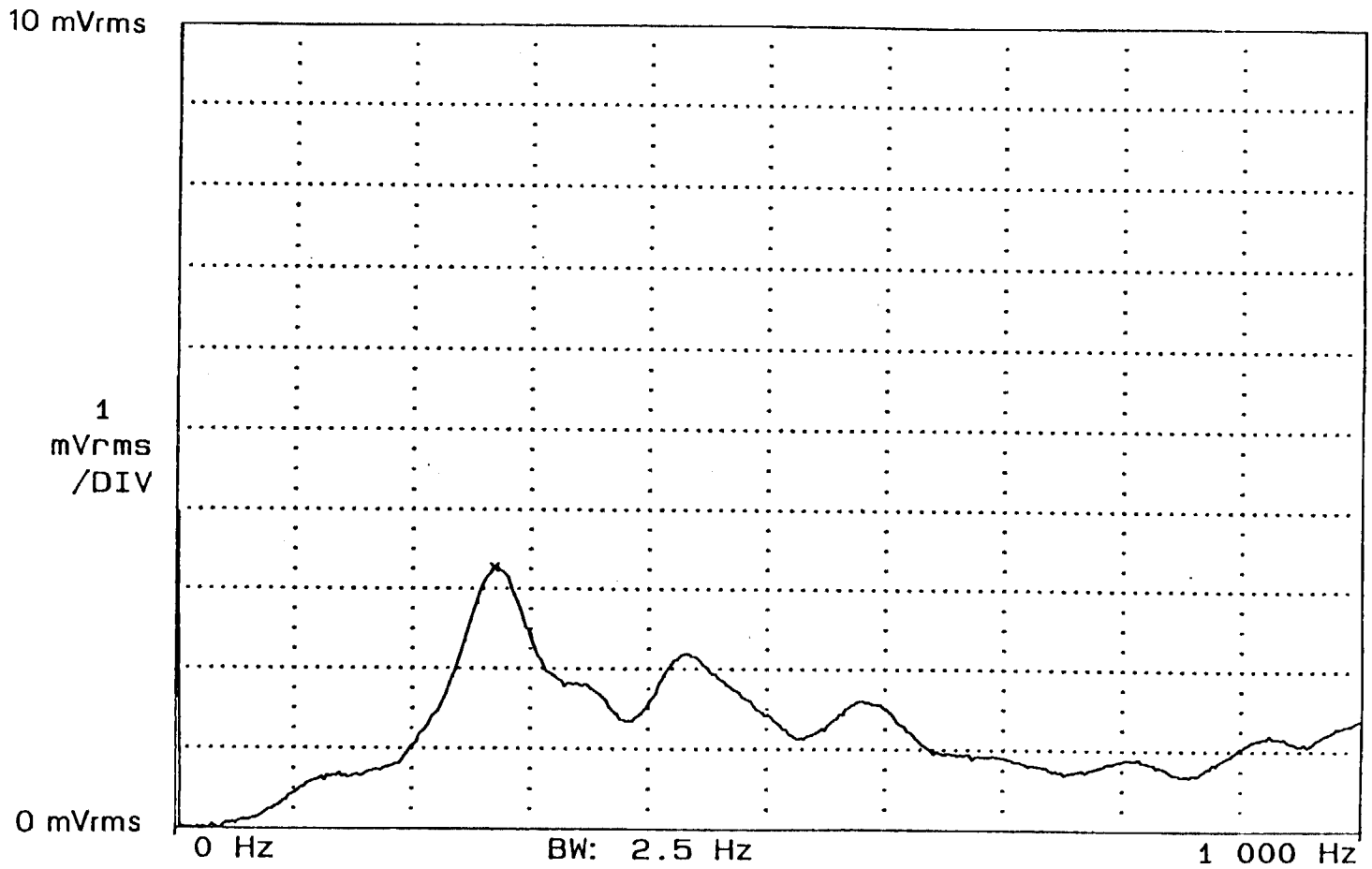

Figure B-17: Longeron mid-span radial response to longeron radial tap. Longeron located just above panel 2.1.

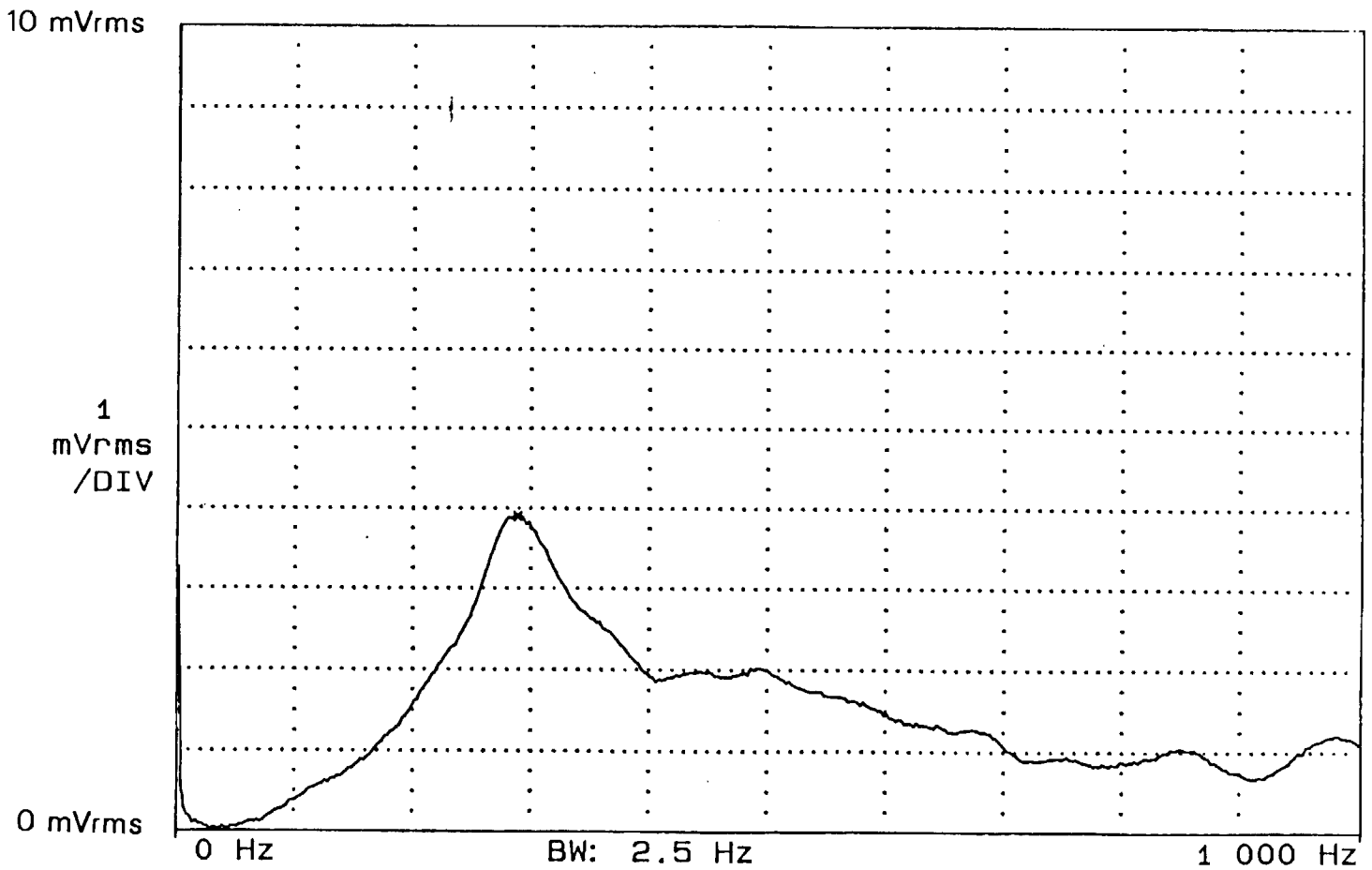

Figure B-18: Longeron mid-span radial response to longeron radial tap. Longeron located just above panel 2.2.

Table I: Acoustical characteristics of the large chamber with glass fiber rolls and the Gulfstream II fuselage test section positioned in the room.

1/3 Octave Band Frequency Hz	Room Characteristics T_{60} seconds	Stand. Dev. seconds	Absorption Coefficient
100	0.083	0.021	0.921
125	0.100	0.023	0.879
160	0.088	0.022	0.909
200	0.090	0.016	0.904
250	0.096	0.014	0.889
315	0.093	0.021	0.897
400	0.091	0.012	0.902
500	0.086	0.014	0.914
630	0.101	0.015	0.876
800	0.097	0.013	0.886
1000	0.079	0.023	0.931

Room volume: 781 m^3 (27566 ft^3)
Fuselage volume: 16 m^3 (552 ft^2)
Adjusted volume (V_a): 766 m^3 (27014 ft^3)
Room surface area: 550 m^2 (5916 ft^2)
Fuselage Surface area: 35 m^2 (378 ft^2)
Adjusted surface area (S_a): 585 m^2 (6294 ft^2)

Absorption Coefficient = $1 - EXP(-0.211/T_{60})$
(For effective surface areas of the wall and fuselage.)

Table II: Listing of laboratory test conditions and related flight tests.

Start NAS#	Resonator Status	Ends* Treated	Cabin Absorption	Vary SPLs	Acoustic Source#	Radial Mics@	Sidewall Glass	Probe Mics+	Comments
1	Oper	No	100%	No	T & R	No	Yes	No	Fuselage SPLs - External Field Setup
23	-	-	-	Yes	T	No	-	No	Microphone Calibrations
62	Oper	No	100%	No	T & R	No	Yes	No	Baseline, re Flights 66 & 67
90	Oper	No	10%	No	T & R	No	Yes	No	Baseline, re Flights 66 & 67
115	Oper	No	0%	No	R	No	Yes	No	Baseline, re Flights 66 & 67
117	Oper	Yes	100%	No	T & R	No	Yes	No	Full end treatments, re Flight 71
141	-	-	-	No	T	No	-	Yes	Probe Calibrations
144	Oper	Yes	100%	Yes	T & R	No	Yes	Yes	Probes in mid-panel
173	Oper	Yes	100%	No	T & R	No	Yes	Yes	Ambient, No Air; No Signal
175	Oper	Yes	100%	No	T & R	No	Yes	Yes	Probes in aft-panel
179	Oper&Rev	Yes	100%	Yes	R	No	Yes	No	Operating Resonators in Cabin
183	Oper&Rev	Yes	0%	Yes	R	No	Yes	No	Operating Resonators in Cabin
187	Inop&Rev	Yes	100%	Yes	R	No	Yes	No	Taped Resonators in Cabin
191	Oper&Rev	Yes	100%	Yes	R	Yes	Yes	No	Operating Resonators in Cabin
195	Inop&Rev	Yes	100%	Yes	R	Yes	Yes	No	Taped Resonators in Cabin
199	Inop	Yes	100%	No	R	Yes	Yes	No	Taped Resonators in Sidewalls, re Flt 72
201	Inop	Yes	0%	No	R	No	Yes	No	Taped Resonators in Sidewalls, re Flt 72
203	Inop	Yes	100%	No	T & R	No	Yes	No	Taped Resonators in Sidewalls, re Flt 72
227	-	-	-	-	T	-	-	No	Final Calibrations - First Set
251	-	-	-	-	T	-	-	No	Initial Calibrations - Second Set
272	Removed	Yes	100%	No	T & R	No	Yes	No	Resonators Removed
296	Oper	Yes	100%	No	T & R	No	No	No	Resonators Active - No Sidewall Glass
304	Oper	Yes	100%	No	T & R	No		No	Replacement & Calibration of M323
306	Oper	Yes	100%	No	T & R	No	No	No	Restart of Test #296
331	Inop	Yes	100%	No	T & R	No	No	No	Resonators Inactive - No Sidewall Glass
355	-	-	-	-	T	-	-	No	Final Calibrations

* Vinyl barriers were added to ends of fuselage section.
\# T = Tone Excitation; R = Random Excitation
@ Cabin microphones were placed in a line across the cabin.
\+ Probe microphones placed in sidewall airspace and sidewall resonator.

Table III: Accelerometer measurement locations for noise excitation and tap tests (refer to Fig. 9).

Accelerometer	Fuselage Station	Water Line	Location
AG01	319	100	Panel Next to Resonator
AG02	319	105	Resonator
AG03	370	71	Fuselage Floor at Aft Isolator
AG04	370	74	Enclosure Floor at Aft Isolator
AG05	263	113	Fuselage Skin
AG06	319	113	Fuselage Skin
AG07	353	113	Fuselage Skin

Table IV: Accelerometer measurement locations for tap tests on enclosure with panels installed.

Panel Number	Panel Location (Refer to Fig. B-7)
1.1	Bay #1, lower panel
1.2	Bay #1, side panel
1.3	Bay #1, side panel
1.4	Bay #1, top panel
2.1	Bay #2, lower panel
2.2	Bay #2, side panel
2.3	Bay #2, side panel
2.4	Bay #2, top panel
3.1	Bay #3, lower panel
3.2	Bay #3, side panel
3.3	Bay #3, side panel
3.4	Bay #3, top panel

Table V: Thermocouple locations during laboratory tests (refer to Fig. 9).

Thermocouple	Fuselage Station	Water Line	Location
TH01	353	128	Fuselage Skin
TH02	318	101	Fuselage Skin
TH03	262	92	Fuselage Skin
TH04	240	120	Fuselage End
TH05	240	80	Fuselage End
TH06	370	120	Fuselage End
TH07	370	80	Fuselage End
TH08	311	140	Sidewall
TH09	279	90	Sidewall Resonator
TH10	279	90	Sidewall
TH11	339	132	Sidewall
TH12	316	113	Sidewall Resonator
TH13	339	132	Sidewall Resonator
TH14	311	140	Sidewall Resonator
TH15	316	113	Sidewall
TH16	315	132	Cabin
TH17	272	99	Cabin
TH18	316	132	Cabin
TH19	345	116	Cabin
TH20	316	73	Under Floor Resonator
TH21	325	73	Under Floor
TH22	293	73	Under Floor

NASA
National Aeronautics and Space Administration

Report Documentation Page

1. Report No.	2. Government Accession No.	3. Recipient's Catalog No.
NASA CR-182075		

4. Title and Subtitle	5. Report Date
Laboratory Test and Acoustic Analysis of Cabin Treatment for Propfan Test Assessment Aircraft	May 1991
	6. Performing Organization Code

7. Author(s)	8. Performing Organization Report No.
H. L. Kuntz and R. J. Gatineau	LR 31879
	10. Work Unit No. 535-03-11-04

9. Performing Organization Name and Address	11. Contract or Grant No.
Lockheed Aeronautical Systems Company - Burbank P. O. Box 551 Burbank, CA 91520	NAS1-18036
	13. Type of Report and Period Covered: Contractor Report

12. Sponsoring Agency Name and Address	14. Sponsoring Agency Code
National Aeronautics and Space Administration Langley Research Center Hampton, VA 23665-5225	

15. Supplementary Notes

Langley Technical Monitor: Kevin P. Shepherd

Interim Report - Task 3

16. Abstract

An aircraft cabin acoustic enclosure, built in support of the Propfan Test Assessment (PTA) program, is described. Helmholtz resonators were attached to the cabin trim panels to increase the sidewall transmission loss (TL). Resonators (448) were located between the trim panels and fuselage shell. In addition, 152 resonators were placed between the enclosure and aircraft floors. The 600 resonators were each tuned to a 235 Hz resonance frequency. After flight testing on the PTA aircraft, the enclosure was tested in the Kelly Johnson Research and Development Center Acoustics Laboratory. Laboratory noise reduction (NR) test results are discussed. The enclosure was placed in a Gulfstream II fuselage section. Broadband (138 dB overall SPL) and tonal (149 dB overall SPL) excitations were used in the laboratory. Tonal excitation simulated the propfan flight test excitation. The fundamental tone was stepped in 2 Hz intervals from 225 Hz through 245 Hz. The resonators increase the NR of the cabin walls around the resonance frequency of the resonator array. The effects of flanking, sidewall absorption, cabin absorption, resonator loading of trim panels, and panel vibrations are presented. Increases in NR of up to 11 dB were measured.

17. Key Words (Suggested by Author(s))	18. Distribution Statement
Helmholtz resonator, Transmission loss, Advanced turboprop aircraft, Acoustics, Interior noise control	Unclassified - Unlimited Subject Category 71

19. Security Classif. (of this report)	20. Security Classif. (of this page)	21. No. of pages	22. Price
Unclassified	Unclassified	144	

NASA FORM 1626 OCT 86